131
Advances in Biochemical Engineering/Biotechnology

For further volumes:
http://www.springer.com/series/10

Aims and Scope

This book series reviews current trends in modern biotechnology and biochemical engineering. Its aim is to cover all aspects of these interdisciplinary disciplines, where knowledge, methods and expertise are required from chemistry, biochemistry, microbiology, molecular biology, chemical engineering and computer science.

Volumes are organized topically and provide a comprehensive discussion of developments in the field over the past 3–5 years. The series also discusses new discoveries and applications. Special volumes are dedicated to selected topics which focus on new biotechnological products and new processes for their synthesis and purification.

In general, volumes are edited by well-known guest editors. The series editor and publisher will, however, always be pleased to receive suggestions and supplementary information. Manuscripts are accepted in English.

In references, Advances in Biochemical Engineering/Biotechnology is abbreviated as *Adv. Biochem. Engin./Biotechnol.* and cited as a journal.

Jian-Jiang Zhong
Editor

Future Trends in Biotechnology

With contributions by

M. Bardor · K. F. Chan · C. Furusawa · X. Han
R. Haryadi · T. Hirasawa · T. Horinouchi · K. Kang
Y. Lee · G. Qi · H. Shimizu · Z. Song · L. Wang · X. Xu
Y. Yong · P. Zhang · Y.-H. P. Zhang · J. J. Zhong

Springer

Editor
Jian-Jiang Zhong
State Key Laboratory of Microbial Metabolism
School of Life Sciences and Biotechnology
Shanghai Jiao Tong University
Shanghai
People's Republic of China

ISSN 0724-6145 ISSN 1616-8542 (electronic)
ISBN 978-3-642-36507-2 ISBN 978-3-642-36508-9 (eBook)
DOI 10.1007/978-3-642-36508-9
Springer Heidelberg New York Dordrecht London

Library of Congress Control Number: 2013931219

Printed on acid-free paper

Springer is part of Springer Science+Business Media (www.springer.com)

Preface

The title of this volume may appear a bit too ambitious to some readers. Biotechnology has been developing so fast in recent decades and has had a great impact on our life and society by addressing various problems including environmental pollution, ecological protection, energy issues, and public health. It is therefore almost impossible for a single volume to provide topics covering the current development and future trends in all aspects of biotechnology. Nevertheless, for this volume we have selected a number of interesting topics from a few important areas of biotechnology. These contributions are based on talks which were held at the 1st Asian Congress on Biotechnology (ACB) in 2011 which was organized under Asian Federation of Biotechnology (AFOB) (http://www.afob.org/) [1] to acknowledge the significant advances in biotechnology innovation and applications.

In order to establish a sustainable society, not reliant on using fossil resources, bioconversion technologies which turn biomass resources into valuable materials have received great attention in recent years. To improve cellular properties for high productivity and high yield production of desired products, the metabolic engineering approach is very useful [2]. Here, optimization of metabolic pathways of cells and creation of stress tolerant cells are important [3]. Prof. Hiroshi Shimizu and his coworkers from Osaka University describe multi-omics information analyses and rational design methods for molecular breeding ("Systems Metabolic Engineering: The Creation of Microbial Cell Factories by Rational Metabolic Design and Evolution").

Recent studies indicate that bacteria usually coordinate their behaviors at population level by producing, sensing, and responding to small signal molecules. This so-called quorum sensing regulation enables bacteria to live in a 'society' with cell–cell communication, and controls many important bacterial behaviors [4]. Profs. Jian-Jiang Zhong and Yang-Chun Yong from Shanghai Jiao Tong University and Jiangsu University review quorum sensing signals and their impacts on microbial metabolism and human health ("Impacts of Quorum Sensing on Microbial Metabolism and Human Health"). Quorum sensing plays an important role both in bacteria

directly and human beings, and a better understanding of this phenomenon would lead to better control of bacteria.

The next two chapters are related to biomanufacturing, which is defined as the manufacture of desired products using living biological organisms (e.g., bacteria, yeasts, animal cells) or some components from one or several biological organisms [5]. Chinese hamster ovary (CHO) cells are the current industrial workhorse for manufacturing the majority of leading recombinant biologics. Glycosylation is an important characteristic of CHO cells, which decorate protein or lipid backbones by carbohydrate moieties, leading to a wide range of bioactive end products. Dr. Zhiwei Song and his colleagues from the Bioprocessing Technology Institute of Singapore describe CHO glycosylation mutants as potential host cells to produce therapeutic proteins with enhanced efficacy ("CHO Glycosylation Mutants as Potential Host Cells to Produce Therapeutic Proteins with Enhanced Efficacy"). In light of the critical impact of glycosylation on biopharmaceutical performances (safety and efficacy), the CHO glycosylation mutants have enormous potential in producing glycoprotein therapeutics with optimal glycosylation profiles, which result in improved safety profile and enhanced efficacy [6].

Another type of biomanufacturing platform is the cell-free biosystem, which is very different from those of the above three chapters. Prof. Y.-H. Percival Zhang and Mr. Chun You from Virginia Tech summarize cell-free biosystems for biomanufacturing ("Cell-Free Biosystems for Biomanufacturing"). Cell-free biosystems are becoming an emerging biomanufacturing platform in the production of low-value biocommodities, fine chemicals, and high-value protein and carbohydrate drugs and their precursors. They believe that cell-free biosystems could become a disruptive technology to microbial fermentation, especially in the production of high-impact low-value biocommodities. This is mainly due to very high product yields and potential low-production costs [7].

"Lipid Bilayer Membrane Arrays: Fabrication and Applications" is a contribution describing the lipid bilayer of biomembranes, which is a universal component of all cell-based biological systems, forming the barrier between cytosol and the cell's exterior, as well as mediating many biological functions by providing a defined interface for cell-surface recognition, signaling, and transport. The importance of the lipid bilayer has raised much interest in fabricating artificial membrane as both free standing lipid membranes and solid supported lipid bilayer membranes. Prof. Xiaojun Han and his coworkers from the Harbin Institute of Technology describe the formation of bilayer lipid membrane arrays. The applications of lipid bilayer arrays are reviewed in the account of biosensors, protein binding studies, and lipid bilayer-based 2D electrophoresis [8].

The last chapter is about RNA aptamers, which are RNA molecules binding target molecules. Those small oligonucleotides derived from the in-vitro selection process are important candidates for therapeutics and diagnostics due to their high affinity and specificity against their target molecules. Prof. Yoon-Sik Lee and Dr. Kyung-Nam Kang from Seoul National University summarize recent trends and applications of RNA aptamers ("RNA Aptamers: A Review of Recent Trends and Applications"). As the global market for aptamers is expected to grow (about

$1.8 billion by 2014), research into the therapeutic and diagnostic applications of RNA aptamers seems to be increasing continuously [9].

Finally, I would like to thank all the authors for their excellent contributions to this book. The kind advice from Professor Thomas Scheper and great assistance from Ms. Karin Bartsch (Project Coordinator), Ms. Elizabeth Hawkins (Editor Chemistry), and other related staff at Springer are certainly appreciated. I do hope readers will enjoy this volume and provide suggestions and comments to me and the other authors.

Shanghai, 2012 Jian-Jiang Zhong

References

1. Asian Federation of Biotechnology. Asian Congress on Biotechnology, http://www.afob.org/
2. Nielsen J (ed) (2005) Biotechnology for the future. Advances in biochemical engineering/biotechnology, vol 100. Springer, Heidelberg.
3. Furusawa C, Horinouchi T, Hirasawa T and Shimizu H (2013) Systems metabolic engineering: the creation of microbial cell factories by rational metabolic design and evolution. Adv Biochem Eng Biotechnol 131:1–23
4. Yong Y-C, Zhong J-J (2013) Quorum sensing and its impact on microbial metabolism and human health. Adv Biochem Eng Biotechnol 131:25–61
5. Zhong JJ, (ed) (2004) Biomanufacturing. Advances in biochemical engineering/biotechnology, vol 87. Springer, Heidelberg.
6. Zhang P, Chan KF, Haryadi R, Bardor M and Song Z (2013) CHO glycosylation mutants as potential host cells to produce therapeutic proteins with enhanced efficacy. Adv Biochem Eng Biotechnol 131:63–87
7. You C, Zhang Y-HP (2013) Cell-free biosystems for biomanufacturing. Adv Biochem Eng Biotechnol 131:89–119
8. Han X, Qi G, Xu X, Wang L (2013) Formation of bilayer lipid membrane arrays and its application. Adv Biochem Eng Biotechnol 131:121–152
9. Kang K-N and Lee Y-S (2013) RNA aptamers: recent trends and applications. Adv Biochem Eng Biotechnol 131:153–169

Contents

Adv Biochem Eng Biotechnol (2013) 131: 1–23
DOI: 10.1007/10_2012_137

Published Online: 27 June 2012

Systems Metabolic Engineering: The Creation of Microbial Cell Factories by Rational Metabolic Design and Evolution

Chikara Furusawa, Takaaki Horinouchi, Takashi Hirasawa and Hiroshi Shimizu

Abstract It is widely acknowledged that in order to establish sustainable societies, production processes should shift from petrochemical-based processes to bioprocesses. Because bioconversion technologies, in which biomass resources are converted to valuable materials, are preferable to processes dependent on fossil resources, the former should be further developed. The following two approaches can be adopted to improve cellular properties and obtain high productivity and production yield of target products: (1) optimization of cellular metabolic pathways involved in various bioprocesses and (2) creation of stress-tolerant cells that can be active even under severe stress conditions in the bioprocesses. Recent progress in omics analyses has facilitated the analysis of microorganisms based on bioinformatics data for molecular breeding and bioprocess development. Systems metabolic engineering is a new area of study, and it has been defined as a methodology in which metabolic engineering and systems biology are integrated to upgrade the designability of industrially useful microorganisms. This chapter discusses multi-omics analyses and rational design methods for molecular breeding. The first is an example of the rational design of metabolic networks for target production by flux balance analysis using genome-scale metabolic models. Recent progress in the development of genome-scale metabolic models and the application of these models to the design of desirable metabolic networks is also described in this example. The second is an example of evolution engineering with omics analyses for the creation of stress-tolerant microorganisms. Long-term culture experiments to obtain the desired phenotypes and omics analyses to identify the phenotypic changes are described here.

Keywords Systems Biotechnology · Strain improvement · Constraint-based flux balance analysis · Experimental evolution

C. Furusawa · T. Horinouchi · T. Hirasawa · H. Shimizu (✉)
Department of Bioinformatic Engineering, Osaka University, 1-5 Yamadaoka, Suita Osaka, 565-0871, Japan
e-mail: shimizu@ist.osaka-u.ac.jp

Contents

1 General Introduction

Microorganisms are used as cell factories for producing valuable chemical compounds such as various primary and secondary metabolites [5, 43, 53, 55, 65] and recombinant proteins [62, 67], all of which play important roles in the pharmaceutical, chemical, and agricultural industries. One of the goals of microbial cell factory development is the establishment of cheap and high-yield bioprocesses to meet commercial requirements. To achieve this, modifications of the metabolic system of the host microorganism are typically required to improve the productivity of target products. This is because the metabolic systems of natural microorganisms are already tuned to optimize their growth in their natural habitat [83]. To acquire the cellular properties necessary for achieving high productivity and high production yield of the target product, the microorganism can be tailored so that it has the following two characteristics [81]. First, the metabolic system of the microorganism should be optimized to maximize production yield and eliminate byproduct formation. Moreover, the balance of coenzyme production and consumption—for example, the recycling of adenosine triphosphate (ATP) and nicotinamide adenine dinucleotide (NAD)—should also be designed so that optimal target production yield is achieved [16, 60, 101]. Second, the cells should be able to tolerate the environmental stresses encountered during the production process. Such environmental stresses include exposure to acids, high/low temperature, high osmotic pressure, and so forth—all of which can reduce cellular growth and target productivity. Therefore, tolerance to environmental stresses is essential for improving bioprocesses [3, 12, 44, 114]. Classical strain improvement techniques have traditionally been used to modify metabolic systems and achieve the desired properties. For example, microorganisms with superior production capabilities have been developed through random mutagenesis following appropriate screening procedures [80]. The properties of metabolic systems have also been improved by molecular biology techniques, resulting in increased target productivity. However,

conventional approaches have not always been successful due to unexpected changes in the metabolic systems caused by various perturbations. Such unexpected responses could arise from the complexity of intracellular systems in which networks of metabolites, genes, and proteins are interconnected to form multi-hierarchical complex networks. Thus, for the rational design of microbial metabolic systems suitable for bioproduction, proper understanding of the systems is necessary.

Recent advances in experimental techniques have facilitated the comprehensive analysis of different cellular states. Vast amounts of omics data are now available, which have improved our understanding of cellular processes [6, 8, 106, 115]. For example, rapid developments in sequencer and DNA handling technologies have allowed routine sequencing of the whole genome of microorganisms [15, 52, 54]. The availability of such rapid and inexpensive genome sequencing technology has had a great impact on the analysis of genotype-phenotype relationships; for example, it has enabled the identification of mutations responsible for specific phenotypes such as stress tolerance [11]. Similarly, comprehensive gene expression analysis by microarrays and protein expression analysis by 2D electrophoresis or mass spectroscopy have provided detailed information on the cellular state and its dynamics [2, 40–42, 99]. Therefore, it is reasonable to expect that appropriate integration of these high-throughput omics data would yield a system-level understanding of complex cellular processes and that this would lead to a new era of biotechnologically useful microorganisms capable of high productivity of target products [22, 33, 63, 69, 81, 84].

In this review, we present two recent approaches in systems biotechnology. Both studies are based on omics data analysis and are aimed at strain improvement for the purpose of bioproduction. The first approach is constraint-based flux balance analysis using genome-scale metabolic models [77]. This allows the prediction of metabolic profiles of microorganisms by in silico simulations and permits the screening of candidate genes that may be manipulated to improve target productivity [30]. The second approach is strain improvement through experimental evolution [87]. After obtaining the evolved microbial strains, omics analysis can be used to analyze genetic/phenotypic changes that have occurred in the evolutionary process. This analysis provides an in-depth understanding of cellular processes, such as the mechanism of stress tolerance. Such systems analyses provide new information on metabolic systems and in turn facilitate the engineering of strains suitable for industrial applications.

2 Genome-Scale Metabolic Models for Strain Improvement

2.1 Introduction

Each microorganism differs in terms of its metabolic capabilities for producing target metabolites because each has evolved for survival in its natural habitat. Therefore, when using microorganisms to produce valuable metabolites, it is often necessary to

retrofit the metabolic system of the host to obtain the desired phenotype. Genetic engineering techniques permit the modification of metabolic systems through the addition or deletion of genes responsible for metabolic reactions. Engineered microorganisms can be obtained through such gene modifications, and these can be used to improve the productivity of target products. This approach is referred to as the metabolic engineering approach [59, 100]. However, due to the complexity of the metabolic system, it is still difficult to "design" an appropriate metabolic network by gene modifications. For example, several key metabolites such as ATP, NADH, and glutamate act as "hubs" of complex metabolic networks, and the effects of local perturbations by gene modifications on the metabolic network can be propagated throughout the network by these key metabolites [14]. Therefore, to design a metabolic network with high productivity, metabolic systems must be analyzed as a whole, which would require huge inputs in terms of experiments, knowledge, and intuition. Against this background, it is evident that to accelerate strain improvement by metabolic engineering, it would be highly desirable to use genome-wide in silico simulations to predict the metabolic state after genetic modification and under varying environmental conditions.

Recently, on the basis of whole-genome information, genome-scale metabolic networks of cells have been reconstructed for many organisms, including representatives of each of the three major domains of life, namely, archaea [35], bacteria [36, 73, 75, 95], and eukarya [28, 29, 94]. At present, more than 50 genome-scale metabolic reconstructions have been published [72]. Using genome-scale metabolic models, it is possible to reliably estimate metabolic fluxes by the flux balance analysis (FBA) method [34, 76, 77]. FBA is an analysis of metabolic flux profiles in which a steady state of metabolic flux is assumed, and the profile of metabolic fluxes is calculated by optimizing an objective function using linear programming. Although genome-scale metabolic models cannot compute the detailed kinetic dynamics of metabolic reactions in a cell, they permit the description of a range of possible metabolic states on the basis of constraints defined by the stoichiometry of metabolic reactions and transport steps at the steady state. It is also possible to obtain a solution (i.e., a set of all metabolic fluxes) that maximizes or minimizes an objective function using linear programming. The biomass production rate is generally adopted as the objective function. The metabolic profiles calculated by the maximization of biomass production can describe those obtained experimentally in many organisms and under various environmental conditions, suggesting that organisms can maximize their growth rate by adaptation and evolution [38, 46]. By using the appropriate genome-scale metabolic network and objective function to be maximized, FBA can be used to predict the relationship between the genotype, environmental conditions, and product yields at the steady state; this data can then be used to improve microbial production [3, 61].

In the next section, we focus on in silico metabolic simulations using genome-scale metabolic models and experimental evaluations. We also address the possible applications of model prediction to metabolic engineering.

2.2 Reconstruction of Genome-Scale Metabolic Models

In general, genome-scale metabolic models of target organisms have been manually built by the following two steps. First, a draft metabolic model is constructed based on public databases such as KEGG [51] and the BioCyc database collection [21], which collects metabolic reactions occurring in the target organism based on gene annotation data. Second, the draft model is further tuned based on available literature because a draft model constructed using only public databases generally contains incorrect and insufficient metabolic pathways due to the incompleteness of database information. The most frequently observed problem is that of missing enzymes in metabolic pathways producing essential components. Therefore, the resulting network is next subjected to the gap-filling process to adequately represent cellular growth [103]. To fill the gaps, data from literature and homology search results of genomes that are closely related to the target organism are generally used. In some cases, metabolic reactions are added to the metabolic model without any background information to realize cellular growth. It should be noted that the benefit of the gap-analysis process is that it can provide indicators of missing enzymes, i.e., enzymes that probably exist in the target organism but have not been identified. After the construction of the metabolic network, to calculate metabolic fluxes as presented below, it is converted into a stoichiometric matrix SS containing the stoichiometry of all reactions in the network. If a given network is composed of m molecular species involved in n reactions, then the stoichiometry matrix is an $m \times n$ matrix. The element S_{ij} of the stoichiometric matrix represents the contribution of the jth reaction to the ith metabolite.

In addition to reconstructing the metabolic network of a target organism, several parameters representing cellular processes are also necessary for in silico simulations using the genome-scale metabolic model [103]. One such essential parameter is the coefficient of the biomass synthesis reaction. This reaction is hypothetical and represents the requirements of precursors and coenzymes for biomass formation. Biomass synthesis involves the linear combination of dozens of components, including amino acids, DNA, RNA, lipids, and cell envelope components. In general, the biomass composition is determined from reported cellular data such as the compositions of amino acids and other macromolecules (DNA, RNA, protein, lipids, and so forth). Other important parameters that are representative of cellular processes, such as the ATP maintenance costs and P/O ratio, are also determined from the reported data. In the FBA scheme, the reconstructed genome-scale metabolic model and parameters for cellular processes are used to estimate the metabolic flux profiles by the linear algebra-based method presented below.

2.3 Constraint-Based Flux Analysis

Detailed information on the kinetic parameters of enzymatic reactions is unavailable at the genome-scale level; therefore, in silico simulations of the kinetic behavior of metabolic reactions have been difficult so far. Instead, in the FBA

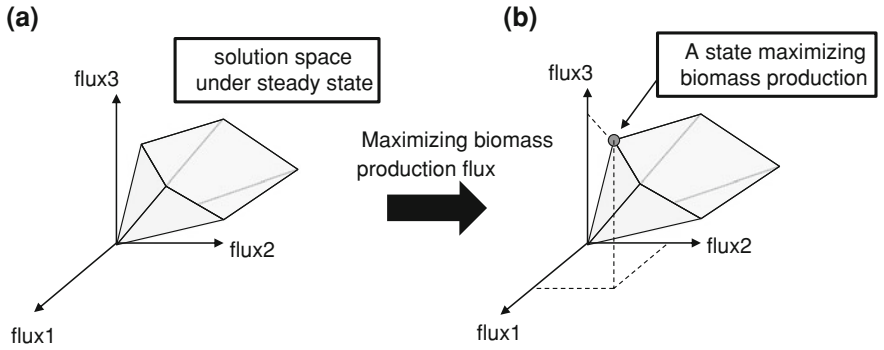

Fig. 1 Schematic representation of the constraint-based flux balance analysis. The axes represent metabolic fluxes. **a** By applying the steady state assumption, we can obtain the feasible solution space. **b** If the biomass production flux is used for an objective function, optimal solutions that maximize the objective function can be calculated by linear programming

scheme, the metabolic flux profile is determined by employing the following assumptions [30].

The first is the steady state assumption in which the concentrations of all metabolites are assumed to remain unchanged over time. In other words, the net sum of all production and consumption fluxes for each internal metabolite is set to zero. This assumption results in a feasible space that is a convex set in the N-dimensional space of metabolic fluxes (where N represents the total number of fluxes), as schematically shown in Fig. 1a. This steady state assumption can be mathematically represented as $S \cdot v = 0$, where S is the stoichiometric matrix and v is a vector of fluxes through the metabolic network. Furthermore, upper and lower bounds are generally employed and are mathematically represented as $v_{\min} \leq v \leq v_{\max}$, where $v_{\min}$ and $v_{\max}$ indicate the minimum and maximum constraints on the fluxes. These bounds of fluxes are used to define the constraints for the maximal enzymatic rate, irreversibility of the reaction, or constant uptake from the environment.

Based on the steady state assumption, the possible flux profile is bound within a closed finite space. However, it is not possible to determine a unique solution for the flux profile by employing only the steady state assumption. Therefore, to determine the flux profile, the second assumption (i.e., maximization or minimization of an objective function) is generally used to obtain a unique solution. The most popular objective function in FBA for obtaining the metabolic flux profile is the biomass synthesis flux, which is represented as a linear combination of metabolic fluxes of building blocks and coenzymes required for biomass synthesis, as mentioned above. Mathematically, maximization of the biomass synthesis flux is solved by linear programming, which corresponds to obtaining the optimal solution at one corner in the feasible flux space (Fig. 1b). This assumption for maximizing biomass synthesis flux is based on the understanding that organisms have evolved toward growth maximization under a given environment. Other objective functions are also used to estimate the metabolic flux profile. For example, to

calculate the metabolic shift after knocking out a metabolic reaction, the Euclidian distance to the wild-type flux profile is often used as an objective function that has to be minimized [93]. Minimization of regulatory on–off switching is also used to predict metabolic changes after gene knock-out [97].

2.4 Example: Flux Balance Analysis of Corynebacterium Glutamicum

For more detailed examination of the processes of reconstruction and experimental verification of genome-scale metabolic models, we study the flux balance analysis of *Corynebacterium glutamicum* as an example [95].

C. glutamicum is a facultatively aerobic, gram-positive bacterium that can grow on various sugars or organic acids [53, 105]. This organism shows high-efficiency production of various amino acids such as glutamate and lysine and is thus widely used for the large-scale production of amino acids [57]. The production of ethanol and organic acids such as lactate and succinate by *C. glutamicum* under oxygen deprivation conditions has been recently proposed [74]. Because of its importance in bioproduction, *C. glutamicum* is an interesting microbial host for metabolic engineering purposes. Therefore, it is highly desirable to construct and explore appropriate in silico metabolic models that can help to predict both cellular behavior and target compound production by this organism.

A genome-scale metabolic model of *C. glutamicum* was developed earlier [95], which can be described as follows. First, a draft model of this microorganism was constructed by collecting metabolic reactions from public databases such as BioCyc and KEGG as well as scientific publications. After performing the gap-filling procedure based on published data and a homology search with genomes of closely related species, a genome-scale metabolic model consisting of 277 genes, 502 metabolic reactions, and 423 metabolites was constructed. Of the total reactions, 428 from the BioCyc and KEGG database collections were included in the model, while the remaining 74 were added based on previously published studies. From the entire set of metabolic reactions, 470 corresponded to intracellular reactions, while 32 were fluxes for transport through the membrane. The biomass synthesis reactions consisted of linear combinations of 43 components, including amino acids, DNA, RNA, lipids, and cell envelope components. The biomass composition was determined from reported data; for example, the requirements of precursors such as pyruvate, acetyl-CoA, and oxaloacetate for biomass production were based on previously reported data [31]. The macromolecular composition was also determined from earlier studies [20]; the total biomass was 52 % protein, 5 % RNA, 1 % DNA, 13 % lipid, 19 % cell wall components, and 10 % other components. *C. glutamicum* cells have a characteristic cell membrane called MAPc that consists of mycolic acids and the polysaccharides peptidoglycan and arabinogalactan. The pathway for the synthesis of this membrane structure was

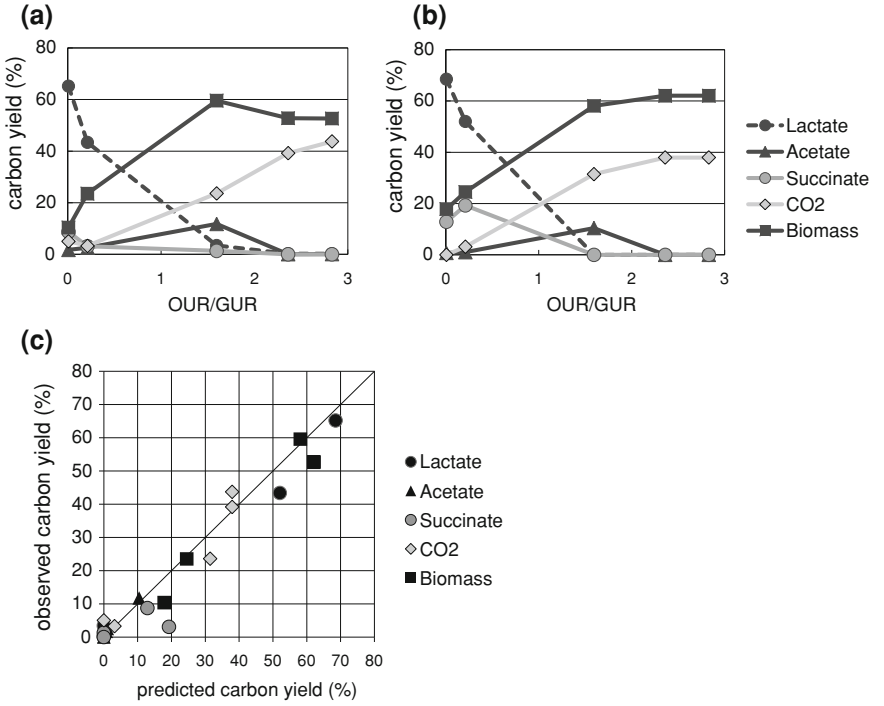

Fig. 2 Changes in the yields of organic acids, biomass, and carbon dioxide when the OUR/GUR ratio is altered. **a** Experimental results with different OUR/GUR ratios. GUR, OUR, and the production rates of CO_2, lactate, acetate, succinate, and biomass are represented in mmol/gDW/h. The values in parentheses represent the carbon yields. **b** Predictions by FBA simulations. The simulation results were obtained using the GUR and OUR values from the experimental data. **c** A scatter plot of carbon yield. The *x*-axis corresponds to the result of FBA simulation, while the *y*-axis shows the experimentally observed carbon yield. The carbon yields in the five sets of experimental and simulation results are presented. The line corresponding to $y = x$ is also shown

included in the model, while the MAPc demand in biomass production was regarded to be consistent with the cell wall composition of *C. glutamicum*.

In general, the reconstructed metabolic models and in silico simulations by these models should be verified experimentally. To construct a genome-scale metabolic model of *C. glutamicum*, a series of culture experiments were performed under different environmental conditions. In the study, the oxygen uptake rate (OUR) was used as the parameter for changing the metabolic profiles of *C. glutamicum*. This is because OUR is known to drastically alter the metabolic profile and is a key factor controlling the productivity of various compounds, such as organic acids, by the microorganism. Culture experiments with five different OURs were performed, and the glucose uptake rate (GUR), OUR, and production rates of CO_2 and organic acids were quantified, as summarized in Fig. 2a. The experimental results showed that under anaerobic and microaerobic conditions (i.e., under conditions of low OUR/GUR ratios), the cells converted most of the

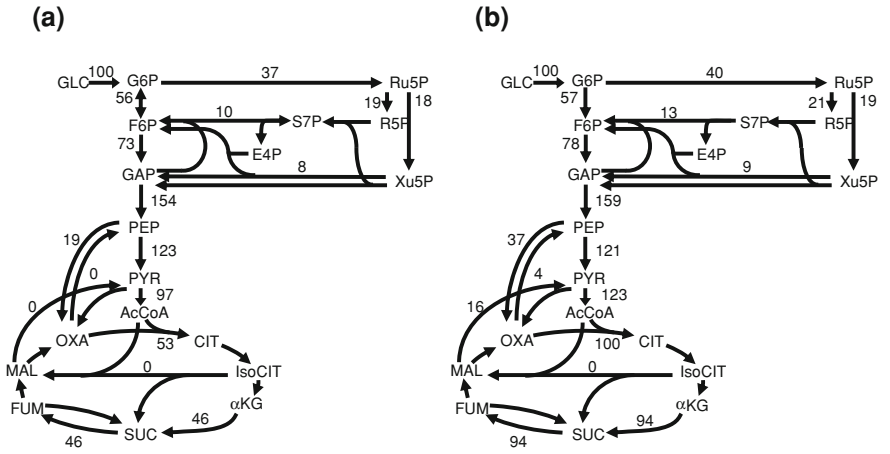

Fig. 3 Metabolic flux profiles of *C. glutamicum* in the exponential growth phase. **a** The metabolic fluxes obtained from the ^{13}C-tracer experiment [96] and **b** simulated metabolic fluxes. The simulation result was obtained by FBA with maximized biomass production flux and using the experimentally observed values of the OUR and GUR parameters. Abbreviations are as follows: *E4P*, erythrose-4-phosphate; *6PG*, 6-phospho-d-gluconate; *Xu5P*, xylulose-5-phosphate; *Pyr*, pyruvate; *F6P*, fructose-6-phosphate; *GAP*, glyceraldehyde-3-phosphate; *R5P*, ribose-5-phosphate; *Ru5P*, ribulose-5-phosphate; *S7P*, sedoheptulose-7-phosphate; *G6P*, glucose-6-phosphate; *LYS*, lysine; *Suc*, succinate; *Cit*, citrate; *IsoCit*, isocitrate; *aKG*, α-ketoglutarate; *MAL*, malate; *FUM*, fumarate; *OAA*, oxaloacetate

glucose to organic acids such as lactate and succinate. As the OUR/GUR ratio increased, the cells altered their metabolism to produce acetate, and a further increase in the OUR/GUR ratio resulted in a metabolic shift to a CO_2 production phase in which the tricarboxylic acid (TCA) cycle was activated.

The results from the FBA simulations using the genome-scale model of *C. glutamicum* were evaluated using the experimental data summarized in Fig. 2a. In these simulations, maximization of the biomass synthesis flux was used as the objective function of FBA. The production yields of organic acids, CO_2, and biomass were calculated by the FBA scheme using the experimentally obtained OUR and GUR values as parameters. The predicted yields are shown in Fig. 2b. Moreover, a scatter plot of carbon yields in 5 sets of experimental and simulation results is shown in Fig. 2c. The predictions of the genome-scale model with maximization of the biomass yield agreed well with the experimentally obtained yields, as shown in Fig. 2c. For example, the FBA simulation predicted that 10 % of the carbon would be secreted as acetate when OUR/GUR $\sim$1.5, which is a value consistent with the experimental results.

To evaluate the accuracy of the predictions by FBA simulations in greater detail, the fluxes estimated by FBA were compared with those obtained in a ^{13}C-tracer experiment [96]. Here, the metabolic profile of exponentially growing *C. glutamicum* under aerobic conditions was used as a reference. The GUR and OUR values were set to those measured experimentally. As shown in Fig. 3, the

predicted flux for the pentose phosphate pathway (PPP) was quite similar to the experimentally observed flux. However, in the anaplerotic and gluconeogenetic pathways—i.e., in pathways where phosphoenolpyruvate is converted to/from oxaloacetate, pyruvate to oxaloacetate, and malate to pyruvate—there appeared to be a discrepancy between the predicted and experimentally obtained results. This was because a cycle of metabolic flux in the anaplerotic and gluconeogenetic pathways does not affect biomass production in the FBA simulation. Therefore, these fluxes were undetermined. However, comparison of the net fluxes from phosphoenolpyruvate/pyruvate to oxaloacetate/malate, which can be uniquely determined by biomass production maximization, revealed that the predicted and experimentally obtained fluxes were quite similar (19.5 in the FBA simulation and 18 in the experiment). The good agreement between the simulations and experimental results strongly suggests that the metabolic profiles of exponentially growing cells can be predicted by our genome-scale model with maximization of the biomass production rate.

Because the in silico prediction of the metabolic profile presented here showed relatively high accuracy, it should be possible to use this for the in silico screening of candidate genes that may be manipulated to improve the productivity of target products. Such in silico screening of gene manipulation candidates would drastically reduce the experimental costs of strain improvement; in fact, this procedure has already been applied to the production of several target metabolites. For example, gene deletion targets for improved lactate productivity were screened using the genome-scale model of *C. glutamicum* [95]. The screening results suggested that the disruption of the succinate production pathway is important for lactate overproduction. Furthermore, the simulation result suggested that the disruption of reactions involved in oxidative phosphorylation increased the lactate production rate. This was due to an increase in demand for NADH oxidation caused by the disruption of oxidative phosphorylation, which resulted in an increase in lactate production for NADH oxidation. Additionally, disrupting some reactions in the PPP resulted in an increase in lactate production, which was due to a decrease in NADPH synthesis in the PPP. Therefore, to compensate for NADPH production, which is required for cell growth, the reaction from malate to pyruvate, catalyzed by malic enzyme, was activated. The simulation results indicated that the increased pyruvate was then converted to lactate. Although these predictions have not been experimentally verified, the screening results can provide valuable information for strain improvement.

2.5 Future Direction

Reliable predictions of the genome-scale metabolic profile allow systematic screening of candidate genes whose manipulation can result in improvement of the target productivity [23, 107]. For example, lycopene productivity by *Escherichia coli* cells was successfully increased by constraint-based flux prediction using the

genome-scale metabolic model [4]. In another example, a comparative analysis of genome-scale metabolic models of *E. coli* and succinic acid-overproducing *Mannheimia succiniciproducens* was performed to enhance succinate productivity by *E. coli*. The comparison provided several candidate genes for disruption, and succinate productivity was increased more than 7-fold by the predicted manipulations [61]. Computational tools for the screening of gene disruption targets have also been extensively developed. For example, Optknock is a method that predicts optimal combinations of gene knock-outs leading to the overproduction of chemicals of interest in a metabolic network [19]. Several variant methods such as OptStrain [85] and RobustKnock [102] as well as successful applications [37, 70] have also been presented. These tools are expected to accelerate the application of genome-scale simulations in the field of systems metabolic engineering.

It is apparent that further development of a metabolic simulation method to improve the productivity of target metabolites is highly desirable. One promising approach to refine the genome-scale metabolic model is to combine multi-omics data with metabolic simulations. For example, it has been demonstrated that incorporating gene regulatory information from transcriptome data can improve the prediction accuracy of FBA simulations [1]. To increase valine and threonine production by *E. coli*, the target genes to be engineered were successfully identified by genome-scale metabolic simulations using transcriptome profiling data [60, 81]. A toolbox to integrate expression data and gene regulatory networks into the metabolic simulation also had been developed [50]. Such metabolic simulations based on multi-omics data will play an increasingly important role in the development of systems metabolic engineering.

Another important expansion of the study using the genome-scale metabolic model is pathway analysis. For example, elementary mode analysis [90–92] and extreme pathway analysis [56, 78, 79, 88] are useful metabolic pathway analysis tools to extract valuable information based on the structure of a metabolic network. These analyses can identify independent pathways that are inherent in a metabolic network. These pathways can represent independent physiological state and thus they can support the operation of cellular metabolism. This decomposition of metabolic network is useful for network design. For example, the efficient metabolic network of *E. coli* that produce ethanol from hexoses and pentoses were designed based on the elementary mode analysis [104]. These analyses also provide the key aspects of the metabolic systems, including network functionality, robustness and gene regulations, based only on the topologies of the network. It is expected that, with the appropriate integration with multi-omics data, this approach based on the topological features of networks can accelerate the prediction accuracy of metabolic systems.

Furthermore, the advancements of synthetic biology can greatly contribute to the metabolic design for the bio-productions. Synthetic biology aims to provide a design principle of biological systems analogous that is to artificial machines, which consist of well-characterized parts; their total behavior is predictable as the sum of these parts [86]. In synthetic biology, many parts in biological systems—including genes, proteins, and well-characterized interactions between

them—are used to construct a cell or cell-system with desired behavior [7, 32]. De novo reaction pathways are also prepared to realize a desired system. Such assemblies of biological parts to design a metabolic system can accelerate systems metabolic engineering. For example, the productions of biofuels by *E. coli* by introducing non-native reaction pathways and de novo pathway design have been extensively studied [25], including the production of ethanol [113], 1-butanol [47], and isobutanol [10], and so forth. Such integration of metabolic engineering, systems biology, and synthetic biology will open the door to a new era of biotechnology.

3 Experimental Evolution for Strain Improvement

3.1 Introduction

An important factor in improving bioproduction is the preparation of microbial strains suitable for the desired production process. Molecular biology has provided tools for altering cellular processes by genetic modifications, which allows the design of suitable strains for bioengineering. However, due to the complex nature of intracellular reaction networks, the appropriate design of cellular activity is still challenging. Although algorithms and modeling frameworks have been developed to predict effective genetic changes, as mentioned in the previous section, more information is required to guide complete strain design. In fact, the side effects of gene manipulation are generally unpredictable, which complicates the rational design of strains.

One possible strategy for obtaining the desired strain is a discovery approach based on high-throughput screening [80]. The combination of variant preparation and screening with the appropriate phenotype allows the creation of useful microbial strains. In fact, the use of random mutagenesis and direct selection has been successful in industrial strain development for decades [18, 27, 71, 98, 108], particularly in the absence of genome or other omics information. These mutagenesis approaches are well suited for obtaining feedback inhibition in biosynthetic pathways because simple selection schemes can be applied based on resistance to toxic analogs of intermediates. However, there are two disadvantages to this strategy of mutagenesis with relatively high mutation rates and high-throughput screening. First, it is generally difficult to identify the mechanisms behind the desired phenotype because multiple genetic and phenotypic changes occur simultaneously during mutagenesis. Without understanding the mechanisms, it is impossible to transfer the obtained phenotype to other strains, even though such transfer of the desired phenotype could accelerate further strain improvement. Second, mutagenesis with a high mutation rate and selection is generally concomitant with the accumulation of unfavorable mutations, which can result in highly specialized but fragile strains for bioproduction.

An alternative approach is experimental evolution in which numerous cycles of mutation and selection are employed. In such a process, the mutation rate can be maintained at a low or moderate level. A cell that achieves high selective advantage by mutations increases its relative abundance and eventually takes over the entire population. Iteration of such takeover events could result in a population in which beneficial mutations are enriched but deleterious mutations are avoided. Furthermore, because gradual phenotypic changes would lead to a higher fitness state, it is expected that the mechanisms responsible for such high fitness can be identified by techniques such as high-resolution omics approaches. For example, pioneering studies by Lenski demonstrated that long-term culture of *E. coli* resulted in significant phenotypic changes, and the mechanisms responsible for these phenotypic changes were partially identified by whole-genome resequencing and other omics analysis [15, 64]. Palsson and colleagues studied the experimental evolution of *E. coli* under conditions in which several carbon sources were used, and they identified mutations responsible for the activation of glycerol and lactate assimilation [26, 38]. Experimental evolution has also been used to study stress tolerances developed under ethanol [45, 112] and isobutanol [11] stress conditions. Furthermore, experimental evolution under conditions that allow the use of a nonnative carbon source was also studied with *E. coli* cells [58]. It is important to note that in these studies, the mechanisms for the achievement of fitness advantage were intensively and systematically studied. Information from such studies has allowed the rational design of improved strains for bioengineering.

3.2 Example: Experimental Evolution of E. coli Under Ethanol Stress

To examine the process of experimental evolution in greater detail, we present the transcriptome analysis of parallel-evolved *E. coli* strains under ethanol stress; the results have provided partial understanding of the mechanism of ethanol tolerance of this microorganism [45].

E. coli cells are widely used for the production of useful materials such as amino acids, enzymes, biofuels, and biopolymers [9, 13, 17, 24, 49, 66, 82, 109–111]. Use of this microorganism in the production of biofuels from biomass resources has increased its importance in recent times [89]. During ethanol production by *E. coli*, ethanol itself acts as a major stress factor that interferes with growth and ethanol production. Thus, developing ethanol tolerance in *E. coli* strains is important for improving ethanol production.

To obtain strains tolerant to ethanol stress and to understand the mechanisms behind it, a series of experimental evolution and transcriptome analysis studies were performed on the tolerant strains obtained. Fig. 4a presents the schematic procedure of the experimental evolution setup used. In this case, six independent series of evolution experiments were performed under 5 % ethanol stress; these

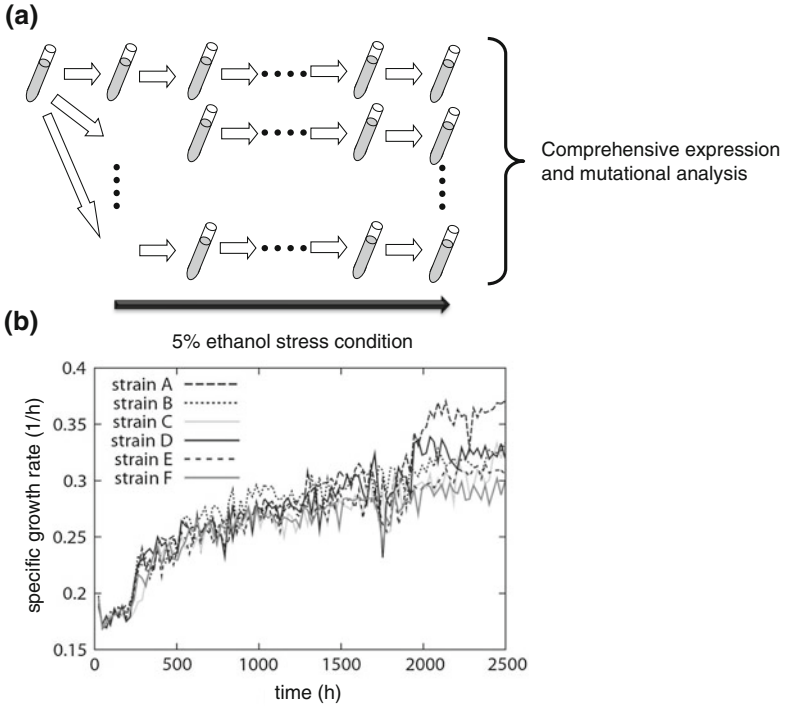

Fig. 4 **a** Schematic representation of the procedure used for the experimental evolution of *E. coli* under 5 % ethanol stress condition. Cells were diluted into fresh medium containing 5 % ethanol every 24 h. The cells were maintained in the exponential growth phase by adjusting the initial cell concentration of each dilution. **b** The time course of specific growth rates in the evolution experiments performed under 5 % ethanol stress. Six parallel series of experiments were performed starting from the same parent strain

were carried out by serial transfer of an aliquot of culture to fresh M9 synthetic medium containing ethanol every 24 h. Fig. 4b shows the change in the specific growth rates in these evolution experiments under 5 % ethanol stress. As shown in the figure, the specific growth rates gradually increased, resulting in an approximately 2-fold increase in comparison with the parental strain. It was confirmed that the phenotype of the evolved strains, i.e., higher growth rate under ethanol stress, was stable after cultivating the cells for more than 100 generations (144 h) in M9 medium without ethanol.

To analyze the phenotypic changes that occurred during adaptive evolution to ethanol stress, microarray expression analyses of the parent strain (named P) and six tolerant strains (named strains A–F in descending order of the final growth rate) were performed in M9 medium with or without 5 % ethanol. Because many expression profiles had to be analyzed, principal component analysis (PCA) was used to represent the changes in the expression levels. Figure 5 shows the PCA results of these 14 expression profiles. The data points corresponding to the addition of ethanol

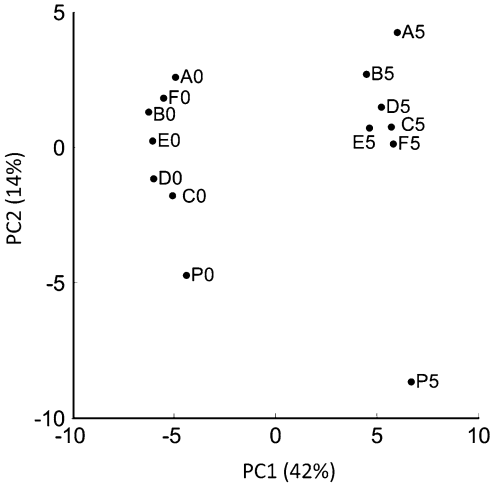

Fig. 5 The PCA score plot of PC1 versus PC2. P0 and A0–F0 represent the expression profiles of strain P and tolerant strains A–F obtained without ethanol addition, respectively. P5 and A5–F5 show the data for the 5 % ethanol condition

(depicted as P5, A5–F5) are shown on the right, while those corresponding to the absence of ethanol are shown on the left, indicating that PC1 represents changes in the expression levels in response to ethanol stress, regardless of phenotypic changes in adaptive evolution. Furthermore, in both cases (i.e., with and without ethanol), the data points of strain P are located at the bottom of the figure, whereas those of the evolved strains are located at the top. It should also be noted that for the expression profiles obtained under ethanol stress conditions (P5, A5–F5), the order of data points along the PC2 axis roughly corresponds to the growth rate under ethanol stress, as shown in the growth rates in Fig. 4b. This indicates that PC2 represents changes in the expression levels that occur during adaptive evolution under ethanol stress conditions aimed at achieving higher growth rates.

To obtain a better understanding of the changes in expression levels, the functional categories in which genes contributing to PC1 or PC2 were statistically overrepresented were screened. The results showed that genes related to iron ion metabolism were commonly upregulated in the tolerant strains. Because it is known that changes in the intracellular redox state activate the genes related to iron ion metabolism, it was suggested that such changes in the redox state occur during adaptive evolution. It was also noted that genes related to the biosynthetic pathways of tryptophan, histidine, valine, leucine, and isoleucine were commonly upregulated in the tolerant strains. It is speculated that the activation or reactivation of these amino acid biosynthesis pathways is responsible for the ethanol stress tolerance observed. This hypothesis was partially supported by the finding that supplementation of isoleucine, tryptophan, and histidine into the medium increased the specific growth rate of the parent strain in an ethanol stress environment. It is expected that these findings would serve as a starting point for understanding the molecular mechanisms involved in ethanol stress tolerance in *E. coli* and would be taken into consideration when designing ethanol-tolerant *E. coli* cells for improved ethanol productivity on an industrial scale.

3.3 Future Trends

In the experimental evolutions, we can obtain cells with higher growth activity by a growth-based selection process. By this scheme, we can obtain various useful strains for engineering purposes, such as stress-tolerant strains. However, cells having other superior phenotypes, such as productivity of target metabolites, are rather difficult to obtain using experimental evolution with simple growth-based selection. One possible strategy to obtain cells with such superior phenotypes is to build a positive correlation between growth activity and the desired phenotypes by appropriate genetic modifications, and then to select cells with higher growth activity [37, 48]. For example, in [48], engineered *E. coli* cells whose growth was correlated with the production of targets (succinate and malate) under an anaerobic condition were constructed by deletion of the central anaerobic fermentation genes (*ldhA*, *adhE*, *ackA*). Then, the cells with high productivity of targets were successfully obtained by the experimental evolution with growth-based selection. Such integration of the rational metabolic network design and the experimental evolution can significantly expand the applicable range of the experimental evolution for the strain improvement.

The advent of next-generation sequencers that reduce the cost of sequencing and greatly increase throughput should permit the identification of mutations fixed in strains obtained by experimental evolution [68]. Furthermore, comprehensive phenotypic analyses, including transcriptome, proteome, and metabolome analyses, provide high-dimensional and high-resolution data of the evolved strains. Using these multi-omics data, we can analyze the phenotype-genotype relationship, which should reveal the mechanisms behind the creation of the desired phenotype. It is anticipated that with the use of multi-omics analyses, bioinformatics, and mathematical modeling of cellular functions, experimental evolution would become a prominent tool for systematic strain improvements.

4 Outlook

At present, systems biotechnology and systems metabolic engineering are in the early stages of development, and technical breakthroughs are required to advance the development of these areas of study [59, 61, 63]. Systems biology-based engineering for strain improvement consists of three steps (Fig. 6). The first is data acquisition. For example, multi-omics analyses provide detailed information on cellular processes in the strains under study. In the case of the genome-scale metabolic analysis presented above, the construction of a metabolic model based on genome analysis and other physiological studies corresponds to this step. In experimental evolution studies, the first step in strain improvement is the production of strains by long-term culture experiments followed by analysis of the phenotype using techniques such as gene expression profiling. The second step

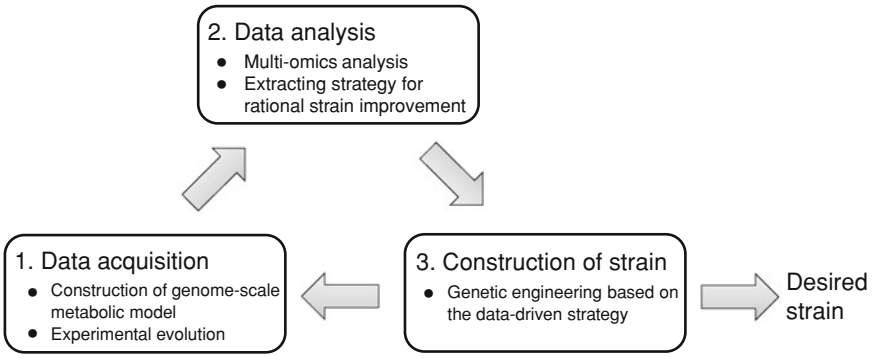

Fig. 6 Summary of systems metabolic engineering for the creation of strains with improved productivity

involves the analysis of data to determine strategies for strain improvement. Bioinformatics analysis and computer modeling play essential roles in this step. Constraint-based flux analysis using genome-scale metabolic models could identify candidate genes that could be manipulated for strain improvement. Bioinformatics analysis of omics data of strains obtained by experimental evolution can provide insight into the mechanisms responsible for the higher fitness of these strains, and this information can provide a basis for strain improvement. The third and final step is the creation of an improved strain based on the data obtained from the above analysis. This could be achieved by using methods such as gene manipulation techniques. In some cases, the obtained strains may again be subjected to multi-omics analyses. In other words, the first step may be repeated with the obtained strain for further strain improvement. To adequately perform these procedures and to obtain strains with the desired phenotypes, further improvements in methodology are necessary. For example, the prediction accuracy of genome-scale metabolic simulation should be improved, which might be possible by integrating multi-omics data. Although the analysis of phenotype-genotype relationships in experimental evolution is challenging, the accumulation of multi-omics data is expected to provide a better understanding of phenotype-genotype relationships in complex cellular dynamics, which could contribute significantly to the advancement of rational metabolic design.

It is predicted that systems biotechnology and systems metabolic engineering will have an increasing impact on industrial biotechnology in the future. These studies might also be important for the synthesis of a minimal cell [39]. Although key innovations might be necessary, these approaches will create a platform for the rational design of microorganisms that can be used to produce cheap high-quality target compounds in large quantities by industrial processes.

References

1. Akesson M, Förster J, Nielsen J (2004) Integration of gene expression data into genome-scale metabolic models. Metab Eng 6(4):285–293
2. Aldor IS, Krawitz DC, Forrest W, Chen C, Nishihara JC, Joly JC, Champion KM (2005) Proteomic profiling of recombinant *Escherichia coli* in high-cell-density fermentations for improved production of an antibody fragment biopharmaceutical. Appl Environ Microbiol 71(4):1717–1728
3. Alper H, Moxley J, Nevoigt E, Fink GR, Stephanopoulos G (2006) Engineering yeast transcription machinery for improved ethanol tolerance and production. Science 384(5805):1565–1568
4. Alper H, Jin YS, Moxley JF, Stephanopoulos G (2005) Identifying gene targets for the metabolic engineering of lycopene biosynthesis in *Escherichia coli*. Metab Eng 7(3):155–164
5. Anderson AJ, Dawes EA (1990) Occurrence, metabolism, metabolic role, and industrial uses of bacterial polyhydroxyalkanoates. Microbiol Rev 54(4):450–472
6. Andrew RJ, Palsson BØ (2006) The model organism as a system: integrating 'omics' data sets. Nat Rev Mol Cell Biol 7:198–210
7. Andrianantoandro E, Basu S, Karig DK, Weiss R (2006) Synthetic biology: new engineering rules for an emerging discipline. Mol Syst Biol 2:0028
8. Arakawa K, Kono N, Yamada Y, Mori H, Tomita M (2005) KEGG-based pathway visualization tool for complex omics data. In Silico Biol 5(4):419–423
9. Aristidou AA, San KY, Bennett GN (1995) Metabolic engineering of *Escherichia coli* to enhance recombinant protein production through acetate reduction. Biotechnol Prog 11(4):475–478
10. Atsumi S, Hanai T, Liao JC (2008) Non-fermentative pathways for synthesis of branched-chain higher alcohols as biofuels. Nature 451(7174):86–89
11. Atsumi S, Wu TY, Machado IM, Huang WC, Chen PY, Pellegrini M, Liao JC (2010) Evolution, genomic analysis, and reconstruction of isobutanol tolerance in *Escherichia coli*. Mol Syst Biol 6:449
12. Attfield PV (1997) Stress tolerance: the key to effective strains of industrial baker's yeast. Nat Biotechnol 15(13):1351–1357
13. Bailey JE (1991) Toward a science of metabolic engineering. Science 252(5013):1668–1675
14. Barabási AL, Oltvai ZN (2004) Network biology: understanding the cell's functional organization. Nat Rev Genet 5:101–113
15. Barrick JE, Yu DS, Yoon SH, Jeong H, Oh TK, Schneider D, Lenski RE, Kim JF (2009) Genome evolution and adaptation in a long-term experiment with *Escherichia coli*. Nature 461(7268):1243–1247
16. Beard DA, Liang SD, Qian H (2002) Energy balance for analysis of complex metabolic networks. Biophys J 83(1):79–86
17. Bongaerts J, Krämer M, Müller U, Raeven L, Wubbolts M (2001) Metabolic engineering for microbial production of aromatic amino acids and derived compounds. Metab Eng 3(4):289–300
18. Brown SW, Oliver SG (1982) Isolation of ethanol-tolerant mutants of yeast by continuous selection. Eur J Appl Microbiol Biotechnol 16:119–122
19. Burgard AP, Pharkya P, Maranas CD (2003) Optknock: a bilevel programming framework for identifying gene knockout strategies for microbial strain optimization. Biotechnol Bioeng 84(6):647–657
20. Burkovski A (2008) Corynebacteria: genomics and molecular biology. Caister Academic Press, Norfolk
21. Caspi R, Altman T, Dale JM, Dreher K, Fulcher CA, Gilham F, Kaipa P, Karthikeyan AS, Kothari A, Krummenacker M, Latendresse M, Mueller LA, Paley S, Popescu L, Pujar A, Shearer AG, Zhang P, Karp PD (2010) The MetaCyc database of metabolic pathways and enzymes and the BioCyc collection of pathway/genome databases. Nucleic Acids Res 38:D473–D479

22. Chellapandi P, Sivaramakrishnan S, Viswanathan MB (2010) Systems biotechnology: an emerging trend in metabolic engineering of industrial microorganisms. J Comp Sci Sys Biol 3(2):43–49
23. Chen X, Alonso AP, Allen DK, Reed JL, Shachar-Hill Y (2011) Synergy between (13)C-metabolic flux analysis and flux balance analysis for understanding metabolic adaptation to anaerobiosis in *E. coli*. Metab Eng 13(1):38–48
24. Chou CP (2007) Engineering cell physiology to enhance recombinant protein production in *Escherichia coli*. Appl Microbiol Biotechnol 76(3):521–532
25. Clomburg JM, Gonzalez R (2010) Biofuel production in *Escherichia coli*: the role of metabolic engineering and synthetic biology. Appl Microbiol Biotechnol 86(2):419–434
26. Conrad TM, Joyce AR, Applebee MK, Barrett CL, Xie B, Gao Y, Palsson BØ (2009) Whole-genome resequencing of *Escherichia coli* K-12 MG1655 undergoing short-term laboratory evolution in lactate minimal media reveals flexible selection of adaptive mutations. Genome Biol 10(10):R118
27. Cornish A, Greenwood JA, Jones CW (1989) Binding-protein-dependent sugar transport by *Agrobacterium radiobacter* and *A. tumefaciens* grown in continuous culture. J Gen Microbiol 135(11):3001–3013
28. Duarte NC, Herrgård MJ, Palsson BØ (2004) Reconstruction and validation of *Saccharomyces cerevisiae* iND750, a fully compartmentalized genome-scale metabolic model. Genome Res 14(7):1298–1309
29. Duarte NC, Becker SA, Jamshidi N, Thiele I, Mo ML, Vo TD, Srivas R, Palsson BØ (2007) Global reconstruction of the human metabolic network based on genomic and bibliomic data. Proc Natl Acad Sci U S A 104(6):1777–1782
30. Edwards JS, Palsson BØ (2000) The *Escherichia coli* MG1655 in silico metabolic genotype: its definition, characteristics, and capabilities. Proc Natl Acad Sci U S A 97(10):5528–5533
31. Eggeling L, Bott M (2005) Handbook of *Corynebacterium glutamicum*. CRC Press, Boca Raton
32. Endy D (2005) Foundations for engineering biology. Nature 438(7067):449–453
33. Farmer WR, Liao JC (2000) Improving lycopene production in *Escherichia coli* by engineering metabolic control. Nat Biotechnol 18(5):533–537
34. Feist AM, Palsson BØ (2008) The growing scope of applications of genome-scale metabolic reconstructions using *Escherichia coli*. Nat Biotechnol 26(6):659–667
35. Feist AM, Scholten JC, Palsson BØ, Brockman FJ, Ideker T (2006) Modeling methanogenesis with a genome-scale metabolic reconstruction of *Methanosarcina barkeri*. Mol Syst Biol 2(2006):0004
36. Feist AM, Henry CS, Reed JL, Krummenacker M, Joyce AR, Karp PD, Broadbelt LJ, Hatzimanikatis V, Palsson BØ (2007) A genome-scale metabolic reconstruction for *Escherichia coli* K-12 MG1655 that accounts for 1260 ORFs and thermodynamic information. Mol Syst Biol 3:121
37. Fong SS, Burgard AP, Herring CD, Knight EM, Blattner FR, Maranas CD, Palsson BØ (2005) In silico design and adaptive evolution of *Escherichia coli* for production of lactic acid. Biotechnol Bioeng 91(5):643–648
38. Fong SS, Palsson BØ (2004) Metabolic gene-deletion strains of *Escherichia coli* evolve to computationally predicted growth phenotypes. Nat Genet 36(10):1056–1058
39. Forster AC, Church GM (2006) Towards synthesis of a minimal cell. Mol Syst Biol 2:45
40. Gasser B, Sauer M, Maurer M, Stadlmayr G, Mattanovich D (2007) Transcriptomics-based identification of novel factors enhancing heterologous protein secretion in yeasts. Appl Env Microbiol 73(20):6499–6507
41. Han MJ, Jeong KJ, Yoo JS, Lee SY (2003) Engineering *Escherichia coli* for increased productivity of serine-rich proteins based on proteome profiling. Appl Env Microbiol 69(10):5772–5781
42. Hibi M, Yukitomo H, Ito M, Mori H (2007) Improvement of NADPH-dependent bioconversion by transcriptome-based molecular breeding. Appl Env Microbiol 73(23):7657–7663

43. Hill J, Nelson E, Timan D, Polasky S, Tiffany D (2006) Environmental, economic, and energetic costs and benefits of biodiesel and ethanol biofuels. Proc Nat Acad Sci U S A 103(30):11206–11210
44. Hirasawa T, Yoshikawa K, Nakakura Y, Nagahisa K, Furusawa C, Katakura Y, Shimizu H, Shioya S (2007) Identification of target genes conferring ethanol stress tolerance to *Saccharomyces cerevisiae* based on DNA microarray data analysis. J Biotechnol 131(1):34–44
45. Horinouchi T, Tamaoka K, Furusawa C, Ono N, Suzuki S, Hirasawa T, Yomo T, Shimizu H (2010) Transcriptome analysis of parallel-evolved *Escherichia coli* strains under ethanol stress. BMC Genomics 11:579
46. Ibarra RU, Edwards JS, Palsson BØ (2002) *Escherichia coli* K-12 undergoes adaptive evolution to achieve in silico predicted optimal growth. Nature 420(6912):186–197
47. Inui M, Suda M, Kimura S, Yasuda K, Suzuki H, Toda H, Yamamoto S, Okino S, Suzuki N, Yukawa H (2008) Expression of Clostridium acetobutylicum butanol synthetic genes in *Escherichia coli*. Appl Microbiol Biotechnol 77(6):1305–1316
48. Jantama K, Haupt MJ, Svoronos SA, Zhang X, Moore JC, Shanmugam KT, Ingram LO (2008) Combining metabolic engineering and metabolic evolution to develop nonrecombinant strains of *Escherichia coli* C that produce succinate and malate. Biotechnol Bioeng 99(5):1140–1153
49. Jarboe LR, Grabar TB, Yomano LP, Shanmugan KT, Ingram LO (2007) Development of ethanologenic bacteria. Adv Biochem Eng Biotechnol 108:237–261
50. Jensen PA, Lutz KA, Papin JA (2011) TIGER: toolbox for integrating genome-scale metabolic models, expression data, and transcriptional regulatory networks. BMC Syst Biol 5:147
51. Kanehisa M, Goto S (2000) KEGG: Kyoto encyclopedia of genes and genomes. Nucleic Acids Res 28(1):27–30
52. Kellis M, Patterson N, Endrizzi M, Birren B, Lander ES (2003) Sequencing and comparison of yeast species to identify genes and regulatory elements. Nature 423(6937):241–254
53. Kinoshita S, Udaka S, Shimono M (1957) Studies on the amino acid fermentation. Appl Microbiol Jpn 3:193–205
54. Kishimoto T, Iijima L, Tatsumi M, Ono N, Oyake A, Hashimoto T, Matsuo M, Okubo M, Suzuki S, Mori K, Kashiwagi A, Furusawa C, Ying BW, Yomo T (2010) Transition from positive to neutral in mutation fixation along with continuing rising fitness in thermal adaptive evolution. PLoS Genet 6(10):e1001164
55. Khosla C, Keasling JD (2003) Metabolic engineering for drug discovery and development. Nat Rev Drug Discov 2(12):1019–1025
56. Klamt S, Stelling J, Ginkel M, Gilles ED (2003) FluxAnalyzer: exploring structure, pathways, and flux distributions in metabolic networks on interactive flux maps. Bioinformatics 19:261–269
57. Kumagai H (2000) Microbial production of amino acids in Japan. Adv Biochem Eng Biotechnol 69:71–85
58. Lee DH, Palsson BØ (2010) Adaptive evolution of *Escherichia coli* K-12 MG1655 during growth on a nonnative carbon source, L-1,2-propanediol. Appl Environ Microbiol 76(13):4158–4168
59. Lee JW, Kim TY, Jang YS, Choi S, Lee SY (2011) Systems metabolic engineering for chemicals and materials. Trends Biotechnol 29(8):370–378
60. Lee KH, Park JH, Kim TY, Kim HU, Lee SY (2007) Systems metabolic engineering of *Escherichia coli* for L-threonine production. Mol Syst Biol 3:149
61. Lee SJ, Lee DY, Kim TY, Kim BH, Lee J, Lee SY (2005) Metabolic engineering of *Escherichia coli* for enhanced production of succinic acid, based on genome comparison and in silico gene knockout simulation. Appl Environ Microbiol 71(12):7880–7887
62. Lee SY (1996) High cell density cultivation of *Escherichia coli*. Trends Biotechnol 14(3):98–105
63. Lee SY, Lee DY, Kim TY (2005) Systems biotechnology for strain improvement. Trends Biotechnol 23(7):349–358

64. Lenski RE, Rose MR, Simpson SC, Tadler SC (1991) Long-term experimental evolution in *Escherichia coli*. I. Adaptation and divergence during 2,000 generations. Am Nat 138(6):1315–1341
65. Leuchtenberger W, Huthmacher K, Drauz K (2005) Biotechnological production of amino acids and derivatives: current status and prospects. Appl Microbiol Biotechnol 69:1–8
66. Li R, Zhang H, Qi Q (2007) The production of polyhydroxyalkanoates in recombinant *Escherichia coli*. Bioresour Technol 98(12):2313–2320
67. Makrides SC (1996) Strategies for achieving high-level expression of genes in *Escherichia coli*. Microbiol Rev 60(3):512–538
68. Mardis ER (2008) The impact of next-generation sequencing technology on genetics. Trends Genet 24(3):133–141
69. Martin VJ, Pitera DJ, Withers ST, Newman JD, Keasling JD (2003) Engineering a mevalonate pathway in *Escherichia coli* for production of terpenoids. Nat Biotechnol 21(7):796–802
70. Montagud A, Navarro E, Fernández de Córdoba P, Urchueguía JF, Patil KR (2010) Reconstruction and analysis of genome-scale metabolic model of a photosynthetic bacterium. BMC Syst Biol 4:156
71. Mortlock RP, Gallo MA (1992) Experiments in the evolution of catabolic pathways using modern bacteria. In: Mortlock RP (ed) The evolution of metabolic function. CRC Press, Boca Raton
72. Oberhardt MA, Palsson BØ, Papin JA (2009) Applications of genome-scale metabolic reconstructions. Mol Syst Biol 5:320
73. Oh YK, Palsson BØ, Park SM, Schilling CH, Mahadevan R (2007) Genome-scale reconstruction of metabolic network in *Bacillus subtilis* based on high-throughput phenotyping and gene essentiality data. J Biol Chem 282(39):28791–28799
74. Okino S, Inui M, Yukawa H (2005) Production of organic acids by *Corynebacterium glutamicum* under oxygen deprivation. Appl Microbiol Biotechnol 68(4):475–480
75. Oliveira AP, Nielsen J, Förster J (2005) Modeling *Lactococcus lactis* using a genome-scale flux model. BMC Microbiol 5:39
76. Orth JD, Thiele I, Palsson BØ (2010) What is flux balance analysis? Nat Biotechnol 28(3):245–248
77. Palsson BØ (2006) Systems biology: properties of reconstructed networks. Cambridge University Press, New York
78. Papin JA, Price ND, Wiback SJ, Fell DA, Palsson BO (2003) Metabolic pathways in the post-genome era. Trends Biochem Sci 28:250–258
79. Papin JA, Stelling J, Price ND, Klamt S, Schuster S, Palsson BO (2004) Comparison of network-based pathway analysis methods. Trends Biotechnol 22:400–405
80. Parekh S, Vinci VA, Strobel RJ (2000) Improvement of microbial strains and fermentation processes. Appl Microbiol Biotechnol 54:287–301
81. Park JH, Lee SY, Kim TY, Kim HU (2008) Application of systems biology for bioprocess development. Trends Biotechnol 26(8):404–412
82. Park JH, Lee KH, Kim TY, Lee SY (2007) Metabolic engineering of *Escherichia coli* for the production of L-valine based on transcriptome analysis and in silico gene knockout simulation. Proc Natl Acad Sci U S A 104(19):7797–7802
83. Patil KR, Akesson M, Neilsen J (2004) Use of genome-scale microbial models for metabolic engineering. Curr Opin Biotechnol 15:64–69
84. Pfleger BF, Pitera DJ, Smolke CD, Keasling JD (2006) Combinatorial engineering of intergenic regions in operons tunes expression of multiple genes. Nat Biotechnol 24(8):1027–1032
85. Pharkya P, Burgard AP, Maranas CD (2004) OptStrain: a computational framework for redesign of microbial production systems. Genome Res 14(11):2367–2376
86. Prather KL, Martin CH (2008) De novo biosynthetic pathways: rational design of microbial chemical factories. Curr Opin Biotechnol 19(5):468–474

87. Sauer U (2001) Evolutionary engineering of industrially important microbial phenotypes. Adv Biochem Eng Biotechnol 73:130–169
88. Schilling CH, Letscher D, Palsson BO (2000) Theory for the systemic definition of metabolic pathways and their use in interpreting metabolic function from a pathway-oriented perspective. J Theor Biol 203:229–248
89. Schubert C (2006) Can biofuels finally take center stage? Nat Biotechnol 24:777–784
90. Schuster S, Hilgetag S (1994) On elementary flux modes in biochemical reaction systems at steady state. J Biol Syst 2:165–182
91. Schuster S, Pfeiffer T, Moldenhauer F, Koch I, Dandekar T (2002) Exploring the pathway structure of metabolism: decomposition into subnetworks and application to *Mycoplasma pneumoniae*. Bioinformatics 18:351–361
92. Schuster S, Hilgetag C, Woods JH, Fell DA (2002) Reaction routes in biochemical reaction systems: algebraic properties, validated calculation procedure and example from nucleotide metabolism. J Math Biol 45:153–181
93. Segrè D, Vitkup D, Church GM (2002) Analysis of optimality in natural and perturbed metabolic networks. Proc Natl Acad Sci U S A 99(23):15112–15117
94. Sheikh K, Förster J, Nielsen LK (2005) Modeling hybridoma cell metabolism using a generic genome-scale metabolic model of *Mus musculus*. Biotechnol Prog 21(1):112–121
95. Shinfuku Y, Sorpitiporn N, Sono M, Furusawa C, Hirasawa T, Shimizu H (2009) Development and experimental verification of a genome-scale metabolic model for *Corynebacterium glutamicum*. Microb Cell Fact 8:43
96. Shirai T, Fujimura K, Furusawa C, Nagahisa K, Shioya S, Shimizu H (2007) Study on roles of anaplerotic pathways in glutamate overproduction of *Corynebacterium glutamicum* by metabolic flux analysis. Microb Cell Fact 6:19
97. Shlomi T, Berkman O, Ruppin E (2005) Regulatory on/off minimization of metabolic flux changes after genetic perturbations. Proc Natl Acad Sci U S A 102(21):7695–7700
98. Silman N, Carver MA, Jones CW (1989) Physiology of amidase production by *Methylophilus methylotrophus*: isolation of hyperactive strains using continuous culture. J Gen Microbiol 135:3153–3164
99. Sindelar G, Wendisch VF (2007) Improving lysine production by *Corynebacterium glutamicum* through DNA microarray-based identification of novel target genes. Appl Microbiol Biotechnol 76:677–689
100. Stephanopoulos G (1998) Metabolic fluxes and metabolic engineering. Metab Eng 1(1):1–11
101. Takac S, Calik G, Mavituna F, Dervakos G (1998) Metabolic flux distribution for the optimized production of L-glutamate. Enzym Microb Technol 23(5):286–300
102. Tepper N, Shlomi T (2010) Predicting metabolic engineering knockout strategies for chemical production: accounting for competing pathways. Bioinformatics 26(4):536–543
103. Thiele I, Palsson BØ (2010) A protocol for generating a high-quality genome-scale metabolic reconstruction. Nat Protocols 5(1):93–121
104. Trinh CT, Uneran P, Srienc F (2008) Minimal *Escherichia coli* cell for the most efficient production of ethanol from hexoses and pentoses. Appl Env Microbiol 74(12):3634–3643
105. Udaka S (1960) Screening method for microorganisms accumulating metabolites and its use in the isolation of *Micrococcus glutamicus*. J Bacteriol 79(5):754–755
106. Vemuri GN, Aristidou AA (2005) Metabolic engineering in the -omics era: elucidating and modulating regulatory networks. Microbiol Mol Biol Rev 69(2):197–216
107. Wang Q, Chen X, Yang Y, Zhao X (2006) Genome-scale in silico aided metabolic analysis and flux comparisons of *Escherichia coli* to improve succinate production. Appl Environ Microbiol 73(4):887–894
108. Weikert C, Sauer U, Bailey JE (1997) Use of a glycerol-limited, long-term chemostat for isolation of *Escherichia coli* mutants with improved physiological properties. Microbiology 143:1567–1574
109. Wendisch VF, Bott M, Eikmanns BJ (2006) Metabolic engineering of *Escherichia coli* and *Corynebacterium glutamicum* for biotechnological production of organic acids and amino acids. Curr Opin Microbiol 9(3):268–274

110. Yan Y, Chemler J, Huang L, Martens S, Koffas MA (2005) Metabolic engineering of anthocyanin biosynthesis in *Escherichia coli*. Appl Environ Microbiol 71(7):3617–3623
111. Yan Y, Liao JC (2009) Engineering metabolic systems for production of advanced fuels. J Ind Microbiol Biotechnol 36:471–479
112. Yomano LP, York SW, Ingram LO (1998) Isolation and characterization of ethanol-tolerant mutants of *Escherichia coli* KO11 for fuel ethanol production. J Ind Microbiol Biotechnol 20(2):132–138
113. Yomano LP, York SW, Zhou S, Shanmugam KT, Ingram LO (2008) Re-engineering *Escherichia coli* for ethanol production. Biotechnol Lett 30(12):2097–2103
114. Yoshikawa K, Tanaka T, Furusawa C, Nagahisa K, Hirasawa T, Shimizu H (2009) Comprehensive phenotypic analysis for identification of genes affecting growth under ethanol stress in *Saccharomyces cerevisiae*. FEMS Yeast Res 9(1):32–44
115. Zhang W, Li F, Nie L (2010) Integrating multiple 'omics' analysis for microbial biology: application and methodologies. Microbiology 156(Pt 2):287–301

Adv Biochem Eng Biotechnol (2013) 131: 25–61
DOI: 10.1007/10_2012_138

Published Online: 6 July 2012

Impacts of Quorum Sensing on Microbial Metabolism and Human Health

Yang-Chun Yong and Jian-Jiang Zhong

Abstract Bacteria were considered to be lonely 'mutes' for hundreds of years. However, recently it was found that bacteria usually coordinate their behaviors at the population level by producing (speaking), sensing (listening), and responding to small signal molecules. This so-called quorum sensing (QS) regulation enables bacteria to live in a 'society' with cell–cell communication and controls many important bacterial behaviors. In this chapter, QS systems and their signal molecules for Gram-negative and Gram-positive bacteria are introduced. Most interestingly, QS regulates the important bacterial behaviors such as metabolism and pathogenesis. QS-regulated microbial metabolism includes antibiotic synthesis, pollutant biodegradation, and bioenergy production, which are very relevant to human health. QS is also well-known for its involvement in bacterial pathogenesis, such as iin nfections by *Pseudomonas aeruginosa* and *Staphylococcus aureus*. Novel disease diagnosis strategies and antimicrobial agents have also been developed based on QS regulation on bacterial infections. In addition, to meet the requirements for the detection/quantification of QS signaling molecules for research and application, different biosensors have been constructed, which will also be reviewed here. QS regulation is essential to bacterial survival and important to human health. A better understanding of QS could lead better control/manipulation of bacteria, thus making them more helpful to people.

Keywords Quorum Sensing · Metabolism · Pathogenesis · Biosensor · Bioenergy

J.-J. Zhong (✉)
Laboratory of Molecular Biochemical Engineering, State Key Laboratory of Microbial Metabolism, School of Life Sciences and Biotechnology, Shanghai Jiao Tong University, 800 Dong Chuan Road, 200240 Shanghai China
e-mail: jjzhong@sjtu.edu.cn

Y.-C. Yong
Biofuels Institute, School of the Environment, Jiangsu University, 301 Xuefu Road, 212013 Zhenjiang, Jiangsu Province, China

Contents

1 Introduction

Social and cooperative traits are believed to be the most important characteristics for human survival and development. Bacteria can easily adapt to various new environmental conditions, and they have thrived on earth ubiquitously with a much longer history and wider occupation than humans. However, bacteria were regarded as deaf mutes for at least 300 years since they were first observed by van Leeuwenhoek [1]. Scientists questioned how, as a simple single deaf germ, bacteria achieved such great success? Recently, researchers discovered that bacteria do not live as a non-communicating single cell, but they are organized like a society that shows unique social and cooperative traits [2]. They can use a so-called "quorum sensing" (QS) mechanism to 'talk to' and 'listen to' each other, and hence they can coordinate population behaviors like "multicellular" species [3]. In general, bacteria synthesize low molecular weight (MW) chemical molecules (serving as signaling molecules called 'autoinducers' [AIs]) and release them into the environment; the concentration of AIs increases with increasing cell densities; once the AIs (and cell density) reach a threshold concentration (the quorum), they bind to their cognate receptor and evoke a response (gene expression) in all individuals of the population [1, 3, 4]. Such a population-level response is cell-density dependent and was first termed as 'QS' by Fuqua in 1994 [5]. By the QS mechanism, bacteria can sense the population density and carry out some population behaviors that would be unproductive if done by individuals alone [2]. At present, scientists recognize that communication and cooperation are not exclusive characteristics for animals but rather are the norm in the bacterial world [1]. Since it was first described, QS has been identified in various bacterial species and involves in many important biological processes, including biofilm formation,

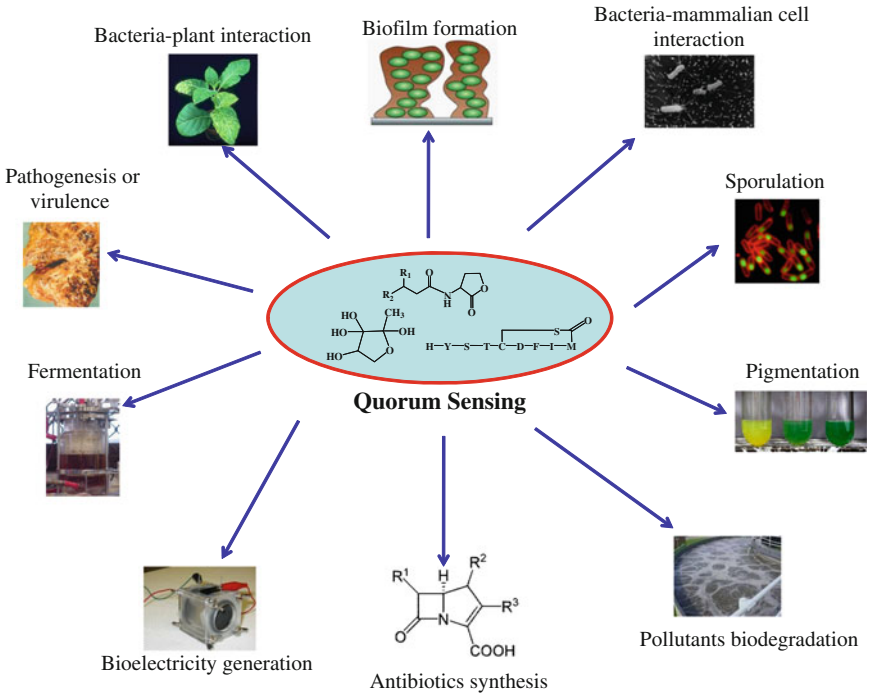

Fig. 1 Involvement of QS in various important biological processes

sporulation, virulence and pathogenesis, pollutant biodegradation, secondary metabolism, and bacteria-host interaction (Fig. 1).

To date, there are several QS systems, including QS in Gram-negative bacteria mediated by acylated homoserine lactone (AHL), hydroxy-palmitic acid methyl ester (PAME), diffusive signal factor (DSF), and *Pseudomonas* quinolone signal (PQS); QS in Gram-positive bacteria mediated by oligopeptide (known as auto-inducing peptides (AIP)), and A-factor; and interspecies QS mediated by autoinducer-2 (AI-2). Here, we selected three representative QS systems for a brief introduction: AHL-mediated QS in Gram-negative bacteria, oligopeptide (known as [AIP])-mediated QS in Gram-positive bacteria, and AI-2 mediated QS for interspecies communication (Fig. 2). AHL-mediated QS is widespread in Gram-negative bacteria. It is comprised of an AHL synthase (LuxI-type family protein) and an AHL receptor (LuxR-type family transcription regulator). AHL-mediated QS was first described in the bioluminescent bacterium *Vibrio fischeri*, in which the LuxI and LuxR proteins controlled the expression of *luxCDABE* operon (a luciferase) ([5], Fig. 2a). LuxI is responsible for the synthesis of the AHL signaling molecule 3OC6HSL (Fig. 3). LuxR is the receptor of 3OC6HSL and the transcription activator of Lux-controlled genes. Once the 3OC6HSL is produced, it can freely diffuse into the environment and accumulate with increasing cell densities. When the concentration of 3OC6HSL reaches its threshold, it will interact

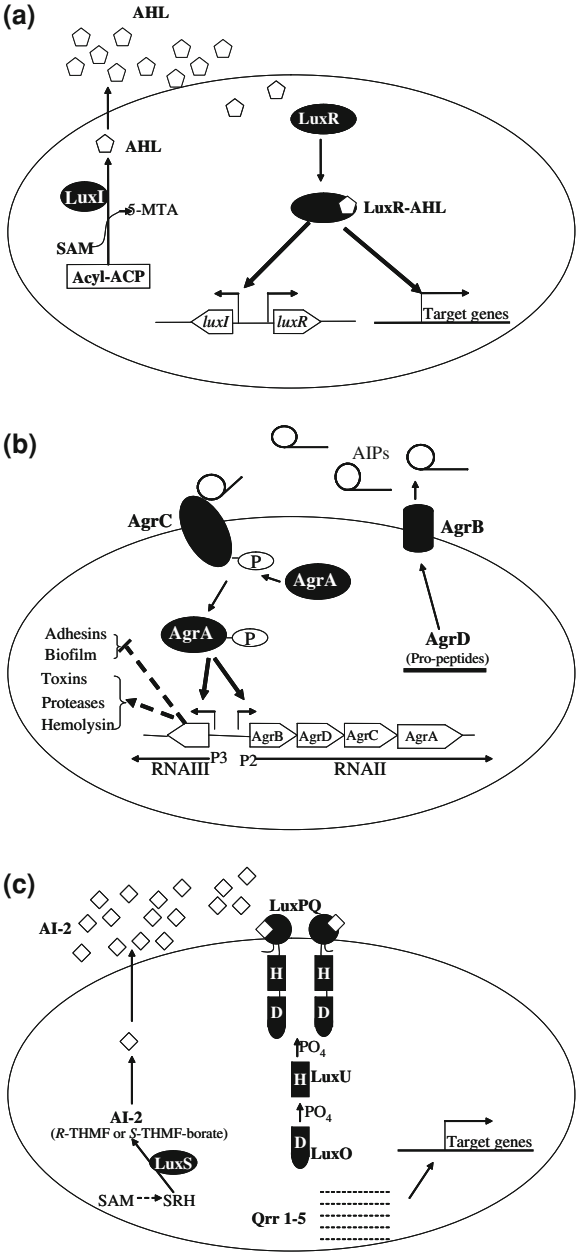

Fig. 2 Three typical QS systems in bacteria: **a** LuxI/R-type AHL-dependent QS system in Gram-negative bacteria (LuxI/R QS system in *V. fisheri*); **b** AIP-dependent QS system in Gram-positive bacteria (*agr* QS system in *S. aureus*); **c** AI-2-dependent interspecies QS system (LuxS QS system in *V. harveyi*) [1, 3, 4, 7, 9, 10, 16]

with the LuxR protein to form the LuxR-HSL complex and then activate the transcription of *luxCDABE* [3]. As this transcription activation and hence the luciferase expression could be activated simultaneously in all individual cells at the population level, *V. fischeri* could provide enough light for its host Hawaiian

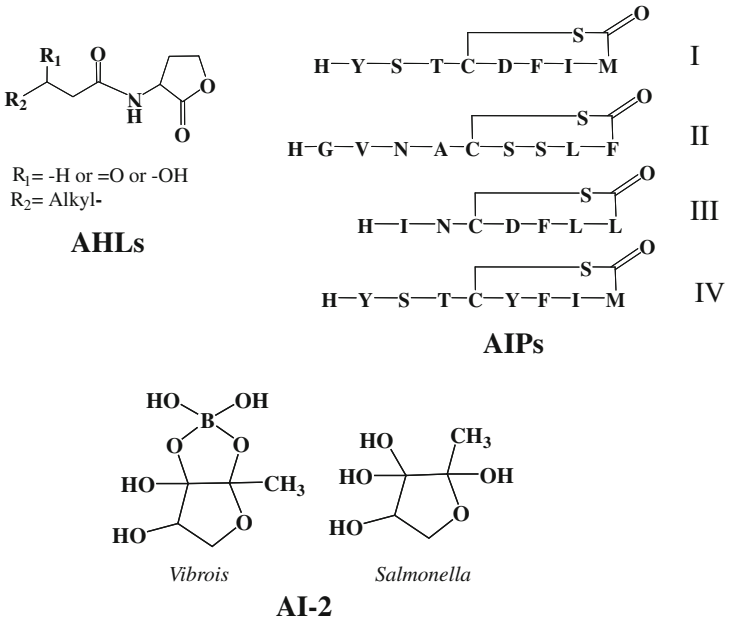

Fig. 3 Typical QS signaling molecules

squid *Euprymma scolopes* for counterillumination to mask its shadow and avoid predation [4, 6]. It is worth noting that the LuxI/R QS system usually has positive feedback for its AHL synthase LuxI [3]. Therefore if the quorum is reached, the AHL synthesis will be accelerated and the expression of QS controlled targets will also be rapidly enhanced.

In Gram-positive bacteria, the QS system is usually comprised of modified oligopeptides (AIP, Fig. 3) as signaling molecules and a two-component type of histidine kinase as signal sensing and transduction modules [7]. Besides using different types of signaling molecules, there are two main differences between AIP-mediated QS and AHL-mediated QS. First, AIP is a modified oligopeptide and cannot freely diffuse across the cell membrane; it should be exported with the aid of exporters. Second, the signaling process for AIP-mediated QS is relayed by two-component histidine kinase. The most typical example of AIP-mediated QS is the *agr* system in *Staphylococcus aureus* ([7, 8]). The *agr* QS system is encoded by *agrBDCA* operon. Gene *agrD* encodes the precursor of the signaling oligopeptide (AIP), and AgrB protein is responsible for the oligopeptide exporting and modification (add thiolactone ring). AgrC and AgrA consist of a two-component histidine kinase-response regulator. AgrC is a transmembrane protein that can bind with AIP. Once AgrC binds with AIP, the intracellular AgrA will be phosphorylated by a two-step phosphorelay. This phosphorylation can activate AgrA to induce the transcription of target genes. Similar to LuxI/R type QS, the phospho-AgrA can also

induce the expression of the *agrBDCA* operon to form a positive feed-back loop. (Fig. 2b).

Both of AHL- and AIP-mediated QS are involved in intraspecies cell–cell communication; the AIs and their cognate receptors are species specific and are only effective in intraspecies communication. In contrast, AI-2 can be synthesized in a remarkably wide variety of bacterial species and can be recognized by other species besides the producer [7, 9–11]. Hence, AI-2 mediated QS is an interspecies cell–cell communication system, and AI-2 is considered to be a universal language in bacterial world. AI-2 is a furanosyl borate diester (3A-methyl-5,6-dihydrofuro [2,3-D] [1,3,2] dioxa-borole-2,2,6,6A tetraol in *Vibrio harveyi*, Fig. 3) synthesized by LuxS from *S*-adenosylmethionine (SAM) [12, 13]. The signaling process relied on several phosphorylation-relay steps [7, 11, 14]. In *V. harveyi*, the signal-relay system is comprised of LuxPQ, LuxU, and LuxO (Fig. 2c). At low cell densities, in the absence of AI-2, LuxQ serves as a kinase and is autophosphorylated. The phosphate was transduced to LuxU and then transferred to LuxO. Phospho–LuxO (LuxO–P) then activates the transcription of Qrr1-5 (genes encoding five small regulatory RNAs (sRNAs)). Qrr sRNAs are master regulators controlling the transcription of a variety of genes [13, 14]. At high cell densities, once AI-2 reaches its critical concentration, it can be detected by the periplasmic proteins LuxP and LuxQ complex. Binding with AI-2 will switch the LuxQ from kinase to phosphatase and result in the dephosphorylation of LuxO–P. Therefore, the Qrr sRNAs are not transcribed and the response is the switch-off of the Qrr sRNAs regulation (Fig. 2c) [7].

It was found that some bacteria simultaneously have several QS systems. These systems may exist in parallel, cross-linked, or hierarchically organized in complex mode [7, 15]. Based on these QS systems, bacteria are not limited to normal cell–cell communication but are capable of signal interception or coercion [16], which allows them to evolve with more sophisticated social traits such as social cheating, exploitation, and kin-selection [17, 18]. Although some other new QS systems have been identified in bacteria and QS was found to be not just limited to the bacterial world, we take the above previously mentioned three typical QS systems as examples in this chapter to discuss the progress of in QS biosensors and the impact of QS on microbial metabolism and human health.

2 Impact of QS on Microbial Metabolism

From the beginning of history, humans have been continuously fighting against and benefiting from the little “bug” of bacteria. Bacterial metabolism is vital to human health. For example, the metabolic pathways of some virulence factor synthesis are crucial for pathogen infection in the human body, and they directly affect human health. In contrast, many other microbial metabolic pathways are related to biofuel production, antibiotic synthesis, biodegradation and bioelectricity production, which are beneficial and vital to the sustainable development of

human society and also closely related to human health. In this section, the QS regulation on microbial metabolism such as fermentation, biodegradation, and bioelectricity generation are discussed.

2.1 Butanediol Fermentation and Acetate Switch

With fermentable carbon sources, bacteria are able to produce a series of acids by using mixed-acid fermentation pathways or various neutral end products (e.g., butanediol or acetoin). The switch to neutral end products allows cells to prevent lethal acidification by limiting acidic end products production [19]. Recently, QS was identified to directly or indirectly regulate the 2,3-butanediol pathway in *Vibrio cholerae*, *Serratia plymuthica*, *Serratia marcescens*, and *Aeromonas hydrophila* [20–22]. In certain strains of *V. cholerae*, the QS systems repressed the *aphA* expression [23], while AphA showed strong repression on the acetoin and 2,3-butanediol synthesis pathway [20]. These studies indicated that QS systems positively regulated 2, 3-butanediol fermentation in *V. cholerae*. Recently, it was found that 2,3-butanediol fermentation in *S. plymuthica* RVH1 and *S. marcescens* MG1 is regulated by SplIR or SwrIR QS system [21]. This study was inspired by an incidental phenomenon in which *splI* mutant (*S. plymuthica* RVH1, deficient in AHL production) grows less well in LB medium compared to the wild-type strain; the *splI* mutant led to continued acidification of the medium and resulted in early growth arrest. Further analysis indicated that inactivation of QS systems in these two *Serratia* strains repressed the acetoin and 2,3-butanediol production and induced the acidic end products. Although the precise mechanism is still unclear, the evidence clearly indicated that the QS system controlled the switch to 2,3-butanediol fermentation in *S. plymuthica* RVH1 and *S. marcescens* MG1. Houdt et al. [21] also showed that the AhyIR QS system regulated the switch from mixed-acids fermentation to 2,3-butanediol fermentation in *A. hydrophila* AH-1 N. Hence, it effectively prevented the accumulation of acids that might lead to lethal acidification and allow further growth using the residual nutrient sources [21]. Butanediol fermentation is the first central metabolism identified to be controlled by QS system.

When grown on acetogenic carbon sources (e.g. D-glucose or L-serine), bacteria can transit from acetate dissimilation (production and secretion) to acetate assimilation (import and utilization) by using an acetate switch at certain conditions [24]. This central regulatory mechanism is crucial for bacteria survival by permitting bacteria growth rapidly when abundant nutrients are present and allowing cells to reclaim the secreted acetate in the absence of these nutrients [24]. However, this switch cannot occur unless the acetate assimilation machinery was activated. Induction of *acs* transcription and Acs activation are required to "flip" the acetate switch [25]. Studer et al. [26] described that wild-type *V. fischeri* showed an acetate switch during growth in a glycerol/tryptone-based medium. Interestingly, the C8HSL synthase (AinS) mutant strain cannot switch from acetate dissimilation to

assimilation, and the acetate accumulated to a lethal pH of about 4.6. Further analysis indicated that the *ainS* mutant showed about 20-fold lower *acs* transcription, which resulted in failure in acetate switch [26]. Meanwhile, the *acs* transcription and acetate switch could be restored by AHL complementation in *ainS* mutant. The evidence indicated that the AinS QS system regulates the *V. fischeri* acetate switch through the *acs* transcription control [26]. All the evidence indicates that QS not only plays important roles in non-essential bioprocesses (biofilm formation, motility), but also is involved in the essential metabolism process at certain conditions. It also implies the possibility to manipulate the of microbial metabolism by tuning QS system regulation to produce value-added products. However, the basic regulation mechanisms and ecological implication still need to be explored.

2.2 QS Regulation on Antibiotics Synthesis

2.2.1 Carbapenem in Gram-Negative Bacteria

The carbapenems are potent members of the most classic and important β-lactam antibiotics, which are widely used in chemotherapy, particularly for nosocomial, multidrug resistant infections [27]. Carbapenems are active against many important Gram-negative and Gram-positive bacteria, such as *S. aureus*, *Haemophilus* spp., and *Pseudomonas aeruginosa* [28]. Different kinds of carbapenems were identified in the metabolites of *Streptomyces*, *Erwinina*, and *Serratia* [28]. *Serratia* sp. ATCC 39006 and *E. carotovora* are able to produce a simple carbapenem antibiotic, 1-carbapen-2-em-3-carboxylic acid (Fig. 4a) [27, 29, 30]. A highly conserved gene cluster containing nine genes (*carRABCDEFGH*) was proven to be responsible for the production of this antibiotic in *Serratia* sp. ATCC 39006 and *Erwinia carotovora* [29, 30]. The *carA–E* genes are predicted as the structure genes for carbapenem synthesis, while *carF* and *carG* encode proteins are involved in the β-lactam resistance. The function of *carH* is unknown. CarR is a transcriptional activator responsible for the regulation of the remaining *car* genes [29, 30]. Interestingly, the expression of *car* operon and antibiotic production showed a cell density dependent manner that is characteristic of QS regulation [31]. Further analysis indicated that *E. carotovora* produced a QS signal molecule 3OC6HSL by an unlinked CarI. Purified protein CarR binds to its ligand 3OC6HSL with a stoichiometry of two molecules of the ligand per dimer of protein. In the presence of 3OC6HSL, the purified CarR could form a high MW complex with 3OC6HSL and bind to the promoter upstream of the first of the biosynthetic genes, *carA* [32, 33]. Therefore, when 3OC6HSL reaches its critical concentration at high cell density, CarR binds with the 3OC6HSL and multimerizes; the CarR-3OC6HSL then binds to the *lux* box of the *carA* promoter to activate the transcription. Thus, the carbapenem synthesis in *E. carotovora* is controlled by CarIR QS system at the transcriptional level [31–34]. In contrast to the LuxIR QS system, the AHL receptor

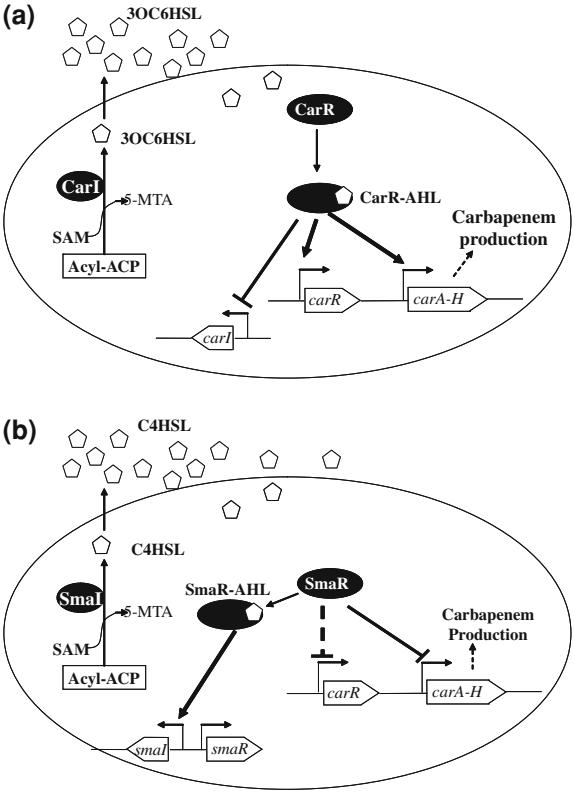

Fig. 4 Models for QS regulation in carbapenem synthesis in **a** *Erwinia carotovora* and **b** *Serratia* sp. ATCC 39006 [28, 199]

CarR shows positive autoregulation in the presence of 3OC6HSL, whereas AHL synthesis (CarI) is negative feedback repressed by the increasing concentration of 3OC6HSL [33] (Fig. 4a). Due to the sharing of a high identity of *car* operon to *E. carotovora* [30], the carbapenem production in *Serratia* sp. ATCC 39006 is expected to be controlled by the CarR/3OC6HSL QS system. Unexpectedly, the *lux* biosensor, which responded to 3OC6HSL, failed to detect AHL in *Serratia* sp. ATCC 39006. However, C4HSL and C6HSL were detected by using the *Chromobacterium violaceum* CV026 bioassay and TLC analysis [30]. More interestingly, although carbapenem production in *Serratia* was unsurprisingly proven to be C4HSL/C6HSL-dependent, the *Serratia* CarR protein showed AHL-independent regulatory activity and is functionally interchangeable with the *Erwinia* homologue [35]. The pheromone-independent nature of CarR inspired the researchers to identify a new SmaIR QS system in *Serratia* sp. ATCC 39006 [30]. SmaI, the homologue of LuxI, directed the synthesis of C4HSL and C6HSL. SmaR, which is the homologue of LuxR and the receptor of C4HSL/C6HSL, was a transcriptional repressor, an uncommon feature of LuxR-type transcriptional regulators [36]. In the absence of C4HSL/C6HSL, SmaR repressed the transcription of *car* gene cluster. In the presence of C4HSL/C6HSL, SmaR lost the repression

ability. Transcriptional analysis showed *Serratia carR* transcription (the AHL-independent transcriptional activator of *car* gene cluster, closely paralleled transcription of *carA*) is under the control of SmaIR QS system [36]. However, the QS regulation on *carR* did not occur directly as the SmaR protein did not bind the *carR* promoter as shown in in vitro gel shift assay [37]. Surprisingly, the purified SmaR directly bound with the *carA* promoter and C4HSL/C6HSL could abolish this binding [37]. It suggested that the SmaIR QS system controlled the carbapenem synthesis in *Serratia* through both an unclear indirect mode with *carR* and a direct control on transcription of structure genes (Fig. 4b). In addition, recent evidence implied that the AI-2 (produced by LuxS) QS system was also involved in the carbapenem synthesis in *Serratia* [38]. This evidence showed the complexity and diversity of QS regulation on carbapenem biosynthesis, which needs further investigation.

2.2.2 Phenazine Antibiotics Produced by *Pseudomonas*

During the past century, approximately 100 natural origin heterocyclic nitrogen-containing phenazines have been identified, and most of these showed antibiotic activity toward various plant bacteria and fungi [39–41]. Thus phenazines and their producers are widely used as biocontrol agents for plant protection. Although a lot of bacteria species could synthesize phenazine compounds, *Pseudomonas* spp. (including *P. fluorescens*, *P. chlororaphis*, and *P. aeruginosa*) were found to be the main producers [40, 42]. *P. fluorescens* only produced one phenazine compound of phenazine-1-carboxylic acid (PCA), while the other two genera simultaneously produced two or more phenazine compounds, which usually included PCA, 1-hydroxyphenazine (1-OH-PHZ), pyocyanin (5-N-methyl-1-hydroxyphenazine, PYO), and phenazine-1-carboxamide (PCN) [39, 40]. In most bacterial species, 1-OH-PHZ, PYO and PCN are derived from the common precursor PCA, while the PCA was synthesized from chorismate. The gene cluster responsible for PCA synthesis has been identified in several strains. Typically, *phzABCDEFG*, which is highly conserved among *P. aeruginosa*, *P. chlororaphis*, and *P. fluorescens*, was characterized and proven to be the biosynthetic operon that is responsible for the PCA synthesis from the chorismate precursor (Fig. 5). Then, PCA can be modified to diverse phenazine derivatives by various specific enzymes. In *P. aeruginosa*, PCA was transformed to PCN, PYO, and 1-OH-PHZ by PhzH, PhzM/PhzS, and PhzS, respectively (Fig. 5). Interestingly, the PCA production in Pseudomonas usually showed a population density-dependent manner; i.e., only a large amount of PCA was produced in the late exponential growth and early stationary phase, which suggested the regulation of QS. The QS system PhzI–PhzR was identified in *P. aureofaciens* 30–84, *P. fluorescens* 2–79, and *P. chlororaphis* PCL1391. Similar to other AHL-mediated QS systems, the *phzI* encodes an AHL synthase (side chain length differs from C4 to C14, with or without hydroxyl group substitution on C-3 position) and *phzR* encodes its cognate transcription regulator [40, 43]. The *phzI* and *phzR* genes are located directly upstream of the *phzABCDEFG* gene cluster, and

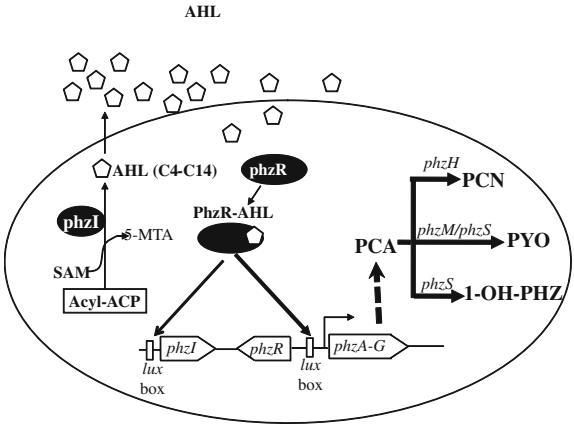

Fig. 5 Model for QS regulation in phenazine synthesis in *Pseudomonas*

positively regulated the transcription of core gene cluster for PCA synthesis through a well-defined *lux* box upstream of *phzA*. However, together with *P. aeruginosa* PAO1, another important biocontrol strain *Pseudomonas* sp. M18 possessed two complete sets of *phzABCDEFG* genes that are 99 % homolog, but without *phzI* and *phzR* [44, 45]. The PCA synthesis in *P. aeruginosa* PAO1 and *Pseudomonas* sp. strain M18 was regulated by another AHL-mediated QS system, i.e., RhlI–RhlR. In this regulatory context, the RhlI–RhlR QS system directly activated the transcription of *phzABCDEFG*, and thus promoted the PCA synthesis [44, 46, 47]. As the *las* and rhl QS systems are organized hierarchically and are interdependent in *P. aeruginosa* PAO1 and *Pseudomonas* sp. M18, the *las* QS system could regulate the PCA synthesis through modulation of the *rhl* QS system [44, 46, 48]. Besides, other environmental factors such as temperature or other global regulators such as GacA/S indirectly influenced the phenazine production through transcriptional or posttranscriptional regulation on the previously mentioned QS systems [47, 49, 50].

2.2.3 Lantibiotics in Gram-Positive Bacteria

Many Gram-positive bacteria produce small (<10 kDa) ribosomally synthesized peptide antibiotics (bacteriocins). These bacteriocins are usually categorized into two classes, i.e., class I (heat stable, post-translationally modified peptides) and class II (non-modified heat stable peptides) [51]. The great interest in these antimicrobial peptides biosynthesis is not just because they are potent antimicrobial agents, but also because they serve as QS pheromones, which in turn regulate the biosynthesis of themselves. Lantibiotics constitute a unique family of antibiotic peptides with a typical intracellular thioether bridges called (β-methyl) lanthionines and are the main members of class I bacteriocin [52]. Lantibiotics have been studied extensively because of their unusual structure properties, broad spectrum of antimicrobial activity, and increasing applications in the food industry [53]. Here we will take nisin and subtilin as examples to illustrate the QS regulation on lantibiotic synthesis (Fig. 6).

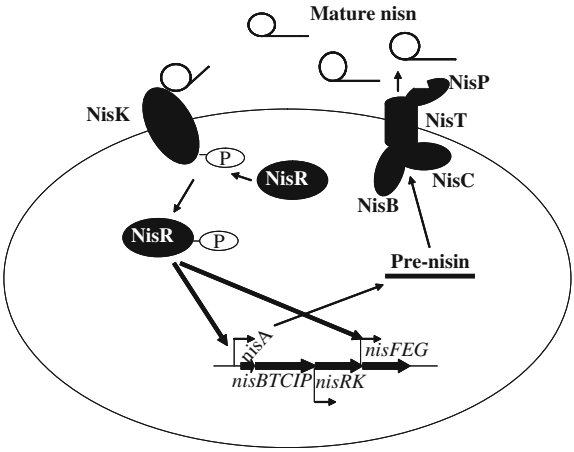

Fig. 6 Model for QS regulation on nisin biosynthesis [51, 52]

The genes for nisin and subtilin biosynthesis are organized in clusters, i.e., *nisABTCIPRKFEG* for nisin in *Lactococcus lactis* and *spaBTCSIFEGRK* in *Bacillus substilis* [54]. The gene clusters contain the structure gene encoding the lantibiotic precursors (*nisA* for nisin and *spaS* for subtilin), genes for post-translational modification (*nisB*, *nisC* and *spaB*, *spaC*, respectively), genes for secretion (*nisT* and *spaT*, respectively), genes for immunity (*nisIFEG* and *spaIFEG*, respectively), and a two-component regulation system (*nisR*, *nisK* and *spaR*, *spaK*, respectively) [54]. Gene *nisP* encodes an extracellular protease to remove the leader peptide of pre-nisin, and this cleavage is achieved by unspecific serine proteases for substilin [55]. Similar to other antimicrobial peptides, production of nisn and subtilin are inducible by the extracellularly accumulated peptides [52, 56, 57]. Production of these peptides usually only startes at the mid- to end-log growth phase, but rapidly reaches the maximum level at the beginning of stationary growth phase [52]. The rapid and massive production is achieved by positive feedback; i.e., the base-level antimicrobial peptide accumulates with increasing cell density When the concentration of peptide reaches its threshold, the peptide interactes with its cognate receptor, resulting in transmembrane signal transduction and leading to induction of the production of itself [52]. This typical QS regulation trait stimulated researchers to elucidate the QS regulation mechanism in nisin and substilin biosynthesis.

Introduction of 4-bp deletion in *nisA* gene of a nisin-producing *L. lactis* resulted in loss of nisin production and abolition of Δ*nisA* transcription [56]. However, the transcription of Δ*nisA* was restored by the exogenous addition of mature nisn or nisin analog into the culture medium. Also the induction of the transcription of Δ*nisA* was directly related to the amount of exogenously added nisin. This study indicates that nisin acts as a pheromone and induces the production of itself [56]. Further analysis showed that the two-component regulation system *nisRK* is indispensable for nisin autoregulation [58]. A QS regulatory circuit was also defined [52]. At the mid- to end-log growth phase, nisin biosynthesis started; the

extracellular nisin accumulated with increasing cell density. When the extracellular nisin reached its critical concentration, nisin interacted with the input domain of sensor kinase protein *nisK*, and the subsequent phosphortransfer from the sensor kinase transmitter domain to the receiver domain of the response regulator *nisR* led to its activation. The activated *nisR* would bind to specific *nis*-box within the promoter of *nisA*, which lead to transcription activation and induced nisin production. Studies also showed that substilin production is regulated by the *spaS–spaRK* QS system, which uses substilin (encoded by *spaS*) as the signaling molecule, and *spaRK* as a two-component signal transduction system [52, 57].

2.3 QS Regulation of Pollutants Biodegradation and Bioelectricity Generation

Although a variety of QS signaling molecules or gene circuits have been identified in bacteria that were isolated from pollutant treatment systems [59–63], only a few reports mentioned the involvement of QS in pollutant biodegradation [63–65]. Valle et al. isolated several AHL-producing bacteria from activated sludge and investigated the effect of AHL on its phenol biodegradation ability [59]. Without AHL addition, the phenol biodegradation by activated sludge was reduced at day 10 and completely lost at day 14. However, with the daily addition of 2 μM AHL mixture, phenol biodegradation ability of activated sludge remained stable at day 14 [59]. This is the first report on the effect of QS signals on pollutant treatment. They explained that the improvement on the performance of activated sludge was due to the change of the microbial community which was induced by AHL addition [59]. However, that work did not show any evidence about for the QS effect on bacterial biodegradation ability or the metabolism of pollutants. Although the mechanism is not mentioned, Kang and Park described an observation that QS signal elimination would lead to a reduction in hexadecane biodegradation by *Acinetobacter* sp. strain DR1 [64]. Recently, we isolated a strain of *P. aeruginosa* that could degrade broad-spectrum aromatics. This strain contained an active RhlIR QS system according to genetic analysis and biosensor detection [63]. AHL production was detected by *C. violaceum* CV026 during aromatics biodegradation. By using TLC and HPLC–MS/MS analysis, C4HSL and C6HSL were identified in its culture supernatant during phenol biodegradation. Interestingly, deletion of *rhlI* or *rhlIR* repressed the phenol biodegradation compared to the wild-type strain, and it could be reversed by complementation with wild-type *rhlI* or *rhlIR*, respectively. This repression by *rhlI* deletion could be relieved by exogenously adding AHL extracts or synthetic BHL. One report indicated that the RhlIR QS system is involved in the regulation of aromatics biodegradation by *P. aeruginosa* [63]. This report showed concrete evidence that the QS system is involved in the bacterial biodegradation ability. Further evidence on transcriptional and enzymatic levels indicated that the RhlIR QS system improved the catechol meta-cleavage

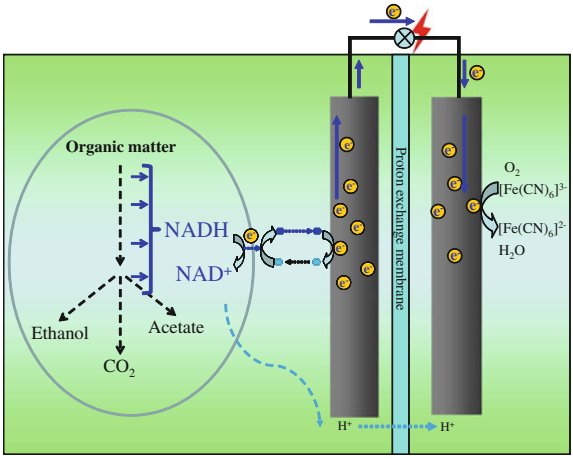

Fig. 7 Simple model for a two-chamber microbial fuel cell

pathway but with no effect on the first degradation step of phenol hydroxylation (unpublished data). It further suggested that the QS regulates metabolism of pollutants' biodegradation.

Besides environmental pollution, another serious problem that the human have encountered is the energy crisis. Microbial fuel cells (MFCs) are considered to be a promising "two birds, one stone" solution for simultaneous clean energy generation and pollutant treatment [66–69]. The bacteria in MFC could convert the chemical energy stored in the waste organic matters to bioelectricity by intracellular metabolism and extracellular electron transfer pathways (Fig. 7). Venkataraman et al. reported that *retS* knockout, which might indirectly activate the QS system, resulted in an increase in the current generation by *P. aeruginosa* (70). Recently, we proposed a novel mechanism in the reinforcement of the current output in the *P. aeruginosa* MFC, i.e., alteration of the electron transfer system to a more efficient electron shuttle by overexpressing the QS cassette [71] and Fig. 8). It was found that *P. aeruginosa* could use different electron shuttles in an MFC under different QS expression patterns, and the bioelectricity could be significantly improved by overexpression of the *rhlIR* QS system. In a dual-chamber MFC, the wild-type *P. aeruginosa* strain mainly used an electron shuttle (rather than phenazines) with a high mid-point potential of 0.20 V (vs. Ag/AgCl–KCl saturated electrode). This high mid-point potential is much closer to the cathodic potential ($\sim$0.3 V) and is believed to be unfavorable for electricity output (Fig. 8). As expected, the wild-type strain only delivered a low current output ($\sim$2.3 $\mu A/cm^2$). However, upon overexpression of the *rhl* QS system in this wild-type strain, the electron shuttle with high mid-point potential disappeared and more strikingly it was substituted by phenazines, which have a relatively low mid-point potential. According to HPLC analysis, the phenazine electron shuttles produced by the QS overexpression strain were pyocyanin and phenazine-1-carboxylate, which had a mid-point potential of -0.17 and -0.28 V, respectively. The substitution of high

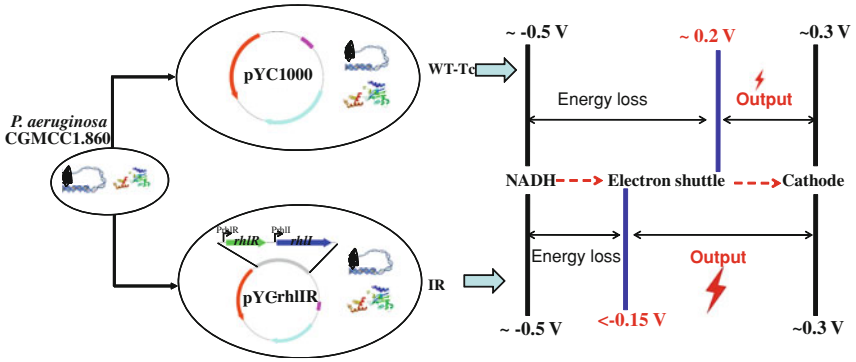

Fig. 8 Schematic illustration of bioelectricity improvement by QS overexpression in *P. aeruginosa*-inoculated MFC (modified from Ref. [71])

mid-potential electron shuttles with low ones directly led to an increase of about 1.6 times of the current output ($\sim$6.0 μA/cm^2) [71]. The results indicated that QS played important roles in bacterial electrochemical behavior.

Taken together, QS was proven to be involved in pollutant biodegradation and bioelectricity production. It may be expected to be an alternative to the solution for cleaner environment and cheaper bioenergy.

2.4 QS Regulatory Network for Synthetic Biology

Synthetic biology is an emerging and fast-moving field includes novel cellular behavior programming for a variety of applications [72–74]. Scientists believed that synthetic biology would be promising to provide solutions for many of the major global problems such as famine, disease, and energy crises [75]. The ultimate goal of synthetic biology is to build synthetic cells module by module—a bottom-up strategy, just like assembling a jumbo jet from a list of mechanical parts [75]. Although it is a long way from such a goal, a lot of genetic parts/circuits have been constructed, such as logic gates, bistable toggle switches, and oscillators. Because of the fancy molecule response characteristics of QS, it was widely used as the building block for genetic circuit construction. For example, an artificial genetic AND gate was constructed based on the hybrid promoter of $P_{luxI\text{–}lacO}$ and constitutively expressed LuxR and LacI [76]. The gene expression under this hybrid promoter can only be activated upon simultaneous addition of two kinds of activators (OHHL and IPTG). Thus, this minimal circuit showed logical AND response for induction with OHHL and IPTG. At the early stage, most constructed genetic parts mainly focused on single-cell behavior because stochastic gene expression caused cell–cell variation in a bacterial population. QS that realizes cooperative behavior at the population level could provide powerful tools for synthetic biology to coordinate microbial population dynamics and to engineer bacterial population behavior [74]. For example, a synthetic predator–prey ecosystem

consisting of two *Escherichia coli* populations was constructed by using a QS circuit to achieve bi-directional communication [77]. In this ecosystem, the predator cells can produce a QS signaling molecule that will activate the suicide gene to kill the prey cells. In contrast, the prey cells can also produce another QS signaling molecule to induce the expression of an antidote protein and then rescue the predator cells. The QS communication system ensured these bacterial behaviors could be coordinated at the population level. More interestingly, this synthetic ecosystem displayed defined eco-behaviors, such as competition or predation depending on the specific experimental conditions [76]. In all, QS is a vital building block in synthetic biology and should be crucial to future synthetic living systems, which are expected to substantially change our life-styles.

3 QS Biosensors

During the past decades, QS was proven to play important roles in many essential bioprocesses, which including microbial metabolism (primary and secondary metabolism), pathogenesis (host colonization, invasion, antibiotic resistance, etc.), plasmid conjugation, motility, and biofilm formation [1, 78]. The importance of QS led to a burst of research on QS mechanism and development of tools for QS signaling molecule detection/quantification. Because AIs are difficult to detect by conventional physical and chemical methods, biosensors that provide rapid and cost-effective alternatives have attracted much attention [2, 79]. During the past decades, there have been a series of QS signaling molecules identified in different bacterial systems (Fig. 3). Meanwhile, a large number of AI-specific receptors have been identified, which provided the possibility to construct various biosensors to meet research and application needs.

3.1 Biosensors for AHL, AIP, and AI-2

The AHL-mediated QS system is the most intensively studied cell–cell communication system, and various bacterial biosensors were constructed for the detection/quantification of AHL in samples ([80], Table 1). LuxR-type proteins usually specifically recognize AHLs produced by its cognate LuxI-type synthase. Therefore, various LuxR-type proteins have been used as detectors for AHL biosensors. For detection of short-chain AHL (C4–C8), LuxR (*V. fischeri*), TraR (*Agrobacterium tumefaciens*), CviR (*Chromobacterium violaceum*), AhyR (*A. hydrophyla*), RhlR (*P. aeruginsoa*), or SmaR (*Serratia* sp.) have been used as the sensing module [2, 81–83]. For long-chain AHL detection (C10–C16), LasR (*P. aeruginosa*) and SinR (*Sinorhizobim meliloti*) have been used [84, 85]. The output modules, which usually are bioluminescent, β-galactosidase, or fluorescence genes, are reassembled downstream of the LuxR-type regulator controlled promoters [80]. In the presence

Table 1 Typical biosensors for detection of QS signaling molecules

Strain/Plasmid	Host	QS system used	Most sensitive AI detected	Ref
pYC-rhlR	*P. aeruginosa* (*rhlI*$^-$*rhlR*$^-$)	RhlI/R	C4HSL	[2]
C. violaceum CV026	*C. violaceum* (*cvi*$^-$)	CviI/R	C6HSL	[82]
pSB401	*E. coli*	LuxI/R	3OC6HSL	[179]
pSF105 + pSF107	*P. fluorescens*	PhzI/R	3OHC6HSL	[180]
pAS-C8	Broad host range	CepI/R	C8HSL	[181]
PJZ384 + PJZ410 + PJZ372	*A. tumefaciens*	TraI/R	3OC8HSL	[105]
PSB1075	*E. coli*	LasI/R	3OC12HSL	[177]
BB170	*V. harveyi* (*luxN*::tn5Kan)	LuxS	AI-2	[94]
MM32	*V. harveyi* (*luxN*::cm, *luxS*::tn5Kan)	LuxS	AI-2	[95]
pRN7035	*Staphylococcus aureus* (*agrD*$^-$)	*agr*	*S. aureus* AIPs (Based on host)	[91]
pRN7062	*S. aureus* (agr-null)	*agr*	Group I AIPs (*S. aureus*)	[91]
pRN7105	*S. aureus* (agr-null)	*agr*	Group II AIPs (*S. aureus*)	[91]
pRN7131	*S. aureus* (agr-null)	*agr*	Group III AIPs (*S. aureus*)	[182]
pRN7107	*S. aureus* (agr-null)	*agr*	Group IV AIPs (*S. aureus*)	[91]
BD2876	*B. subtilis* (*comQ*$^-$)	*com* (*B. substilis* 168)	Group I ComX	[183]
BD3020	*B. subtilis* (*comQ*$^-$)	*com* (*B. subtilis* RO-E-2)	Group II ComX	[92]
BD2962	*B. subtilis* (*comQ*$^-$)	*com* (*B. mojavensis* RO-H-1)	Group III ComX	[183]
BD2877	*B. subtilis* (*comQ*$^-$)	*com* (*B. substilis* natto NAF4)	Group IV ComX	[183]

of its cognate AHL, the LuxR-AHL complex could activate the transcription of the output module and hence result in luminescence, enzyme activity, or fluorescence (reviewed in [80]). In addition, natural pigments are used as the output module. The pigments chosen usually are natural AHL controlled ones. Therefore, the simple design idea is to change the pigment production control from self-synthesized AHL to exogenously added AHL. By mutation on AHL synthase, the self-synthesized AHL is abolished and the QS-regulated pigment production can respond to the exogenous AHL [2, 82, 83]. *C. violaceum* CV026, which was constructed based on the CviI/R QS system, is a commonly used biosensor for C6HSL [82]. *C. violaceum* CV026 is a *cviI* mutant without AHL production, and its violacin (purple pigment) production responded to the exogenously added C6HSL. However, strain CV026

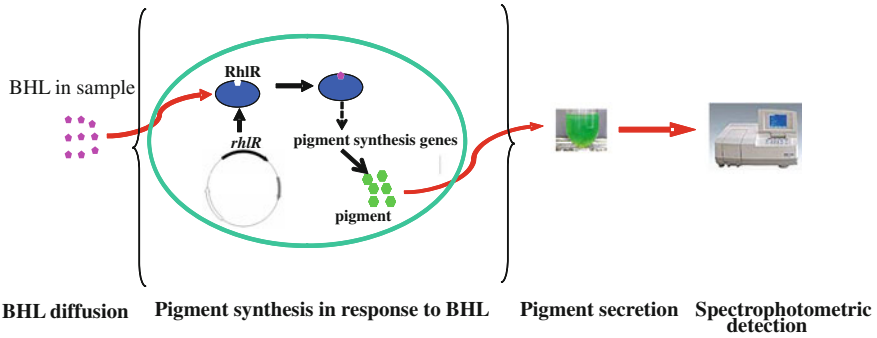

Fig. 9 The schematic illustration of the pigment-based whole-cell BHL biosensor (modified from Ref. [2])

can respond to other AHLs (C63OHSL, C8HSL, and C4HSL) although with less activity than the natural *C. violaceum* AHL (C6HSL). More interestingly, the violacin induced by short chain AHL (C4–C8) can be inhibited by long-chain AHLs (C10–C12) [82]. By quantification of extraction of the induced violacin by spectrophotometer, Blosser and Gray developed a quantification method for C6HSL by using another *C. violaceum* mutant CVblu [86]. Recently, we constructed a C4HSL biosensor by using an RhlI/R QS system [2] (Fig. 9). Similarly, a C4HSL-negative mutant was constructed and an overexpressed RhlR was used as the AHL sensing module. The engineered *P. aeruginosa* can produce a blue–green pigment in a specific response to the exogenous C4HSL. By optimization of the sensing conditions, a high sensitivity (10^4-fold more than CV026, and 300-fold more than LC–MS) for C4HSL quantification was achieved (Fig. 10). When applied in pollutant samples, the selected host strain *P. aeruginosa* CGMCC 1.860 is an aromatic resistant strain. Remarkably, this biosensor was successfully applied for C4HSL quantification in environment samples with toxic aromatic pollutants [2].

Regarding the genetic polymorphism of the AIP QS system, the AIP sensing/response system in Gram-positive bacteria is highly specific [87, 88]. For example, *S. aureus* has been divided into four groups based on the specific interactions between AIP and ArgC [89, 90]. Each group produced the structurally distinct AIP (different amino acid sequences and lengths), and only activated the *agr* response in itself and in the same group members, but showed intra-group inhibition on *agr* response [88, 90]. Therefore, a series of AIP biosensors have been constructed for application in different species and groups (Table 1). The most common AIP biosensors are constructed in the AIP gene mutant (e.g., *agrD* mutant of *S. aureus*, *comQ* mutant of *Bacillus* species) of itself or the same group members. The reporter genes (*gfp*, *yfp*, *lacZ*, *lux*, etc., optimized for expression in Gram-positive bacteria) are usually harbored on plasmids and transcriptional fused reporter genes with the AIP QS controlled promoters (e.g., P3 promoter in *agr* system in *S. aureus*, *srfA* promoter in com system in *Bacillus*) (Table 1). These biosensors use the host-expressed AIP receptors (e.g., AgrC in *S. aureus*) to detect the

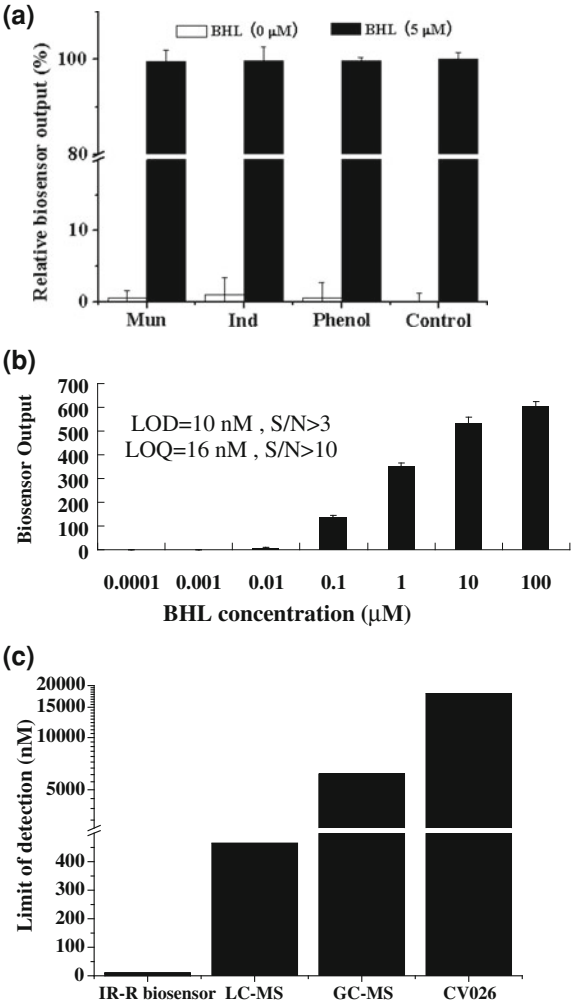

Fig. 10 Characterization of a genetically engineered BHL biosensor (*P. aeruginosa* IR-R). **a** The effect of different interferences on the biosensor output. Mun, municipal wastewater; Ind, industrial wastewater; PHE, phenanthrene; NAP, naphthalene. **b** Dose-dependent response to synthetic BHL. **c** Comparison of limit of detection (LOD) with previous reported BHL quantification methods. CV026, *C. violaceum* CV026 biosensor. (modified from Ref. [2])

exogenous AIP, process the signaling based on the AIP QS system in the host, and then activate the reporters by the inducible promoters (Fig. 3). This kind of biosensor can only specifically respond to the AIP of itself or the same group. However, by heterogeneously expressing another group AgrC in *agrC* and *agrD* double mutant, the strain of *S. aureus* could be converted to detect other groups of AIP [91]. Similarly, the ComX pheromones in *Bacillus* are defined as four different groups [92]. Biosensors for different groups of ComX were constructed in a *Bacillus substilis* mutant (*comQ*::Kan, ComQ is responsible for the maturation of

ComX precursor) by replacing the original *comXP* genes with another *comXP* that belongs to other groups [93].

For AI-2 detection, a well-known QS reporter kit (designed for detection of QS molecule AI-2 in *Vibrio*, ATCC # BAA 1116–1121) was developed by Bassler et al. (*V. harveyi* BB170 (*luxN*::tn5Kan) and *V. harveyi* MM32 (*luxN*::cm, *luxS*::tn5Kan)) is commonly used [94, 95]. Because the AI-2 QS system regulates the luciferase operon in *V. harveyi*, *V. harveyi* should be a suitable host for biosensor construction by rewiring the bioluminescence with exogenous AI-2. In *V. harveyi*, there is another QS system that used AI-1 (N-(3-hydroxybutanoyl)-L-homoserine lactone) as a signaling molecule interfering with the AI-2 signaling process [7]. Therefore, both of the AI-2 biosensors, BB170 and MM32, had an insertion mutation on the LuxN receptor needed for AI-1 detection [94]. They only responded to exogenous AI-2 by producing induced luminescence [94]. Because its original LuxS is intact in BB170, BB170 can synthesize AI-2 and produce low base-level bioluminescence without exogenous AI-2. It is also widely used as a simple tool for a qualitative test for the production of AI-2 in various bacteria [96–98]. However, for BB170 detection, supernatants from *V. harveyi* BB152 (*luxLM*::Tn5; AI-1^{-}; AI-2^{+}) and MM77 (*luxLM*::Tn5, *luxS*::Tn5; AI-1^{-}; AI-2^{-}) are usually required to serve as positive and negative controls [99]. By mutation on AI-2 synthase LuxS and AI-1 receptor LuxN, the strain MM32 thus produced no endogenous AI-2 and only responded to exogenous AI-2; it showed better performance than BB170 with lower base-level luminescence [95]. However, it should be noted that these biosensors were sensitive to growth conditions (such as pH and glucose) and bioluminescence could be inhibited by a high concentration of AI-2 [100–103].

3.2 Improvement on QS Biosensors

Even though a number of QS biosensors have been constructed so far, there are only a few reports on QS biosensor improvement. By using genetic and protein engineering strategies, one can expect to enhance the biosensor sensitivity, as well as the wide or narrow substrate spectrum [104]. It is reasonable to expect to enhance the biosensor sensitivity by engineering the sensor module (higher concentration of sensor module or higher bounding activity with target). Overexpression of the LuxR-type protein is confirmed as a useful strategy to synthesze more AHL detectors intracellularly and hence enhance the sensitivity of AHL biosensors [2, 105]. By overexpression of RhlR using a multi-copy plasmid, the sensitivity of a C4HSL biosensor was significantly enhanced [2]. Also, by using T7 expression system to overproduce TraR, the limit of detection (3 pM for 3OC8HSL) for this biosensor was reduced by at least 100-fold [105]. Moreover, Ling et al. constructed a *P. aeruginosa* biosensor for detection of a broad spectrum of AHLs by using a reporter plasmid containing *tacp-lasR*, *tacp-rhlR*, and *lasB*'-*lacZ* [106]. This reporter plasmid confers to non-signaling *P. aeruginosa* the ability to respond to a

wide variety of exogenous AHLs (C4HSL, C6HSL, 3OC6HSL, C7HSL, C12HSL, and 3OC12HSL) by induction of β-galactosidase [107]. Another versatile plasmid that tandemly assembles 8 *luxI*-family gene promoters (*luxI*, *cviI*, *ahlI*, *rhlI*, *cepI*, *phzI*, *traI*, and *ppuI*) upstream of a promoterless *lacZ* gene was constructed by Steindler et al. [108]. This plasmid biosensor was demonstrated to be useful to identify QS LuxR-family orphans in bacterial strains not producing AHLs [108]. If it is co-transformed with plasmid harboring different LuxR-type receptors, a super biosensor that could detect much a very broad spectrum of AHLs would be expected.

By using site-directed mutagenesis or direct evolution, a series of autoinducer receptor variants that respond to different AHLs at different levels and specificities were obtained [109–112]. By two-generation screening of the variants exhibiting increased response to C8HSL (only showing a weak interaction with wild-type LuxR) in LuxR mutant libraries (constructed by error-prone PCR and DNA shuffling), a LuxR-G2E variant that maintained a wild-type response to 3OC6HSL (the native AHL) and showed 100-fold increase in sensitivity to C8HSL was obtained [109]. As a result, LuxR-G2E could detect a much broader substrate spectrum (C5HSL, C6HSL, 3OC6HSL, C8HSL, C10HSL, C12HSL, 3OC12HSL, C14HSL) than the wild type [109, 111]. By an additional two rounds of directed evolution based on LuxR-G2E, the substrate spectrum was further broadened; LuxR-G4E obtained showed a strong response to C4HSL, which could not be detected by G2E [110]. In contrast, a specificity-enhancing variant of LuxR-G2E, which only responded to straight-chain AHL but no longer responded to 3OC6HSL and 3OC12HSL, was obtained by using a novel dual positive–negative selection system [111]. The alternation in autoinducer specificity of TraR or AgrC was also achieved by site-directed mutagenesis [109, 112]. Three residue changes in the AgrC-IV receptor were identified to be sufficient to convert the AIP recognizing specificity to AgrC-I [112]. Although most of these studies did not focus on biosensors, these AI receptor variants with different specificities and sensitivities could be used for biosensor construction, and improvement in specificity or sensitivity would be expected. The results of these studies imply that the biosensor specificity and sensitivity could be efficiently manipulated by engineering the AI receptors with various molecular strategies such as directed evolution, site-directed mutagenesis, and promoter engineering. Moreover, in the near future, with adequately detailed structure–function information on autoinducer receptor, we can expect computational design of new receptors with desired specificity and sensitivity [113, 114] to have customized QS biosensors.

Most of the reported QS biosensors were constructed for pure laboratory research use (for detection of samples with several extraction/purification steps and in well-defined culture condition), while a few efforts have been made toward their application in real environmental samples. Intended for application in samples containing toxic pollutants, we previously isolated aromatics resistant *P. aeruginosa* from rubber rubbish and used it as a host strain to construct a whole-cell biosensor for quantification of C4HSL in wastewater samples [2]. As expected, the biosensor response was not affected by toxic aromatics, and it was

demonstrated to be successfully applied in synthetic and real wastewater samples (Fig. 10). Two in situ AHL biosensors were also constructed recently [115, 116]. By using an indigenous soil bacterium as the host strain, a biosensor containing a P_{luxI} controlled *gfp*-reporter plasmid was constructed [115]. This biosensor was introduced into compost soil microcosms; after incubation, cells were harvested and analyzed by flow cytometry. By using this in situ technology, the AHL-producing microcosms were successfully discriminated [115]. Another approach for in situ AHL monitoring used a self-transmissible biosensor plasmid. Lumjiaktase et al. [116] constructed a RP4 replicon based AHL biosensor plasmid. This plasmid could self-spread within mixed biofilm, and it was applied for in situ identification of AHL-producing bacteria in lake sediment [116].

4 Effect of QS on Pathogen Infection and its Application in Diagnosis and Drug Discovery

4.1 QS Regulation on Pathogen Infection

The pathogen infection process is like a war between pathogens and human defense systems (immune defense and antimicrobial agents' treatment). Surpassing and overtaking the human defenses is the main goal for pathogens in achieving successful infections. The QS systems provide a sophisticated mechanism for pathogens to escape from the host immune defense at the early colonization stage, and to overwhelm and destroy the host defenses by rapid production of massive virulence factors once the population expands to a critical level (reviewed in [117–119]). In addition, QS systems also render antibiotic resistant strategies for pathogens to fight against the antimicrobial treatment [120–123]. Therefore, there is great interest in elucidating the QS effect on pathogenesis, which will provide insights on pathogen infection and the opportunity to develop new diagnostic or treatment tools. Here, we take two significant pathogens as examples to briefly introduce QS regulation on Gram-negative and Gram-positive bacterial infections.

4.1.1 *Pseudomonas aeruginosa*

P. aeruginosa is an important opportunistic pathogen that is commonly involved in nosocomial infections and burn wound infection; it is a leading cause of death in cystic fibrosis (CF) lung disease [124, 125]. So far, at least three QS systems have been identified in *P. aeruginosa* and are proven to be involved in its pathogenesis [15] (Fig. 11). Two of these are LasIR and RhlIR QS systems, which use 3OC12HSL and C4HSL as signaling molecules, respectively [126–129]. The third QS system is an AHL-independent system that consists of a LysR-type regulator PqsR and the

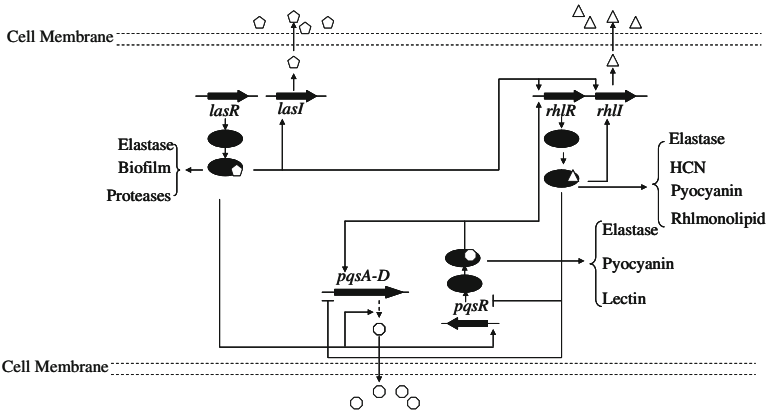

Fig. 11 Model for QS networks in *P. aeruginosa* and its regulation on virulences [3, 15, 16]. *Solid arrows* indicate positive regulation; *solid T-bars* indicate, negative regulation

pseudomonas quinolone signal (PQS, 2-heptyl-3-hydroxy-4-quinolone) called PQS system [130, 131].

P. aeruginosa usually secretes a variety of extracellular virulence determinants to kill or change signal transduction in mammalian cells. However, expression of these toxins is metabolically expensive [132]; early secretion of toxins will trigger the innate immunity system, which is a disaster for pathogens. Therefore, toxin expression should be exquisitely regulated so that it is secreted at the right time and location [132]. It has been determined that most of the virulence factors are regulated by the fine-tuned QS systems in *P. aeruginosa* [133]. According to transcriptome analysis, the *las* and *rhl* QS systems controlled the transcription of over 300 genes, representing about 6 % of the *P. aeruginosa* genome [134]. These include a large number of virulent genes such as *lasAB*, *rhlAB*, *hcnABC*, and *phzCDE* [134]. By comparative analysis between site-specific QS gene deletion mutants and wild-type strains, *las* and *rhl* QS systems were found to regulate the production of multiple virulence factors including elastase [135], alkaline protease [136], hydrogen cyanide [137], exotoxin A [138], rhamnolipid [139], pyocyanin [140], and lectins [141] (Fig. 6). More interestingly, an additional timing regulation mechanism (suggested at the LasR and RhlR receptor level) besides AHL accumulation may exist to ensure that the virulence factors are produced at the right time [134]. The PQS system has been shown to control several virulence factors, such as pyocyanin, elastase, and lectin [118, 142] (Fig. 6). Because the three QS systems are cross-linked, one specific virulence factor might be simultaneously regulated by two or three systems; this regulation may occur in parallel, crossover, or hierarchically [15] (Fig. 6). Besides various virulent weapons, *P. aeruginosa* evolved some defense helmets such as the formation of biofilm and resistance to multiple antibiotics, which were also regulated by QS systems [143, 144]. In addition, in vivo and clinical studies also confirmed the importance of QS regulation on *P. aeruginosa* infection. Both C4HSL and 3OC12HSL have

Table 2 Typical antibiotics biosynthesis controlled by QS systems

Antibiotics	Strain	QS system involved	Ref
Carbapenem	*Serratia* sp. ATTCC 39006	SmaI/R	[30]
	E. carotovora	CarI/R	[33]
	Serratia sp. ATTCC 39006	LuxS	[38]
Prodigiosin	*Serratia* sp. ATTCC 39006	SmaI/R	[30]
	S. marcescens ATCC 274	LuxS	[38]
Thailandamide	*Burkholderia thailandensis*	ThaA/?	[184]
Phenazines	*P. chlororaphis* 30–84	PhzI/R	[185]
	P. fluorescens 2–79	PhzI/R	[180]
	P. chlororaphis PCL1391	PhzI/R	[186]
	P. aeruginosa PAO1	RhlI/R, PQS	[15, 140]
	Pseudomonas sp. M18	RhlI/R	[44, 46]
Pimaricin	*Streptomyces natalensis*	PimM/PI	[187, 188]
Mupirocin	*P. fluorescens* NCIMB 10586	MupI/R	[189]
Pyoluteorin	*Pseudomonas* sp. M18	RhlI/VqsR	[190, 191]
		PQS	[192]
Pyrrolnitrin	*B. cepacia*	CepI/R	[193]
	Serratia plymuthica	SplI/R	[194]
Bactobolin	*B. thailandensis* E264	BtaI2/R2	[195]
Fosfomycin	*Streptomyces fradiae*	FomR/?	[196]
Nisin	*L. lactis*	Nisin/NisRK	[56]
Subtilin	*B. subtilis*	Subtilin/SpaRK	[57]
Blp Bacteriocins	*Streptococcus thermophilus*	Blp/BlpRH	[197]
Plantaricin	*Lactobacillus plantarum*	Plantarcin/PlnB/PlnC/D	[198]

been detected in sputum from *P. aeruginosa* infected patients with CF [145, 146]. Studies on various animal infection models showed that mutation on QS regulon leads to less severe tissue destruction, reduced pneumonia, reduced infections dissemination, and reduced mortality compared to wild-type *P. aeruginosa* [147–152]. These results indicate that QS systems are active during *P. aeruginosa* infection and functional QS systems play essential roles in acute or chronic infections (Table 2).

4.1.2 *Staphylococcus aureus*

S. aureus is a typical Gram-positive pathogen that uses QS to control its pathogenesis [118]. *S. aureus* is considered to be another versatile and dangerous human pathogen. It causes multiple high mortality infections such as bacteremia, endocarditis, sepsis, and toxic shock syndrome (reviewed in [153, 8]). *S. aureus* is very dangerous to humans not just because of its capability to produce a diverse arsenal of virulence factors and its increasing resistance to multi-antibiotics [8], but also because it is commensally colonized in 30 to 50 % of healthy adults [153]. *Agr* The QS system is responsible for its switch from a colonizing commensal bacterium to an aggressive pathogen [118, 154]. The *agr* system in *S. aureus* has been

studied as a model QS system in Gram-positive bacteria as introduced in Sect. 1, and its effect on *S. aureus* infections will be discussed here.

According to transcriptomic and proteomic analyses, over 20 virulent genes are regulated by the *agr* QS system [155, 156]. As described in Sect. 1 and Fig. 2b, *agr* regulation is mainly relies on the P3 promoter controlled RNAIII. RNAIII is a 514-nt bifunctional RNA, i.e., mRNA encoding δ-hemolysin and a regulatory RNA [156, 157]. The regulatory RNA RNAIII is the QS effector that regulates a variety of virulence factors. The *agr* response virulence factors are comprised of two groups, i.e., cell surface factors (group I) responsible for early-stage attachment to host cells and evasion of host innate immune systems, and extracellular virulence factors (group II) responsible for the invasion and toxin production [118, 156]. Murphy et al. [156] showed that cell surface associated factors are predominately expressed during early-log-phase and repressed by the *agr* system at high cell densities. The extracellular virulence factors, including exoenzymes and toxins, are produced at the basal level during early-log-phase and upregulated by the *agr* system at high cell densities [156]. This *agr* regulation mechanism facilitated the initial *S. aureus* colonization on host cells and strictly repressed the expression of exoenzymes and toxins to evade the host immune system during the early stage. The upregulation of exoenzymes and toxins facilitates the bacteria to rapidly invade the host cells and causes disease when high cell density is reached. In contrast to *P. aeruginosa*, the QS system activates the detachment of biofilm in *S. aureus* by repressing the group I factors that are responsible for biofilm formation at high cell densities [158]. The detached cells can colonize other sites to cause a spreading invasion or infect other persons to cause person-to-person transmission [8, 153]. Although the mechanism is still controversial, it is in line with its metastatic infections and high frequency observations of acquired nosocomial infections [153].

4.2 QS as a Potential Biomarker for Pathogen Detection and Disease Diagnosis

As described previously, a considerable amount of in vitro and in vivo evidences shows that QS plays an important role in pathogen infections. Therefore, researchers hypothesized that QS may serve as a biomarker for diagnostic purposes in the management of bacteria-related diseases [159, 160].

Some PCR-based methods have been developed to use QS as a biomarker to specifically detect various pathogens [161–163]. By designing a set of primers targeting the QS genes of pathogens, some pathogens were specifically detected and the presence of pathogens in various samples was rapidly discriminated [161–163]. For example, by using a set of primers targeting *sdiA* QS genes in *Salmonella* spp., a total of 101 different serotypes of *Salmonella* (155 strains) could be specifically detected [81 non-*Salmonella* strains (24 different species) showed negative results]. Moreover, this PCR-based method was successfully applied to specifically detect

Salmonella in contaminated human fecal samples with a detection limit of 10^2 CFU/g [161]. Although the PCR-based diagnostic method could specifically check for the presence of the targeting pathogen, it is hard to provide information about the QS activity in the infected samples. However, the activity of QS is much more important than its existence for determining the infection stage. For example, the activation of QS is the key step to switch *S. aureus* from a commensal to an aggressive pathogen (Sect. 4.1.2). Specific quantification of QS signaling molecules or effectors, which was the advantage of biosensor, could give us insight into the activity of QS.

Various biosensor systems for the detection/quantification of QS signaling molecules have been developed (introduced in Sect. 4). Kumari et al. attempted to detect AHLs in clinical samples and test whether AHL could be employed as a biomarker for bacteria-related disorders by using the *gfp*-based biosensing system [160]. They successfully detected the presence of AHLs in saliva and stool samples. More interestingly, the levels of AHLs were significantly different between samples from healthy volunteers and samples from patients with Crohn's disease [159, 160]. The difference was further confirmed by using HPLC–MS/MS analysis [159]. Although it is difficult to conclude the precise relationship between AHLs (type and concentration) and the bacteria-related disorder due to the limited number of samples analyzed, they suggested that QS signaling molecules may be potential biomarkers for the diagnosis of bacteria-related diseases [159, 160]. However, special attention should be paid to the following aspects: A significant number of clinical samples should be carefully analyzed to test whether QS signaling molecules could be considered as biomarkers for each specific disease. Before testing, rigorous studies should be conducted to assess analytical performance when applied to such clinical samples. Notably, the co-existence of different QS signaling molecules may cause cross-inhibition on biosensor detection (e.g., long-chain AHL would inhibit violacin of *C. violaceum* CV026, which responded to short-chain AHL). The concentration of QS signaling molecules is much lower at the early infection stage, which might result in negative results by biosensor diagnosis for early diagnosis. Therefore, a combination of PCR and the QS biosensor method could provide comprehensive information about QS during pathogen infection. However, a combination of QS diagnosis with another conventional strategy has been strongly suggested for pathogen infection diagnosis, and the sensitivity of QS biosensor should be improved for early diagnosis.

4.3 QS as an Antimicrobial Target for Drug Discovery

Considering the increasing antibiotic resistance and threat of postantibiotic era [164, 165], new strategies to combat microbial infections has attracted much attention. The selective pressure/motivation for bacterial resistance evolution is the stress imposed by conventional antibiotics that are aimed at bacterial viability [165, 166]. New strategies targeting the functions essential for infections rather

than bacterial viability have been investigated over the past decades [164]. Anti-virulence, which did not impose any growth stress and thus no risk of resistance, was considered to be a promising strategy [164, 165].

As described in Sect. 3.1, a QS system acting as a global regulator controlled a variety of virulence factors in many clinically important pathogens. Moreover, many QS-deficient pathogens lost the ability to infect or at least caused less severe infections. Therefore, interference with the QS system was considered to be a compelling approach to fight against microbial infections [165]. Theoretically, interruption in any step of the QS regulatory circuit (autoinducer synthesis, autoinducer-receptor interaction, signal transduction, etc.) would abolish its regulation on microbial infection. Based on the different targets, the identified inhibitors or antagonists could be divided into at least four groups. The group I inhibitors target autoinducer synthesis and accumulation. SAM (S-adenosylmethionine) analogs (interfering with AHL synthesis) [167] and SRH (S-ribosyl-L-homocysteine) analogs (interfering with AI-2 synthesis) [168, 169] are the main representatives of this group. In addition, enzymes with autoinducer degradation abilities (review in [170]) and antibodies that sequestrate the autoinducers [171] could abolish pheromone accumulation and disrupt the QS. Autoinducer receptors are the target of Group II inhibitors/antagonists. Analogs of autoinducers are a large family of this group. The various analogs with QS inhibition activity could bind to the autoinducer receptors to prevent interaction with its actual autoinducer, resulting in disruption of QS [172]. The signal transduction process and the downstream QS effectors are the targets of groups III and IV, respectively. These two groups are mainly composed of the inhibitors of peptide-dependent and AI-2 QS systems.

By using QS bioreporter strains for in vitro screening, researchers identified a large number of potential QS inhibitors or antagonists (reviewed in [172]) from synthetic or natural compound libraries. Most of the inhibitors and antagonists showed strong inhibition on the production of virulence factors by important pathogens [172]. For example, two inhibitors that resembled the acyl-homoserine lactone molecule were screened out from a library of 200,000 compounds by using an ultra-high throughput in vitro screening based on PAO-MW1 bioreporter strains [173]. More importantly, one of these two inhibitors (12-carbon aliphatic tail attached to a phenyl ring) inhibited 129 QS-controlled genes in *P. aeruginosa* PAO1 at a concentration of 100 μM. With the addition of this inhibitor, the pyocyanin production was inhibited by about 90 % and elastase production was reduced by 60 % [173]. Remarkably, the in vivo anti-virulence/anti-infection activity of several inhibitors or antagonists has been confirmed in different animal infection models [171, 172, 174]. Interestingly, some inhibitors/antagonists disrupted QS with several different mechanisms. For example, the well-known halogenated furanone, (5Z)-4-bromo-5-(bromomethylene)-3-butyl-2(5H)-furanone, showed broad-spectrum QS inhibition activity by interfering with AHL receptors [175, 176] or inhibiting AI-2 synthase LuxS [177]. To date, a large series of inhibitors and antagonists of the bacterial QS system have been identified (reviewed in [172]), and most of these showed strong inhibition on production of virulence factors. Although many potential inhibitors/antagonists have been

obtained, more in vivo research should be conducted to address their efficiency on infection control. Because QS is a widespread global regulatory mechanism, the ecological effect of QS disruption/interference on other commensal beneficial microbial flora should be taken into account. More importantly, although no risk of microbial resistance was claimed, attention should be directed to concrete long-term and rigorous evidence to address whether there is the possibility for bacteria to evolve resistance to QS disruption [178].

5 Concluding Remarks and Perspectives

This chapter reviewed the recent progress in QS regulation on microbial metabolism and bacterial pathogenesis. It introduced recent endeavors in novel antimicrobial agents development based on quorum quenching, disease diagnosis based on QS signaling molecule detection, and sensitive QS biosensors developed for various applications.

The findings of QS regulation on microbial metabolism have provided us with a possibility to manipulate the target metabolic pathway at the population level. Population- level control could coordinate the cell populations to maximize production ability, and it is substantially different from previous regulation patterns that only focused on the individual cells. We envision that QS regulatory circuits can also serve as a model system to be incorporated into the traditional fermentation/biodegradation process, and hence control the fermentation or pollutant degradation processes at the population level. To date, knowledge of QS regulation on pathogenesis is still limited to several model bacteria. Development of novel antimicrobial agents or diagnosis strategies based on QS mechanisms is heavily dependent on our knowledge in its role on pathogenesis. Systematic research on the role of QS in disease-related bacteria should be addressed because QS quenching is expected to be the next generation of antimicrobial strategy.

QS may be one of the most important bacterial regulatory systems for human life. It is not only a key regulon in death (mortal infections), but it also provides hope for life because it is related to the production of fuels and antibiotics, as well as diagnosis. QS expected to be the target of the next generation of antimicrobial agents, and it may be is the sole hope for the postantibiotic era. Bacteria are surely a double-edged sword for human beings, but the QS regulatory system links these two sides. QS can to reduce the danger of bacteria and fully use their advantages for the benefit of human life.

Acknowledgments We gratefully acknowledge the financial support from the National Natural Science Foundation of China (project Nos. 30821005 and 20876096) and the National Key Basic Research Program of China (973 Program, Nos. 2009CB118906 and 2012CB721006). YCY thanks the financial support from the Biofuels Institute and the start-up grant from Jiangsu University. JJZ appreciates the National 985 Project and the University Distinguished Professorship program (SJTU).

References

1. Bassler BL, Losick R (2006) Bacterially speaking. Cell 125:237–246
2. Yong YC, Zhong JJ (2009) A genetically engineered whole-cell pigment-based bacterial biosensing system for quantification of N-butyryl homoserine lactone quorum sensing signal. Biosens Bioelectron 25:41–47
3. Fuqua C, Greenberg EP (2002) Listening in on bacteria: acyl-homoserine lactone signalling. Nat Rev Mol Cell Biol 3:685–695
4. Waters CM, Bassler BL (2005) Quorum sensing: cell-to-cell communication in bacteria. Annu Rev Cell Dev Biol 21:319–346
5. Fuqua C, Winans SC, Greenberg EP (1994) Quorum sensing in bacteria: the LuxR-LuxI family of cell density-responsive transcriptional regulators. J Bacteriol 176:269–275
6. Visick KL, Foster J, Doino J et al. (2000) *Vibrio fischeri lux* genes play an important role in colonization and development of the host light organ. J Bacteriol 182:4578–4586
7. Ng WL, Bassler BL (2009) Bacterial quorum-sensing network architectures. Ann Rev Genet 43:197–222
8. George EA, Muir TW (2007) Molecular mechanisms of agr quorum sensing in virulent *Staphylococci*. ChemBioChem 8:847–855
9. Xavier KB, Bassler BL (2003) LuxS quorum sensing: more than just a numbers game. Curr Opin Microbiol 6:191–197
10. Winzer K, Hardie KR, Williams P (2003) LuxS and autoinducer-2: their contribution to quorum sensing and metabolism in bacteria. Adv Appl Microbiol 53:291–396
11. Ng WL, Wei Y, Perez LJ et al. (2010) Probing bacterial transmembrane histidine kinase receptor-ligand interactions with natural and synthetic molecules. Proc Natl Acad Sci 107:5575–5580
12. Chen X, Schauder S, Potier N et al. (2002) Structural identification of a bacterial quorum-sensing signal containing boron. Nature 415:545–549
13. Ruder WC, Lu T, Collins JJ (2011) Synthetic biology moving into the clinic. Science 333:1248–1252
14. Tu KC, Long T, Svenningsen SL et al. (2010) Negative feedback loops involving small regulatory RNAs precisely control the *Vibrio harveyi* quorum-sensing response. Mol Cell 37:567–579
15. Williams P, Camara M (2009) Quorum sensing and environmental adaptation in *Pseudomonas aeruginosa*: a tale of regulatory networks and multifunctional signal molecules. Curr Opin Microbiol 12:182–191
16. Atkinson S, Williams P (2009) Quorum sensing and social networking in the microbial world. J R Soc Interface 6:959–978
17. Sandoz KM, Mitzimberg SM, Schuster M (2007) Social cheating in *Pseudomonas aeruginosa* quorum sensing. Proc Natl Acad Sci U S A 104:15876–15881
18. Diggle SP, Griffin AS, Campbell GS et al. (2007) Cooperation and conflict in quorum-sensing bacterial populations. Nature 450:411-U7
19. Johansen L, Bryn K, Stomer FC (1975) Physiological and biochemical role of the butanediol pathway in *Aerobacter* (Enterobacter) *aerogenes*. J Bacteriol 123:1124–1130
20. Kovacikova G, Lin W, Skorupski K (2005) Dual regulation of genes involved in acetoin biosynthesis and motility/biofilm formation by virulence activator AphA and the acetate-responsive LysR-type regulator AlsR in *Vibrio cholerae*. Mol Microbiol 57:420–433
21. Houdt RV, Moons P, Buj MH et al. (2006) N-Acyl-L-homoserine lactone quorum sensing controls butanediol fermentation in *Serratia plymuthica* RVH1 and *Serratia marcescens* MG1. J Bacteriol 188:4570–4572
22. Houdt RV, Aertsen A, Michies CW (2007) Quorum-sensing-dependent switch to butanediol fermentation prevents lethal medium acidification in *Aeromonas hydrophila* AH-1N. Res Microbiol 158:379–385

23. Lenz DH, Mok KC, Lilley BN et al. (2004) The small RNA chaperone Hfq and multiple small RNAs control quorum sensing in *Vibrio harveyi* and *Vibrio cholerae*. Cell 118:69–82
24. Wolfe AJ (2005) The acetate switch. Microbiol Mol Biol Rev 69:12–50
25. Wolfe AJ (2008) Quorum sensing flips the acetate switch. J Bacteriol 190:5735–5737
26. Studer SV, Mandel MJ, Ruby EG (2008) AinS quorum sensing regulates the *Vibrio fischeri* acetate switch. 190:5915–5923
27. McGowan SJ, Holden MTG, Bycroft BW et al. (1999) Molecular genetics of carbapenem antibiotic biosynthesis. Antonie Van Leeuwenhoek 75:135–141
28. Coulthurst SJ, Barnard AML, Salmond GPC (2005) Regulation and biosynthesis of carbapenem antibiotics in bacteria. Nat Rev Microbiol 3:295–306
29. McGowan SJ, Sebaihia M, Porter LE et al. (1996) Analysis of bacterial carbapenem antibiotic production genes reveals a novel β-lactam biosynthetic pathway. Mol Microbiol 22:415–426
30. Thomson NR, Crow MA, McGowan SJ et al. (2000) Biosynthesis of carbapenem antibiotic and prodigiosin pigment in *Serratia* is under quorum sensing control. Mol Microbiol 36:539–556
31. Bainton NJ, Stead P, Chhabra SR et al. (1992) N-(3-oxohexanoyl)-L-homoserine lactone regulates carbapenem antibiotic production in *Erwinia carotovora*. Biochem J 288:997–1004
32. Welch M, Todd DE, Whitehead NA et al. (2000) N-Acyl homoserine lactones binding to the CarR receptor determines quorum-sensing specificity in *Erwinia*. EMBO J 19:631–641
33. McGowan SJ, Barnard AML, Bosgelmez G et al. (2005) Carbapenem antibiotic biosynthesis in *Erwinia carotovora* is regulated by physiological and genetic factors modulating the quorum sensing-dependent control pathway. Mol Microbiol 55:526–545
34. McGowan SJ, Sebaihia M, Jones S et al. (1995) Carbapenem antibiotic production in *Erwinia carotovora* is regulated by CarR, a homologue of the LuxR transcriptional regulator. Microbiol SGM 141:541–550
35. Cox ARJ, Thomson NR, Bycroft B et al. (1998) A pheromone-independent CarR protein control carbapenem antibiotic synthesis in the opportunistic human pathogen *Serratia marcescens*. Microbiol SGM 144:201–209
36. Slater H, Crow M, Everson L et al. (2003) Phosphate availability regulates biosynthesis of two antibiotics, prodigiosin and carbapenem, in *Serratia* via both quorum-sensing-dependent and -independent pathways. Mol Microbiol 47:303–320
37. Fineran RC, Slater H, Everson L et al. (2005) Biosynthesis of tripyrrole and β-lactam secondary metabolites in *Serratia*: integration of quorum sensing with multiple new regulatory components in the control of prodigiosin and carbapenem antibiotic production. Mol Microbiol 56:1495–1517
38. Coulthurst SJ, Kurz CL, Salmond GPC (2004) *luxS* mutants of *Serratia* defective in autoinducer-2-dependent quorum sensing show strain-dependent impacts on virulence and production of carbapenem and prodigiosin. Microbiol SGM 150:1901–1910
39. Chin-A-Woeng TFC, Bloemberg GV, Lugtenberg BJJ (2003) Phenazines and their role in biocontrol by *Pseudomonas* bacteria. New Phytolog 157:503–523
40. Juhas M, Eberl L, Tummler B (2005) Quorum sensing: the power of cooperation in the world of Pseudomonas. Environ Microbiol 7:459–471
41. He YW, Zhang LH (2008) Quorum Sensing and Virulence Regulation in *Xanthomonas campestris*. FEMS Microbiol Rev 32:842–857
42. Mavrodi DV, Blankenfeldt W, Thomashow LS (2006) Phenazine compounds in fluorescent Pseudomonas spp. biosynthesis and regulation. Annu Rev Phytopathol 44:417–445
43. Kay E, Humair B, Denerbaud V et al. (2006) Two GacA-dependent small RNAs modulate the quorum sensing response in *Pseudomonas aeruginosa*. J Bacteriol 188:6026–6033
44. Huang JF, Xu YQ, Zhang HY et al. (2009) Temperature-dependent expression of *phzM* and its regulatory genes *lasI* and *ptsP* in rhizosphere isolate *Pseudomonas* sp. strain M18. Appl Environ Microbiol 75:6568–6580

45. Latifi A, Foglino M, Tanaka K et al. (1996) A hierarchical quorum-sensing cascade in Pseudomonas aeruginosa links the transcriptional activators LasR and RhlR (VsmR) to expression of the stationary-phase sigma factor RpoS. Mol Microbiol 21:1137–1146
46. Lu JS, Huang XQ, Zhang MY et al. (2009) The distinct quorum sensing hierarchy of *las* and *rhl* in *Pseudomonas* sp. M18. Curr Microbiol 59:621–627
47. Stover CK, Pham XQm Erwin AL et al. (2000) Complete genome sequence of *Pseudomonas aeruginosa* PAO1, and opportunistic pathogen. Nature 406:959–964
48. Li YQ, Du XL, Lu ZJ et al. (2011) Regulatory feedback loop of two phz gene clusters through 5′-untranslated regions in Pseudomonas sp. M18. PLoS ONE 6:e19413
49. Chin-A-Woeng TFC, van den Broek D, de Voer G et al. (2001) Phenazine-1-carboxamide production in the biocontrol strain Pseudomonas chlororaphis PCL1391 is reulated by multiple factors secreted into the growth medium. Mol Plant Microbe Inter 14:969–979
50. Haas D, Defago G (2005) Biological control of soil-borne pathogens by fluorescent *Pseudomonas*. Nat Rev Microbiol 3:307–319
51. Eijsink VGH, Axelsson L, Diep DB et al. (2002) Production of class II bacteriolcins by lactic acid bacteria; an example of biological warfare and communication. Antonie Van Leewenhoek 81:639–654
52. Kleerebezem M (2004) Quorum sensing control of lantibiotic production; nisin and subtilin autoregulate their own biosynthesis. Peptides 25:1405–1414
53. Twomey D, Ross RP, Ryan M (2002) Lantibiotics produced by lactic acid bacteria: structure, function and applications. Antonie Van Leeuwenhoek 82:165–185
54. Siezen RJ, Kuipers OP, de Vos WM (1996) Comparison of lantibiotic gene clusters and encoded proteins. Antonie Van Leeuwenhoek 69:171–184
55. van der Meer JR, Polman J, Beerthuyzen MM et al. (1993) Characterization of the *Lactococcus lactis* nisin A operon genes *nisP*, encoding a subtilisin-like serine protease involved in precursor processing, and *nisR*, encoding a regulatory protein involved in nisin biosynthesis. J Bacteriol 175:2578–2588
56. Kuipers OP, Beerthuyzen MM, de Ruyter PGGA et al. (1995) Autoregulation of nisin biosynthesis in *Lactococcus lactis* by signal transduction. J Biol Chem 270:27299–27304
57. Stein T, Heinzmann S, Kiesau P et al. (2003) The spa-box for transcriptional activation of subtilin biosynthesis and immunity in *Bacillus subtilis*. Mol Microbiol 47:1627–1636
58. Klein C, Kaletta C, Entian KD (1993) Biosynthesis of the lantibiotic subtilin is regulated by a histidine kinase/response regulator system. Appl Environ Microbiol 59:296–303
59. Valle A, Bailey MJ, Whiteley AS et al. (2004) N-Acyl-L-homoserine lactones (AHLs) affect microbial community composition and function in activated sludge. Environ Microbiol 6:424–433
60. Hu JY, Fan Y, Lin YH et al. (2003) Microbial diversity and prevalence of virulent pathogens in biofilms developed in water reclamation system. Res Microbiol 154:623–629
61. Morgan-Sagastume F, Boon N, Dobbelaere S et al. (2005) Production of acylated homoserine lactones by *Aeromonas* and *Pseudomonas* strains isolated from municipal activated sludge. Can J Microbiol 51:924–933
62. Yeon KM, Cheong WS, Oh HS et al. (2009) Quorum sensing: a new biofouling control paradigm in a membrane bioreactor for advanced wastewater treatment. Environ Sci Technol 43:380–385
63. Yong YC, Zhong JJ (2010) N-Acylated homoserine lactone production and involvement in the biodegradation of aromatics by an environmental isolate of *Pseudomonas aeruginosa*. Process Biochem 45:1944–1948
64. Kang YS, Park W (2010) Contribution of quorum-sensing system to hexadecane degradation and biofilm formation in *Acinetobacter* sp. strain DR1. J Appl Microbiol 109:1650–1659
65. Bassler BL (2010) Small cells–big future. Mol Biol Cell 21:3786–3787
66. Logan BE (2009) Exoelectrogenic Bacteria that Power Microbial Fuel Cells. Nat Rev Microbiol 7:375–381

67. Lovley DR (2006) Bug juice: harvesting electricity with microorganisms. Nat Rev Microbiol 4:497–508
68. Yong YC, Zhong JJ (2010) Recent advances in biodegradation in China: new microorganisms and pathways, Biodegradation engineering, and bioenergy from pollutants biodegradation. Proc Biochem 45:1937–1943
69. Yong YC, Dong XC, Chan-Park MB et al. (2012) Macroporous and monolithic three-dimensional anode for high-performance Microbial Fuel Cells. ACS Nano 6:2394–2400
70. Venkataraman A, Rosenbaum M, Arends JBA et al. (2010) Quorum sensing regulates electric current generation of *Pseudomonas aeruginosa* PA14 in bioelectrochemical systems. Electro Commun 12:459–462
71. Yong YC, Yu YY, Li CM et al. (2011) Bioelectricity enhancement via overexpression of quorum sensing system in *Pseudomonas aeruginosa*-inoculated microbial fuel cells. Biosens Bioelectron 30:87–92
72. Schwille P (2011) Bottom-up synthetic biology: engineering in a thinker's world. Science 333:1252–1254
73. Song H, Payne S, Tan C, You L (2011) Programming microbial population dynamics by engineered cell–cell communication. Biotechnol J 6:837–849
74. Collins J (2012) Bits and pieces come to life. Nature 483:S8–S10
75. Balagadde FK, Song H, Ozaki J et al. (2008) A synthetic *Escherichia coli* predator-prey ecosystem. Mol Syst Biol 4:187
76. Sayut DJ, Niu Y, Sun L (2009) Construction and enhancement of a minimal genetic AND gate. Appl Environ Microbiol 75:637–642
77. Song H, Payne S, Gray M et al. (2009) Spatiotemporal modulation of biodiversity in a synthetic chemical-meiated ecosystem. Nat Chem Biol 5:929–935
78. Williams P, Winzer K, Chan WC et al. (2007) Look who's talking: communication and quorum sensing in the bacterial world. Philos Trans R Soc B Biol Sci 362:1119–1134
79. D'Souza SF (2001) Microbial biosensors. Biosens Bioelectron 16:337–353
80. Steindler L, Venturi V (2007) Detection of quorum-sensing N-acyl homoserine lactone signal molecules by bacterial biosensors. FEMS Microbiol Lett 266:1–7
81. Swift S, Karlyshev AV, Fish L et al. (1997) Quorum sensing in *Aeromonas hydrophila* and *Aeromonas salmonicidia*: Identification of the LuxRI homologs AhyRI and AsaRI and their cognate N-acylhomoserine lactone signal molecules. J Bacteriol 179:5271–5281
82. McClean KH, Winson MK, Fish L et al. (1997) Quorum sensing and *Chromobacterium violaceum*: exploitation of violacein production and inhibition for the detection of N-acylhomoserine lactones. Microbiol SGM 143:3703–3711
83. Poulter S, Carlton TM, Su X et al. (2010) Engineering of new prodigiosin-based biosensors of *Serratia* for facile detection of short-chain N-acylhomoserine lactone quorum-sensing molecules. Environ Microbiol Rep 2:322–328
84. Llamas I, Keshavan N, Gonzalez JE (2004) Use of Sinorhizobium meliloti as an indicator for specific detection of long-chain N-acyl homoserine lactones. Appl Environ Microbiol 70:3715–3723
85. Struss A, Pasini P, Ensor CM (2010) Paper strip whole cell biosensors: a portable test for the semiquantitative detection of bacterial quorum sensing molecules. Anal Chem 82:4457–4463
86. Blosser RS, Gray KM (2000) Extraction of violacein from *Chromobacterium violaceum* provides a new quantitative bioassay for N-acyl homoserine lactone autoinducers. J Microbiol Methods 40:47–55
87. Dufour P, Jarraud S, Vandenesch F et al. (2002) High genetic variability of the agr locus in *Staphylococcus* species. J Bacteriol 184:1180–1186
88. Mandic-Mulec I, Kraigher B, Cepon U et al. (2003) Variability of the quorum sensing system in natural isolates of *Bacillus* sp. Food Technol Biotechnol 41:23–28
89. Ji G, Beavis R, Novick RP (1997) Bacterial interference caused by autoinducing peptide variants. Science 276:2027–2030

90. Jarraud S, Lyon GJ, Figueiredo AM et al. (2000) Exofoliation-producing strains define a fourth agr specificity group in *Staphylococcus aureus*. J Bacteriol 182:6517–6522
91. Lyon GJ, Mayville P, Muir TW et al. (2000) Rational design of a global inhibitor of the virulence response in *Staphylococcus aureus*, based in part on localization of the site of inhibtion to the receptor-histidine kinase, AgrC. Proc Natl Acad Sci U S A 97:13330–13335
92. Ansaldi M, Marolt D, Stebe T et al. (2002) Specific activation of the *Bacillus* quorum-sensing systems by isoprenylated pheromone variants. Mol Microbiol 44:1561–1573
93. Stefanic P, Mandic-Mulec I (2009) Social interaction and distribution of *Bacillus substilis* pherotypes at microscale. J Bacteriol 191:1756–1764
94. Bassler BL, Wright M, Showalter RE et al. (1993) Intercellular signalling in *Vibrio harveyi*: sequence and function of genes regulating expression of luminescence. Mol Microbiol 773–786
95. Miller ST, Xavier KB, Campagna SR et al. (2004) *Salmonella typhimurium* recognizes a chemically distinct form of bacterial quorum-sensing signal AI-2. Mol Cell 15:677–687
96. Jones MB, Blaser MJ (2003) Detection of a *luxS*-signaling molecule in *Bacillus anthracis*. Infect Immun 71:3914–3919
97. Han XG, Lu CP (2009) Detection of autoinducer-2 and analysis of the profile of luxS and pfs transcription in *Streptococcus suis* serotype 2. Curr Microbiol 58:146–152
98. Novak EA, Shao HJ, Daep CA et al. (2010) Autoinducer-2 and QseC control biofilm formation and in vivo virulence of *Aggregatibacter actinomycetemcomitans*. Infect Immun 78:2919–2926
99. Li X, Han Y, Yang Q et al. (2010) Detection of quorum sensing signal molecules and mutation of *luxS* gene in *Vibrio ichthyoenteri*. Res Microbiol 161:51–57
100. DeKeermaecker SC, Vanderleyden J (2003) Constraints on detection of autoinducer-2 (AI-2) signalling molecules using *Vibrio harveyi* as a reporter. Microbiol SGM 149:1953–1956
101. Turovskiy Y, Chikindas ML (2006) Autoinducer-2 bioassay is a qualitative, not quantitative method influenced by glucose. J Microbiol Methods 66:497–503
102. Vilchez R, Lemme A, Thiel V et al. (2007) Analyzing traces of autoinducer-2 requires standardization of the *Vibrio harveyi* bioassay. Anal Bioanal Chem 387:489–496
103. Zhu J, Pei D (2007) A LuxP-based fluorescent sensor for bacterial autoinducer II. ACS Chem Biol 3:110–119
104. Van der Meer JR, Belkin S (2010) Where microbiology meets microengineering: design and applications of reporter bacteria. Nat Rev Microbiol 8:511–522
105. Zhu J, Chai Y, Zhong Z et al. (2003) Agrobacterium bioassay strain for ultrasensitive detection of N-acylhomoserine lactone-type quorum-sensing molecules: detection of autoinducers in *Mesorhizobium huakuii*. Appl Environ Microbiol 69:6949–6953
106. Ling EA, Ellison ML, Pesci EC (2009) A novel plasmid for detection of N-acyl homoserine lactones. Plasmid 62:16–21
107. Chai Y, Winans SC (2004) Site-directed mutagenesis of a LuxR-type quorum-sensing transcription factor: alteration of autoinducer specificity. Mol Microbiol 51:765–776
108. Steindler L, Devescovi G, Subramoni S et al. (2008) A versatile plasmid biosensor useful to identify quorum sensing LuxR-family orphans in bacterial strains. J Microbiol Methods 73:273–275
109. Collins CH, Arnold FH, Leadbetter JR (2005) Directed evolution of *Vibrio fischeri* LuxR for increased sensitivity to a broad spectrum of acyl-homoserine lactones. Mol Microbiol 55:712–723
110. Hawkins AC, Aronld FH, Stuermer R et al. (2007) Directed evolution of *Vibrio fischeri* LuxR for improved response to butanoyl-homoserine lactone. Appl Environ Microbiol 73:5775–5781
111. Collins CH, Leadbetter JR, Arnold FH (2006) Dual selection enhances the signaling specificity of a variant of the quorum-sensing transcription activator LuxR. Nat Biotech 24:708–712
112. Chen LC, Tsou LT, Chen FJ (2009) Ligand-receptor recognition for activation of quorum sensing in Staphylococcus aureus. J Microbiol 47:572–581

113. DeGrado WF (2003) Biosensor design. Nature 423:132–133
114. Looger LL, Dwyer MA, Smith JJ et al. (2003) Computational design of receptor and sensor proteins with novel functions. Nature 423:185–190
115. Burmolle M, Hansen LH, Sorensen SJ (2005) Use of a whole-cell biosensor and flow cytometry to detect AHL production by an indigenous soil community during decomposition of litter. Microb Ecol 50:221–229
116. Lumjiaktase P, Aguilar C, Battin T et al. (2010) Construction of self-transmissible green fluorescent protein-based biosensor plasmids and their use for identification of N-acyl homoserine-producing bacteria in lake sediments. Appl Environ Microbiol 76:6119–6127
117. Boyen F, Eeckhaut V, Immerseel FV et al. (2009) Quorum sensing in veterinary pathogens: mechanisms, clinical importance and future perspectives. Vet Mcirobiol 135:187–195
118. Antunes LCM, Ferreira RBR, Buckner MMC et al. (2010) Quorum sensing in bacterial virulence. Microbiol SGM 156:2271–2282
119. Asad S, Opal SM (2008) Bench-to-beside review: quorum sensing and the role of cell-to-cell communication during invasive bacterial infection. Crit Care 12:236
120. Yao Y, Vuong C, Kocianova S et al. (2006) Characterization of the *Staphylococcus epidermidis* accessory-gene regulator response: quorum-sensing regulation of resistance to human innate host defense. J Infect Dis 193:841–848
121. Tavio MM, Aquili VD, Poveda JB et al. (2010) Quorum-sensing regulator *sdiA* and *marA* is involved in in vitro-selected multidrug resistance of *Escherichia coli*. J Antimicrob Chemoth 65:1178–1186
122. Poole K (2001) Multidrug efflux pumps and antimicrobial resistance in *Pseudomonas aeruginosa* and related organisms. J Mol Microbiol Biotech 3:255–263
123. Maseda H, Sawada I, Saito K et al. (2004) Enhancement of the *mexAB-oprM* efflux pump expression by a quorum-sensing autoinducer and its cancellation by a regulator, mexT, of the *mexEF-oprN* efflux pump operon in *Pseudomonas aeruginosa*. Antimicrob Agents Chemoth 48:1320–1328
124. Koch C, Hoiby N (1993) Pathogenesis of cystic fibrosis. Lancet 341:1065–1069
125. Bodey GP, Bolivar R, Fainstein V et al. (1983) Infections caused by *Pseudomonas aeruginosa*. Rev Infect Dis 5:279–313
126. Passador L, Cook JM, Gambello MJ et al. (1993) Expression of *Pseudomonas aeruginosa* virulence genes requires cell-to-cell communication. Science 260:1127–1130
127. Pearson JP, Gray KM, Passador L et al. (1994) Structure of the autoinducer required for expression of *Pseudomonas aeruginosa* virulence genes. Proc. Natl. Acad. Sci. U S A 91:197–201
128. Ochsner UA, Koch AK, Fiechter A et al. (1994) Isolation and characterization of a regulatory gene affecting rhamnolipid biosurfactant synthesis in *Pseudomonas aeruginosa*. J Bacteriol 176:2044–2054
129. Ochsner UA, Reiser J (1995) Autoinducer-mediated regulation of rhamnolipid biosurfactant synthesis in *Pseudomonas aeruginosa*. Proc Natl Acad Sci U S A 92:6424–6428
130. Pesci EC, Milbank JBJ, Pearson JP et al. (1999) Quinolone signaling in the cell to cell communication system of *Pseudomonas aeruginosa*. Proc Natl Acad Sci U S A 96:11229–11234
131. Gallagher LA, McKnight SL, Kuznetsova MS et al. (2002) Functions required for extracellular quinolone signalling by *Pseudomonas aeruginosa*. J Bacteriol 184:6472–6480
132. Staskawicz BJ, Mudgett MB, Dangl JL et al. (2001) Common and contrasting themes of plant and animal diseases. Science 292:2285–2289
133. Smith RS, Iglewski BH (2003) *P. aeruginosa* quorum-sensing systems and virulence. Curr Opin Microbiol 6:56–60
134. Schuster M, Lostroh CP, Ogi T et al. (2003) Identification, timing, and signal specificity of *Pseudomonas aeruginosa* quorum-controlled genes: a transcriptome analysis. J Bacteriol 185:2066–2079
135. Toder DS, Ferrell SJ, Nezezon JL et al. (1994) *lasA* and *lasB* genes of *Pseudomonas aeruginosa*: analysis of transcription and gene product activity. Infect Immun 62:1320–1327

136. Latifi A, Winson MK, Foglino M et al. (1995) Multiple homologues of LuxR and LuxI control expression of virulence determinants and secondary metabolites trough quorum sensing in *Pseudomonas aeruginosa* PAO1. Mol Microbiol 17:333–343
137. Pessi G, Haas D (2000) Transcriptional control of the hydrogen cyanide biosynthetic genes *hcnABC* by the anaerobic regulator ANR and the quorum-sensing regulators LasR and RhlR in *Pseudomonas aeruginosa*. J Bacteriol 182:6940–6949
138. Gambello MJ, Kaye S, Iglewski BH (1993) LasR of *Pseudomonas aeruginosa* is a transcriptional activator of the alkaline protease gene (apr) and an enhancer of exotoxin A expression. Infect Immun 61:1180–1184
139. Oschsner UA, Reiser J (1995) Autoinducer-mediated regulation of rhamnolipid biosurfactant synthesis in *Pseudomonas aeruginosa*. Proc Natl Acad Sci U S A 92:6424–6428
140. Brint JM, Ohman DE (1995) Synthesis of multiple exoproducts in *Pseudomonas aeruginosa* is under the control of RhlR-RhlI, another set of regulators in strain PAO1 with homology to the autoinducer-responsive LuxR-LuxI family. J Bacteriol 177:7155–7163
141. Winzer K, Falconer C, Garber NC et al. (2000) The *Pseudomonas aeruginosa* lectins PA-IL and PA-IIL are controlled by quorum sensing and by RpoS. J Bacteriol 182:6401–6411
142. Cao H, Krishnan G, Goumnerov B et al. (2001) A quorum sensing-associated virulence gene of *Pseudomonas aeruginosa* encodes a LysR-like transcription regulator with a unique self-regulatory mechanism. Proc Natl Acad Sci U S A 98:14613–14618
143. Kirsts MJ, Parsek MR (2006) Does *Pseudomonas aeruginosa* use intercellular signaling to build biofilm communities? Cell Microbiol 8:1841–1849
144. Hoiby N, Bjarnsholt T, Givskov M et al. (2010) Antibiotic resistance of bacterial biofilms. Intl J Antimicrob Agents 35:322–332
145. Erickson DL, Endersby R, Kirkham A et al. (2002) *Pseudomonas aeruginosa* quorum-sensing systems may control virulence factor expression in the lungs of patients with cystic fibrosis. Infect Immun 70:1783–1790
146. Singh PK, Schaefer AL, Parsek MR et al. (2000) Quorum-sensing signals indicate that cystic fibrosis lungs are infected with bacterial biofilms. Nature 407:762–764
147. Rumbaugh KP, Griswold JA, Iglewski BH et al. (1999) Contribution of quorum sensing to the virulence of *Pseudomonas aeruginosa* in burn wound infections. Infect Immun 67:5854–5862
148. Tang HB, DiMango E, Bryan R et al. (1996) Contribution of specific *Pseudomonas aeruginosa* virulence factors to pathogenesis of pneumonia in a neonatal mouse model of infection. Infect Immun 64:37–43
149. Pearson JP, Feldman M, Iglewski BH et al. (2000) *Pseudomonas aeruginosa* cell-to-cell signaling is required for virulence in a model of acute pulmonary infection. Infect Immun 68:4331–4334
150. Smith RS, Harris SG, Phipps R et al. (2002) The *Pseudomonas aeruginosa* quorum-sensing molecule N-(3-oxododecanoyl) homoserine lactone contributes to virulence and induces inflammation in vivo. J Bacteriol 184:1132–1139
151. Wu H, Song Z, Givskov M et al. (2001) *Pseudomonas aeruginosa* mutations in lasI and rhlI quorum sensing systems result in milder chronic lung infection. Microbiol SGM 147:1105–1113
152. Collier DN, Anderson L, McKnight SL et al. (2002) A bacterial cell to cell signal in the lungs of cystic fibrosis patients. FEMS Microbiol Lett 215:41–46
153. Lowy FD (1998) Medical progress-*Staphylococcus aureus* infections. N Eng J Med 339:520–532
154. Roux A, Payne SM, Gilmore MS (2009) Microbial telesensing: probing the environment for friends, foes, and food. Cell Host Microbe 6:115–124
155. Ziebandt AK, Becher D, Ohlsen K et al. (2004) The influence of agr and σB in growth phase dependent regulation of virulence factors in *Staphylococcus aureus*. Proteomics 4:3034–3037

156. Dunman PM, Murphy E, Haney S et al. (2001) Transcription profiling-based identification of *Staphylococcus aureus* genes regulated by the *agr* and/or *sarA* loci. J Bacteriol 183:7341–7353
157. Novick RP, Ross HF, Projan SJ et al. (1993) Synthesis of staphylococcal virulence factors is controlled by a regulatory RNA molecule. EMBO J 12:3967–3975
158. Boles BR, Horswill AR (2008) Agr-mediated dispersal of *Staphylococcus aureus* biofilms. PLoS Pathog 4:e1000052
159. Kumari A, Pasini P, Daunert S (2008) Detection of bacterial quorum sensing N-acyl homoserine lactones in clinical samples. Anal Bioanal Chem 391:1619–1627
160. Kumari A, Pasini P, Deo SK et al. (2006) Biosensing systems for the detection of bacterial quorum signaling molecules. Anal Chem 78:7603–7609
161. Halatsi K, Oikonomou I, Lambiri M et al. (2006) PCR detection of *Salmonella* spp. Using primers targeting the quorum sensing gene *sdiA*. FEMS Microbiol Lett 259:201–207
162. Oikonomou I, Halatsi K, Kyriacou A (2008) Selective PCR: a novel internal amplification control strategy for enhanced senstivity in *Salmonella* diagnosis. Lett Appl Microbiol 46:456–461
163. Zhu H, Sun SJ, Dang HY (2008) PCR detection of *Serratia* spp. Using primers targeting *pfs* and *luxS* genes involved in AI-2-dependent quorum sensing. Curr Microbiol 57:326–330
164. Clatworthy AE, Pierson E, Hung DT (2007) Targeting virulence: a new paradigm for antimicrobial therapy. Nat Chem Biol 3:541–548
165. Rasko DA, Sperandio V (2010) Anti-virulence strategies to combat bacteria-mediated disease. Nat Rev Drug Discov 9:117–128
166. Werner G, Strommenger B, Witte W et al. (2008) Acquired vancomycin resistance in clinically relevant pathogens. Future Microbiol 3:547–562
167. Musk DJ, Hergenrother PJ (2006) Chemical countermeasures for the control of bacterial biofilms: Effective compounds and promising targets. Curr Med Chem 13:2163–2177
168. Zhao G, Wan W, Mansouri S et al. (2003) Chemical synthesis of S-ribosyl-L-homocysteine and activity assay as a LuxS substrate. Bioorg Med Chem Lett 13:3897–3900
169. Alfaro JF, Zhang T, Wynn DP et al. (2004) Synthesis of LuxS inhibitors targeting bacterial cell–cell communication. Org Lett 6:3043–3046
170. Czajkowski R, Jafra S (2009) Quenching of acylhomoserine lactone-dependent quorum sensing by enzymatic disruption of signal molecules. Acta Biochim Pol 56:1–16
171. Park J, Jagasia R, Kaufmann GF et al. (2007) Infection control by antibody disruption of bacterial quorum sensing signaling. Chem Biol 14:1119–1127
172. Ni N, Li M, Wang J et al. (2009) Inhibitors and antagonists of bacterial quorum sensing. Med Res Rev 29:65–124
173. Muh U, Schuster M, Heim R et al. (2006) Novel *Pseudomonas aeruginosa* quorum-sensing inhibitors identifed in an ultra-high-throughput screen. Antimicrob Agents Chemoth 50:3674–3679
174. Hentzer M, Wu H, Andersen JB et al. (2003) Attenuation of *Pseudomonas aeruginosa* virulence by quorum sensing inhibitors. EMBO J 22:3803–3815
175. Manefield M, Rasmussen TB, Hentzer M et al. (2002) Halogenated furanones inhibit quorum sensing through accelerated LuxR turnover. Microbiol SGM 148:1119–1127
176. Defoirdt T, Miyamoto CM, Wood TK et al. (2007) The natural furanone (5Z)-4- bromo-5-(bromomethylene)-3-butyl-2(5H)-furanone disrupts quorum sensing-regulated gene expression in *Vibrio harveyi* by decreasing the DNA-binding activity of of the transcriptional regulator protein LuxR. Environ Microbiol 9:2486–2495
177 Zang T, Lee BWK, Cannon LM et al. (2009) A naturally occurring brominated furanone covalently modifies and inactivates LuxS. Bioorg Med Chem Lett 19:6200–6204
178. Defoirdt T, Boon N, Bossier P (2010) Can bacteria evolve resistance to quorum sensing disruption. PLOS Pathog 6:e1000989
179. Winson MK, Swift S, Fish L et al. (1998) Construction and analysis of *luxCDABE*-based plasmid sensors for investigating N-acyl homoserine lactone-mediated quorum sensing. FEMS Microbiol Lett 163:185–192

180. Khan SR, Mavrodi DV, Jog GJ et al. (2005) Activation of the phz operon of Pseudomonas fluorescens 2–79 requires the LuxR homolog PhzR, N-(3-OH-Hexanoyl)-L-homoserine lactone produced by the LuxI homolog PhzI, and a cis-acting phz box. J Bacteriol 187:6517–6527
181. Riedel K, Hentzer M, Geisenberger O et al. (2001) N-Acylhomoserine-lactone-mediated communication between *Pseudomonas aeruginosa* and *Burkholderia cepacia* in mixed biofilms. Microbiology 147:3249–3262
182. Lyon GJ, Wright JS, Muir TW et al. (2002) Key determinants of receptor activation in the agr autoinducing peptides of *Staphylococcus aureus*. Biochemistry 41:10095–10104
183. Tortosa P, Logsdon L, Kraigher B et al. (2001) Specificity and genetic polymorphism of the *Bacillus* competence quorum sensing system. J Bacteriol 183:451–460
184. Ishida K, Lincke T, Behnken S et al. (2010) Induced biosynthesis of cryptic polyketide metabolites in a *Burkholderia thailandensis* quorum sensing mutant. J Am Chem Soc 132:13966–13968
185. Khan SR, Herman J, Krank J et al. (2007) N-(3-Hydroxyhexanoyl)-L-homoserine lactone is the biologically relevant quormone that regulates the phz operon of *Pseudomonas chlororaphis* strain 30–84. Appl Environ Microbiol 73:7443–7455
186. Chin-A-Woeng TFC, van den Broek D, de Voer G et al. (2001) Phenazine-1-carboxamode production in the biocontrol strain *Pseudomonas chlororaphis* PCL1391 is regulated by multiple factors secreted into the growth medium. Mol Plant Microbe Interact 14:969–979
187. Recio E, Colinas A, Rumbero A et al. (2004) PI factor, a novel type quorum-sensing inducer elicits pimaricin production in *Streptomyces natalensis*. J Biol Chem 279:41586–41593
188. Anton N, Santos-Aberturas J, Mendes MV et al. (2007) PimM, a PAS domain positive regulator of pimaricin biosynthesis in *Streptomyces natalensis*. Microbiol SGM 153:3174–3183
189. EI-Sayed AK, Hothersall J, Thomas CM (2001) Quorum-sensing-dependent regulation of biosynthesis of the polyketide antibiotic mupirocin in *Pseudomonas fluorescens* NCIMB 10586. Microbiol SGM 147:2127–2139
190. Yan A, Huang XQ, Liu HM et al. (2007) An *rhl*-like quorum-sensing system negatively regulates pyoluteorin production in *Pseudomonas* sp. M18. Microbiol SGM 153:16–28
191. Huang XQ, Zhang XH, Xu YQ (2008) Positive regulation of pyoluteorin biosynthesis in *Pseudomonas* sp. M18 quorum-sensing regulator VqsR. J Microbiol Biotechnol 18:828–836
192. Lu JS, Huang XQ, Li K et al. (2009) LysR family transcriptional regulator PqsR as repressor of pyoluteorin biosynthesis and activator of phenazine-1-carboxylic acid biosynthesis in *Pseudomonas* sp. M18. J Biotechnol 143:1–9
193. Schmidt S, Blom JF, Pernthaler J et al. (2009) Production of the antifungal compound pyrrolnitrin is quorum sensing-regulated in members of the *Burkholderia cepacia* complex. Environ Microbiol 11:1422–1437
194. Liu X, Bimerew M, Ma Y et al. (2007) Quorum-sensing signaling is required for production of the antibiotic pyrrolnitrin in a rhizospheric biocontrol strain of *Serratia plymuthica*. FEMS Microbiol Lett 270:299–305
195. Seyedsayamdost MR, Chandler JR, Blodgett JAV et al. (2010) Quorum-sensing-regulated bactobolin production by *Burkholoderia thailandensis* E264. Org Lett 12:716–719
196. Woodyer RD, Shao Z, Thomas PM et al. (2006) Heterologous production of fosfomycin and identification of the minimal biosynthetic gene cluster. Chem Biol 13:1171–1182
197. Fontaine L, Boutry C, Guedon E et al. (2007) Quorum-sensing regulation of the production of Blp bacteriocins in *Streptococcus thermophilus*. J Bacteriol 189:7195–7205
198. Straume D, Kjos M, Nes IF et al. (2007) Quorum-sensing based bacteriocins production is down-regulated by N-terminally truncated species of gene activators. Mol Genet Genomics 278:283–293
199. Barnard AML, Bowden SD, Burr T et al. (2007) Quorum sensing, virulence and secondary metabolite production in plant soft-rotting bacteria. Phil Trans R Soc B 362:1165–1183

Adv Biochem Eng Biotechnol (2013) 131: 63–87
DOI: 10.1007/10_2012_163

Published Online: 10 November 2012

CHO Glycosylation Mutants as Potential Host Cells to Produce Therapeutic Proteins with Enhanced Efficacy

Peiqing Zhang, Kah Fai Chan, Ryan Haryadi, Muriel Bardor and Zhiwei Song

Abstract CHO glycosylation mutants, pioneered by Stanley and co-workers, have proven to be valuable tools in glycobiology and biopharmaceutical research. Here we aim to provide a summary of our efforts to isolate industrially applicable CHO glycosylation mutants, termed CHO-gmt cells, using cytotoxic lectins and zinc-finger nuclease technology. The genetic defects in the glycosylation machinery in these cells lead to the production of recombinant glycoproteins with consistent and unique glycan structures. In addition, these mutant cells can be easily adapted to serum-free medium in suspension cultures, the condition used by the biotech industry for large-scale production of recombinant therapeutics. In light of the critical impact of glycosylation on biopharmaceutical performances, namely, safety and efficacy, the CHO-gmt lines have enormous potential in producing glycoprotein therapeutics with optimal glycosylation profiles, thus, representing a panel of ideal host cell lines for producing recombinant biopharmaceuticals with improved safety profiles and enhanced efficacy.

Keywords Biopharmaceutical · CHO · EPO · Glucocerebrosidase · Glycosylation mutant · IgG

Abbreviations

AAL	*Aleuria aurantia* lectin
ADCC	Antibody-dependent cellular cytotoxicity
CDC	Complement-dependent cytotoxicity
CDG	Congenital disorder of glycosylation
CHO	Chinese hamster ovary
Con A	Concanavalin A
CST	CMP-sialic acid transporter
EPO	Erythropoietin

P. Zhang · K. F. Chan · R. Haryadi · M. Bardor · Z. Song (✉)
Bioprocessing Technology Institute, Agency for Science,
Technology and Research (A*STAR),
20 Biopolis Way, #06-01 Centros, Singapore 138668, Singapore
e-mail: song_zhiwei@bti.a-star.edu.sg

ER	Endoplasmic reticulum
ERT	Enzyme replacement therapy
Gal	Galactose
GalNAc	*N*-acetylgalactosamine
GCase	Glucocerebrosidase
G-CSF	Granulocyte-colony stimulating factor
GlcNAc	*N*-acetylglucosamine
GnT I	*N*-acetylglucosaminyltransferase I
HPAEC-PAD	High pH anion exchange chromatography with pulsed amperometric detection
IgG	Immunoglobulin G
IFN	Interferon
MAA	*Maackia amurensis* agglutinin
MALDI-TOF	Matrix-assisted laser desorption/ionization coupled with a time-of-flight analyzer
Man	Mannose
MS	Mass spectrometry
Neu5Gc	*N*-glycolylneuraminic acid
NST	Nucleotide sugar transporter
RCA	*Ricinus communis* agglutinin
Sia	Sialic acid
UGnT	UDP-GlcNAc transporter
UGT	UDP-galactose transporter
ZFN	Zinc-finger nuclease

Contents

1 Introduction

Since the 1980s, development of the pharmaceutical industry has been mainly catalyzed by the rapid expansion of biotherapeutics [1–4]. The majority of biotherapeutics are glycoproteins, including monoclonal antibodies, receptor-IgG fusion proteins, hormones, growth factors, and therapeutic enzymes, which are recombinantly produced in cell cultures [4]. Glycosylation has been extensively documented as pivotal for a number of drug properties, ranging from bioactivity [3], immunogenicity [5], to in vivo circulation [6]. Therefore, an important consideration for choosing a suitable host cell line is its capability of producing "human-like", safe, and efficacious glycoforms of the drug substance. This requirement, together with its resistance to major pathogenic viruses, the ability to grow in serum-free, suspension culture conditions, makes Chinese hamster ovary (CHO) cells the current industrial workhorse for the majority of leading recombinant biologics [7].

Glycosylation, the decoration of protein or lipid backbones by carbohydrate moieties, entails a series of metabolic reactions in the endoplasmic reticulum (ER) and Golgi apparatus, which ultimately generate a wide range of end products [8, 9]. This heterogeneity in glycoforms will translate into varied therapeutic drug performance [7]. As a result, there are regulatory requirements for producing consistent glycosylation profiles during drug manufacturing processes [10, 11]. The industrial practice for maintaining consistent glycosylation profiles and selecting favorable glycoforms mainly relies on extensive purification steps that eliminate the unwanted glycoforms. For example, the high degree of sialylation, a favorable property for recombinant human erythropoietin (rhEPO) that leads to extended in vivo circulatory half-life, is often maximized by a two-step ion exchange chromatography process. About 50 % of rhEPO is discarded during the process because of insufficient sialylation. Therefore, for consistency and process economy purposes, a CHO cell line that is capable of producing more favorable, and in addition, a narrower range of glycan structures, will be an ideal recombinant host for the production of therapeutic glycoproteins.

CHO glycosylation mutant cell lines offer a viable option for such glycosylation-optimized hosts. Pioneered by Stanley and co-workers, a comprehensive collection of CHO glycosylation mutants, most notably the Lec mutants, have been isolated (reviewed in [12]). These mutants carry genetic lesions in different components of the glycosylation machinery, resulting in altered glycan structures [13]. With a few exceptions, glycans produced by the mutants are predominantly premature intermediates that typically constitute a minor fraction in the glycan pool produced by the wild-type CHO cells. Interestingly, some of the glycan intermediates represent highly favorable structures for therapeutic applications. For example, *N*-glycans terminated with mannose (Man) residues allow glucocerebrosidase to be effectively targeted to macrophages in the enzyme replacement therapy (ERT) of Gaucher's disease [14]. In another example, *N*-glycans without core fucose have been shown

Table 1 List of the currently available CHO-gmt mutants in our lab

Mutant line	Genotype	Glycomic features		Ref.
		N-glycan	*O*-glycan	
CHO-gmt1	*CST-*	Asialo	T	Lim et al. (2006) [17]
CHO-gmt2	*UGT-*	GlcNAc-terminated	Tn and STn	Unpublished data
CHO-gmt3	*Slc35c1-/-*	Afucosylated	Wild type	Unpublished data
CHO-gmt4	*GnT I-*	Pauci-/Oligo-mannose	Wild type	Goh et al. (2010) [27]
CHO-gmt5	*CST- and Slc35c1-/-*	Asialo, afucosylated	T	Zhang et al. (2012) [19]

Abbreviations for glycogenes: *CST* CMP-sialic acid transporter; *UGT* UDP-galactose transporter; SLC35C1, the Golgi GDP-fucose transporter; GnT I, *N*-acetylglucosaminyltransferase I.Notations for *O*-glycan structures: T, Galβ1,3-GalNAcα-(Ser/Thr); Tn, GalNAcα-(Ser/Thr); STn, Siaα2,6-GalNAcα-(Ser/Thr)

to significantly enhance the antibody-dependent cellular cytotoxicity (ADCC) effect of IgG for cancer therapy [15].

Studies on previously reported CHO glycosylation mutants [12] have made significant contributions to our understanding of the glycosylation pathway in mammalian cells. Proof-of-concept investigations also discovered that there exists potential benefits for producing certain biotherapeutics in the glycosylation mutants [14, 15]. However, their industrial application has been limited due to their resistance to bioprocess development. In fact, the adaptation of the Lec mutants to a serum-free medium in a large-scale suspension culture has been unsuccessful (unpublished data and personal communications). Here we will focus on our effort to develop new CHO mutant lines using lectin selection as well as zinc-finger nuclease technology, an emerging method for site-specific gene silencing [16]. We have used these mutants to establish structure–function relationships of glycosylation-related proteins, particularly nucleotide sugar transporters [17–19]. The ultimate goal of this work, however, is to apply these mutants to produce recombinant therapeutics with enhanced efficacy through optimized glycosylation.

2 Isolation and Characterization of the CHO-gmt Mutants

The fact that CHO is functionally hemizygous for many genes implies a relatively higher rate of mutant development and this thus enhances the ease of selecting for these recessive mutants arising from the loss of a single functional allele [20]. A specific example is the CMP-sialic acid transporter (CST) which has only one functional allele [21]. Treatment of wild-type CHO cells with an α2,3-linked sialic acid-specific lectin, *Maackia amurensis* agglutinin (MAA) [22, 23], enabled us to readily select for CST-deficient mutants [17].

Using the well-established lectin selection and the recent ZFN methods, we have established a panel of CHO glycosylation mutant (CHO-gmt) lines (Table 1).

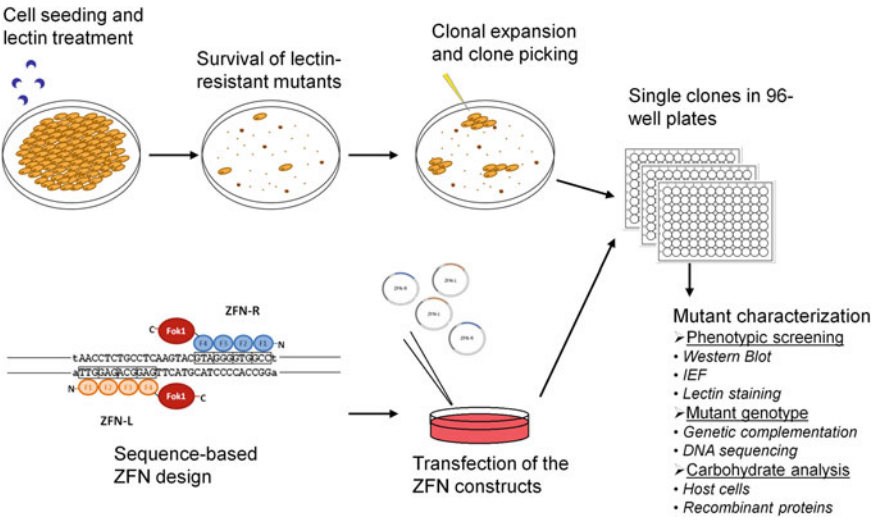

Fig. 1 Illustration of the general workflow for isolation and characterization of CHO glycosylation mutants using cytotoxic lectins and ZFNs

These include cells with single or multiple genetic defects in the glycosylation machinery. The glycosylation potential of these mutants was characterized by matrix-assisted laser desorption/ionization time-of-flight mass spectrometry (MALDI-TOF MS), using mutant cell pellets as well as recombinant glycoproteins as reporter molecules. We will briefly describe the isolation and characterization methods below. The general workflow is illustrated in Fig. 1.

2.1 Isolation of CHO Mutants Using Cytotoxic Lectins

Lectins are carbohydrate binding proteins with different sugar recognition specificities and exhibit cell agglutination activities through binding to cell surface glycans [24]. Many lectins are cytotoxic and kill cells by inducing apoptosis [25, 26]. A number of cytotoxic lectins have been applied in isolating CHO glycosylation mutants, including WGA, PHA, and Con A [12]. These naturally occurring mutants were believed to arise from rare spontaneous mutation event(s) and contain genetic defects in glycosyltransferase enzymes or nucleotide sugar transporters that are involved at different steps of the glycosylation pathway. Phenotypically, these mutants possess altered cell-surface *N*-glycans that lack the specific carbohydrate residue(s) required for specific lectin recognition and binding, thus are capable of surviving the cytotoxic lectin treatment. Different mutants have different levels of sensitivity/resistance to different types of lectins, thus it is possible to isolate a variety of different glycosylation mutants with different lectins. In our lab, we have isolated a panel of CHO mutants using *Maackia*

amurensis agglutinin (MAA) [17] and *Ricinus communis* agglutinin-I (RCA-I) lectins [27].

MAA is a plant lectin that shows high specificity toward α2,3-linked sialic acid [22, 23]. MAA was chosen for selecting CHO glycosylation mutants because CHO cells only express α2,3-linked sialic acid but not α2,6-linked sialic acid on their *N*-glycans. Indeed, using MAA we successfully isolated CHO-gmt1 (previously known as MAR-11) [17]. Similar to the Lec2 CHO mutants isolated by Stanley, CHO-gmt1 also carries a mutated CMP-sialic acid transporter gene [17]. This mutant survived the MAA treatment at 50 μg/ml concentration while the wild-type CHO cells, which contain abundant sialylated glycoconjugates at the cell surface, were killed. Because there are at least two sialyltransferases involved in the formation of the Siaα2,3-Gal linkage on *N*-glycans (namely ST3Gal III and ST3Gal IV) [28], isolating a mutant of both transferases will be practically impossible. However, mutations in the glycosylation pathway that are upstream of sialic acid incorporation, i.e., the formation of acceptor glycan structures, would in theory confer resistance to MAA. Consistent with this hypothesis, we have isolated another MAA-resistant CHO mutant, CHO-gmt2 that has a mutated UDP-galactose transporter (unpublished data). This transporter is essential for the formation of galactosylated glycans, which are acceptor structures for sialic acids. Thus, MAA is a versatile lectin that allows the isolation of different mutants of asialo phenotypes.

RCA-I, a 120-kDa tetra-hemagglutinin, is known to bind terminal β1,4-galactose residues and is highly toxic to wild-type CHO cells [29]. Later it was found that RCA-I is a promiscuous lectin showing binding affinities towards a range of glycan epitopes, including fully sialylated, bi-antennary *N*-glycans [30]. Therefore, RCA-I-resistant CHO mutants should theoretically possess genetic defects in the glycosylation steps upstream of galactosylation. We have isolated a large number of RCA-I-resistant mutants [27]. Strikingly, all these mutants were found to have genetic lesions in the same gene, *N*-acetylglucosaminyltransferase I (GnT I) [27]. As a result of the GnT I malfunction, the *N*-glycosylation process is stalled at $Man_5GlcNAc_2$, a structure which is not recognized by RCA-I. It is intriguing that we were able to isolate only GnT I mutants, but not mutants of other glycosylation-related genes that can result in the formation of RCA-I-insensitive glycan structures. While the mechanism merits further investigation, we speculate that it could be caused by the nonspecific binding of RCA-I to several *N*-glycan structures except oligomannose-type glycans, as shown by a study on lectin specificity using remodeled glycans (the $Man_5GlcNAc_2$ structure was not tested in the study) [30].

A representative cell line among the more than 100 RCA-I-resistant mutants is CHO-gmt4 (previously known as JW152) [27]. Similar to Lec1 CHO mutants [31], CHO-gmt4 lacks GnT I activity due to a mutation in the *Mgat1* gene. This line carries a C to T nonsense mutation at position 1015 in the open reading frame, resulting in a truncated GnT I protein with a deletion of amino acids at its C-terminus. Carbohydrate analysis of the CHO-gmt4 cell pellet confirmed the loss of GnT I activity. In the other RCA-I-resistant lines, we have identified and reported different types of mutations in the GnT I locus, including nonsense,

missense, insertion, and deletion mutations. These mutants were isolated over a wide range of RCA-I concentrations (2–40 μg/ml) [27]. Hence, the stringent selectivity for the *GnT I*-genotype is independent of RCA-I concentration as long as it is concentrated enough to kill the wild-type CHO cells. Therefore, the use of RCA-I offers a highly efficient method to isolate CHO mutants that are specialized in producing mannose-terminated *N*-glycans.

MAA was used to isolate CHO mutants because it is extremely cytotoxic and highly specific toward α2,3-linked sialic acid, which is abundantly expressed on the CHO cell surface. Therefore, MAA should be able to isolate various CHO mutants with genetic defects upstream of the addition of sialic acid to the galactose on the *N*-linked glycosylation pathway. Conversely, all the CHO cells that have survived RCA-I treatment so far have a dysfunctional GnT I [27]. Therefore, CHO mutants isolated by MAA, such as CHO-gmt1 and CHO-gmt2, can be further treated with RCA-I to isolate new cell lines with double mutations.

The choice of parental cell line is crucial when isolating lectin-resistant CHO mutants for bioprocess purposes. Since the application of CHO cells in basic research in the late 1950s, there have been many strains/variants of CHO used in different labs, such as CHO-K1, Pro-3, and Pro-5. However, only a few CHO variants are used in the industry, including CHO-K1, CHO-DXB11, and CHO-DG44. The latter two are deficient in dihydrofolate reductase (DHFR) and are often used as host cells for gene amplification. We isolated all our mutants from CHO-K1 and CHO-DG44 populations due to their industrial popularity: they have been shown to be adaptable to suspension culture under serum- or protein-free conditions. They are "robust" cell lines and are able to achieve high cell densities, thus enabling high titer of recombinant proteins. Mutants isolated from CHO-K1 were also shown to be capable of easier adaptation to suspension cultures. Conversely, we and others have been unable to adapt the Lec mutants to suspension culture in chemically defined media (unpublished data and personal communications).

2.2 Generation of CHO Mutants Using Zinc-Finger Nuclease

While cytotoxic lectin-based negative selection allows the isolation of some CHO mutants, it is challenging to isolate mutants with simultaneous genetic deficiency in multi-alleilic genes. In addition, there might be limited or no choice of cytotoxic lectins for some glycan structures. The recent advancement in zinc-finger nuclease (ZFN) technology offers an alternative, highly efficient approach to knock out the gene of interest [16]. Using the ZFN technology, we have knocked out the gene encoding the Golgi GDP-fucose transporter (SLC35C1) from CHO-gmt1 [19] and CHO-K1 (unpublished data), respectively.

Zinc-finger nucleases are customized restriction enzymes created by fusing a zinc-finger DNA binding domain to the cleavage domain of the endonuclease FokI. In the ZFNs, each zinc-finger domain typically contains three or four

zinc-finger units, each recognizing a 3-base sequence via 7 amino acids located within the finger unit. Because FokI is functional only upon dimerization, two ZFNs must simultaneously bind two sites on the opposite strands of the DNA separated by 5–7 bps. This results in the dimerization of the two FokI domains on the substrate and subsequently induces DNA double-stranded break (DSB). Cells repair the DSB by nonhomologous end joining, and often introduce insertion or deletion mutations during the repair process [32].

A comprehensive approach for designing ZFN constructs of high affinity, high fidelity yet low toxicity relies on a large randomized library and selection expertise [33], which limits this approach to only a few experienced groups [34–36]. An alternative approach is the modular assembly method in which individual fingers are designed to target nucleotide triplets by virtue of publically available information on finger motifs for many triplet DNA sequences [32, 37]. Among the validated motifs, fingers that bind the 5'-GNN-3' (where N can be either A, T, G, or C) are the best studied and shown to have the strongest DNA binding [38–40]. Furthermore, 5'-GNG'-3' triplets represent a better binding site than other 5'-GNN-3' triplets. Because the two binding sites for two ZFNs on opposite DNA strands should be 5–7 bp apart for efficient FokI dimerization, the ideal target sequence for two four-fingered ZFNs should be: 5'-NNCNNCNNCNNC-$(N)_{5\text{-}7}$-GNNGNNGNNGNN-3'. In addition to the 5'-GNG'-3' sequences, DNA triplets such as CTG, TGG, AAG, and AAA have also been successfully targeted by ZFNs in the literature. Identification of ideal targeting sites within the gene of interest can be aided by a web-based program, ZiFiT, provided by the Zinc Finger Consortium at: http://zifit.partners.org/ZiFiT/ [41, 42]. The structural scaffold for zinc-finger proteins is conserved and can be adopted from published reports [34, 35]. To prevent homodimerization of FokI linked to the same ZFN, FokI-KK and FokI-EL variants were created and shown to have reduced the chance for homodimerization [43]. Thus, linking FokI-KK and FokI-EL to each of the two ZFNs allows the formation of an active FokI endonuclease dimer upon DNA binding of both zinc finger domains on opposite strands. This ensures high-fidelity targeting and minimizes a potential off-target effect.

We decided to generate a fucose-deficient CHO mutant by disrupting the gene encoding the GDP-fucose transporter, *Slc35c1*, using the modular assembly method. Scanning the open reading frame of the Chinese hamster GDP-fucose transporter using the ZiFiT program [42], one potential ZFN target site was identified in the first exon of the *Slc35c1* open reading frame (5'-tAACCT CTGCCTCAAGTACGTAGGGGTGGCCt-3'). Two ZFNs were then designed by searching for finger motifs recognizing each 5'-GNN'3' triplet in the literature and fusing them to the ZFN scaffold, which was then linked to FokI-KK and FokI-EL, respectively. Parental cells (CHO-gmt1) were transiently transfected with a mixture of two constructs each expressing one of the two ZFNs. Two days after transfection, cells were detached by trypsinization and single cells were seeded into 96-well plates by limiting dilution. After clonal expansion, genomic DNA of each clone was extracted and sequenced using a specific primer pair flanking the ZFN target sites. Through DNA sequencing analysis, mutants that harbor genetic

lesions (deletions or insertions) in one or both *Slc35c1* alleles were identified. This workflow (illustrated in Fig. 1) led to the generation of the fucose-deficient CHO-gmt5, due to deletions in both alleles [19].

Recently, we also applied the same method to target the GDP-fucose transporter (*Slc35c1*) in CHO-K1 cells. To increase the selection efficiency after transfection with ZFN constructs, cells were incubated with a fluorescently conjugated *Aleuria aurantia* lectin (AAL), a fucose-specific lectin, and sorted by a fluorescence-activated cell sorter (FACS) [44]. Cells within the AAL-negative region were pooled and cultured. The AAL-assisted sorting was repeated a few times to progressively enrich the AAL-negative population, eventually resulting in a homogeneous pool of AAL-negative cells. Finally, single cells were seeded to allow for clonal expansion. Mutants of *Slc35c1* were identified through genetic complementation, genomic DNA sequencing, and carbohydrate analysis (see below). The FACS-based mutant selection protocol gave rise to CHO-gmt3, a mutant of *Slc35c1* on the genetic background of CHO-K1 (unpublished data).

2.3 Characterization Methods

Identification of ZFN-derived CHO mutants is relatively more straightforward, where the majority of the effort is devoted to sequencing of the genomic DNA flanking the ZFN-target locus. Therefore, we will mainly describe our workflow for characterization of lectin-resistant mutants. Some of the procedures can also be applied to characterize ZFN-derived mutants.

There are three layers of characterization that we routinely perform to identify the genotype of the lectin-resistant CHO mutants, their glycosylation status, and potential of glycosylating recombinant proteins. In order to rapidly characterize the glycosylation status of a mutant, we often utilize a reporter molecule, human erythropoietin (EPO). EPO is a heavily glycosylated protein with 3 *N*- and 1 *O*-glycosylation sites. It is estimated that the attached carbohydrate moieties can account for about 40 % of its total molecular weight. EPO is a blockbuster biopharmaceutical drug with annual sales exceeding 10 billion US dollars worldwide from the innovator versions. Sialic acids on the attached glycans have a profound impact on the bioactivity of EPO through critical modulation of its in vivo circulation. In fact, the circulatory half-life of sialylated EPO was found to be around 2 h whereas that of desialylated EPO was dramatically reduced to about 2 min. The high percentage of glycans on the total molecular mass renders EPO a sensitive model molecule to indicate changes in glycosylation of the host cells. Aberrant glycosylation of EPO often leads to a change in its molecular mass and/or its isoelectric point due to the change in the degree of sialylation. These two attributes can be detected by SDS-PAGE/Western blot and isoelectric focusing (IEF), respectively.

A large number of CHO mutants can be mapped along the sialylation pathway that ranges from glucosidase and mannosidase cleavage in the ER and early Golgi,

to glycan chain elongation by the sequential actions of GlcNAc transferases and galactosyltransferases, and the capping of the glycan branch by sialyltransferases. A prerequisite for the incorporation of GlcNAc, Gal, and Sia is the corresponding nucleotide sugars in the Golgi lumen. These nucleotide sugar building blocks are synthesized in the cytosol or nucleus and transported across the Golgi membrane by dedicated nucleotide sugar transporters (NSTs). Loss of function in any of these genes, including certain glycosidases, glycosyltransferases and NSTs, will lead to the production of premature *N*-glycans that are free of sialic acid.

An EPO expression construct is transiently transfected into a mutant line and the recombinant EPO secreted into the culture medium is collected 3 days after the transfection. The conditioned medium is then subjected to SDS-PAGE followed by Western blot using an EPO-specific antibody. By comparing the molecular weights of the EPO produced by the mutant cells with that produced by the wild-type CHO cells, one can confirm whether the glycans attached to the EPO protein produced by the mutant cells are truncated. By applying this method, we found that EPO produced in an RCA-I-resistant mutant, clone 25002, had a lower apparent molecular weight (Fig. 2a), suggesting a blockage in the glycosylation pathway. Subsequently, we were able to focus on genes within that category and identified GnT I as the gene defective in clone 25002 as well as in all RCA-I-resistant mutants including CHO-gmt4 through genetic complementation.

IEF represents an orthogonal method to SDS-PAGE/Western blot-based phenotypic characterization. When coupled with immunodetection using an EPO-specific antibody, the IEF assay allows sensitive glycoform profiling of recombinant EPO in crude culture media. It is especially useful when the mutation does not cause a significant change in EPO molecular weight. For example, CHO-gmt1 has a mutation in the CST gene and produces predominantly asialoglycans. The lack of sialic acids on recombinant EPO produced in CHO-gmt1 did not translate into an obvious decrease in its apparent molecular weight. However, when this EPO preparation was subjected to IEF, it was apparent that the sialylation was dramatically abolished, revealing that CHO-gmt1 is indeed a glycosylation mutant. Similarly, IEF analysis of rhEPO produced in RCA-I-resistant mutants, including clone 25002 (Fig. 2b) and CHO-gmt4 [27], also confirmed the failure of sialylation in these cell lines.

SDS-PAGE/Western blot and IEF methods can also be applied to the genetic complementation test in order to identify the defective gene. We previously reported the construction of a glycosylation toolbox with 31 major glycogenes cloned into mammalian expression vectors [45]. These glycogenes cover all the essential steps from ER to Golgi leading to sialylation of the *N*-glycans. Individual glycogenes can be co-transfected with the EPO construct into a mutant cell line. A successful genetic complementation will restore the glycosylation pathway which will in turn result in the restoration of electrophoretic and charge properties of rhEPO. Indeed, complementation of a functional GnT I in CHO-gmt4 restores the defective glycosylation step, allowing subsequent glycan chain elongation, as evidently demonstrated by the restoration of EPO molecular weight to the level

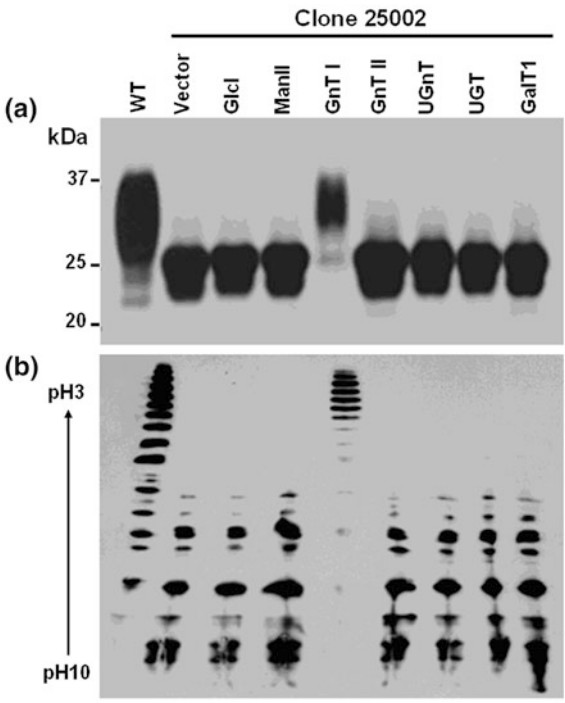

Fig. 2 Phenotypic analysis of an RCA-I-resistant mutant, clone 25002, and identification of GnT I as the defective gene by genetic complementation followed by SDS-PAGE/Western blot and IEF analyses of rhEPO. Recombinant EPO produced by wild-type (denoted as WT) and mutant 25002 cells was analyzed by SDS-PAGE or IEF followed by Western blot. (**a**) Co-transfection of GnT I, but not other glycogenes, resulted in restoration of EPO apparent molecular weight. (**b**) Co-transfection of GnT I, but not other glycogenes, resulted in restoration of EPO sialylation to a higher degree as compared to WT. Note that the EPO produced by clone 25002 in the presence of GnT I is better sialylated than that produced by the wild-type CHO cells. Vector, stands for empty vector; GlcI, stands for α-glucosidase I; Man II, α-mannosidase II; GnT I, *N*-acetylglucosaminyltransferase I; GnT II, *N*-acetylglucosaminyltransferase II; UGnT, UDP-GlcNAc transporter; UGT, UDP-galactose transporter; GalT1, galactose transferase 1

of rhEPO produced in wild-type CHO cells [27]. Figure 2 shows the complementation of another CHO mutant line, clone 25002, also harboring a dysfunctional GnT I. In contrast, heterologous expression of several other glycogenes selected from the glycogene toolbox failed to restore the electrophoretic pattern of rhEPO. As expected, genetic complementation with a functional GnT I enabled the completion of the glycosylation reactions and led to efficient sialylation of rhEPO as revealed by the SDS-PAGE (Fig. 2a) and the IEF assay (Fig. 2b). Similar to CHO-gmt4 (JW152) and Lec1 reported earlier [27], clone 25002 also produced highly sialylated recombinant EPO following GnT I complementation (Fig. 2b). This forms the basis of our proposal for utilizing the genetically complemented RCA-I-resistant CHO mutants (such as CHO-gmt4 and clone 25002) to produce highly sialylated glycoprotein drug substances.

Once the defective gene in a mutant has been identified via genetic complementation, the exact mutation at the molecular level will be ascertained by sequencing the corresponding transcript or genomic locus.

The third layer of mutant characterization is carbohydrate structural analysis. After validating the mutant by DNA sequencing, we routinely perform glycomic analysis of the mutant cells using MALDI-TOF MS. Analysis using a whole cell pellet is performed according to published reports mainly established by Dell and co-workers [13, 46]. Briefly, *N*-glycans are released by PNGase F treatment from cells that are cultured in T flasks or suspension and harvested at mid-log phase. Subsequently, *O*-glycans are released by alkaline reductive elimination which was shown to prevent degradation of the reducing-end sugar ("peeling" effect). Both glycan pools are then permethylated and analyzed in the positive ion mode using a MALDI-TOF/TOF system for glycan profiling. Glycan peaks that may correspond to isobaric structures can be further subjected to MS/MS by collision-induced dissociation (CID) for unambiguous structural assignment. The obtained *N*- and *O*-glycomic profiles will provide important insights into the glycosylation potential of the mutant cell lines. To further understand the glycosylation capability of the mutants, we also express recombinant glycoproteins that represent commercially important biopharmaceuticals, such as antibodies (IgG), EPO-Fc fusion protein, and interferon-γ (IFN-γ). *N*-glycans attached to these glycoproteins are released and analyzed by the same MALDI-TOF MS workflow. To yield quantitative data on distribution of different glycan structures, the underivatized *N*-glycans are subjected to high pH anion exchange chromatography coupled with pulsed amperometric detection (HPAEC-PAD). Through such analysis, identity as well as abundance of major glycan species can be determined. Furthermore, sialylation extent, a critical quality attribute of many recombinant glycoproteins, is also assessed by quantitative methods such as the thiobarbituric acid (TBA) assay, and recently, using a rapid and highly sensitive high-throughput method (HTM) [47].

3 Applications of CHO-gmt Mutants

The heterogeneic nature of glycosylation raises four major challenges in basic research and biopharmaceutical applications: First, little is known about how glycosylation is regulated at the systems level despite numerous studies showing that the outcome of the glycosylation can be affected by expression, localization of glycogene-encoded proteins and their interplay with other factors, and cell culture ages. Second, the (often) huge diversity of glycan structures produced by cells and those carried by a protein makes it extremely difficult to delineage the structure–function relationship of an individual glycan. Third, because of the above two challenges, it is difficult to establish the association between a glycoform of a drug and its corresponding efficacy. Finally, having identified the favorable drug glycoform, the heterogeneity issue still impedes the effort to maximize the recombinant production of only the efficacious glycoforms in cell culture.

The introduction of CHO glycosylation mutants (especially the Lec mutants) by Stanley and co-workers has provided valuable tools to address some of these questions. The mutants can serve as null background in certain glycogenes, thus allowing the identification of novel glycogenes with complementary functions [48] as well as structure–function relationships of the known glycogenes. In addition, the mutants provide a more homogenous pool of glycans and represent indispensable hosts for functional glycomic study. These aspects have been extensively reviewed and we will highlight some unique applications of the CHO-gmt mutants in basic research and biopharmaceutical production.

3.1 CHO-gmt in Basic Research: Structure–Function Analysis of NST Proteins

Biosynthesis of glycans requires a huge diversity of proteins, including glycosidases, glycosyltransferases, and nucleotide sugar transporters (NSTs). NSTs are an indispensable group of proteins for glycosylation; they transport nucleotide sugars that are synthesized in the cytosol (such as UDP- and GDP-sugars) or nucleus (CMP-sialic acid) into the lumen of the Golgi apparatus. Incorporation of these nucleotide sugars into the acceptor glycans ultimately gives rise to glycan structural diversity. The importance of NSTs in glycosylation can be further supported by evidences from three major aspects: First, mutation of NST in cultured cells (such as CHO cells) leads to aberrant glycan structures that are essentially devoid of the corresponding sugar [13]; second, rare mutations of several NST proteins have been reported in humans which lead to congenital disorders of glycosylation (CDG) [21, 49, 50], a class of inherited diseases that are often associated with severe developmental defects; third, up-regulation of certain NSTs have been implicated in some pathological conditions such as cancer [51].

NSTs are type III membrane proteins with 6–10 putative transmembrane helices [52]. Because of the difficulty in solving their structures, structure–function establishment typically relies on a heterologous system such as yeast or CHO glycosylation mutants. For example, Lec2 and Lec8, which are mutants of the CMP-Sia transporter (CST) and UDP-Gal transporter (UGT), respectively, proved to be indispensable tools for identifying sequences that determine the activity and specificity of the transporters [53–55].

The availability of CHO-gmt1 allowed us to perform further analysis of the CMP-Sia transporter, with particular focus on identifying critical elements located within the transmembrane regions [17] as well as hydrophilic loops of the CST [52]. The nonsense mutation in CHO-gmt1 at position 301 (cDNA numbering) results in a truncated CST protein of 100 amino acids, making it the smallest among all the reported CST mutants [17]. CHO-gmt1 has been shown to

have lower sialic acid content than another CST mutant, Lec2, both under adherent and suspension culture conditions, suggesting a lower residual CST activity [12, 17]. This feature makes CHO-gmt1 a highly sensitive background for structure–function analysis of CST. Using a "GFP-scan" approach, we identified several loop sequences having critical impact on CST activity. Subsequent targeted mutagenesis and expression of the mutant CST constructs in CHO-gmt1 allowed us to pinpoint the minimal critical sequence motifs [18].

Another NST protein, the GDP-fucose transporter, has been shown to be an important player in development and cancer. Overexpression of this protein is responsible for fucosylation of alpha-fetoprotein (AFP-L3 fraction), which is linked to hepatocellular carcinoma [51]. Conversely, loss-of-function mutations in the gene encoding this transporter, *Slc35c1*, form the molecular basis for leukocyte adhesion deficiency type II (LAD-II) [49, 50]. However, the structure–function relationship of this protein was not solved due to the lack of a heterologous system. We knocked out *Slc35c1* from CHO-gmt1 and used the resulting cell line, CHO-gmt5, as a tool towards this purpose. By targeted mutagenesis and functional analysis of the mutant *Slc35c1* constructs in CHO-gmt5 cells, we identified the cytosolic C-terminal tail sequence, and specifically, a conserved lysine cluster and Glu-Met motif, as the critical elements that determine the transport activity of the GDP-fucose transporter [19].

Similar applications of CHO glycosylation mutants in basic research have been extensively demonstrated by Lec mutants [12] and will not be reviewed here.

3.2 Potential Applications of CHO-gmt Lines in the Production of Recombinant Therapeutics

Glycans attached to the therapeutic proteins can have a profound impact on their safety and efficacy profiles. Nonhuman glycan structures can potentially provoke the immune response leading to neutralization of the drug or in more severe cases, anaphylactic reactions [56]. Galα1,3-Gal (or αGal in short) is known as the major xenoantigen in xenograft transplantation and is also responsible for allergic reactions that occurred after administration of the monoclonal antibody, Cetuximab [57]. Another major nonhuman glycan epitope derived from mammalian cell culture is *N*-glycolylneuraminic acid (Neu5Gc) [5]. The impact of glycan structure on drug efficacy is context-dependent [58]. Our panel of CHO-gmt mutants can be applied to produce a range of drug glycoforms. Their applications will be discussed in the context of three major categories of biopharmaceuticals, monoclonal antibodies (IgG), hormones and growth factors, as well as glycosylated enzymes.

3.2.1 CHO-gmt1, 3 and 5 for the Production of Certain Therapeutic Antibodies

Most therapeutic monoclonal antibodies on the market are of IgG1 isotype which are a class of heterotetrameric proteins, consisting of two light chains and two heavy chains. IgG1 molecules are glycoproteins with an *N*-glycan attached to Asn^{297} located within the CH2 domain of each heavy chain. The attached *N*-glycans display significant structural heterogeneity and differ from each other due to terminal modifications. Recombinant IgG1 antibodies produced in CHO cells typically contain mainly complex-type, bi-antennary *N*-glycans with 0–2 terminal galactose residues with core fucose [59, 60]. Sialylated glycan species typically represent less than 5 % of the total glycan pool [59, 60].

The major application of antibodies is for the treatment of cancer and autoimmune diseases such as breast cancer and rheumatoid arthritis [4]. To effectively eliminate cancer cells, the specific targeting of cancer cell surface antigen by IgG must be complemented by cytotoxic effector functions, including complement-dependent cytotoxicity (CDC) and antibody-dependent cellular cytotoxicity (ADCC) effects. Induction of the effector functions is achieved through binding of the Fc domain of the antibody to components of the complement pathway such as C1q or Fcγ receptors (FcγR) expressed on the surface of leukocytes (e.g., natural killer or NK cells). Studies have shown that the *N*-glycan attached to Asn^{297} of the IgG CH2 domain can mediate the binding of Fc to components of the complement complex and Fc receptors [61]. Specifically, the level of terminal Gal residues was found to positively correlate with the CDC effect as a result of C1q binding in the context of an anti-CD20 antibody, Rituxan. However, terminal Gal was shown to be dispensable for ADCC activity, shown in the context of an anti-Her2 antibody, Herceptin.

The most dramatic effect of Fc *N*-glycan on the ADCC effect can be attributed to the core fucose residue. Most Fc *N*-glycans contain a fucose residue that is α1,6-linked to the reducing end GlcNAc residue on recombinant IgG produced in CHO cells. However, removal of the core fucose resulted in a marked increase in ADCC activity due to increased binding of Fc to FcγRIIIa expressed on the NK cell surface [62, 63]. In vivo studies provided consistent results [60, 64–66]. Mechanistically, Try^{296}, adjacent to the *N*-glycan carrier Asn^{297}, assumes a more flexible conformation for FcγRIIIa binding in afucosylated Fc than in fucosylated Fc, as evidently shown by X-ray crystallographic and NMR studies [67, 68]. Reducing the core fucosylation level of the Fc *N*-glycan represents a rational strategy to enhance the efficacy of monoclonal antibodies that rely on the ADCC effect to treat diseases. Approaches towards decreasing the fucosylation level mainly involved gene targeting of the fucosylation pathway, for example, knockdown of the fucosyltransferase (Fut8) by RNAi [69], or knockout of Fut8 [70] and GDP-mannose 4,6-dehydratase (GMD) [71] by homologous recombination, ZFN-based gene inactivation of Fut8 [72] and Slc35c1 [73]. Recently, we also disrupted both alleles of Slc35c1 in CHO-K1 using ZFN technology (unpublished data). The resulting cell line, CHO-gmt3, was found to have completely lost the interaction with a

fucose-specific lectin, AAL, suggesting the lack of fucosylation. Therefore, CHO-gmt3 offers an alternative choice for the production of fucose-free IgG with enhanced ADCC effect.

Sialylation of Fc *N*-glycan can also affect in vivo performance of IgG. The presence of terminal sialic acid reduced the ADCC activity [74, 75]. Conversely, sialylation via α2,6 linkage contributes to the anti-inflammatory effect in the context of IVIG [74, 75]. CHO-gmt1 was found to contain lower amounts of sialic acids on its cell surface than Lec2 [17]. Recombinant IFN-γ produced in CHO-gmt1 carry predominantly asialoglycans. Thus, CHO-gmt1 represents an alternative host for antibody production with a minimal sialylation background that will reduce the variability in efficacy caused by sialic acid-mediated ADCC variation. Another application of CHO-gmt1 is for the production of anti-inflammatory antibodies. The lack of sialic acids on CHO-gmt1-produced IgG will expose the Gal residues for in vitro sialylation using an α2,6-sialyltransferase. Again, using CHO-gmt1 in this semisynthetic approach will reduce the variability caused by different sialylation in wild-type cells.

It is tempting to speculate that removal of fucose together with sialic acid will have a combinatorial effect on ADCC. Towards this end, we knocked out Slc35c1 on the basis of the CHO-gmt1 mutant line [19]. The resulting "double mutant," CHO-gmt5, harbors loss-of-function mutations in transporters for CMP-sialic acid and GDP-fucose [19]. Carbohydrate analysis of recombinant EPO-Fc produced in CHO-gmt5 showed a deficiency in both sialic acid and fucose on its *N*-glycans [19]. The industrial potential of this mutant cell line will be assessed in terms of the IgG ADCC effect. Nevertheless, the clean background of asialo-, afucosylated phenotype strongly justifies the relevance of CHO-gmt5 as a "biobetter" host for the production of more homogeneous IgG glycoforms.

3.2.2 GnT I-Complemented CHO-gmt4 for the Production of Highly Sialylated Glycoprotein Therapeutics

Many hormones, blood and growth factors are glycoproteins [4, 76]. Glycosylation of these proteins has a wide range of effects, including increasing solubility, conferring resistance to proteolytic degradations, and modulating the in vivo bioactivities [3]. Notably, sialylation of the attached glycans can have a critical impact on the circulatory half-lives of many drugs within this category, by protecting the drugs against clearance mediated by the liver asialoglycoprotein receptor which recognizes the underlying sugar motifs [77, 78]. In fact, studies showed that removal of sialic acids resulted in a dramatic decrease in drug half-lives from hours to minutes [79]. Conversely, increasing the content of sialic acid led to marked increase in in vivo circulation [6, 80]. To maintain optimal drug performance, a significant portion of under-sialylated glycoforms is discarded during purification processes. Increasing the sialic acid content can be a viable approach to enhance drug efficacy via extended in vivo circulation, maximizing the "druggable" portion

of the recombinant glycoproteins, which leads to significant reduction of drug cost. Effort towards increasing the sialic acid content in glycoprotein drugs, especially in the context of EPO and IFN-γ, mainly relied on metabolic and genetic engineering approaches, which yielded variable, sometimes contradictory results [7, 45, 81–84].

During our characterization of the CHO-gmt4 mutant, we found that complementing the mutant cells with a functional GnT I resulted in not only restoration of, but also increase in, rhEPO sialylation ([27] and Fig. 2b). This is not due to clonal variation; in fact we have tested a panel of RCA-I-resistant mutants as well as Lec1 (a mutant of GnT I) and the same observation still holds. Using quantitative HPAEC-PAD, it was found that the sialic acid content of rhEPO-Fc produced in GnT I-complemented CHO-gmt4 was increased by about 20 % as compared to that of the wild-type CHO-derived EPO-Fc [27]. While the mechanism for this phenomenon merits further investigation, it evidently demonstrates the advantage of GnT I-complemented CHO-gmt4 for the production of highly sialylated glycoproteins, making it an ideal host for "biobetter" versions of the innovator drugs.

3.2.3 CHO-gmt4 for the Production of Recombinant Glucocerebrosidase

Gaucher's disease is a lysosomal storage disorder. It is caused by rare mutations in the gene encoding glucocerebrosidase (GCase), or acid β-glucosidase [14]. GCase breaks down glucosylceramide (GlcCer) and loss-of-function mutation in this gene results in the accumulation of GlcCer in macrophages. Treatment of Gaucher's disease relies on enzyme replacement therapy (ERT) in which exogenous GCase is administered intravenously into the patients. Therapeutic preparations of GCase were first purified from human placenta, and later produced recombinantly in CHO cells due to the growing demand [14]. GCase is a glycoprotein with five potential *N*-linked glycosylation sites, the first four of which are occupied by *N*-glycans [85]. Effective targeting of GCase to macrophage cells depends on terminal mannose residues on the *N*-glycans, which are recognized by a mannose receptor on the macrophage cell surface for drug internalization [86]. Recombinant GCase produced in CHO cell culture carries complex-type *N*-glycans with mannose residues capped by GlcNAc, which is in turn protected by terminal Gal and then Sia residues. In order to generate mannose-terminated *N*-glycans, GCase purified from the cell culture process has to undergo sequential glycosidase treatment steps to remove Sia, Gal, and GlcNAc [86]. This process introduces substantial cost and potential variability to the final druggable GCase. Alternative expression systems (primarily based on transgenic plants) that are capable of producing mannose-terminated *N*-glycans have been tested for recombinant production of GCase [87–92]. Recently, taliglucerase alfa, a recombinant GCase produced in carrot cells, has been approved by the FDA for the treatment of Gaucher's disease (reviewed in [58]). There are still several potential problems that exist with the plant expression platform. First is the

presence of β1,2-linked xylose residue which is highly immunogenic in humans [90, 93]. Second, GCase has to be targeted to the storage vacuole in plant cells [90]. This requires a cell disruption step to extract GCase, which introduces additional cost and unit operations as compared to harvesting GCase directly from the conditioned media using the CHO system.

The fact that CHO-gmt4 produces predominantly pauci- and oligomannose-type *N*-glycans (Man3 and Man5) makes it an ideal host for recombinant production of GCase. GCase carrying Man3 and Man5-terminated *N*-glycans has been shown to be safe and has a bioactivity comparable to that of the glycan-remodeled innovator drug, Cerezyme [90]. In addition, CHO-gmt4 can be cultured in suspension using serum-free media. This will translate into cell culture and purification strategies similar to those developed for Cerezyme, except that the steps for glycan remodeling are removed. We are currently developing the bioprocess and purification technologies towards the production of recombinant GCase with uncompromised bioactivity while maintaining low cost.

3.2.4 Potential Applications of the CHO-gmt Mutants in *O*-Glycosylated Protein Production

The majority of the glycoprotein therapeutics are *N*-glycosylated proteins. And together with more in-depth understanding of the *N*-glycosylation biosynthetic pathway and its functional importance on drug efficacy, more focus has been placed on engineering and characterization of *N*-glycans in the context of biopharmaceuticals. In contrast, *O*-glycosylation modifications were found on a small number of biopharmaceutical drugs, such as TNFR2-Fc fusion protein (Enbrel) and granulocyte-colony stimulating factor (G-CSF), and their impact on drug properties are less understood. However, with the advancement in *O*-glycan analytical techniques and more stringent regulatory requirements, there is a need for developing cell lines and bioprocesses that can produce highly consistent, functionally favorable *O*-glycosylated protein drugs. A promising drug candidate of this category is lubricin, a highly *O*-glycosylated protein secreted into the synovial fluid with a cartilage protective function [94]. *O*-glycosylation of lubricin was found to be critical for mediating the lubrication function but is structurally highly heterogeneous [95, 96]. Obviously, a host cell line that is capable of producing lubricin with more homogeneous *O*-glycans will offer a desirable production platform. Carbohydrate analysis of the CHO-gmt lines showed unique and highly reproducible structures. For example, *O*-glycomic profiling of CHO-gmt1 cells predominantly showed a T structure, with an extremely low level of sialylation (unpublished data). Thus, a production host cell line can be selected from the panel of CHO-gmt lines, depending on the favorable *O*-glycan structures.

3.3 Bioprocess Advantages of the CHO-gmt Lines

While CHO glycosylation mutant cell lines represent unique host backgrounds in glycosylation pattern, their applications in recombinant production have been impeded by several factors, including the inability to adapt to a serum-free suspension platform. Transfection efficiency was also hampered in a ZFN-derived CHO mutant line [97]. A recent report showed that RNAi suppression of Golgi NSTs resulted in ER stress, leading to down-regulated protein secretion [98]. Clearly, these issues have to be resolved in order to render CHO glycosylation mutants relevant to bioprocess development.

Owing to the robust parental background of CHO-K1, the CHO-gmt mutants were found to be adaptable to serum-free, suspension cultures. In fact, our unpublished results showed the CHO-gmt mutants can reach peak viable cell densities of about 1.1×10^7 cells/ml in batch cultures in shake flasks. The growth curves are comparable to that of CHO-K1. Transfection efficiencies of the mutant cells were found to be comparable to CHO-K1 through the use of reporter molecules including GFP, IgG, EPO, and a complement of assays such as cell sorting, fluorescence microscopy, and ELISA. Additionally, activation of ER stress was not detected in the CHO-gmt mutant cells, as revealed by the absence of XBP-1 splicing. On the basis of these findings, we envisage that the workflow and strategy for cell line and bioprocess development of the CHO-gmt cells should be similar to that of CHO-K1, thus enabling the development of high-producing CHO-gmt cell lines for stable production of biopharmaceutical proteins with optimized glycosylation patterns.

4 Future Perspectives

Lectin-based negative selection of spontaneous mutants, together with sequence-based gene disruption by homologous recombination and the recent ZFN technology, has led to the generation of a sizable collection of CHO glycosylation mutants in our lab. Recently, the draft genome sequence of the CHO-K1 has been published [99], thus enabling sequence-based ZFN design for targeting any glycosylation-related genes to create novel mutant lines. While a potential future direction is to generate mutants of new genotypes, the fact that mutants of multiple glycogene defects can be isolated [19] points to a possible direction of creating more, multi-deficient glycosylation mutants. These single- or multi-deficient CHO mutants, together with the collection of functional glycosylation genes [45], may represent valuable tools for systematic understanding of the regulation mechanism of glycosylation at pathway and systems levels. From a bioprocess point of view, the panel of CHO-gmt mutants will enable the production of glycoproteins with defined, homogenous glycosylation profiles, which may be translated into better, more consistent drug performance. Additionally, glycosylation mutants can be isolated

from established drug-producing cell lines, given the dynamic, heterogeneous nature of CHO cytogenetics [100]. It is tempting to speculate that the second-wave of biopharmaceutical drugs produced from glycosylation mutant lines derived by lectins or ZFNs, will have higher efficacy and safety profiles.

Acknowledgments The authors would like to thank Ms. Natasha Pereira for critical review of the manuscript. This work is supported by the Biomedical Research Council, Agency for Science, Technology and Research (A*STAR), Singapore.

References

1. Walsh G (2000) Biopharmaceutical benchmarks. Nat Biotechnol 18(8):831–833
2. Walsh G (2003) Biopharmaceutical benchmarks–2003. Nat Biotechnol 21(8):865–870
3. Walsh G, Jefferis R (2006) Post-translational modifications in the context of therapeutic proteins. Nat Biotechnol 24(10):1241–1252
4. Walsh G (2010) Biopharmaceutical benchmarks 2010. Nat Biotechnol 28(9):917–924
5. Ghaderi D, Taylor RE, Padler-Karavani V, Diaz S, Varki A (2010) Implications of the presence of *N*-glycolylneuraminic acid in recombinant therapeutic glycoproteins. Nat Biotechnol 28(8):863–867
6. Elliott S, Lorenzini T, Asher S, Aoki K, Brankow D, Buck L, Busse L, Chang D, Fuller J, Grant J, Hernday N, Hokum M, Hu S, Knudten A, Levin N, Komorowski R, Martin F, Navarro R, Osslund T, Rogers G, Rogers N, Trail G, Egrie J (2003) Enhancement of therapeutic protein in vivo activities through glycoengineering. Nat Biotechnol 21(4):414–421
7. Hossler P, Khattak SF, Li ZJ (2009) Optimal and consistent protein glycosylation in mammalian cell culture. Glycobiology 19(9):936–949
8. Parodi AJ (2000) Protein glucosylation and its role in protein folding. Annu Rev Biochem 69:69–93
9. Haltiwanger RS, Lowe JB (2004) Role of glycosylation in development. Annu Rev Biochem 73:491–537
10. International Conference on Harmonisation; guidance on specifications: test procedures and acceptance criteria for biotechnological/biological products. Notice. Food and Drug Administration, HHS (1999). Fed Regist 64 (159):44928–44935
11. International Conference on Harmonisation; guidance on Q5E Comparability of Biotechnological/Biological Products Subject to Changes in Their Manufacturing Process; availability. Notice (2005). Fed Regist 70 (125):37861–37862
12. Patnaik SK, Stanley P (2006) Lectin-resistant CHO glycosylation mutants. Methods Enzymol 416:159–182
13. North SJ, Huang HH, Sundaram S, Jang-Lee J, Etienne AT, Trollope A, Chalabi S, Dell A, Stanley P, Haslam SM (2010) Glycomics profiling of Chinese hamster ovary cell glycosylation mutants reveals *N*-glycans of a novel size and complexity. J Biol Chem 285(8):5759–5775
14. Hoppe H (2000) Cerezyme–recombinant protein treatment for Gaucher's disease. J Biotechnol 76(2–3):259–261
15. Shinkawa T, Nakamura K, Yamane N, Shoji-Hosaka E, Kanda Y, Sakurada M, Uchida K, Anazawa H, Satoh M, Yamasaki M, Hanai N, Shitara K (2003) The absence of fucose but not the presence of galactose or bisecting *N*-acetylglucosamine of human IgG1 complex-type oligosaccharides shows the critical role of enhancing antibody-dependent cellular cytotoxicity. J Biol Chem 278(5):3466–3473

16. Le Provost F, Lillico S, Passet B, Young R, Whitelaw B, Vilotte JL (2010) Zinc finger nuclease technology heralds a new era in mammalian transgenesis. Trends Biotechnol 28(3):134–141
17. Lim SF, Lee MM, Zhang P, Song Z (2008) The Golgi CMP-sialic acid transporter: a new CHO mutant provides functional insights. Glycobiology 18(11):851–860
18. Chan KF, Zhang P, Song Z (2010) Identification of essential amino acid residues in the hydrophilic loop regions of the CMP-sialic acid transporter and UDP-galactose transporter. Glycobiology 20(6):689–701
19. Zhang P, Haryadi R, Chan KF, Teo G, Goh J, Pereira NA, Feng H, Song Z (2012) Identification of functional elements of the GDP-fucose transporter SLC35C1 using a novel Chinese hamster ovary mutant. Glycobiology 22(7):897–911
20. Siminovitch L (1976) On the nature of hereditable variation in cultured somatic cells. Cell 7(1):1–11
21. Martinez-Duncker I, Dupre T, Piller V, Piller F, Candelier JJ, Trichet C, Tchernia G, Oriol R, Mollicone R (2005) Genetic complementation reveals a novel human congenital disorder of glycosylation of type II, due to inactivation of the Golgi CMP-sialic acid transporter. Blood 105(7):2671–2676
22. Wang WC, Cummings RD (1988) The immobilized leukoagglutinin from the seeds of *Maackia amurensis* binds with high affinity to complex-type Asn-linked oligosaccharides containing terminal sialic acid-linked alpha-2,3 to penultimate galactose residues. J Biol Chem 263(10):4576–4585
23. Knibbs RN, Goldstein IJ, Ratcliffe RM, Shibuya N (1991) Characterization of the carbohydrate binding specificity of the leukoagglutinating lectin from *Maackia amurensis*. Comparison with other sialic acid-specific lectins. J Biol Chem 266(1):83–88
24. Sharon N, Lis H (2004) History of lectins: from hemagglutinins to biological recognition molecules. Glycobiology 14(11):53R–62R
25. Li WW, Yu JY, Xu HL, Bao JK (2011) Concanavalin A: a potential anti-neoplastic agent targeting apoptosis, autophagy and anti-angiogenesis for cancer therapeutics. Biochem Biophys Res Commun 414(2):282–286
26. Lim SF, Chuan KH, Liu S, Loh SO, Chung BY, Ong CC, Song Z (2006) RNAi suppression of Bax and Bak enhances viability in fed-batch cultures of CHO cells. Metab Eng 8(6):509–522
27. Goh JS, Zhang P, Chan KF, Lee MM, Lim SF, Song Z (2010) RCA-I-resistant CHO mutant cells have dysfunctional GnT I and expression of normal GnT I in these mutants enhances sialylation of recombinant erythropoietin. Metab Eng 12(4):360–368
28. Harduin-Lepers A, Vallejo-Ruiz V, Krzewinski-Recchi MA, Samyn-Petit B, Julien S, Delannoy P (2001) The human sialyltransferase family. Biochimie 83(8):727–737
29. Baenziger JU, Fiete D (1979) Structural determinants of *Ricinus communis* agglutinin and toxin specificity for oligosaccharides. J Biol Chem 254(19):9795–9799
30. Iskratsch T, Braun A, Paschinger K, Wilson IB (2009) Specificity analysis of lectins and antibodies using remodeled glycoproteins. Anal Biochem 386(2):133–146
31. Chen W, Stanley P (2003) Five Lec1 CHO cell mutants have distinct Mgat1 gene mutations that encode truncated *N*-acetylglucosaminyltransferase I. Glycobiology 13(1):43–50
32. Carroll D, Morton JJ, Beumer KJ, Segal DJ (2006) Design, construction and in vitro testing of zinc finger nucleases. Nat Protoc 1(3):1329–1341
33. Maeder ML, Thibodeau-Beganny S, Osiak A, Wright DA, Anthony RM, Eichtinger M, Jiang T, Foley JE, Winfrey RJ, Townsend JA, Unger-Wallace E, Sander JD, Muller-Lerch F, Fu F, Pearlberg J, Gobel C, Dassie JP, Pruett-Miller SM, Porteus MH, Sgroi DC, Iafrate AJ, Dobbs D, McCray PB Jr, Cathomen T, Voytas DF, Joung JK (2008) Rapid "open-source" engineering of customized zinc-finger nucleases for highly efficient gene modification. Mol Cell 31(2):294–301
34. Urnov FD, Miller JC, Lee YL, Beausejour CM, Rock JM, Augustus S, Jamieson AC, Porteus MH, Gregory PD, Holmes MC (2005) Highly efficient endogenous human gene correction using designed zinc-finger nucleases. Nature 435(7042):646–651

35. Doyon Y, McCammon JM, Miller JC, Faraji F, Ngo C, Katibah GE, Amora R, Hocking TD, Zhang L, Rebar EJ, Gregory PD, Urnov FD, Amacher SL (2008) Heritable targeted gene disruption in zebrafish using designed zinc-finger nucleases. Nat Biotechnol 26(6):702–708
36. Santiago Y, Chan E, Liu PQ, Orlando S, Zhang L, Urnov FD, Holmes MC, Guschin D, Waite A, Miller JC, Rebar EJ, Gregory PD, Klug A, Collingwood TN (2008) Targeted gene knockout in mammalian cells by using engineered zinc-finger nucleases. Proc Natl Acad Sci USA 105(15):5809–5814
37. Kim HJ, Lee HJ, Kim H, Cho SW, Kim JS (2009) Targeted genome editing in human cells with zinc finger nucleases constructed via modular assembly. Genome Res 19(7): 1279–1288
38. Dreier B, Segal DJ, Barbas CF 3rd (2000) Insights into the molecular recognition of the 5'-GNN-3' family of DNA sequences by zinc finger domains. J Mol Biol 303(4):489–502
39. Liu Q, Xia Z, Zhong X, Case CC (2002) Validated zinc finger protein designs for all 16 GNN DNA triplet targets. J Biol Chem 277(6):3850–3856
40. Segal DJ, Dreier B, Beerli RR, Barbas CF 3rd (1999) Toward controlling gene expression at will: selection and design of zinc finger domains recognizing each of the 5'-GNN-3' DNA target sequences. Proc Natl Acad Sci USA 96(6):2758–2763
41. Sander JD, Zaback P, Joung JK, Voytas DF, Dobbs D (2007) Zinc finger targeter (ZiFiT): an engineered zinc finger/target site design tool. Nucleic Acids Res 35 (Web Server issue):W599–605
42. Sander JD, Maeder ML, Reyon D, Voytas DF, Joung JK, Dobbs D (2010) ZiFiT (Zinc Finger Targeter): an updated zinc finger engineering tool. Nucleic Acids Res 38 (Web Server issue):W462–468
43. Miller JC, Holmes MC, Wang J, Guschin DY, Lee YL, Rupniewski I, Beausejour CM, Waite AJ, Wang NS, Kim KA, Gregory PD, Pabo CO, Rebar EJ (2007) An improved zinc-finger nuclease architecture for highly specific genome editing. Nat Biotechnol 25(7):778–785
44. Haryadi R, Zhang P, Chan KF, Song Z (2012) CHO-gmt5, a novel CHO glycosylation mutant for producing afucosylated and asialylated recombinant antibodies. Bioengineered 4(2):1–5
45. Zhang P, Tan DL, Heng D, Wang T, Mariati Yang Y, Song Z (2010) A functional analysis of *N*-glycosylation-related genes on sialylation of recombinant erythropoietin in six commonly used mammalian cell lines. Metab Eng 12(6):526–536
46. North SJ, Hitchen PG, Haslam SM, Dell A (2009) Mass spectrometry in the analysis of N-linked and O-linked glycans. Curr Opin Struct Biol 19(5):498–506
47. Markely LR, Ong BT, Hoi KM, Teo G, Lu MY, Wang DI (2010) A high-throughput method for quantification of glycoprotein sialylation. Anal Biochem 407(1):128–133
48. Ishida N, Ito M, Yoshioka S, Sun-Wada GH, Kawakita M (1998) Functional expression of human golgi CMP-sialic acid transporter in the golgi complex of a transporter-deficient Chinese hamster ovary cell mutant. J Biochem 124(1):171–178
49. Luhn K, Wild MK, Eckhardt M, Gerardy-Schahn R, Vestweber D (2001) The gene defective in leukocyte adhesion deficiency II encodes a putative GDP-fucose transporter. Nat Genet 28(1):69–72
50. Lubke T, Marquardt T, Etzioni A, Hartmann E, von Figura K, Korner C (2001) Complementation cloning identifies CDG-IIc, a new type of congenital disorders of glycosylation, as a GDP-fucose transporter deficiency. Nat Genet 28(1):73–76
51. Moriwaki K, Noda K, Nakagawa T, Asahi M, Yoshihara H, Taniguchi N, Hayashi N, Miyoshi E (2007) A high expression of GDP-fucose transporter in hepatocellular carcinoma is a key factor for increases in fucosylation. Glycobiology 17(12):1311–1320
52. Liu L, Xu YX, Hirschberg CB (2010) The role of nucleotide sugar transporters in development of eukaryotes. Semin Cell Dev Biol 21(6):600–608
53. Aoki K, Ishida N, Kawakita M (2001) Substrate recognition by UDP-galactose and CMP-sialic acid transporters. Different sets of transmembrane helices are utilized for the specific recognition of UDP-galactose and CMP-sialic acid. J Biol Chem 276(24):21555–21561

54. Aoki K, Ishida N, Kawakita M (2003) Substrate recognition by nucleotide sugar transporters: further characterization of substrate recognition regions by analyses of UDP-galactose/CMP-sialic acid transporter chimeras and biochemical analysis of the substrate specificity of parental and chimeric transporters. J Biol Chem 278(25):22887–22893
55. Takeshima-Futagami T, Sakaguchi M, Uehara E, Aoki K, Ishida N, Sanai Y, Sugahara Y, Kawakita M (2012) Amino acid residues important for CMP-sialic acid recognition by the CMP-sialic acid transporter: analysis of the substrate specificity of UDP-galactose/CMP-sialic acid transporter chimeras. Glycobiology. doi:10.1093/glycob/cws116
56. Commins SP, Platts-Mills TA (2010) Allergenicity of carbohydrates and their role in anaphylactic events. Curr Allergy Asthma Rep 10(1):29–33
57. Chung CH, Mirakhur B, Chan E, Le QT, Berlin J, Morse M, Murphy BA, Satinover SM, Hosen J, Mauro D, Slebos RJ, Zhou Q, Gold D, Hatley T, Hicklin DJ, Platts-Mills TA (2008) Cetuximab-induced anaphylaxis and IgE specific for galactose-alpha-1,3-galactose. N Engl J Med 358(11):1109–1117
58. Lingg N, Zhang P, Song Z, Bardor M (2012) The sweet tooth of biopharmaceuticals: Importance of recombinant protein glycosylation analysis. Biotechnol J. doi: 10.1002/biot.201200078
59. Ho SC, Bardor M, Feng H, Mariati, Tong YW, Song Z, Yap MG, Yang Y (2012) IRES-mediated Tricistronic vectors for enhancing generation of high monoclonal antibody expressing CHO cell lines. J Biotechnol 157(1):130–139
60. Junttila TT, Parsons K, Olsson C, Lu Y, Xin Y, Theriault J, Crocker L, Pabonan O, Baginski T, Meng G, Totpal K, Kelley RF, Sliwkowski MX (2010) Superior in vivo efficacy of afucosylated trastuzumab in the treatment of HER2-amplified breast cancer. Cancer Res 70(11):4481–4489
61. Raju TS (2008) Terminal sugars of Fc glycans influence antibody effector functions of IgGs. Curr Opin Immunol 20(4):471–478
62. Shields RL, Lai J, Keck R, O'Connell LY, Hong K, Meng YG, Weikert SHA, Presta LG (2002) Lack of fucose on human IgG1 N-linked oligosaccharide improves binding to human Fc gamma RIII and antibody-dependent cellular toxicity. J Biol Chem 277(30):26733–26740
63. Peipp M, Lammerts van Bueren JJ, Schneider-Merck T, Bleeker WWK, Dechant M, Beyer T, Repp R, van Berkel PHC, Vink T, van de Winkel JGJ, Parren PWHI, Valerius T (2008) Antibody fucosylation differentially impacts cytotoxicity mediated by NK and PMN effector cells. Blood 112(6):2390–2399
64. Niwa R, Shoji-Hosaka E, Sakurada M, Shinkawa T, Uchida K, Nakamura K, Matsushima K, Ueda R, Hanai N, Shitara K (2004) Defucosylated chimeric anti-CC chemokine receptor 4 IgG1 with enhanced antibody-dependent cellular cytotoxicity shows potent therapeutic activity to T-cell leukemia and lymphoma. Cancer Res 64(6):2127–2133
65. Suzuki E, Niwa R, Saji S, Muta M, Hirose M, Iida S, Shiotsu Y, Satoh M, Shitara K, Kondo M, Toi M (2007) A nonfucosylated anti-HER2 antibody augments antibody-dependent cellular cytotoxicity in breast cancer patients. Clin Cancer Res 13(6):1875–1882
66. Cardarelli PM, Moldovan-Loomis MC, Preston B, Black A, Passmore D, Chen TH, Chen S, Liu J, Kuhne MR, Srinivasan M, Assad A, Witte A, Graziano RF, King DJ (2009) In vitro and in vivo characterization of MDX-1401 for therapy of malignant lymphoma. Clin Cancer Res 15(10):3376–3383
67. Matsumiya S, Yamaguchi Y, Saito J, Nagano M, Sasakawa H, Otaki S, Satoh M, Shitara K, Kato K (2007) Structural comparison of fucosylated and nonfucosylated Fc fragments of human immunoglobulin G1. J Mol Biol 368(3):767–779
68. Radaev S, Sun P (2002) Recognition of immunoglobulins by Fcgamma receptors. Mol Immunol 38(14):1073–1083
69. Imai-Nishiya H, Mori K, Inoue M, Wakitani M, Iida S, Shitara K, Satoh M (2007) Double knockdown of alpha1,6-fucosyltransferase (FUT8) and GDP-mannose 4,6-dehydratase (GMD) in antibody-producing cells: a new strategy for generating fully non-fucosylated therapeutic antibodies with enhanced ADCC. BMC Biotechnol 7:84

70. Yamane-Ohnuki N, Kinoshita S, Inoue-Urakubo M, Kusunoki M, Iida S, Nakano R, Wakitani M, Niwa R, Sakurada M, Uchida K, Shitara K, Satoh M (2004) Establishment of FUT8 knockout Chinese hamster ovary cells: an ideal host cell line for producing completely defucosylated antibodies with enhanced antibody-dependent cellular cytotoxicity. Biotechnol Bioeng 87(5):614–622
71. Kanda Y, Imai-Nishiya H, Kuni-Kamochi R, Mori K, Inoue M, Kitajima-Miyama K, Okazaki A, Iida S, Shitara K, Satoh M (2007) Establishment of a GDP-mannose 4,6-dehydratase (GMD) knockout host cell line: a new strategy for generating completely non-fucosylated recombinant therapeutics. J Biotechnol 130(3):300–310
72. Malphettes L, Freyvert Y, Chang J, Liu PQ, Chan E, Miller JC, Zhou Z, Nguyen T, Tsai C, Snowden AW, Collingwood TN, Gregory PD, Cost GJ (2010) Highly efficient deletion of FUT8 in CHO cell lines using zinc-finger nucleases yields cells that produce completely nonfucosylated antibodies. Biotechnol Bioeng 106(5):774–783
73. Ishiguro T, Kawai S, Habu K, Sugimoto M, Shiraiwa H, Iijima S, Ozaki S, Matsumoto T, Yamada-Okabe H (2010) A defucosylated anti-CD317 antibody exhibited enhanced antibody-dependent cellular cytotoxicity against primary myeloma cells in the presence of effectors from patients. Cancer Sci 101(10):2227–2233
74. Anthony RM, Nimmerjahn F, Ashline DJ, Reinhold VN, Paulson JC, Ravetch JV (2008) Recapitulation of IVIG anti-inflammatory activity with a recombinant IgG Fc. Science 320(5874):373–376
75. Kaneko Y, Nimmerjahn F, Ravetch JV (2006) Anti-inflammatory activity of immunoglobulin G resulting from Fc sialylation. Science 313(5787):670–673
76. Leader B, Baca QJ, Golan DE (2008) Protein therapeutics: a summary and pharmacological classification. Nat Rev Drug Discov 7(1):21–39
77. Van Hall EV, Vaitukaitis JL, Ross GT, Hickman JW, Ashwell G (1971) Effects of progressive desialylation on the rate of disappearance of immunoreactive HCG from plasma in rats. Endocrinology 89(1):11–15
78. Grewal PK (2010) The Ashwell-Morell receptor. Methods Enzymol 479:223–241
79. Fukuda MN, Sasaki H, Lopez L, Fukuda M (1989) Survival of recombinant erythropoietin in the circulation: the role of carbohydrates. Blood 73(1):84–89
80. Egrie JC, Browne JK (2001) Development and characterization of novel erythropoiesis stimulating protein (NESP). Br J Cancer 84(Suppl 1):3–10
81. Wong NS, Yap MG, Wang DI (2006) Enhancing recombinant glycoprotein sialylation through CMP-sialic acid transporter over expression in Chinese hamster ovary cells. Biotechnol Bioeng 93(5):1005–1016
82. Wang Z, Park JH, Park HH, Tan W, Park TH (2011) Enhancement of recombinant human EPO production and sialylation in Chinese hamster ovary cells through Bombyx mori 30Kc19 gene expression. Biotechnol Bioeng 108(7):1634–1642
83. Chee Furng Wong D, Tin Kam Wong K, Tang Goh L, Kiat Heng C, Gek Sim Yap M (2005) Impact of dynamic online fed-batch strategies on metabolism, productivity and *N*-glycosylation quality in CHO cell cultures. Biotechnol Bioeng 89(2):164–177
84. Fukuta K, Yokomatsu T, Abe R, Asanagi M, Makino T (2000) Genetic engineering of CHO cells producing human interferon-gamma by transfection of sialyltransferases. Glycoconj J 17(12):895–904
85. Berg-Fussman A, Grace ME, Ioannou Y, Grabowski GA (1993) Human acid beta-glucosidase. *N*-glycosylation site occupancy and the effect of glycosylation on enzymatic activity. J Biol Chem 268(20):14861–14866
86. Pastores GM (2010) Recombinant glucocerebrosidase (imiglucerase) as a therapy for Gaucher disease. BioDrugs 24(1):41–47
87. Brumshtein B, Salinas P, Peterson B, Chan V, Silman I, Sussman JL, Savickas PJ, Robinson GS, Futerman AH (2010) Characterization of gene-activated human acid-beta-glucosidase: crystal structure, glycan composition, and internalization into macrophages. Glycobiology 20(1):24–32

88. He X, Galpin JD, Tropak MB, Mahuran D, Haselhorst T, von Itzstein M, Kolarich D, Packer NH, Miao Y, Jiang L, Grabowski GA, Clarke LA, Kermode AR (2012) Production of active human glucocerebrosidase in seeds of Arabidopsis thaliana complex-glycan-deficient (cgl) plants. Glycobiology 22(4):492–503
89. Pastores GM (2010) Velaglucerase alfa, a human recombinant glucocerebrosidase enzyme replacement therapy for type 1 Gaucher disease. Curr Opin Investig Drugs 11(4):472–478
90. Shaaltiel Y, Bartfeld D, Hashmueli S, Baum G, Brill-Almon E, Galili G, Dym O, Boldin-Adamsky SA, Silman I, Sussman JL, Futerman AH, Aviezer D (2007) Production of glucocerebrosidase with terminal mannose glycans for enzyme replacement therapy of Gaucher's disease using a plant cell system. Plant Biotechnol J 5(5):579–590
91. Sinclair G, Pfeifer TA, Grigliatti TA, Choy FY (2006) Secretion of human glucocerebrosidase from stable transformed insect cells using native signal sequences. Biochem Cell Biol 84(2):148–156
92. Zimran A, Brill-Almon E, Chertkoff R, Petakov M, Blanco-Favela F, Munoz ET, Solorio-Meza SE, Amato D, Duran G, Giona F, Heitner R, Rosenbaum H, Giraldo P, Mehta A, Park G, Phillips M, Elstein D, Altarescu G, Szleifer M, Hashmueli S, Aviezer D (2011) Pivotal trial with plant cell-expressed recombinant glucocerebrosidase, taliglucerase alfa, a novel enzyme replacement therapy for Gaucher disease. Blood 118(22):5767–5773
93. Bardor M, Faveeuw C, Fitchette AC, Gilbert D, Galas L, Trottein F, Faye L, Lerouge P (2003) Immunoreactivity in mammals of two typical plant glyco-epitopes, core alpha(1,3)-fucose and core xylose. Glycobiology 13(6):427–434
94. Rhee DK, Marcelino J, Baker M, Gong Y, Smits P, Lefebvre V, Jay GD, Stewart M, Wang H, Warman ML, Carpten JD (2005) The secreted glycoprotein lubricin protects cartilage surfaces and inhibits synovial cell overgrowth. J Clin Invest 115(3):622–631
95. Jay GD, Harris DA, Cha CJ (2001) Boundary lubrication by lubricin is mediated by O-linked beta(1–3)Gal-GalNAc oligosaccharides. Glycoconj J 18(10):807–815
96. Estrella RP, Whitelock JM, Packer NH, Karlsson NG (2010) The glycosylation of human synovial lubricin: implications for its role in inflammation. Biochem J 429(2):359–367
97. Wong AW, Baginski TK, Reilly DE (2010) Enhancement of DNA uptake in FUT8-deleted CHO cells for transient production of afucosylated antibodies. Biotechnol Bioeng 106(5): 751–763
98. Xu YX, Liu L, Caffaro CE, Hirschberg CB (2010) Inhibition of Golgi apparatus glycosylation causes endoplasmic reticulum stress and decreased protein synthesis. J Biol Chem 285(32):24600–24608
99. Xu X, Nagarajan H, Lewis NE, Pan S, Cai Z, Liu X, Chen W, Xie M, Wang W, Hammond S, Andersen MR, Neff N, Passarelli B, Koh W, Fan HC, Wang J, Gui Y, Lee KH, Betenbaugh MJ, Quake SR, Famili I, Palsson BO (2011) The genomic sequence of the Chinese hamster ovary (CHO)-K1 cell line. Nat Biotechnol 29(8):735–741
100. Davies SL, Lovelady CS, Grainger RK, Racher AJ, Young RJ, James DC (2012) Functional heterogeneity and heritability in CHO cell populations. Biotechnol Bioeng. doi:10.1002/bit.24621

Adv Biochem Eng Biotechnol (2012) 131: 89–119
DOI: 10.1007/10_2012_159

Published Online: 31 October 2012

Cell-Free Biosystems for Biomanufacturing

Chun You and Y.-H. Percival Zhang

Abstract Although cell-free biosystems have been used as a tool for investigating fundamental aspects of biological systems for more than 100 years, they are becoming an emerging biomanufacturing platform in the production of low-value biocommodities (e.g., H_2, ethanol, and isobutanol), fine chemicals, and high-value protein and carbohydrate drugs and their precursors. Here we would like to define the cell-free biosystems containing more than three catalytic components in a single reaction vessel, which although different from one-, two-, or three-enzyme biocatalysis can be regarded as a straightforward extension of multienzymatic biocatalysis. In this chapter, we compare the advantages and disadvantages of cell-free biosystems versus living organisms, briefly review the history of cell-free biosystems, highlight a few examples, analyze any remaining obstacles to the scale-up of cell-free biosystems, and suggest potential solutions. Cell-free biosystems could become a disruptive technology to microbial fermentation, especially in the production of high-impact low-value biocommodities mainly due to the very high product yields and potentially low production costs.

Keywords Biocommodity engineering · Bioeconomy · Biofuels · Biomanufacturing · Cascade enzyme biocatalyst · Cell-free synthetic biology · Synthetic pathway biotransformation

Revised book chapter for Advances in Biochemical Engineering/Biotechnology.
Volume: Future Trends in Biotechnology.
Volume editor: Jian-Jiang Zhong.

C. You · Y.-H. P. Zhang (✉)
Biological Systems Engineering Department, Virginia Tech, 304 Seitz Hall, Blacksburg, VA 24061, USA
e-mail: ypzhang@vt.edu

Y.-H. P. Zhang
Institute for Critical Technology and Applied Science (ICTAS), Virginia Tech, Blacksburg, VA 24061, USA

Y.-H. P. Zhang
Gate Fuels Inc., 2200 Kraft Drive, Suite 1200B, Blacksburg, VA 24060, USA

Contents

1 Introduction

Biomanufacturing is defined as manufacturing the desired products by using living biological organisms (e.g., bacteria, yeasts, plants) or some components from one or several biological organisms. Biomanufacturing has great potential to become a defining technology, especially in the sustainability revolution [1, 2]. Research and development in the fields of biotechnology, bioengineering, and nanomaterials have dramatic impacts on both the products that we are able to create and the ways in which we create them. Potential products that could be produced through biomanufacturing can be listed in an increasing order of selling prices: biocommodities ($0.3–several US dollars per kg), specialties and biomaterials (tens of dollars per kg), fine chemicals (hundreds of dollars per kg), pharmaceuticals (thousands of dollars/kg), to protein drugs (more than tens of thousands of dollars per kg) (Fig. 1).

Biomanufacturing can be classified into two platforms: living organisms and cell-free biosystems [3, 4]. Living organisms, especially microorganisms, have been utilized for several thousand years to produce a number of products that meet mankind's needs. As a result, living entities dominate as whole-cell biocatalysts in current biomanufacturing systems. With the development of genetic engineering, protein engineering, systems biology, and synthetic biology, we have gained the ability to modify living organisms to produce natural products at high yields or produce non-natural products. However, the potential of cell-free biosystems in biomanufacturing is often ignored. Herein we define cell-free biosystems composed of more than three catalytic components in one reactor. Thus, we intentionally exclude the use of one to three catalytic components as has been widely used to produce fructose from glucose, produce glucose from starch, and produce chiral alcohols, on large scales [5–9]. Therefore, we do not review traditional enzyme-mediated biocatalysis in this chapter.

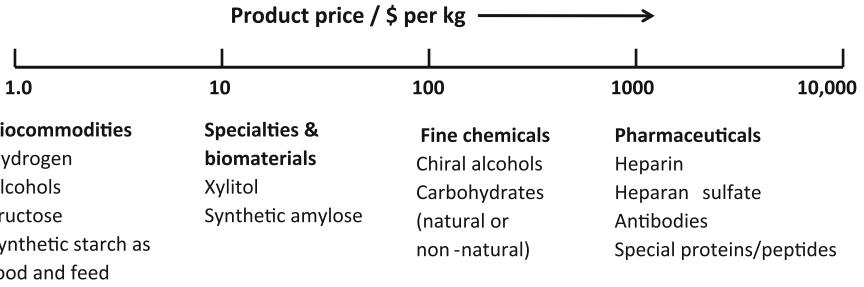

Fig. 1 Typical products produced by cell-free biosystems in terms of their selling prices from biocommodities, specialties and renewable materials, and fine chemicals to pharmaceuticals

Table 1 Comparison of cell-free biosystems and a living organism for biomanufacturing

Features	Cell-free biosystems	Living organism
Product yield	Theoretic or high	Low or modest
Product titer	High	Low or modest
Reaction rate	Fast	Slow
Process control	Easy	Difficult
Reaction conditions	Broad	Narrow

Cell-free biosystems have many advantages over living-organism biomanufacturing, such as high product yield, fast reaction rate, high product titer, unprecedented level of control and freedom of design, and broad reaction conditions [3, 4, 10–12] (Table 1). Cell-free biomanufacturing usually gives a yield of the desired product that is often close to a theoretical value when the reactions are irreversible or when the products can be removed in situ. Living systems suffer from low product yields [13, 14] because a significant fraction of carbohydrate and/or energy is used for duplication of cells and formation of side-products when using living organism for manufacturing [15]. For example, all hydrogen-producing microorganisms regardless of whether natural or genetically modified cannot produce hydrogen at yields of more than four moles per mole of glucose, called the Thauer limit [16], because complete oxidation of glucose with water as an oxidant cannot generate any ATP supporting living systems. Conversely, cell-free enzyme cocktails are able to produce nearly 12 moles of hydrogen per mole of glucose [17]. Much higher reaction rates are believed to be possible for cell-free systems than living organisms because (i) neither cell membrane nor wall is present to slow down substrate/product transport, (ii) no energy is needed for transport of substrate/product across the membrane, and (iii) much higher concentrations of biocatalysts can be present in the reactors and no side reactions "slow" the production of the desired product [11]. For example, the highest power density of microbial fuel cells is expected to be around 0.79 mW/cm^2 [18], while enzymatic fuel cells can generate power densities of up to 8.5–24 mW/cm^2 [19, 20]. Sometimes too slow productivities mean low potential in industrial biomanufacturing [14, 21]. A high concentration of fermentation products can greatly

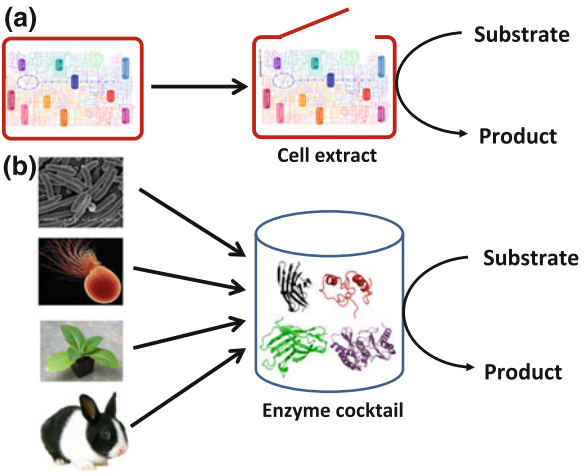

Fig. 2 Cell-free biosystems can use a cell extract from one host **a** or purified enzyme from different hosts **b** for biomanufacturing

decrease product separation costs [15] while often inhibiting the growth of living organisms, resulting in low product titers. Cell-free biosystems can be controlled much more easily than living organism because the latter has complicated feedback control for gene regulation, protein transcription, translation, and metabolite fluxes. Therefore, cell-free protein synthesis (CFPS) has become an alternative choice for fast synthesis of recombinant proteins in academic laboratories. Furthermore, cell-free protein synthesis has reached a 100-L milestone [22]. In principal, enzymes, especially thermostable enzymes, can tolerate higher levels of organic solvents or toxic chemical compounds than living organisms, resulting in high product titers. Recently, Sieber and co-workers demonstrated that the enzyme cocktails can produce isobutanol even at a concentration of more than 4 % [23]. Additionally, cell-free biosystems can be conducted under much broader reaction conditions than living organisms, for example in organic solvents, ionic liquids, or in the presence of compounds that are toxic to microorganisms [24]. Most building blocks of cell-free systems are highly exchangeable [25]. For example, high-yield enzymatic hydrogen can be produced by using enzymes isolated or originated from bacterium, yeast, plant, rabbit, and archaebacterium [26]. Given the advantages of cell-free systems over living organisms, cell-free biosystems are emerging as a powerful biomanufacturing platform to expand the capabilities of natural biological systems without using whole-cell cells.

Cell-free biosystems may be classified into two distinctive platforms according to their preparation method. The first is based on whole cell extract by breaking the cell membrane (Fig. 2a). The second is based on purified enzymes from different sources that are then mixed together (Fig. 2b). The cell extract can be prepared easily but some cellular components may influence the whole system's performance and the whole cell extract has a short half-life time [27, 28]. Systems made of purified components require labor-intensive preparation and seem costly but they can be stabilized after each component is carefully optimized and their

performance is more precisely controlled [14, 29]. Specific attributes of two cell-free biosystems enable their applicability to different products.

2 History of Cell-Free Biosystems

The power of cell-free biosystems has been appreciated as a fundamental research tool for more than 100 years. In 1897, Eduard Buchner discovered a yeast extract (not living yeast) that can convert glucose to ethanol [30], leading to his Nobel Prize in Chemistry in 1907. Later, many scientists used cell-free systems to study the basic biological mechanisms and some have received the Nobel Prize for their efforts. An incomplete winners list includes Arthur Harden and Hans von Euler-Chelpin for their investigation of the fermentation of sugar and fermentative enzymes [31], Otto Warburg for his discovery of the nature and mode of action of respiratory enzymes [32], Carl and Gerty Cori for their discovery of the course of the catalytic conversion of glycogen [33, 34], Hans Krebs for his elucidation of the citric acid cycle [35], Melvin Calvin for his investigation of carbon dioxide assimilation in plants [36], and Nirenberg for his elucidation of the genetic codon by using a cell-free system to translate a poly-uracil RNA sequence [37].

Enzyme-based biotransformation became a manufacturing tool approximately 50 years after the discovery of enzymes. The developments of enzyme-based biotransformation can be divided roughly into three phases:

Phase 1 (1960s)—one-enzyme biotransformation [5, 38]. To solve enzyme stability and recycling issues, enzyme immobilization technology was developed. Invertase may be the first immobilized enzyme used commercially for the production of Golden Syrup by Tate and Lyle during World War II. Tanabe Seiyaku Co. (Japan) started the industrial production of L-methionine by using immobilized aminoacylase in a packed bed reactor in 1969. The Clinton Corn Processing Company (USA) produced fructose syrup using glucose isomerase in 1967. Current annual fructose production exceeds 9 million tons [38] and the longest published working lifetime of immobilized glucose isomerase is 687 days at 55 °C and pH 7.5 (Kato Kagaku, Japan) [5]. Semisynthetic beta-lactamase-resistant beta-lactam antibiotics (e.g., cloxacillin, flucloxacillin) are produced by using amidases [5, 39]. Enzymatic acrylamide production was initiated in 1985 and more than 100,000 metric tons of acrylamide per year is produced by using immobilized nitrile hydratases [38]. Progress is accelerating due to fast developments in protein engineering tools including directed evolution, rational design, and their combination [40], high cell-density fermentation for low-cost recombinant protein production [41], the discovery and utilization of thermoenzymes [42], and enzyme immobilization in nanomaterials [3]. As a result, enzyme-mediated biocatalysis is an alternative choice for numerous transformations from commodities to pharmaceuticals [43, 44].

Phase 2 (1990s)—multienzyme one pot for relatively complicated biotransformation. Multienzyme one pot has numerous benefits compared to single-enzyme

reactors in cascade: fewer unit operations, smaller reactor volume, higher volumetric and space–time yields, shorter cycle times, and less waste generated. Also, by coupling steps together, unfavorable equilibria can be driven towards the formation of desired products [4, 45, 46]. For instance, enzymatic hydrolysis of crystalline cellulose requires a synergetic action of endoglucanase, cellobiohydrolase, and beta-glucosidase because a single enzyme cannot hydrolyze cellulose efficiently [47, 48]. For cofactor-dependent enzyme reactions that consume reduced NAD(P)H, in situ NAD(P)H-regenerated by another enzyme is becoming more and more accepted, especially for the synthesis of high-value chiral compounds in the pharmaceutical industry [3, 49, 50]. Similarly, NAD(P)H is usually generated by using a pair of a hydrogen-donor substrate and a single enzyme, including formate/formate dehydrogenase [51], glucose/glucose dehydrogenase [52], glucose-6-phosphate/glucose-6-phosphate dehydrogenase [42], dihydrogen/hydrogenase [53], and phosphite/phosphite dehydrogenase [54]. In the organic chemistry field, the synthesis of monosaccharides, activated monosaccharides, oligosaccharides, and glycopeptides by using multienzyme one pot has been intensively investigated [55–58].

Phase 3 (2000s)—the utilization of numerous enzymes (i.e., more than three) for implementing very complicated biotransformations. This cell-free biotransformation scheme has three representative directions: (i) cell-free protein synthesis, which utilizes natural protein synthesis systems in cell lysates for fast synthesis of proteins for research purposes and the production of high-value antibodies or other proteins [59, 60], (ii) in vitro synthetic biology for the production of high-value fine chemicals and pharmaceuticals [27, 61–64], and (iii) synthetic pathway biotransformation (SyPaB) for the production of low-value biocommodities [3, 4, 25]. Herein, we focus on the use of more than three catalytic units in one reactor because of its ability to implement biochemical reactions that living organisms cannot.

3 Examples of Cell-Free Biosystems for Biomanufacturing

We highlight several examples of cell-free biosystems so that readers can easily understand the advantages and applications of cell-free biosystems.

3.1 Cell-Free Biosystems for Biocommodity Engineering

Biocommodities are low-value and large-volume products, including biofuels, biochemicals, bioplatics, feed and food [4, 65]. Among them, transportation biofuels have received wide attention due to their nearly zero net greenhouse gas emissions, enhanced energy security, and new biomanufacturing job creation. Because feedstock costs usually account for more than half of biocommodity

selling prices [65, 66], economically viable production of biocommodities requires high product yields and low production costs. Although living microorganisms can duplicate themselves easily and have seemingly low biocatalyst preparation costs, we argue that cell-free biosystems could be an alternative choice due to the unique advantages mentioned earlier: high product yields, fast reaction rates, and potentially very low biocatalyst costs as bulk enzymes become stable and are produced at low cost in the future [3].

There is no question that hydrogen would be the best energy carrier for the transport sector in the future due to the high-energy utilization efficiency through fuel cells and nearly zero pollutants for end-users. Hydrogen can be produced through a number of approaches based on a variety of feedstocks [67]. The production of biohydrogen from low-cost biomass is an excellent solution for producing low-cost hydrogen without net carbon emissions [16, 68, 69]. However, natural and genetically modified hydrogen-producing microbes cannot produce hydrogen in yields of more than four moles hydrogen per mole glucose, called the Thauer limit [14, 16, 70]. Chemical catalysis, such as gasification and aqueous phase reforming, suffers from low product yields due to low chemical selectivity. To solve these problems, a non-natural enzymatic pathway composed of enzymes from bacteria, yeasts, animals, plants, and archae was constructed for generating high-yield hydrogen from starch in 2007 [26] (Fig. 3). The Royal Society (the UK's National Academy of Science) has praised this breakthrough as "the beginning stage of a cheap, green and high-yield hydrogen production" and as a good example of synthetic biology [71]. This synthetic pathway contains (i) a chain-shortening phosphorylation reaction on glucan for producing glucose-1-phosphate (G1P) catalyzed by glucan phosphorylase (Eq. 1); (ii) the conversion of G1P to glucose-6-phosphate (G6P) catalyzed by phosphoglucomutase (Eq. 2); (iii) a pentose phosphate pathway and gluconeogenesis pathway containing ten enzymes for producing 12 NADPH and 6 CO_2 per G6P (Eq. 3); and (iv) the generation of hydrogen from NADPH catalyzed by hydrogenase (Eq. 4).

$$(C_6H_{10}O_5)_n + P_i \rightleftharpoons (C_6H_{10}O_5)_{n-1} + G1P \quad (1)$$

$$G1P \rightleftharpoons G6P \quad (2)$$

$$G6P + 12NADP^+ + 7H_2O \rightleftharpoons 12\ NADPH + 12\ H^+ + 6CO_2 + P_i \quad (3)$$

$$12\ NADPH + 12\ H^+ \rightleftharpoons 12H_2 + 12NADP^+ \quad (4)$$

The combination of Eqs. (1)–(4) results in Eq. 5:

$$(C_6H_{10}O_5)_n + 7H_2O \rightarrow (C_6H_{10}O_5)_{n-1} + 12H_2 + 6CO_2 \quad (5)$$

Thermodynamic analysis of Eq. (5) suggests that the overall reactions from starch or cellulosic materials and water are spontaneous and endothermic ($\Delta G = -50$ kJ/mol and $\Delta H^o = +598$ kJ/mol) [17, 26]. These reactions are driven

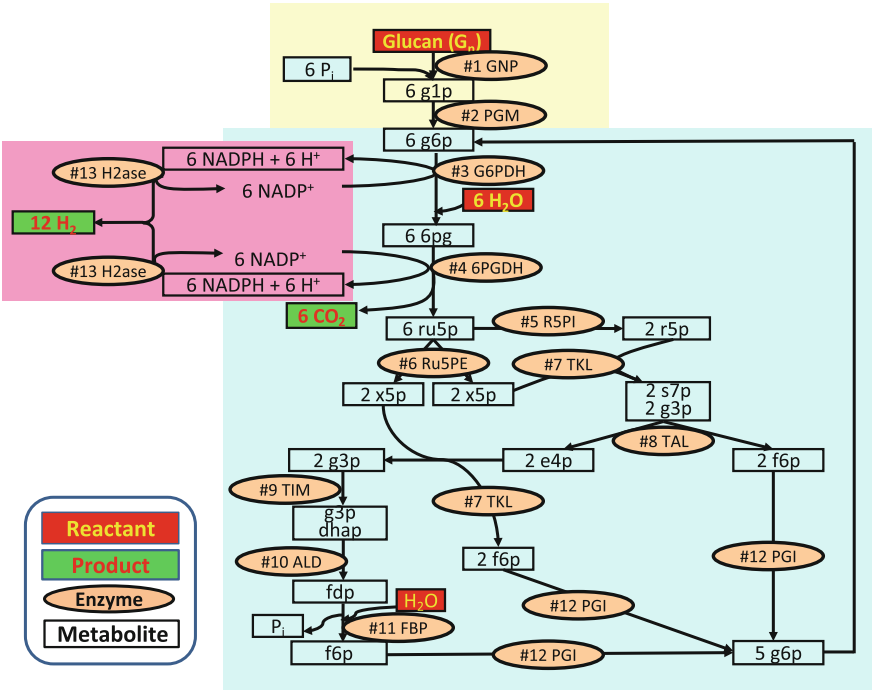

Fig. 3 The synthetic pathway for complete conversion of glucan and water to hydrogen and carbon dioxide. *PPP* pentose phosphate pathway. The enzymes are: *GNP* glucan phosphorylase; *PGM* phosphoglucomutase; *G6PDH* G-6-P dehydrogenase; *6PGDH* 6-phosphogluconate dehydrogenase; *R5PI* phosphoribose isomerase; *Ru5PE* ribulose 5-phosphate epimerase; *TKL* transketolase; *TAL* transaldolase; *TIM* triose phosphate isomerase; *ALD* aldolase; *FBP* fructose-1,6-bisphosphatase; *PGI* phosphoglucose isomerase; and H2ase, hydrogenase. The metabolites and chemicals are: *g1p* glucose-1-phosphate; *g6p* glucose-6-phosphate; *6pg* 6-phosphogluconate; *ru5p* ribulose-5-phosphate; *x5p* xylulose-5-phosphate; *r5p* ribose-5-phosphate; *s7p* sedoheptulose-7-phosphate; *g3p* glyceraldehyde-3-phosphate; *e4p* erythrose-4-phosphate; *dhap* dihydroxyacetone phosphate; *fdp* fructose-1,6-diphosphate; *f6p* fructose-6-phosphate; and *Pi* inorganic phosphate. Modified from Ref. [26]

by entropy gains rather than enthalpy losses. The removal of gaseous products, H_2 and CO_2, from the aqueous phase favors the unidirectional reaction for hydrogen formation. When cellobiose is used as the substrate with a reaction time in the range of one week for a complete reaction, the overall yields of H_2 and CO_2 are 11.2 moles of H_2 and 5.64 moles of CO_2 per mole of anhydroglucose unit of cellobiose, corresponding to 93.1 and 94 % of the theoretical yields (Eq. 5). In principle, the theoretical yield of hydrogen (i.e., 12 H_2 per glucose equivalent) can be obtained when a continuous reaction is conducted. Over the past few years, intensive efforts have been made pertaining to (i) decreasing enzyme costs and prolonging enzyme lifetime [17, 42, 72–75], (ii) producing all recombinant cytoplasmic enzymes at low costs [42, 76], and (iii) purifying recombinant proteins at

low cost using heat precipitation [42, 75], ammonia sulfate precipitation [77, 78], cellulose-binding module-based adsorption and immobilization [79–82].

Ethanol is the most important gasoline additive because it can decrease air pollutants generated by internal combustion (Otto) engines. It can be produced through microbial anaerobic fermentation by the yeast *Saccharomyces cerevisiae* or by other microorganisms such as *Escherichia coli* and *Zymomonas mobilis* [83]. As early as 1897, Eduard Buchner discovered a yeast extract that converted glucose to ethanol [30]. Much later, Welch and Scopes (1985) started investigating the feasibility of high-yield production of ethanol by a reconstituted yeast glycolytic enzyme system—12 enzymes in total including ten enzymes required for the conversion of glucose to pyruvate and two enzymes required for the conversion of pyruvate to ethanol [84]. In this system, ATP accumulation (i.e., two ATP produced per glucose) prevents complete conversion of glucose to ethanol so that costly ATPase or highly toxic arsenate had to be carefully supplemented in Welch's systems to achieve the high yield of ethanol. To solve this problem, Volker and co-workers designed a non-natural synthetic ethanol-producing pathway comprising six enzyme-catalyzed reactions only [23] (Fig. 4). In it, only four enzymes are required for the conversion of glucose to pyruvate. This synthetic pathway requires neither ATP nor CoA and has a balanced NAD cofactor. Since this pathway has a much lower Gibbs energy than those in yeast and *Z. mobilis*, it is anticipated that this cell-free pathway could have very fast production rates after optimization.

Isobutanol is a four-carbon liquid alcohol that has several advantages over ethanol, such as, lower water absorption, better blending ability, higher energy density, and compatibility with current internal combustion engines [85]. Volker and co-workers also designed a synthetic pathway that can produce isobutanol from glucose by using a cell-free enzyme mixture (Fig. 4). This pathway is composed of two parts: the production of pyruvate from glucose and the generation of isobutanol through the enzymes in valine biosynthesis pathways along with 2-keto-acid decarboxylases (KDC) and alcohol dehydrogenase (ADH). One of the most beautiful aspects of this cell-free system is that this enzyme system can work well even in the presence of 4 % (v/v) isobutanol, whereas low levels of isobutanol (e.g., 1–2 % v/v) stops microbial isobutanol production [86].

Fructose is the sweetest monosaccharide. High-fructose corn syrup (HFCS) is a mixture of fructose and glucose produced from starch, which has simply replaced sucrose as a sweetener. On average, one person in the USA consumes approximately 20 kg of HFCS per year. HFCS is made from starch through a series of enzymatic conversions: (i) starch liquefaction mediated by amylose, (ii) starch saccharification to glucose mediated by glucoamylase, and (iii) conversion of glucose to fructose mediated by glucose (xylose) isomerase (Fig. 5). In this typical process, fructose yield cannot be very high because the last step is reversible and the process runs at equilibrium. To solve this problem, Benner and his coworker designed a novel enzymatic pathway in one pot containing (i) starch phosphorylase, (ii) phosphoglucomutase, (iii) phosphoglucose isomerase, and (iv) fructose-6-phosphatase (Fig. 5). In the last step, the net hydrolysis of fructose-6-phosphate

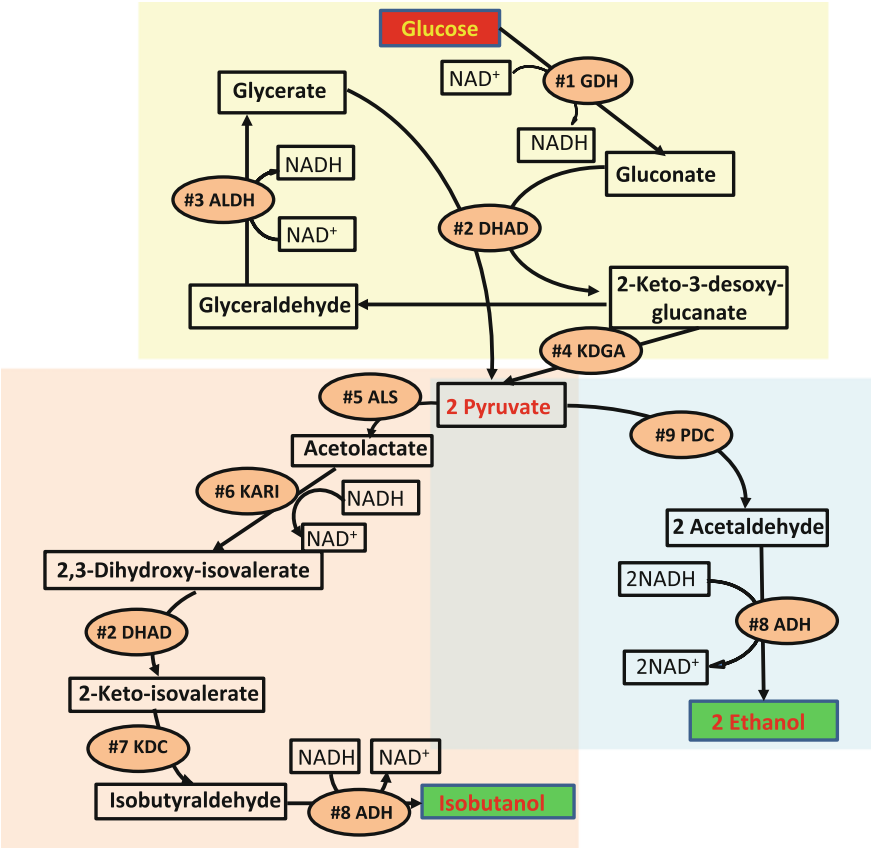

Fig. 4 Schematic representation of a novel cell-free reaction pathway from glucose to ethanol and isobutanol. In the first part of the reaction (*top box*), glucose is converted into two molecules of pyruvate by four enzymes, then pyruvate can be either directed to ethanol (*lower right box*) or isobutanol synthesis (*lower left box*) in the second part of the reaction cascade. The molecules of CO_2 and H_2O are not shown for clarity. Enzymes are *GDH* glucose dehydrogenase; *DHAD* (gluconate/glycerate) dihydroxy acid dehydratase; *ALDH* glyceraldehyde dehydrogenase; *KDGA* 2-keto-3-desoxygluconate aldolase; *ALS* acetolactate synthase; *KARI* ketolacid reductoisomerase; *KDC* 2-ketoacid decarboxylase; *PDC* pyruvate decarboxylase complex; and *ADH* alcohol dehydrogenase. Modified from Ref. [23]

yields fructose via a transaldolase-catalyzed reaction between fructose-6-phosphate and glyceraldehyde to yield fructose and glyceraldehyde-3-phosphate, which is then hydrolyzed to regenerate glyceraldehyde and inorganic phosphate by using a 3-phosphoglycerate phosphatase. Because the final step is exergonic and irreversible, this process pulls all of the equilibrium intermediates to the desired product. This pathway design illustrates a general idea that the energetics of a pathway should be considered when designing multistep biocatalytic transformations [87].

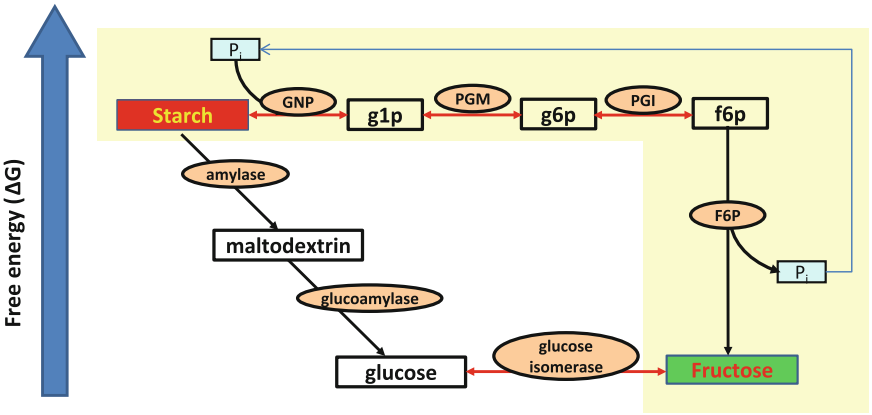

Fig. 5 Schematic representation of enzymatic fructose production from starch. *GNP* alpha-glucan phosphorylase; *PGM* phosphoglucomutase; *PGI* phosphoglucose isomerase; *F6P* fructose-6-phosphatase. *Arrows* in *red* are reversible reactions. Modified from Ref. [87]

3.2 Cell-Free Biosystems for High-Value Product Synthesis

Cell-free systems can be used to produce high-value pharmaceuticals. Organic chemical synthesis plays a dominant role in producing chemicals in the modern pharmaceutical industry, although it is being challenged by enzyme-mediated biocatalysis [44]. For example, fondaparinux (trade name Arixtra) is a synthetic antithrombin III-binding pentasaccharide. Its chemical synthesis involves a large number of chemical synthesis reactions, resulting in very low yields of products (e.g., less than 0.5 %) and the generation of toxic intermediates [88]. As a result, Arixtra is a costly drug. In 2011, Xu et al. reported 10- and 12-step chemoenzymatic synthesis of two structurally homogeneous ultralow molecular weight heparins in 45 and 37 % overall yield, respectively, starting from simple disaccharides [89]. These ultra-low molecular weight heparins display excellent in vitro anticoagulant activity and comparable pharmacokinetic properties to Arixtra in a rabbit model. This enzymatic approach may be scaled up easily and shows great potential for a more cost-efficient way to synthesize this important drug class.

Sheldon and his coworker developed a one-pot procedure including four enzymes for the synthesis of carbohydrates from glycerol and an aldehyde (i.e., butanal) (Fig. 6). The first step is the conversion of glycerol to glycerol-3-phosphate at a cost of pyrophosphate mediated by phytase. The second enzyme (glycerol phosphate oxidase) converts glycerol-3-phosphate to DHAP and generates H_2O_2 as a by-product, where a third enzyme catalase is responsible for degrading H_2O_2 to water and oxygen. The fourth enzyme fructose-1,6-bisphosphate aldolase links DHAP and butanal to butanal-DHAP. At the last step, the first enzyme phytase releases phosphate from butanal-DHAP and generates 5-deoxy-5-ethyl-D-xylulose. Although the four enzymes have different optimal pHs, the four enzymes are put in one pot during the whole process. The pH of the reaction vessel

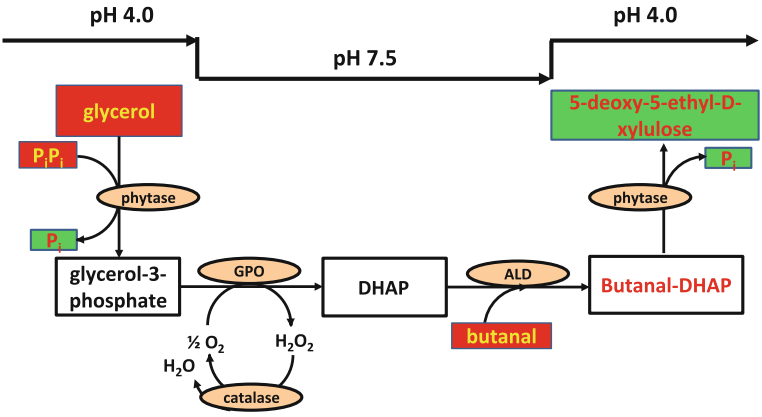

Fig. 6 Schematic representation of enzymatic transformation from glycerol to carbohydrates in one pot with pH shifts. *GPO* glycerol phosphate oxidase; *ALD* fructose-1,6-bisphosphate aldolase. Modified from Ref. [158]

is changed from pH 4.0 to pH 7.0 and then to pH 4.0, ensuring the cascading reactions occur in the desired order. The phytase on/off-switch at its respective pH 4.0 and 7.0 was the key to controlling phosphorylation and dephosphorylation [55].

Cell-free biosystems have been developed for the biosynthesis of radio-labeled purines (ATP and GTP) and pyrimidines (UTP and CTP) from glucose and ammonia, which requires 28 and 18 enzymes, respectively [63, 64]. Compared to the chemical synthesis, both purine and pyrimidine biosynthesis pathways can be reconstructed de novo for the incorporation of isotopes into specific sites. This work enables NMR detection for probing structural and dynamic characteristics of nucleic acids.

Enzymatic fuel cells (EFCs) represent a new type of fuel cell devices that can convert chemical energy stored in fuels into electricity mediated by redox enzymes [4, 90]. EFCs are an appealing micro-power source suitable for powering portable electronics because they have a number of features such as high-energy storage density; no flammability or explosion risk; biodegradability; low fuel costs; no costly, rare or heavy metals needed; and rapid "recharge" by injecting a sugar solution [91]. Nearly all EFCs extract only a small fraction of chemical energy in fuels by utilizing only one or a few oxidoreductase enzymes. The complete oxidation of fuels into electricity through engineered cascade pathways would have four benefits: (i) high energy utilization efficiency, (ii) high energy storage density, (iii) low product inhibition, and (iv) high power density [4, 92–94]. EFCs can utilize a large range of chemical compounds as fuels, including methanol, ethanol, glycerol, pyruvate, and glucose (these fuels are listed in increasing order of carbon number in the compound). To increase the fuel utilization efficiency, cascade enzymes can be employed. For example, three cascading redox enzymes have been used in an anode for the complete oxidization of one-carbon methanol to CO_2 [95].

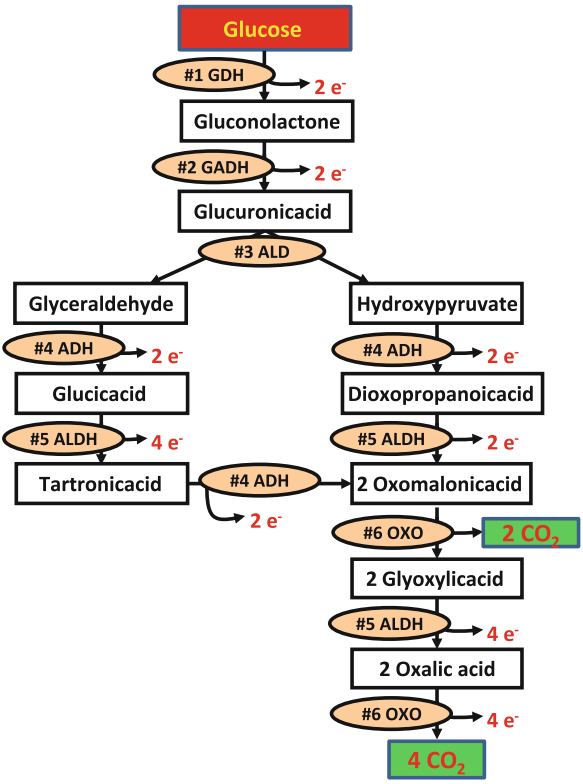

Fig. 7 Schematic representation of complete oxidation of glucose for electricity generation through six enzymes. Modified from Ref. [100]

Similarly, two-carbon ethanol has been oxidized using an 11-enzyme pathway to generate more electrons [96]. Three-carbon glycerol and pyruvate have been oxidized using two cascading dehydrogenases [97] and enzymes in the Krebs cycle [98, 99], respectively. Furthermore, Minteer et al. have proposed the complete oxidation of glucose using glycolysis and the TCA cycle [92]. Their pathway design is more complicated than the one proposed here and involves ATP/GTP and acetyl-CoA. However, acetyl-CoA and ATP are labile and cannot be utilized for an extended period of time. Recently, Xu and Minteer [100] published another paper on glucose oxidation to CO_2 through a new pathway that does not involve ATP and acetyl-CoA (Fig. 7). However, this design suffers from a very low power density because aldolase that breaks the C–C bond has a very low activity on non-phosphorylated carbohydrates [101, 102].

Zhang and coworkers utilized four thermophilic enzymes in cascade for deep oxidation of glucose without the use of ATP [94]. Polyphosphate glucokinase converts glucose to glucose-6-phosphate using low-cost, stable polyphosphate rather than costly ATP [81]. Two NAD-dependent dehydrogenases (glucose-6-phosphate dehydrogenase and 6-phosphogluconate dehydrogenase) that were immobilized on the bioanode were responsible for generating two NADH per glucose-6-phosphate (i.e., four electrons were generated per glucose via a

diaphorase-vitamin K(3) electron shuttle system at the anode). When the temperature was increased to 50 °C, the maximum power density increased to 0.322 mW/cm^{-2}, which was approximately eight times higher than that based on mesophilic enzymes at the same temperature. These results suggest that the deep oxidation of glucose could be achieved by using multiple dehydrogenases in synthetic cascade pathways and that high power output could be achieved by using thermostable enzymes at elevated temperatures.

3.3 Cell-Free Protein Synthesis

While cell-free protein synthesis (CFPS) has been used for decades as a foundational research tool for understanding transcription and translation, recent advances have made possible cost-effective micro-scale to manufacturing scale synthesis of complex proteins [22]. CFPS is becoming a more acceptable tool for the fast synthesis of recombinant proteins, especially when the proteins are in vivo cytotoxic, regulatory, or unstable proteins that are difficult to express in living cells and/or the proteins contain unnatural amino acids [10, 59, 103]. CFPS is usually conducted by using a crude cell lysate from any given organism (e.g., bacterial, plant, or animal cells) supplemented with the DNA template encoding the desired protein, NTPs, a highly processive RNA polymerase, amino acids, and an energy supply while the cell lysate provides the translational machinery, accessory enzymes, tRNA, and cofactors [10]. The use of cell lysate greatly simplifies CFPS but it may have some negative impacts due to other cellular components in cell extracts, for example, a rapid depletion of energy charge [59] and the degradation of protein products or template nucleic acids by proteases or nucleases [29]. In 2001, Shimizu et al. reported a protein-synthesizing system reconstituted from recombinant tagged protein factors purified to homogeneity [29]. The system – termed the "protein synthesis using recombinant elements" (PURE) system—contains all necessary translation factors, purified with high specific activity, and allows efficient protein production. This system has more than 100 well-defined molecules for implementing this complicated protein biosynthesis. The PURE system exhibits high translational efficiency with the added advantage of simple manipulation of reaction conditions and easy purification of untagged protein product. As a result, New England Biolabs Inc. sells the PURE fast protein synthesis kit.

Currently CFPS can produce protein in yields exceeding grams of target protein per liter of reaction volume, in batch reactions lasting multiple hours, with cost decreases to several orders of magnitude, and at scales reaching the 100-L milestone by SutroBio [11]. These advances have inspired new applications in the synthesis of protein libraries for functional genomics and structural biology, the production of protein therapeutics [104], personalized medicines [105], vaccines [106], short antimicrobial peptides [107], and the expression of virus-like particles, among others.

4 Challenges

The potential of cell-free biosystems for biomanufacturing is often ignored or underappreciated by many bioengineers and scientists because this paradigm shift is an out-of-the-box solution so that most do not realize that technological breakthroughs in other fields may be game changing in their field. A good example is no-till farming replacing tilling or discing farmland. Mankind has tilled land for thousands of years so it was easy to forget that the primary goal of tilling was to kill weeds. Beveridge described it as conditional thinking in his famous book entitled "The art of Scientific Investigation" [108]. Even long after the invention of selective herbicides and complementary herbicide-resistant seeds, farmers continued to till their land due to the ruling paradigm. The situation changed when several agricultural engineering pioneers in the nonpoint water pollution field realized that tilling was not necessary with proper herbicide and improved seed use. In reality, these no-tilling pioneers did not invent any new technologies but proposed a new concept to solve a key problem in their field. Now no-till farming is widely adopted because of the environmental and economic benefits [109]. Similarly, doubts regarding cell-free biosystems may include (i) enzymes cannot be produced and purified at low cost, (ii) enzymes are not stable enough, (iii) coenzymes are expensive and labile, and (iv) optimal conditions for numerous enzymes are different (Table 2). To address the above challenges, the respective solutions are listed in Table 2.

4.1 Low-Cost Enzyme Production and Purification

Cell-free protein synthesis usually uses cell extracts to decrease enzyme costs, while most cell-free biosystems prefer using partially purified enzymes that avoid unnecessary side-reactions and may prolong reaction time up to weeks, months, or even years. Low-cost production of bulk enzymes has been achieved but most academic researchers do not know this because most purchase costly enzymes from Sigma or other enzyme vendors. For example, bulk enzymes, such as protease and amylase produced by *Bacillus* sp., cellulase produced by *Trichoderma* and *Aspergillus* sp., have selling prices of ca. 5–10 US dollars per kg of dry protein [4, 110]. The cost of protein production is highly related to its expression level. The higher the expression level, the lower the cost of the purified protein. Codon usage optimization is a common way to enhance recombinant protein expression levels. For example, more than 500-fold improvement in the expression of soluble *Thermotoga maritima* 6-phosphogluconate dehydrogenase has been achieved in *E. coli* by codon usage optimization, accounting for >30 % of the total cellular protein [42]. Some recombinant formate dehydrogenase expression levels in *E. coli* are as high as 50 % cellular proteins [111]. It is estimated that current costs of recombinant proteins produced by *E. coli* BL 21 are approximately 100 US

Table 2 Challenges of cell-free systems and respective solutions

Challenge	Solution	Ref
Recombinant protein expression	High-cell density fermentation	Shiloach and Fass [41], Studier [160]
Enzyme purification	Secretory protein	Zhang [4]
	Cell extract	Bujara et al. [27], Swartz [28]
	Heat precipitation	Wang and Zhang [42], Sun et al. [75]
	Ammonia sulfate precipitation	Zhang and Mielenz [77], Scopes [78]
	Simple adsorption and immobilization	Liao et al. [81], Myung et al. [82]
	Resin-free chromatographic separation	Banki et al. [161]
	Fusion proteins	Zhang [114], Iturrate et al. [162], Bulow et al. [163]
	Multienzyme co-purification and immobilization	You et al. [112], Chen et al. [164], Nahalka et al. [165]
Enzyme stability	Thermostable enzymes	Table 3
	Enzyme immobilization	Demain and Vaishnav [166], Kirk et al. [167]
	Enzyme engineering through rational design and/or directed evolution	Ye et al. [40]
Costly and labile coenzymes	Coenzyme immobilization and recycling	Liu and Wang [168]
	Use of stable and low-cost biomimetic coenzyme	Campbell et al. [142], Ryan et al. [151], Campbell et al. [157]
Different optimal conditions for enzymes	Compromised reaction conditions	Zhang et al. [26]
	Adjusted reaction conditions in terms of time	Schoevaart et al. [55], Schoevaart et al. [158]
	Discovery of enzymes from one source	Zhang [4], Wang and Zhang [42], Myung et al. [74], Sun et al. [75]
	Engineered enzymes	Ye et al. [40], Chen and Arnold [169]

dollars per kg of dry protein including materials, labor, and capital depreciation [43]. As enzyme production is scaled up, production costs would decrease further. Dr. Tao at EnzymeWorks (China) pointed out that current enzyme costs in his company were approximately 70 US dollars per kg of enzyme because they can grow the *E. coli* cell densities of more than 100 g dry cell weight per liter without the use of costly pure oxygen (personal communication). It is anticipated that the cost of bulk recombinant enzymes will decrease greatly when their markets are ready.

The impression of costly enzyme purification is often gained from high-purity enzymes produced by academic labs and for pharmaceutical protein drugs, which are purified through a series of chromatographic methods. However, cell-free biosystems can utilize relatively low-quality enzymes as building blocks. Please bear in mind that cell extracts without purification could work well. In addition, several

low-cost scalable protein purifications are available and have been developed recently. For example, ammonia sulfate precipitation can be used as the first step of most protein purifications [77]. Instead of using commercial costly protein purification resins like Ni–NTA resin, and glutathione Sepharose 4B, low-cost cellulosic materials can be used for protein adsorption/desorption, purification, and immobilization [79–82]. For highly thermophilic enzymes expressed by *E. coli*, heat precipitation could be the simplest way to obtain purified proteins from *E. coli* cell extracts [42, 75]. In our laboratory, we have systematically investigated heat precipitation for the purification of recombinant enzymes produced from *E. coli*. We found that six recombinant enzymes cloned from *T. maritima* and produced in *E. coli*, for example, 6-phosphogluconate dehydrogenase [42], ribose-5-phosphate isomerase [75], aldolase [112], transaldolase [113], transketolase, and xylulokinase can be purified to more than 80–90 % homogeneity by simple heat treatment at 80 °C for 20 min.

Inspired by integrated circuits and natural metabolons [114], we developed a new protein purification method which can enrich, purify, and immobilize three cascade enzymes in one step (Fig. 8a). This method was based on the highly species-specific interaction between cohesins and dockerins from natural cellulosomes [112, 115–117]. A synthetic protein scaffold called scaffoldin was constructed containing a CBM3 module and three cohesins. The CBM3 module can tightly bind on cellulosic materials and cohesins are responsible for binding with the specific dockerin-containing enzymes. Dockerins can be located in either the N- or C-terminal of the target protein [118]. After mixing four cell extracts containing the synthetic scaffoldin and dockerin-containing target proteins with cellulosic materials (e.g., regenerated amorphous cellulose, RAC) and centrifugation, the synthetic three-enzyme metabolon can be purified and immobilized on RAC (Fig. 8a). Triosephosphate isomerase (TIM), aldolase (ALD), and fructose 1,6-bisphosphatase (FBP) were chosen for demonstration purposes. The protein expression levels of dockerin-containing TIM, ALD, and FBP were low (Fig. 8b, Lane 1, 2, 3), but they can be easily enriched and purified by mixing with the synthetic scaffoldin (Lane 5, 6, and 7). The self-assembled three-enzyme metabolon can be obtained in one step (Fig. 8b, Lane 9 and Fig. 8c). Such an enzyme complex also has the unique feature of substrate channeling because of the proximity of the cascade enzymes [114]. This enzyme complex showed more than one order of magnitude enhancements on reaction rates compared to the non-complexed TIM, ALD, and FBP mixture [112] (Fig. 9). In conclusion, numerous methods can decrease enzyme purification costs.

4.2 Prolonging Enzyme Lifetime

Most enzymes in academic laboratories deactivate rapidly, giving researchers an impression that enzymes are not stable. In reality, a few enzymes are very stable with a shelf lifetime of years and have been widely used in daily life, for example,

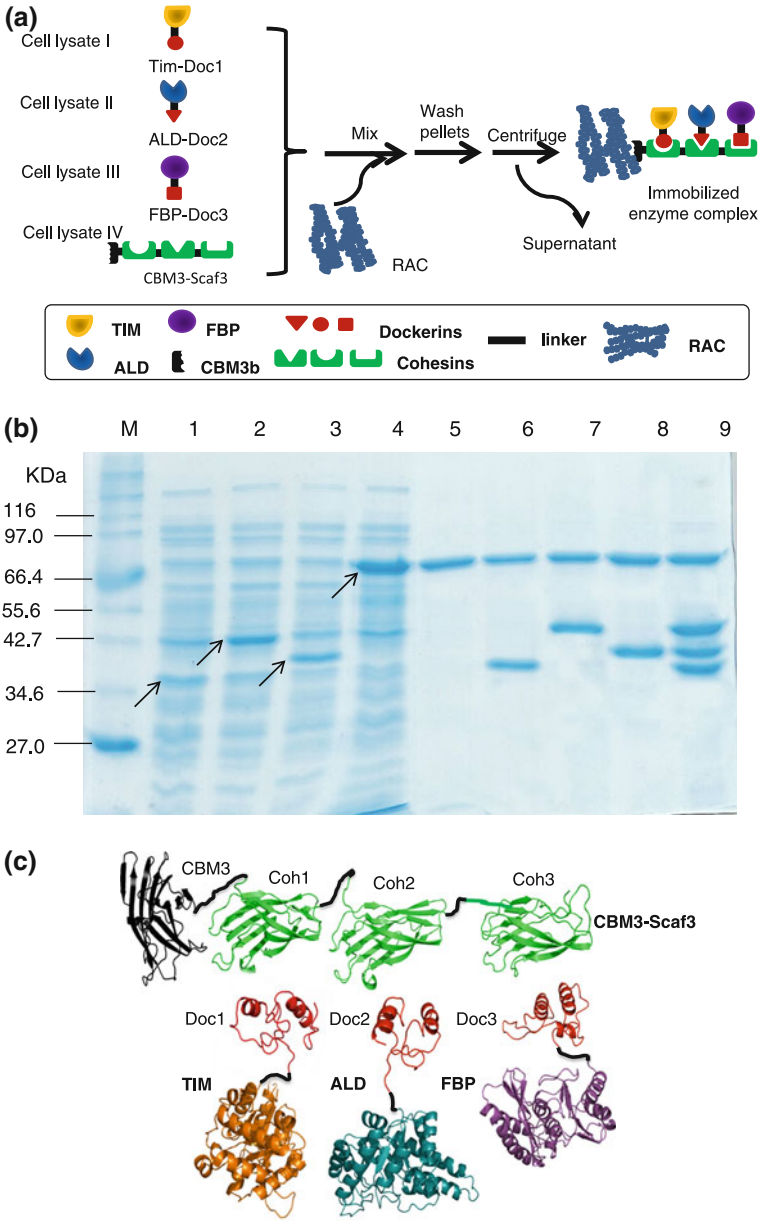

Fig. 8 **a** Schematic representation for the purification and co-immobilization of the synthetic three-enzyme complex, where the mini-scaffoldin contained three different types of cohesins and one family 3 carbohydrate-binding module, and three enzymes contained respective dockerin. **b** SDS-PAGE analysis of the *E. coli* cell extracts containing the recombinant proteins and RAC pull-down proteins (**a**). Lane M, protein marker; Lane 1–4, cell extract containing TIM-Doc1, ALD-Doc2, FBP-Doc3, and CBM-Scaf3, respectively; Lane 5, RAC adsorbed mini-scaffoldin, Lane 6–8, RAC adsorbed CBM-Scaf3 and TIM-Doc1, ALD-Doc2, and FBP-Doc3, respectively; and Lane 9, RAC adsorbed CBM-Scaf3, TIM-Doc1, ALD-DoC2, and FBP-Doc3. **c** Schematic representation of the self-assembled three-enzyme complex containing TIM-Doc1, ALD-Doc2, FBP-Doc3, and CBM-Scaf3 containing three different types of cohesins and one family 3 carbohydrate-binding module. Modified from Ref. [159]

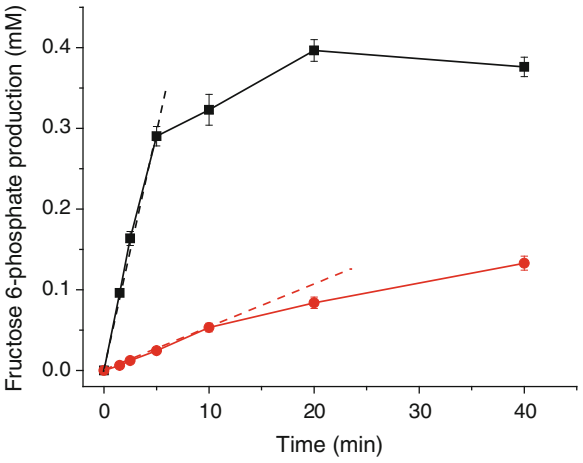

Fig. 9 Profiles of fructose-6-phosphate production catalyzed by 2-μM synthetic enzyme complex (■) and 2-μM noncomplexed enzyme mixture (●) in 2.5-mM glycerealdehyde-3-phosphate at 60 °C, where the slope of the *dashed lines* was defined as the initial reaction rate. Modified from Ref. [112]

protease used in detergents, or enzymes used in diabetic test strips. Another famous example is immobilized glucose isomerase lasting for more than 2 years [5].

Enzyme deactivation can be addressed by using thermoenzymes, enzyme immobilization, protein engineering through directed evolution and rational design, and their combination. Our economic analyses pertaining to enzymatic hydrogen production suggest that enzyme costs would be minimal when total turnover numbers (TTN) of all enzymes are larger than 10^7–10^8 mol of product per mol of enzyme [4, 77]. When cell-free biosystems are used to produce high value products, acceptable TTN values could be lower. On the basis of our experiences, it is very easy to obtain enzymes with such high TTN values by using natural thermostable enzymes (Table 3). Also, Bommarius and his coworker suggest a very simple way to calculate the TTN value of an enzyme: $\mathrm{TTN} = k_{\mathrm{cat}}/k_{\mathrm{d}}$, where k_{cat} and k_{d} are the turn-over number and degradation constant of the enzyme, respectively [119].

The discovery and utilization of thermoenzymes may be the simplest strategy. During the past few years, we have produced a number of thermophilic enzymes in *E. coli*, such as *Clostridium thermocellum* cellodextrin phosphorylase [17], *C. thermocellum* cellobiose phosphorylase [17], *C. thermocellum* glucan phosphorylase [72], *C. thermocellum* phosphoglucomutase [73], *T. maritima* 6-phophogluconate dehydrogenase [42], *T. maritima* fructose bisphosphatase [74], and *T. maritima* pentose phosphate isomerase [75]. Most of them have TTN values of more than 10^7 as shown in Table 3.

Enzyme immobilization technology has been used to prolong the lifetime of enzymes for a long time [3, 120–122]. For instance, a one-step protein purification and immobilization method has been developed by using low-cost, ultra-high adsorption capacity RAC to adsorb CBM-tagged thermophilic *C. thermocellum* phosphoglucose isomerase (PGI) [82]. The resulting immobilized PGI is highly active and ultra-stable compared to the nonimmobilized PGI, with a TTN of more than 10^9 mol of product per mol of enzyme at 60 °C (Table 3). In the food

Table 3 Examples of stable enzyme building blocks suitable for biocommodity production

EC family	Enzyme name	Microorganism source	Form	Condition	TTN (mol/mol)	Ref.
1.1.1.44	6-Phosphogluconate hydrogenase	*T. maritima*	Free	80 °C	2.4×10^8	Wang and Zhang [42]
2.2.1.2	Transaldolase	*T. maritima*	Free	60 °C	1.7×10^7	Huang et al. [113]
3.1.3.11	Fructose 1,6-Bisphosphatase	*T. maritima*	Free	60 °C	2×10^7	Myung et al. [74]
5.4.2.2	Phosphoglucomutase	*C. thermocellum*	Free	60 °C	7.1×10^7	Wang and Zhang [73]
5.3.1.5	Xylose (glucose) isomerase		Immobilized	50–60 °C	5.0×10^8	Zhang [4]
5.3.1.6	Ribose-5-phosphate isomerase	*T. maritima*	Free	60–70 °C	2.2×10^8	Sun et al. [75]
5.3.1.9	Phosphoglucose isomerase	*C. thermocellum*	Free Immobilized	60 °C	3.2×10^7 1.1×10^9	Myung et al. [82]

industry, immobilized thermophilic glucose isomerase exhibits TTN values of $\sim 5 \times 10^8$ mol of product per mol of enzyme. As a result, no company has a motivation to further prolong the lifetime of this enzyme.

Directed evolution and rational design are powerful approaches to enhancing the thermostability of enzymes [123, 124]. Among different desired properties of engineered enzymes, improving enzyme stability is the easiest. A number of companies and academic laboratories have developed tools for enhancing enzyme lifetime. For example, some enzyme companies and start-ups, such as Codexis, Biomethodes, EnzymeWorks, and Arzeda have demonstrated a number of successful examples for enhancing enzyme stability meeting their customers' needs. For example, Codexis is developing a stable carbonic andrase used for capturing high-temperature and low-pH CO_2 from the waste gas of power stations. Also, a combination of rational and random design also have a significant effect on enzyme stability [40].

4.3 Redox Enzyme Engineering

Since both NADP and NAD are not stable in vitro and are costly, it is important to replace them with low-cost biomimetic cofactors especially when cell-free systems are used to produce low-value biofuels and biochemicals (Fig. 10). The bulk prices of NADP, NAD, and nicotinate mononucleotide (NMN) are $4,500, $1,500, and $250 per kg, respectively (personal communication from Alex Tao). Biomimetic cofactors, such as NMN and 1-benzyl-1,4-dihydronicotinamide (BDN), not only have much lower selling prices but also have much better stability.

Redox enzyme engineering was initiated by Perham's group over 20 years ago [125]. By using molecular modeling and comparing amino acid sequences responsible for cofactor binding sites, they changed NADP-preferred glutathione dihydrogen to NAD-preferred by site directed mutagenesis [125]. After this, by using rational design, a number of studies were conducted by swapping cofactor preferences from NADP to NAD [126–132], from NAD to NADP [133–137], and relaxing or broadening cofactor specificity [138–142].

In the 1990s, Lowe and coworkers developed a series of biomimetic analogues of NAD(P) based on triazine dyes [143–147]. Some natural dehydrogenases, such as horse liver alcohol dehydrogenase, can utilize such biomimetic cofactors for implementing redox reactions [146]. Later, Fish et al. determined that the pyrophosphate and adenosine groups associated with NAD are not essential in the hydride transfer and proposed the use of BDN or its analogues to replace natural cofactors [148]. Later, they also showed that wild-type horse liver alcohol dehydrogenase [149] and monooxygenase [150] can work on such biomimics. However, most wild-type redox enzymes cannot work on such biomimics. Clark and Fish demonstrated that a P450 mutant with two amino acid changes can work on these biomimics [151]. Also, another group demonstrated that engineered P450 can utilize Zn dust as an electron source rather than natural cofactors [152, 153]. In

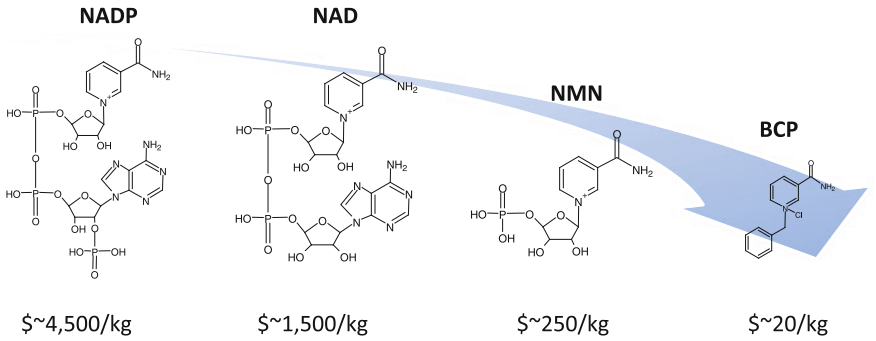

Fig. 10 Structures of natural cofactors and biomimetic cofactors

2011, Zhao and coworkers presented a bio-orthogonal system that catalyzed the oxidative decarboxylation of L-malate with a dedicated biomimetic cofactor, nicotinamide flucytosine dinucleotide, where the redox enzymes were engineered by using saturation mutagenesis of the key amino acid sites [154].

NMN is a precursor of NAD(P) with a much smaller size as compared to NAD(P) (Fig. 6). A few wild-type redox enzymes function using NMN, including liver alcohol dehydrogenase [155] and glutamic dehydrogenase [156]. Recently, Scott et al. demonstrated that engineered *Pyrococcus furiosus* alcohol dehydrogenase has an ability to work on NMN [157].

Although the importance of redox enzyme engineering is gaining recognition for future biomanufacturing [1, 4, 14, 28], redox enzyme engineering remains at an early stage because no framework or general rules exist for engineering redox enzymes on non-natural cofactors [157]. This direction may become one of the top R&D priorities of cell-free biosystems, especially for the production of biocommodities but not for the production of pharmaceuticals that can use more costly natural cofactors.

4.4 Compromised Reaction Conditions

Although numerous enzymes used for the proof-of-concept cell-free biotransformation experiments have different optimal conditions [17, 26], they can work together under compromised conditions (e.g., 30–32 °C) where hyperthermophilic hydrogenase exhibited a very low activity. According to our experiences and literature data, most enzymes from different sources are highly exchangeable in cell-free biosystems [25]. In future applications, we will discover and utilize nearly all enzymes from one source and/or engineer some unmatched enzymes to make their optimal condition match most of other enzymes.

5 Conclusion

The significant advantages provided by cell-free biosystems (Table 1) are motivating their transition from basic research tools to a future biomanufacturing platform. Although a few obstacles to cell-free biosystems remain, all of them can be addressed by using well-known technologies (Table 2). The development of cell-free biosystems may have a similar trend to modern computers. The first prototypes were extremely costly, with low performance, and few applications. After the performance of each part (e.g., CPU, RAM) was improved greatly and standard parts were produced on a large scale, it was simple and less costly to assemble a customized high-performance computer at low prices by using the available standardized parts. Now it is time to discover and develop more stable enzymes as standardized building blocks and engineer redox enzymes that can work with less costly and more stable biomimic cofactors. Cell-free biosystems will eventually become a new biotechnology platform for biomanufacturing numerous products, especially for biocommodities because they are highly cost-sensitive to both product yields (or energy efficiencies) and production costs.

Acknowledgments This work was supported partially by the Shell Game Charger Program, DOE BioEnergy Science Center (BESC), DOE ARPA-E Petro project, the College of Agriculture and Life Sciences Bioprocessing and Biodesign Research Center at Virginia Tech, and NSF SBIR.

References

1. Zhang Y-HP, Huang W-D (2012) Constructing the electricity-carbohydrate-hydrogen cycle for a sustainability revolution. Trends Biotechnol 30:301–306
2. Thiel KA (2004) Biomanufacturing, from bust to boom…to bubble? Nat Biotechnol 22:1365–1372
3. Zhang Y-HP, Myung S, You C, Zhu ZG, Rollin J (2011) Toward low-cost biomanufacturing through cell-free synthetic biology: bottom-up design. J Mater Chem 21:18877–18886
4. Zhang Y-HP (2010) Production of biocommodities and bioelectricity by cell-free synthetic enzymatic pathway biotransformations: challenges and opportunities. Biotechnol Bioeng 105:663–677
5. Vasic-Racki D (2006) History of industrial biotransformations—Dreams and realities. In: Liese A, Seebald S, Wandrey C (eds) Industrial biotransformations. Wiley-VCH, Weinheim, pp 1–37
6. Lopez-Gallego F, Schmidt-Dannert C (2010) Multi-enzymatic synthesis. Curr Opin Chem Biol 14:174–183
7. Ricca E, Brucher B, Schrittwieser JH (2011) Multi-enzymatic cascade reactions: overview and perspectives. Adv Synth Catal 353:2239–2262
8. Santacoloma PA, Sin Gr, Gernaey KV, Woodley JM (2010) Multienzyme-catalyzed processes: next-generation biocatalysis. Org Proc Res Dev 15:203–212
9. Schoffelen S, van Hest JCM (2012) Multi-enzyme systems: bringing enzymes together in vitro. Soft Matter 8:1736–1746
10. Katzen F, Chang G, Kudlicki W (2005) The past, present and future of cell-free protein synthesis. Trends Biotechnol 23:150–156

11. Hodgman CE, Jewett MC (2012) Cell-free synthetic biology: thinking outside the cell. Metab Eng 14:261–269
12. Bujara M, Schümperli M, Billerbeck S, Heinemann M, Panke S (2010) Exploiting cell-free systems: Implementation and debugging of a system of biotransformations. Biotechnol Bioeng 106:376–389
13. Zhang YHP, You C, Chen H, Feng R (2012) Surpassing photosynthesis: High-efficiency and scalable CO_2 utilization through artificial photosynthesis. In ACS Symposium Series . Recent Advances in Post-Combustion CO_2 Capture Chemistry. American Chemical Society, pp275–292
14. Zhang Y-HP (2011) Simpler is better: high-yield and potential low-cost biofuels production through cell-free synthetic pathway biotransformation (SyPaB). ACS Catal 1:998–1009
15. Huang WD, Zhang Y-HP (2011) Analysis of biofuels production from sugar based on three criteria: Thermodynamics, bioenergetics, and product separation. Energy Environ Sci 4:784–792
16. Maeda T, Sanchez-Torres V, Wood TK (2012) Hydrogen production by recombinant *Escherichia coli* strains. Microb Biotechnol. doi: 10.1111/j.1751-7915.2011.00282.x
17. Ye X, Wang Y, Hopkins RC, Adams MWW, Evans BR, Mielenz JR, Zhang Y-HP (2009) Spontaneous high-yield production of hydrogen from cellulosic materials and water catalyzed by enzyme cocktails. ChemSusChem 2:149–152
18. Logan BE (2009) Exoelectrogenic bacteria that power microbial fuel cells. Nat Rev Microbiol 7:375–381
19. Gellett W, Schumacher J, Kesmez M, Le D, Minteer SD (2010) High current density air-breathing laccase biocathode. J Electrochem Soc 157:B557–B562
20. Zebda A, Gondran C, Le Goff A, Holzinger M, Cinquin P, Cosnier S (2011) Mediatorless high-power glucose biofuel cells based on compressed carbon nanotube-enzyme electrodes. Nat Commun 2:370
21. Zhang Y-HP (2010) Renewable carbohydrates are a potential high density hydrogen carrier. Int J Hydrogen Energy 35:10334–10342
22. Carlson ED, Gan R, Hodgman CE, Jewett MC (2012) Cell-free protein synthesis: applications come of age. Biotechnol Adv 30:1185–1194
23. Guterl J-K, Garbe D, Carsten J, Steffler F, Sommer B, Reiße S, Philipp A, Haack M, Rühmann B, Kettling U, et al (2012) Cell-free metabolic engineering—production of chemicals via minimized reaction cascades. ChemSusChem. doi: 10.1002/cssc.201200365
24. Wang Y, Huang W, Sathitsuksanoh N, Zhu Z, Zhang Y-HP (2011) Biohydrogenation from biomass sugar mediated by in vitro synthetic enzymatic pathways. Chem Biol 18:372–380
25. Zhang Y-HP, Sun J-B, Zhong J–J (2010) Biofuel production by in vitro synthetic pathway transformation. Curr Opin Biotechnol 21:663–669
26. Zhang Y-HP, Evans BR, Mielenz JR, Hopkins RC, Adams MWW (2007) High-yield hydrogen production from starch and water by a synthetic enzymatic pathway. PLoS One 2:e456
27. Bujara M, Schümperli M, Pellaux R, Heinemann M, Panke S (2011) Optimization of a blueprint for in vitro glycolysis by metabolic real-time analysis. Nat Chem Biol 7:271–277
28. Swartz JR (2011) Transforming biochemical engineering with cell-free biology. AIChE J 58:5–13
29. Shimizu Y, Inoue A, Tomari Y, Suzuki T, Yokogawa T, Nishikawa K, Ueda T (2001) Cell-free translation reconstituted with purified components. Nat Biotechnol 19:751–755
30. Buchner E (1897) Alkoholische Gärung ohne Hefezellen (Vorläufige Mitteilung). Berichte der Deutschen Chemischen Gesellschaft 30:117–124
31. Harden A, Young WJ (1907) The alcoholic ferment of yeast-juice. Proc Roy Soc London 77B:405–422
32. Warburg OH (1926) Über den Stoffwechsel der Tumoren. Springer, Berlin
33. Cori CF (1931) Mammalian carbohydrate metabolism. Physiol Rev 11:143–275
34. Cori GT, Cori CF (1936) The formation of hexosephosphate esters in frog muscle. J Biol Chem 116:119–128

35. Krebs HA, Eggleston LV (1944) Metabolism of acetoacetic acid in animal tissues. Nature 154:209–210
36. Calvin M, Benson AA (1948) The path of carbon in photosynthesis. Science 107:476–480
37. Nirenberg MW, Matthaei JH (1961) The dependence of cell-free protein synthesis in E. coli upon naturally occurring or synthetic polyribonucleotides. Proc Natl Acad Sci USA 47:1588–1602
38. Michels P, Rosazza J (2009) The evolution of microbial transformations for industrial applications. SIM News 2009:36–52
39. Demain AL (2004) Pickles, pectin, and penicillin. Annu Rev Microbiol 58:1–42
40. Ye X, Zhang C, Zhang YHP (2012) Engineering a large protein by combined rational and random approaches: stabilizing the *Clostridium thermocellum* cellobiose phosphorylase. Mol BioSyst 8:1815–1823
41. Shiloach J, Fass R (2005) Growing *E. coli* to high cell density—a historical perspective on method development. Biotechnol Adv 23:345–357
42. Wang Y, Zhang Y-HP (2009) Overexpression and simple purification of the *Thermotoga maritima* 6-phosphogluconate dehydrogenase in *Escherichia coli* and its application for NADPH regeneration. Microb Cell Fact 8:30
43. Tufvesson Pr, Lima-Ramos J, Nordblad M, Woodley JM (2011) Guidelines and cost analysis for catalyst production in biocatalytic processes. Org Proc Res Dev 15:266–274
44. Bornscheuer UT, Huisman GW, Kazlauskas RJ, Lutz S, Moore JC, Robins K (2012) Engineering the third wave of biocatalysis. Nature 485:185–194
45. Daines AM, Maltman BA, Flitsch SL (2004) Synthesis and modifications of carbohydrates, using biotransformations. Curr Opin Chem Biol 8:106–113
46. Chi Y, Scroggins ST, Frechet JMJ (2008) One-pot multi-component asymmetric cascade reactions catalyzed by soluble star polymers with highly branched non-interpenetrating catalytic cores. J Am Chem Soc 130:6322–6323
47. Lynd LR, Weimer PJ, van Zyl WH, Pretorius IS (2002) Microbial cellulose utilization: fundamentals and biotechnology. Microbiol Mol Biol Rev 66:506–577
48. Liao HH, Zhang XZ, Rollin JA, Zhang Y-HP (2011) A minimal set of bacterial cellulases for consolidated bioprocessing of lignocellulose. Biotechnol J 6:1409–1418
49. Wildeman SMAD, Sonke T, Schoemaker HE, May O (2007) Biocatalytic reductions: from lab curiosity to "first choice". Acc Chem Res 40:1260–1266
50. Wichmann R, Vasic-Racki D (2005) Cofactor regeneration at the lab scale. Adv Biochem Eng Biotechnol 92:225–260
51. Bozic M, Pricelius S, Guebitz GM, Kokol V (2010) Enzymatic reduction of complex redox dyes using NADH-dependent reductase from *Bacillus subtilis* coupled with cofactor regeneration. Appl Microbiol Biotechnol 85:563–571
52. Xu Z, Jing K, Liu Y, Cen P (2007) High-level expression of recombinant glucose dehydrogenase and its application in NADPH regeneration. J Ind Microbiol Biotechnol 34:83–90
53. Mertens R, Liese A (2004) Biotechnological applications of hydrogenases. Curr Opin Biotechnol 15:343–348
54. Johannes TW, Woodyer RD, Zhao H (2007) Efficient regeneration of NADPH using an engineered phosphite dehydrogenase. Biotechnol Bioeng 96:18–26
55. Schoevaart R, van Rantwijk F, Sheldon RA (2000) A four-step enzymatic cascade for the one-pot synthesis of non-natural carbohydrates from glycerol. J Org Chem 65:6940–6943
56. Zhang J, Shao J, Kowal P, Wang PG (2005) Enzymatic Synthesis of Oligosaccharides. Wiley-VCH Verlag GmbH & Co.KGaA, Weinheim
57. Fessner W-D, Helaine V (2001) Biocatalytic synthesis of hydroxylated natural products using aldolases and related enzymes. Curr Opin Biotechnol 12:574–586
58. Endo T, Koizumi S (2000) Large-scale production of oligosaccharides using engineered bacteria. Curr Opin Struct Biol 10:536–541
59. Wang Y, Zhang Y-HP (2009) Cell-free protein synthesis energized by slowly-metabolized maltodextrin. BMC Biotechnol 9:58

60. Calhoun KA, Swartz JR (2005) An economical method for cell-free protein synthesis using glucose and nucleoside monophosphates. Biotechnol Prog 21:1146–1153
61. Hold C, Panke S (2009) Towards the engineering of in vitro systems. J Royal Soc Interface 6:S507–S521
62. Panke S, Held M, Wubbolts M (2004) Trends and innovations in industrial biocatalysis for the production of fine chemicals. Curr Opin Biotechnol 15:272–279
63. Schultheisz HL, Szymczyna BR, Scott LG, Williamson JR (2008) Pathway engineered enzymatic de Novo purine nucleotide synthesis. ACS Chem Biol 3:499–511
64. Schultheisz HL, Szymczyna BR, Williamson JR (2009) Enzymatic synthesis and structural characterization of 13C, 15 N-poly(ADP-ribose). J Am Chem Soc 131:14571–14578
65. Lynd LR, Wyman CE, Gerngross TU (1999) Biocommodity engineering. Biotechnol Prog 15:777–793
66. Zhang Y-HP (2011) What is vital (and not vital) to advance economically-competitive biofuels production. Proc Biochem 46:2091–2110
67. Zhang Y-HP (2011) Hydrogen production from carbohydrates: a mini-review. ACS Symp Ser 1067:203–216
68. Adams MWW, Stiefel EI (1998) Biological hydrogen production: not so elementary. Science 282:1842–1843
69. Cortright RD, Davda RR, Dumesic JA (2002) Hydrogen from catalytic reforming of biomass-derived hydrocarbons in liquid water. Nature 418:964–967
70. Thauer K, Jungermann K, Decker K (1977) Energy conservation in chemotrophic anaerobic bacteria. Bacteriol Rev 41:100–180
71. The Royal Society of the UK (2007) Synthetic biology: call for views. http://royalsociety.org/page.asp?changes=0&latest=1&id=6731
72. Ye X, Rollin J, Zhang Y-HP (2010) Thermophilic α-glucan phosphorylase from *Clostridium thermocellum*: cloning, Characterization and enhanced thermostability. J Mol Cat B Enzym 65:110–116
73. Wang Y, Zhang Y-HP (2010) A highly active phosphoglucomutase from *Clostridium thermocellum*: Cloning, purification, characterization, and enhanced thermostability. J Appl Microbiol 108:39–46
74. Myung S, Wang YR, Zhang Y-HP (2010) Fructose-1,6-bisphosphatase from a hyperthermophilic bacterium *Thermotoga maritima*: Characterization, metabolite stability and its implications. Proc Biochem 45:1882–1887
75. Sun FF, Zhang XZ, Myung S, Zhang Y-HP (2012) Thermophilic *Thermotoga maritima* ribose-5-phosphate isomerase RpiB: Optimized heat treatment purification and basic characterization. Protein Expr Purif 82:302–307
76. Sun J, Hopkins RC, Jenney FE, McTernan PM, Adams MWW (2010) Heterologous expression and maturation of an NADP-dependent [NiFe]-hydrogenase: a key enzyme in biofuel production. PLoS One 5:e10526
77. Zhang Y-HP, Mielenz JR (2011) Renewable hydrogen carrier—carbohydrate: constructing the carbon-neutral carbohydrate economy. Energies 4:254–275
78. Scopes RK (1993) Protein purification: principles and practice, 3rd edn. Springer, New York
79. Hong J, Wang Y, Ye X, Zhang Y-HP (2008) Simple protein purification through affinity adsorption on regenerated amorphous cellulose followed by intein self-cleavage. J Chromatogr A 1194:150–154
80. Hong J, Ye X, Wang Y, Zhang Y-HP (2008) Bioseparation of recombinant cellulose binding module-protein by affinity adsorption on an ultra-high-capacity cellulosic adsorbent. Anal Chim Acta 621:193–199
81. Liao HH, Myung S, Zhang Y-HP (2012) One-step purification and immobilization of thermophilic polyphosphate glucokinase from *Thermobifida fusca* YX: glucose-6-phosphate generation without ATP. Appl. Microbiol Biotechnol 93:1109–1117

82. Myung S, Zhang X-Z, Zhang Y-HP (2011) Ultra-stable phosphoglucose isomerase through immobilization of cellulose-binding module-tagged thermophilic enzyme on low-cost high-capacity cellulosic adsorbent. Biotechnol Prog 27:969–975
83. Bai FW, Anderson WA, Moo-Young M (2008) Ethanol fermentation technologies from sugar and starch feedstocks. Biotechnol Adv 26:89–105
84. Welch P, Scopes RK (1985) Studies on cell-free metabolism: Ethanol production by a yeast glycolytic system reconstituted from purified enzymes. J Biotechnol 2:257–273
85. Li S, Wen J, Jia X (2011) Engineering *Bacillus subtilis* for isobutanol production by heterologous *Ehrlich* pathway construction and the biosynthetic 2-ketoisovalerate precursor pathway overexpression. Appl Microbiol Biotechnol 91:577–589
86. Atsumi S, Hanai T, Liao JC (2008) Non-fermentative pathways for synthesis of branched-chain higher alcohols as biofuels. Nature 451:86–89
87. Moradian A, Benner SA (1992) A biomimetic biotechnological process for converting starch to fructose: thermodynamic and evolutionary considerations in applied enzymology. J Am Chem Soc 114:6980–6987
88. Petitou M, van Boeckel CAA (2004) A synthetic antithrombin iii binding pentasaccharide is now a drug! What comes next? Angew Chem Int Ed 43:3118–3133
89. Xu Y, Masuko S, Takieddin M, Xu H, Liu R, Jing J, Mousa SA, Linhardt RJ, Liu J (2011) Chemoenzymatic synthesis of homogeneous ultralow molecular weight heparins. Science 334:498–501
90. Moehlenbrock M, Minteer S (2008) Extended lifetime biofuel cells. Chem Soc Rev 37:1188–1196
91. Zhang Y-HP, Xu J-H, Zhong JJ (2012) A new high-energy density hydrogen carrier - carbohydrate - might be better than methanol. Int. J. Energy Res. Epub, doi: 10.1002/er.2897
92. Minteer SD, Liaw BY, Cooney MJ (2007) Enzyme-based biofuel cells. Curr. Opin. Biotechnol. 18:228–234
93. Cooney MJ, Svoboda V, Lau C, Martin G, Minteer SD (2008) Enzyme catalysed biofuel cells. Energy Environ Sci 1:320–337
94. Zhu ZG, Sun F, Zhang X, Zhang Y-HP (2012) Deep oxidation of glucose in enzymatic fuel cells through a synthetic enzymatic pathway containing a cascade of two thermostable dehydrogenases. Biosens Bioelectron 36:110–115
95. Palmore GTR, Bertschy H, Bergens SH, Whitesides GM (1998) A methanol/dioxygen biofuel cell that uses NAD^+-dependent dehydrogenases as catalysts: application of an electro-enzymatic method to regenerate nicotinamide adenine dinucleotide at low overpotentials. J Electroanal Chem 443:155–161
96. Sokic-Lazic D, Minteer SD (2008) Citric acid cycle biomimic on a carbon electrode. Biosens Bioelectron 24:939–944
97. Arechederra RL, Treu BL, Minteer SD (2007) Development of glycerol/O-2 biofuel cell. J Power Sources 173:156–161
98. Sokic-Lazic D, Minteer SD (2009) Pyruvate/air enzymatic biofuel cell capable of complete oxidation. Electrochem Solid-State Lett 12:F26–F28
99. Moehlenbrock MJ, Toby TK, Waheed A, Minteer SD (2010) Metabolon catalyzed pyruvate/air biofuel cell. J Am Chem Soc 132:6288–6289
100. Xu S, Minteer SD (2011) Enzymatic biofuel cell for oxidation of glucose to CO_2. ACS Catal 1:91–94
101. Marsh JJ, Lebherz HG (1992) Fructose-bisphosphate aldolases: an evolutionary history. Trends Biochem Sci 17:110–113
102. Hibbert EG, Senussi T, Costelloe SJ, Lei W, Smith MEB, Ward JM, Hailes HC, Dalby PA (2007) Directed evolution of transketolase activity on non-phosphorylated substrates. J Biotechnol 131:425–432
103. Boyer ME, Stapleton JA, Kuchenreuther JM, Wang C-w, Swartz JR (2008) Cell-free synthesis and maturation of [FeFe] hydrogenases. Biotechnol Bioeng 99:59–67
104. Kim D-M, Swartz JR (2004) Efficient production of a bioactive, multiple disulfide-bonded protein using modified extracts of *Escherichia coli*. Biotechnol Bioeng 85:122–129

105. Kanter G, Yang J, Voloshin A, Levy S, Swartz JR, Levy R (2007) Cell-free production of scFv fusion proteins: an efficient approach for personalized lymphoma vaccines. Blood 109:3393–3399
106. Bundy BC, Franciszkowicz MJ, Swartz JR (2008) Escherichia coli-based cell-free synthesis of virus-like particles. Biotechnol Bioeng 100:28–37
107. Lee K-H, Kwon Y-C, Yoo SJ, Kim D-M (2010) Ribosomal synthesis and in situ isolation of peptide molecules in a cell-free translation system. Protein Expr Purif 71:16–20
108. Beveridge WIB (1960) The art of scientific investigation. Vintage, New York
109. Smith P, Powlson DS, Glendining MJ, Smith JU (1998) Preliminary estimates of the potential for carbon mitigation in European soils through no-till farming. Glob Change Biol 4:679–685
110. Klein-Marcuschamer D, Oleskowicz-Popiel P, Simmons BA, Blanch HW (2012) The challenge of enzyme cost in the production of lignocellulosic biofuels. Biotechnol Bioeng 109:1083–1087
111. Tishkov VI, Popov VO (2006) Protein engineering of formate dehydrogenase. Biomol Eng 23:89–110
112. You C, Myung S, Zhang Y-HP (2012) Facilitated substrate channeling in a self-assembled trifunctional enzyme complex. Angew Chem Int Ed 51:8787–8790
113. Huang SY, Zhang Y-HP, Zhong JJ (2012) A thermostable recombinant transaldolase with high activity over a broad pH range. Appl Microbiol Biotechnol 93:2403–2410
114. Zhang Y-HP (2011) Substrate channeling and enzyme complexes for biotechnological applications. Biotechnol Adv 29:715–725
115. Bayer EA, Morag E, Lamed R (1994) The cellulosome–a treasure-trove for biotechnology. Trends Biotechnol 12:379–386
116. You C, Zhang X-Z, Sathitsuksanoh N, Lynd LR, Zhang Y-HP (2012) Enhanced microbial cellulose utilization of recalcitrant cellulose by an ex vivo cellulosome-microbe complex. Appl Environ Microbiol 78:1437–1444
117. You C, Zhang X-Z, Zhang YHP (2012) Mini-scaffoldin enhanced mini-cellulosome hydrolysis performance on low-accessibility cellulose (Avicel) more than on high-accessibility amorphous cellulose. Biochem Eng J 63:57–65
118. Moraïs S, Barak Y, Hadar Y, Wilson DB, Shoham Y, Lamed R, Bayer EA (2011) Assembly of xylanases into designer cellulosomes promotes efficient hydrolysis of the xylan component of a natural recalcitrant cellulosic substrate. MBio 2 e00233-11
119. Rogers TA, Bommarius AS (2010) Utilizing simple biochemical measurements to predict lifetime output of biocatalysts in continuous isothermal processes. Chem Eng Sci 65: 2118–2124
120. Cao L, Langen Lv, Sheldon RA (2003) Immobilised enzymes: carrier-bound or carrier-free? Curr Opin Biotechnol 14:387–394
121. Cao L (2005) Immobilised enzymes: science or art? Curr Opin Chem Biol 9:217–226
122. Hartmann M, Jung D (2010) Biocatalysis with enzymes immobilized on mesoporous hosts: the status quo and future trends. J Mater Chem 20:844–857
123. Arnold FH, Volkov AA (1999) Directed evolution of biocatalysts. Curr Opin Chem Biol 3:54–59
124. Eijsink VG, Bjork A, Gaseidnes S, Sirevag R, Synstad B, van den Burg B, Vriend G (2004) Rational engineering of enzyme stability. J Biotechnol 113:105–120
125. Scrutton NS, Berry A, Perham RN (1990) Redesign of the coenzyme specificity of a dehydrogenase by protein engineering. Nature 343:38–43
126. Zhang L, Ahvazi B, Szittner R, Vrielink A, Meighen E (1999) Change of nucleotide specificity and enhancement of catalytic efficiency in single point mutants of *Vibrio harveyi* aldehyde dehydrogenase. Biochemistry 38:11440–11447
127. Yaoi T, Miyazaki K, Oshima T, Komukai Y, Go M (1996) Conversion of the coenzyme specificity of isocitrate dehydrogenase by module replacement. J Biochem 119:1014–1018

128. Bastian S, Liu X, Meyerowitz JT, Snow CD, Chen MMY, Arnold FH (2011) Engineered ketol-acid reductoisomerase and alcohol dehydrogenase enable anaerobic 2-methylpropan-1-ol production at theoretical yield in *Escherichia coli*. Metab Eng 13:345–352
129. Rosell A, Valencia E, Ochoa WF, Fita I, Pares X, Farres J (2003) Complete reversal of coenzyme specificity by concerted mutation of three consecutive residues in alcohol dehydrogenase. J Biol Chem 278:40573–40580
130. Döhr O, Paine MJI, Friedberg T, Roberts GCK, Wolf CR (2001) Engineering of a functional human NADH-dependent cytochrome P450 system. Proc Natl Acad Sci USA 98:81–86
131. Banta S, Swanson BA, Wu S, Jarnagin A, Anderson S (2002) Alteration of the specificity of the cofactor-binding pocket of *Corynebacterium* 2,5-diketo-D-gluconic acid reductase A. Protein Eng Des Sel 15:131–140
132. Banta S, Swanson BA, Wu S, Jarnagin A, Anderson S (2002) Optimizing an artificial metabolic pathway: Engineering the cofactor specificity of *Corynebacterium* 2,5-Diketo-D-gluconic acid reductase for use in vitamin C biosynthesis. Biochemistry 41:6226–6236
133. Bocanegra JA, Scrutton NS, Perham RN (1993) Creation of an NADP-dependent pyruvate dehydrogenase multienzyme complex by protein engineering. Biochemistry 32:2737–2740
134. Mittl PRE, Berry A, Scrutton NS, Perham RN, Schulz GE (1993) Structural differences between wild-type NADP-dependent glutathione reductase from *Escherichia coli* and a redesigned NAD-dependent mutant. J Mol Biol 231:191–195
135. Steen IH, Lien T, Madsen MS, Birkeland N-K (2002) Identification of cofactor discrimination sites in NAD-isocitrate dehydrogenase from *Pyrococcus furiosus*. Arch Microbiol 178:297–300
136. Watanabe S, Kodaki T, Makino K (2005) Complete reversal of coenzyme specificity of xylitol dehydrogenase and increase of thermostability by the introduction of structural zinc. J Biol Chem 280:10340–10349
137. Glykys DJ, Banta S (2009) Metabolic control analysis of an enzymatic biofuel cell. Biotechnol Bioeng 102:1624–1635
138. Woodyer RD, van der Donk WA, Zhao H (2003) Relaxing the nicotinamide cofactor specificity of phosphite dehydrogenase by rational design. Biochemistry 42:11604–11614
139. Wiegert T, Sahm H, Sprenger GA (1997) The substitution of a single amino acid residue (Ser-116 → Asp) alters NADP-containing glucose-fructose oxidoreductase of Zymomonas mobilis into a glucose dehydrogenase with dual coenzyme specificity. J Biol Chem 272:13126–13133
140. Katzberg M, Skorupa-Parachin N, Gorwa-Grauslund M-F, Bertau M (2010) Engineering cofactor preference of ketone reducing biocatalysts: A mutagenesis study on a γ-Diketone reductase from the yeast Saccharomyces cerevisiae serving as an example. Int J Mol Sci 11:1735–1758
141. Sanli G, Banta S, Anderson S, Blaber M (2004) Structural alteration of cofactor specificity in Corynebacterium 2,5-diketo-D-gluconic acid reductase. Protein Eng 13:504–512
142. Campbell E, Wheeldon IR, Banta S (2010) Broadening the cofactor specificity of a thermostable alcohol dehydrogenase using rational protein design introduces novel kinetic transient behavior. Biotechnol Bioeng 107:763–774
143. Burton SJ, Vivian Stead C, Ansell RJ, Lowe CR (1996) An artificial redox coenzyme based on a triazine dye template. Enzym Microb Technol 18:570–580
144. Ansell RJ, Dilmaghanian S, Stead CV, Lowe CR (1997) Synthesis and properties of new coenzyme mimics based on the artificial coenzyme Blue N-3. Enzym Microb Technol 21:327–334
145. Ansell RJ, Small DAP, Lowe CR (1997) Characterisation of the artificial coenzyme CL4. J Mol Catal B Enzym 3:239–252
146. Ansell RJ, Lowe CR (1999) Artificial redox coenzymes: biomimetic analogues of NAD^+. Appl Microbiol Biotechnol 51:703–710
147. Ansell RJ, Small DAP, Lowe CR (1999) Synthesis and properties of new coenzyme mimics based on the artificial coenzyme CL4. J Mol Recognit 12:45–56

148. Lo HC, Leiva C, Buriez O, Kerr JB, Olmstead MM, Fish RH (2001) Bioorganometallic chemistry. 13. regioselective reduction of NAD^+ models, 1-benzylnicotinamde triflate and beta-nicotinamide ribose-5′-methyl phosphate, with in situ generated $[Cp^*Rh(Bpy)H]^+$: structure–activity relationships, kinetics, and mechanistic aspects in the formation of the 1,4-NADH derivatives. Inorg Chem 40:6705–6716
149. Lo HC, Fish RH (2002) Biomimetic NAD^+ models for tandem cofactor regeneration, horse liver alcohol dehydrogenase recognition of 1,4-NADH derivatives, and chiral synthesis. Angew Chem Int Ed 41:478–481
150. Lutz J, Hollmann F, Ho TV, Schnyder A, Fish RH, Schmid A (2004) Bioorganometallic chemistry: biocatalytic oxidation reactions with biomimetic NAD^+/NADH co-factors and $[Cp^*Rh(bpy)H]^+$ for selective organic synthesis. J Organomet Chem 689:4783–4790
151. Ryan JD, Fish RH, Clark DS (2008) Engineering cytochrome P450 enzymes for improved activity towards biomimetic 1,4-NADH cofactors. ChemBioChem 9:2579–2582
152. Nazor J, Schwaneberg U (2006) Laboratory evolution of P450 BM-3 for mediated electron transfer. ChemBioChem 7:638–644
153. Nazor J, Dannenmann S, Adjei RO, Fordjour YB, Ghampson IT, Blanusa M, Roccatano D, Schwaneberg U (2008) Laboratory evolution of P450 BM3 for mediated electron transfer yielding an activity-improved and reductase-independent variant. Protein Eng Des Sel 21:29–35
154. Ji D, Wang L, Hou S, Liu W, Wang J, Wang Q, Zhao ZK (2011) Creation of bioorthogonal redox systems depending on nicotinamide flucytosine dinucleotide. J Am Chem Soc 133:20857–20862
155. Plapp BV, Sogin DC, Dworschack RT, Bohlken DP, Woenckhaus C, Jeck R (1986) Kinetics and native and modified liver alcohol dehydrogenase with coenzyme analogs: isomerization of enzyme-nicotinamide adenine dinucleotide complex. Biochemistry 25:5396–5402
156. Fisher HF, McGregor LL (1969) The ability of reduced nicotinamide mononucleotide to function as a hydrogen donor in the glutamic dehydrogenase reaction. Biochem Biophys Res Commun 34:627–632
157. Campbell E, Meredith M, Minteer SD, Banta S (2012) Enzymatic biofuel cells utilizing a biomimetic cofactor. Chem Commun 48:1898–1900
158. Schoevaart R, van Rantwijk F, Sheldon RA (1999) Carbohydrates from glycerol: an enzymatic four-step, one-pot synthesis. Chem Commun 31:2465–2466
159. You C, Zhang Y-HP (2012) Self-assembly of synthetic metabolons through synthetic protein scaffolds: one-step purification, co-immobilization, and substrate channeling. ACS Syn. Biol. doi: 10.1021/sb300068g
160. Studier FW (2005) Protein production by auto-induction in high density shaking cultures. Protein Expr Purif 41:207–234
161. Banki MR, Feng L, Wood DW (2005) Simple bioseparations using self-cleaving elastin-like polypeptide tags. Nat Methods 2:659–662
162. Iturrate L, Sanchez-Moreno I, Doyaguez EG, Garcia-Junceda E (2009) Substrate channelling in an engineered bifunctional aldolase/kinase enzyme confers catalytic advantage for C–C bond formation. Chem Commun 2009:1721–1723
163. Bulow L, Ljungcrantz P, Mosbach K (1985) Preparation of a soluble bifunctional enzyme by gene fusion. Nat Biotechnol 3:821–823
164. Chen X, Liu Z, Zhang J, Zhang W, Kowal P, Wang P (2002) Reassembled biosynthetic pathway for large-scale carbohydrate synthesis: α-gal epitope producing "superbug". ChemBioChem 4:47–53
165. Nahalka J, Liu Z, Chen X, Wang PG (2003) Superbeads: Immobilization in "sweet" chemistry. Chem Eur J 9:372–377
166. Demain AL, Vaishnav P (2009) Production of recombinant proteins by microbes and higher organisms. Biotechnol Adv 27:297–306
167. Kirk O, Borchert TV, Fuglsang CC (2002) Industrial enzyme applications. Curr Opin Biotechnol 13:345–351

168. Liu W, Wang P (2007) Cofactor regeneration for sustainable enzymatic biosynthesis. Biotechnol Adv 25:369–384
169. Chen K, Arnold FH (1993) Turning the activity of an enzyme for unusual environments: sequential random mutagenesis of subtilisin E for catalysis in dimethylformamide. Proc Natl Acad Sci USA 90:5618–5622

Adv Biochem Eng Biotechnol (2013) 131: 121–152
DOI: 10.1007/10_2012_135

Published Online: 29 June 2012

Lipid Bilayer Membrane Arrays: Fabrication and Applications

Xiaojun Han, Guodong Qi, Xingtao Xu and Lei Wang

Abstract The lipid bilayer is one of the most important self-assembled structures in nature. In addition to compartmentalizing the cell, the lipid bilayer maintains many physical and biological characteristics of cell membranes, including lateral fluidity. It provides a wealth of opportunities for the study of membrane properties. Recently there has been an increasing interest in lipid bilayer arrays fabrication and their applications. In this review, the leading methods for creating lipid bilayer arrays are categorized as mechanical methods, pre-patterning substrate, direct UV patterning, direct blotting or stamping, polymer liftoff technique, robotic micro spotting, and microfluidics. The applications of bilayer arrays for cell adhesion and activation, lipid bilayer based 2D electrophoresis, and high-throughput binding assays are also presented.

Keywords Cell adhesion · High-throughput binding assay · Lipid bilayer arrays · Photolithography

Abbreviations

TR-PE	Texas Red 1, 2-dihexadecanoyl-*sn*-glycero-3-phosphoethanolamine
D-291	4-(4-(didecylamino) styryl)-*N*-methylpyridinium iodide (4-di-10-ASP)
NBD-PE	(*N*-(7-nitrobenz-2-oxa-1,3-diazol-4-yl)-1,2-dihexadecanoyl-*sn*glycero-3-phosphoethanolamine, triethylammonium salt)
Egg PC	Egg phosphatidylcholine
POPC	1-palmitoyl-2-oleoyl-*sn*-glycero-3-phosphocholine
NBD-PG	1-Acyl-2-{12-[(7-nitro-2-1,3-benzoxadiazol-4-yl)amino]lauroyl}-*sn*-glycero-3-[phospho-rac-(1-glycerol)] (ammonium salt)
TR-BSA	Bovine serum albumin labeled with Texas Red X-SE

X. Han (✉) · G. Qi · X. Xu · L. Wang
School of Chemical Engineering and Technology, Harbin Institute of Technology, No. 92, West Da-Zhi Street, Harbin 150001, China
e-mail: hanxiaojun@hit.edu.cn

Rh-PE	1,2-dipalmitoyl-*sn*-glycero-3-phosphoethanolamine-*N*-(lissamine-rhodamine B sulfonyl)
DOPC	1,2-dioleoyl-*sn*-glycero-3-phosphocholine
Oregon Green-DHPE	Oregon Green labeled 1,2-dihexadecanoyl-*sn*-glycero-3-phosphoethanolamine
Marina Blue-DHPE	Marina Blue labeled 1,2-dihexadecanoyl-*sn*-glycero-3-phosphoethanolamine
DNP-cap-DPPE	1,2-dipalmitoyl-*sn*-glycero-3-phosphoethanolamine-*N*-[6-[(2,4-dinitrophenyl)amino]hexanoyl] (ammonium salt)
GPI	Glycan-phosphatidyl inositol
PG	Phosphatidylglycerol
PC	Phosphatidylcholine
PS	Phosphatidylserine
DPPC	1,2-dipalmitoyl-*sn*-glycero-3-phosphocholine
NBD PS	1,2-dioleoyl-*sn*-glycero-3-phospho-L-serine-*N*-(7-nitro-2-1,3-benzoxadiazol-4-yl) (diammonium salt)
FITC	Fluorescein isothiocyanate
DOTAP	1,2-dioleoyl-3-trimethylammoniumpropane (chloride salt)
Biotin-cap DOPE	1,2-dioleoyl-*sn*-glycero-3-phosphoethanolamine-*N*-(cap biotinyl) (sodium salt)
T_m	Phase transition temperature
SAM	Self assembled monolayer
PDMS	Poly(dimethyl siloxane)
AFM	Atomic force microscopy
CFM	Continuous flow microspotter

Contents

1 Introduction

A biomembrane consists of a lipid bilayer with embedded proteins [1]. The lipid bilayer is a universal component of all cell-based biological systems, forming the barrier between cytosol and the cell's exterior, as well as mediating many biological functions by providing a defined interface for cell-surface recognition, signaling, and transport. The importance of the lipid bilayer has aroused great interest in fabricating artificial membranes as both freestanding lipid membranes [2–9] and solid supported lipid bilayer membranes [10–17]. Supported lipid bilayer membranes can be formed by spontaneous fusion of lipid vesicles onto hydrophilic surfaces, such as silica [12, 18]. Supported lipid bilayers are typically separated from the solid substrate by a thin (~ 1 nm) film of water [19], which serves as a lubricant for the lipids in the bilayer to diffuse laterally. The fluidity of supported lipid bilayers distinguishes them from other surfaces, such as self-assembled monolayers (SAMs). These model membranes have been very useful fro various research investigations, including ion channel activity, lipid phase separation, charged lipids manipulation, cell signaling, cell–cell interaction, membrane base biosensor, and protein binding.

Since Boxer et al. pioneered the patterning of the lipid bilayer using the lithographically fabricated corrals [16], lipid bilayer arrays have received considerable attention because of their potential use in studies of the physical and biological properties of membranes, lipid mobility kinetics, diagnostics, and cellular interactions with lipid-associated biomolecules. The lipid bilayer can be patterned in two ways: homogenous arrays (all patterns contain the same biomolecules) and heterogeneous arrays (all patterns contain different biomolecules, which is useful for high-throughput biosensing).

The aim of this review is to give readers an abundance of information on how to fabricate lipid bilayer arrays, as well as how to apply lipid bilayer arrays in research on cell adhesion and activation, 2D membrane electrophoresis, and high-throughput binding assays.

2 Fabrication Methods of Lipid Bilayer Membrane Arrays

2.1 Forming Patterned Lipid Bilayers by Mechanical Scratching

The simplest method to fabricate patterned lipid bilayers is to mechanically scratch the substrate with sharp tools, such as tweezers, after lipid bilayer formation [12, 18, 20–22]. By using tweezers to scratch the silicon oxide substrate in the

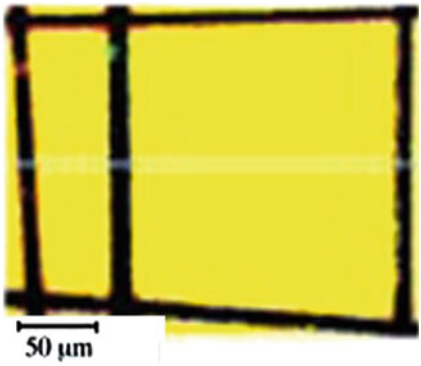

Fig. 1 Fluorescence image of a supported egg PC bilayer containing both 1 % Texas Red DHPE and 2 % D-291 (*green* dye labeled lipid) patterned into boxes by scratch marks. The *yellow* color in the image results from the mixture of *green* and *red* fluorescence lipids in the bilayer. Reprinted with permission from Ref. [20]. Copyright 1999 American Chemical Society

vertical and horizontal directions, one can create a checkerboard pattern. The boundaries created using this method are stable in basic buffer (above pH 8) or Millipore water for weeks to confine the fluid lipid bilayer. It is believed that the hydration layers on the silica substrate play a substantial role in maintaining the stability of a scratch barrier [20] because water molecules at a silica–buffer interface become ordered as the pH is raised; this highly ordered hydration layer is a poor lubricant for a spreading membrane. However, the lipid bilayer membranes spread under mildly acidic conditions. One example of this method is shown in Fig. 1 [20]. The black grids are a scratched area on the substrate created using a pair of tweezers. The *yellow* regions are the patterned lipid bilayers containing both green dye and red dye labeled lipids.

2.2 *Forming Lipid Bilayer Arrays Using Pre-patterned Substrates*

2.2.1 Pre-patterning Surface Using Photolithography

In 1997, Groves et al. developed the first method for patterning solid supported lipid bilayer membranes using a photolithography technique [16]. Standard positive photoresist was spun onto wafers with a thickness of 1 µm. The wafers were then exposed to ultraviolet (UV) light through a photolithographic mask. After developing and Ar plasma etching, the photoresist patterned surfaces were ready for membrane deposition. For fabrication of Al_2O_3 and Au barriers, the photoresist was exposed with the inverse mask and used as a template for metal deposition. This method has been extensively used to fabricate lipid bilayer arrays [23–25].

Using this method, Creamer et al. created micrometer-sized hydrophilic boxes [25]. After cleaning the positive resist patterned substrates, 10–100 pL droplets of liposome were placed into each hydrophilic box (Fig. 2a). Each box can be addressed with different compositions of lipid bilayers. Three types of lipid bilayers were formed in the 50 × 50 µm well plates as shown in Fig. 2b. The lipid

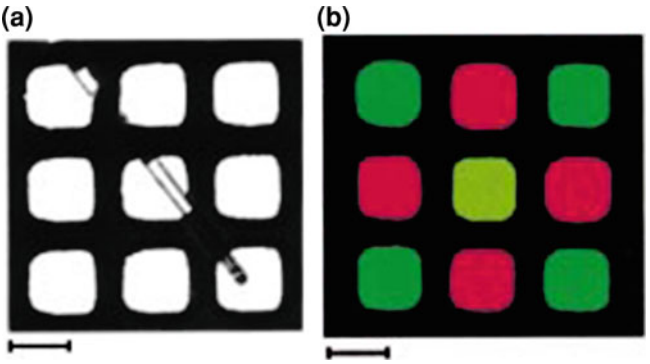

Fig. 2 **a** Bright field image of a microcapillary tube containing liposome solution situated over an array of patterned hydrophilic glass plates. **b** An epifluorescence image of a 3 × 3 array of glass well plates containing addressed Egg-PC lipid bilayer membranes with various dyes. The scale bar is 50 μm. Reprinted with permission from Ref. [25]. Copyright 1999 American Chemical Society

bilayers appearing red in color contain 1 % TR-PE fluorescent probes, whereas those appearing green contain 3 % NBD-PE probes. The dark *yellow* lipid bilayer in the center contains both kinds of fluorophores.

2.2.2 Pre-patterning Surfaces by Microcontact Printing of SAMs

Microcontact printing of SAMs has proven to be an effective method for micro- or nano-fabrication [26–28]. This method was adopted to fabricate lipid bilayer arrays by Evans' group [29], as illustrated in Fig. 3. A PDMS stamp [30] was used to make patterned SAM surfaces. The ink used was home made cholesterylpolyethyleneoxy thiol (CPEO3). The CPEO3 molecules dissolved in dichloromethane (1 mM) were stamped on a "plasma cleaned" gold electrode to form an array of 20 × 20 μm "wells" (left diagram in Fig. 3). The wells were "backfilled" with mercaptoethanol by placing the substrate in a 1 mM solution of mercaptoethanol in dichloromethane. The patterned lipid bilayer formed after incubating the patterned SAM surface into a lipid vesicle solution for 20 min, as schematically shown in Fig. 3 (right diagram). The patterned bilayer formation was proven by the characteristic capacitance of 0.9 μF cm^{-2} for this type of lipid membrane. The benefit of this method for patterned lipid bilayers is that the majority of the gold substrate is covered by an integral (blocking) SAM, thus reducing the leakage current of ions through areas of a defective lipid layer.

2.2.3 Pre-patterning SAM Surfaces by Soft UV

Han et al. introduced a method to fabricate lipid bilayer arrays on solid substrate based on a soft UV (365 nm) patterned SAM surfaces [10, 31]. Two compounds containing photocleavable Ortho-nitrobenzyl moieties were synthesized. They

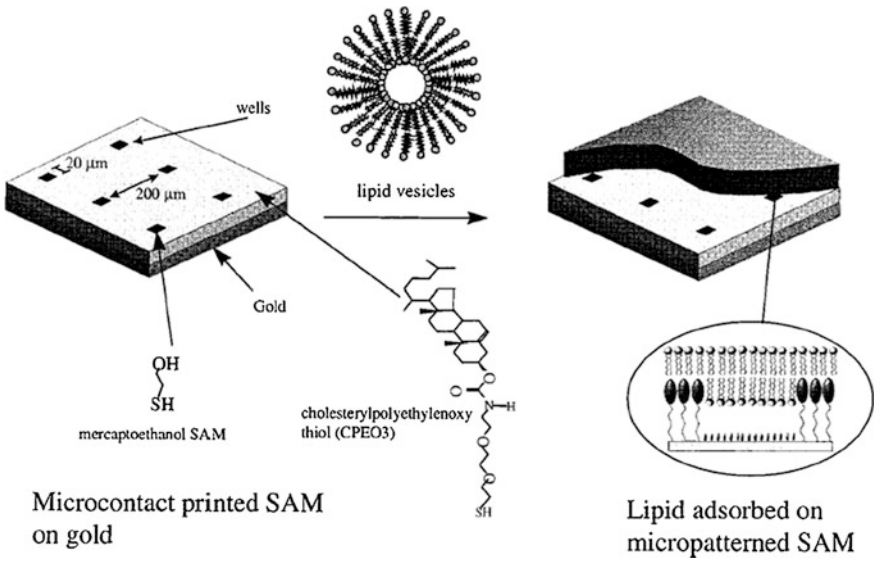

Fig. 3 Schematic illustration of lipid bilayer formation on a micropatterned SAM. Reprinted with permission from Ref. [29]. Copyright 1999 American Chemical Society

created patterned lipid bilayers on both gold and silica surfaces using these two compounds respectively. The procedure for fabricating a patterned lipid bilayer on a silica substrate is illustrated in Fig. 4a–d. 3-aminopropyldimethylethoxysilane (APMES) was used to form amine-terminated SAMs (Fig. 4a). The photocleavable molecule was then attached to an amine functionalized surface by surface reaction (Fig. 4b). Subsequently, the surface was exposed to soft UV light (365 nm) through a chromium mask containing the desired pattern shapes (Fig. 4c). After rinsing with dichloromethane, the light-exposed regions were cleaved to the amine surface (hydrophilic), while the rest of the regions were still hydrophobic. Thus, a prepatterned SAM surface containing both hydrophilic patches and hydrophobic areas was created. After immersing the patterned SAM substrate into lipid vesicle solutions for 1 h, the patterned lipid bilayers were formed, as schematically shown in Fig. 4d. The fluorescence image of lipid bilayer arrays is shown in Fig. 4e. The bright dots are lipid bilayers doped with 1 % TR-PE.

2.2.4 Pre-patterning SAMs Surface by Deep UV

Han et al. found the diffusion coefficient of a patterned lipid bilayer using soft UV patterned SAM is only 0.14 $\mu m^2\ s^{-1}$, which is approximately 10 times less than that of the bilayer on silica substrates. The low mobility is partially from the amine surface after soft UV (Fig. 4c). It is well known that deep UV can cleave the SAM from silica substrates and leave a –OH hydrophilic surface, which is an ideal surface for forming fluid lipid bilayer membranes. Thus, deep UV (254 nm) was

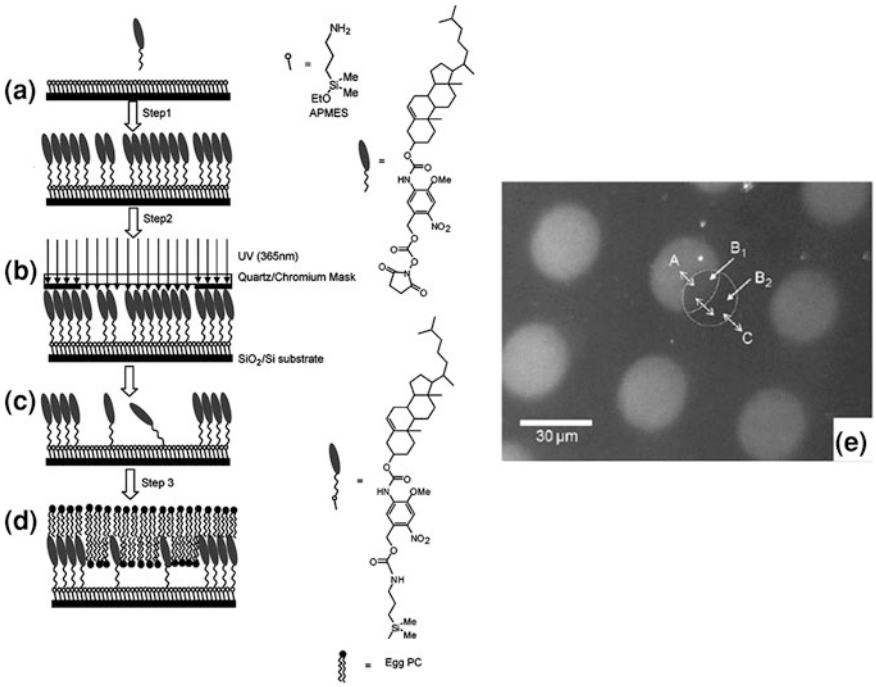

Fig. 4 **a–d** Schematic of the fabrication steps required to form a patterned lipid bilayer on a silica surface, **e** Fluorescence image of the lipid bilayer array in circular shape. The scale bar is 30 μm. Reproduced with permission from Ref. [10]. Copyright 2007 Wiley-VCH

used to pattern SAMs for forming lipid bilayer arrays [32, 33]. The process of this method is illustrated in Fig. 5a, [32]. Han et al. synthesized a cholesterol derivative that was attached to an amine functionalized surface. After exposing the resultant surface (top graph in Fig. 5a) to deep UV through a mask, the patterned SAM surface (middle graph in Fig. 5a) was created. The lipid bilayer array formed after immersing the patterned surface into the vesicle solution for 1 h (bottom graph in Fig. 5a). Figure 5b shows the patterned lipid bilayer created using this method on a silica surface, which has a diffusion coefficient of 1.22 $\mu m^2 s^{-1}$.

The other silanes (*N*-octadecylsiloxanes [34–38], and chlorotrimethylsilane [33]) were also used to create lipid bilayer arrays using deep UV.

2.2.5 Pre-pattering Surface Using UV Polymerized Lipids

Morigaki et al. [39–41] developed a method to create a patterned lipid bilayer based the idea of imprinting a pattern within the lipid bilayer by photochemical polymerization. The general procedure is schematically illustrated in Fig. 6. After a polymerizable lipid bilayer is deposited onto a solid support substrate (Fig. 6a),

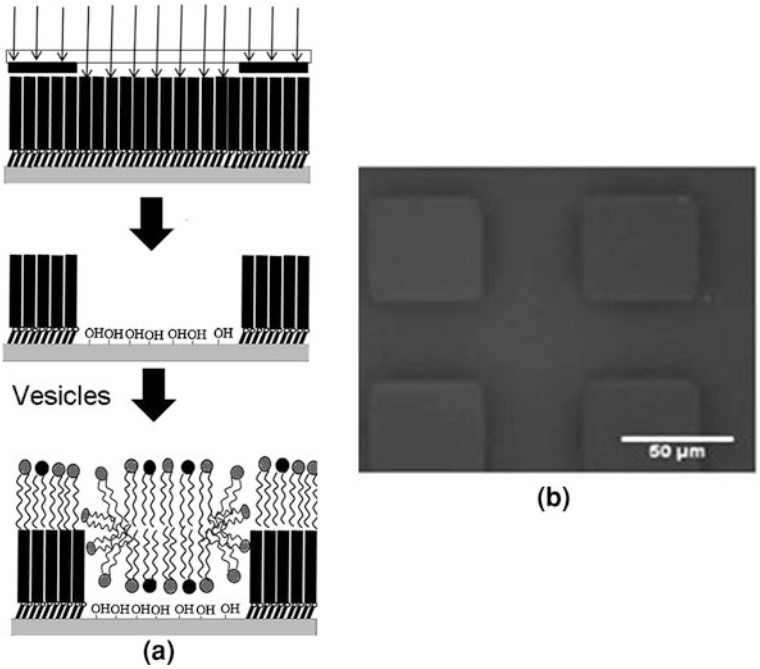

Fig. 5 **a** Schematic diagram for the fabrication of lipid membranes on a deep-UV patterned SAM; **b** fluorescence image of lipid bilayer arrays created using this method (scale bar = 50 μm). Reproduced with permission from Ref. [32]. Copyright 2009 Wiley-VCH

the bilayer is subsequently polymerized by UV light through a mask containing the desired pattern (Fig. 6b) in an aqueous solution. The nonpolymerized lipid is selectively removed by an organic solvent, while the polymerized lipids (solvent resistant) remain on the substrate (Fig. 6c). The polymerized lipids serve as barriers for patterning lipid bilayers (Fig. 6d). Figure 6e is the fluorescent image of lipid bilayer arrays formed using this method. The bright regions are backfilled fluid of lipid bilayer membranes containing dye label lipids, while the dark grids are polymerized lipids.

2.2.6 Pre-patterning Surfaces Using Nanoshaving Lithography

Shi et al. [42] obtained nanosized lipid bilayer line arrays on borosilicate supports by using nanoshaving lithography. The principle of this method is illustrated in Fig. 7a. Basically a bovine serum albumin (BSA) monolayer is first deposited on a borosilicate substrate by incubation with a phosphate–buffered saline (PBS) solution containing 10 mg mL^{-1} BSA. After drying, immobilized protein molecules are selectively removed from the surface with an ultrasharp atomic force

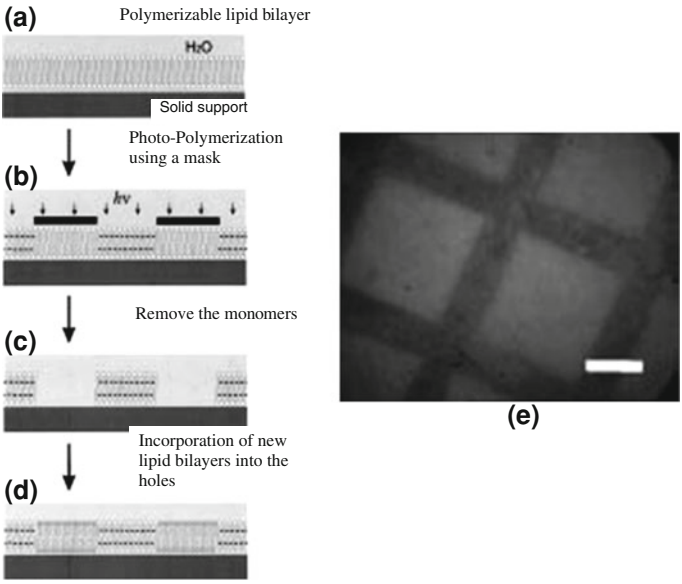

Fig. 6 **a–d** Schematic illustration of the bilayer patterning and introduction of new lipid bilayers; **e** fluorescence image of the lipid bilayer array created using this method. The scale bar is 100 μm. Reproduced with permission from Ref. [41]. Copyright 2001 Wiley-VCH

microscopy (AFM) tip in air to create vacant lines with varying widths at a speed of 40 μm s^{-1} (Fig. 7b). Finally, the lipid bilayer formes on the vacant line regions by vesicle fusion (Fig. 7c). Shi et al. created a series of line widths from 600 to 15 nm and found the smallest bilayer lines created by this method were 55 nm. The diffusion coefficient of the lipid bilayer in the lines is $\sim$2.5 μm^2 s^{-1} with a mobile fraction of $\sim$0.97.

Apart from the method mentioned above to pre-pattern the surfaces, the proteins (TR-BSA [43] and fibronectin [13, 44–46]) were stamped onto the surface to form corrals using PDMS stamp, which were subsequently used to form lipid bilayer arrays.

2.3 Patterning Lipid Bilayers by Direct UV Exposure

Parikh et al. [47–49] described directly patterning microvoids or holes to serve as fluidity barriers within supported lipid bilayer membranes using deep UV light (10–20 mW cm^{-2}). They placed a mask on top of the supported lipid bilayer membranes (top graph in Fig. 8a), then exposed them to deep UV light (middle graph in Fig. 8a). The lipid bilayer exposed to deep UV was photo decomposed,

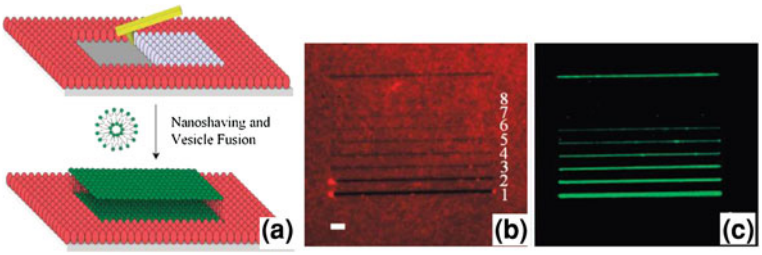

Fig. 7 **a** Schematic diagram of AFM-based nanoshaving lithography for nanoscale lipid bilayer membrane formation. The *red* and *gray* ellipsoids represent adsorbed BSA molecules. The *gray* ones are being removed by the AFM tip. A subsequently deposited lipid bilayer is shown in *green*. Fluorescence images of a nanoshaved BSA monolayer **b** and lipid bilayer lines **c**: the *top* line, ~200 nm in width, was used as a reference marker; the widths of shaved lines in **b** from 1 to 8 are ~600, ~300, ~142, ~103, ~78, ~55, ~36, and ~15 nm, respectively. The scale bar is 3 μm. Reprinted with permission from Ref. [42]. Copyright 2008 American Chemical Society

leaving voids to serve as barriers for the unexposed lipid bilayer (bottom graph in Fig. 8a). Figure 8b shows the mask used for creating the lipid bilayer arrays pictured in Fig. 8c. The method is applicable for patterning bilayers formed on large substrates, and is independent of bilayer composition. Using this method, stable patterns of hydrophilic voids can be directly engineered within a fluid lipid bilayer membrane. Because the voids can be backfilled with secondary lipid vesicles, this method provided a way for manipulating membrane compositions, probing 2D reaction—diffusion processes, and creating functional microdomains in well-defined patterns.

2.4 Patterning Lipid Bilayers by Direct Blotting or Stamping

The supported lipid bilayer membranes undergo self-limiting lateral expansion when the bilayer material is removed or deposited onto the surface. Based on this, Hovis et al. [50, 51] introduced methods of blotting or printing bilayer material for patterning fluid lipid bilayer membranes on solid supports. Similar to the micro contact printing technique, PDMS material was chosen to make the stamp. The blotting and stamping methods to fabricate patterned lipid bilayer are illustrated in Fig. 9. Figure 9a illustrates the blotting method. Figure 9b shows the fluorescence image of a supported lipid bilayer after blotting for 10 min in water with a PDMS stamp containing a grid pattern and waiting 30 min for self-limiting lateral expansion of the patterned bilayer membrane. The bright regions are patterned bilayers containing dye-labeled lipids, while the dark grid pattern is where the bilayer has been removed. Figure 9c schematically shows the stamping methods. Figure 9d is a fluorescence image of a grid pattern of lipid bilayers formed

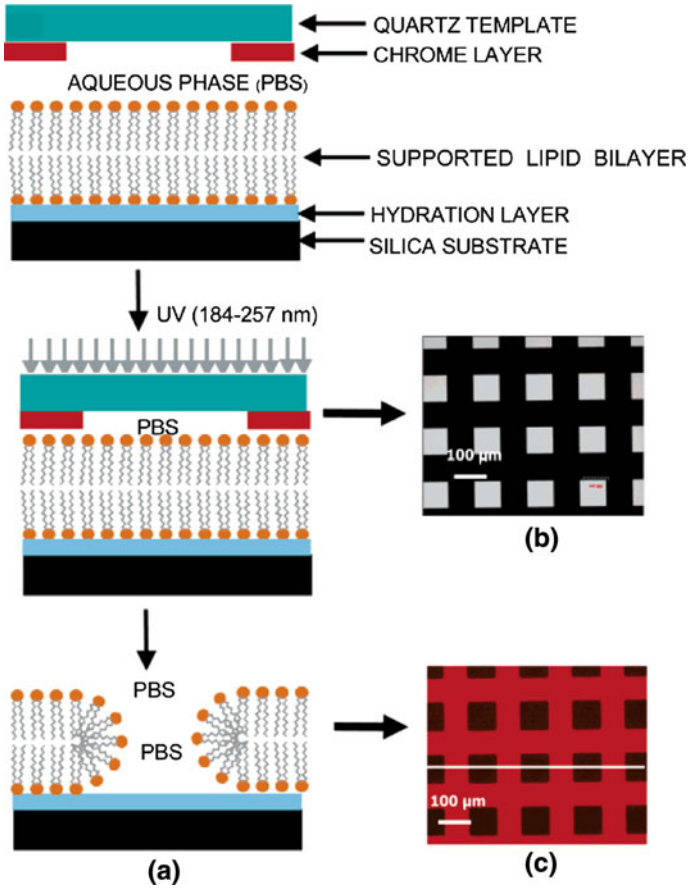

Fig. 8 Direct patterning of void arrays within bilayer membranes using deep UV photolithography. **a** A schematic diagram of the key process steps. **b** Bright-field image of 100 μm square features on the quartz/chrome mask, where *bright* squares are quartz and *dark* regions reveal the chrome background. **c** Fluorescence images of POPC bilayers containing 1 mol % TR-PE. Reprinted with permission from Ref. [47]. Copyright 2004 American Chemical Society

by stamping. They explored two different ways to "ink" the PDMS stamp. One is to ink it from a supported lipid bilayer when doing blotting as shown in Fig. 9a. The other is to place stamps in the vesicle solution, making the vesicle rupture and form bilayers on the PDMS surface. The second way requires at least 1 h for hydrophobic PDMS stamps and 1–5 min for hydrophilic (oxygen plasma treated) PDMS stamps.

Hydrogel stamps were applied to fabricate arrays of proteins [53, 54], bacteria [55], and mammalian cells [56]. Inspired by these works, Majd et al. [52] first used hydrogel stamps to fabricate lipid bilayer arrays. Rather than forming lipid bilayers

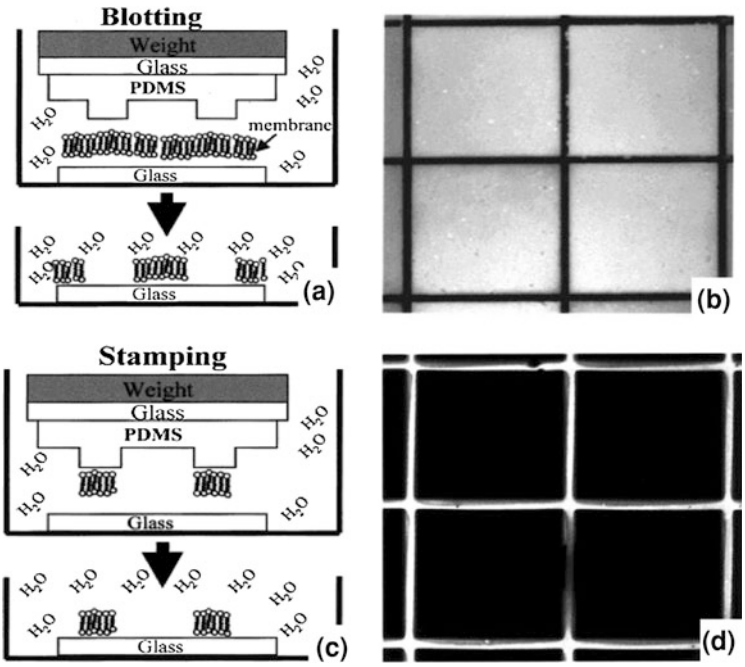

Fig. 9 Schematic illustration and consequent microscopy images of the blotting method **a** and **b** and printing method **c** and **d** used to create patterned bilayers on the surface. The dimensions of both images are 480 × 470 μm. Reprinted with permission from Ref. [50]. Copyright 2000 American Chemical Society

on the surface of PDMS stamps, the lipid vesicles were adsorbed into the porous hydrogel stamps, which allowed the stamp to produce more than 100 bilayer arrays without reinking. They did not find a significant loss in the fluorescence intensity of the spots over 100 stamping events (Fig. 10a). Figure 10b and c shows fluorescence images of lipid bilayer arrays on glass obtained after 6 and 100 stamping events, respectively. Figure 10d shows the FRAP on the last (100th) array. The diffusion coefficient of the 100th bilayer array is similar to that of the 6th bilayer arrays, indicating that the quality of the stamped arrays remained constant over 100 stamping events.

2.5 Fabricating Lipid Bilayer Arrays Using Microfluidics

Microfluidics has been used to fabricate lipid bilayer arrays during the last ten years [57–66]. It usually involves introducing a solution of lipid vesicles through multichannels imbedded within PDMS to produce parallel lanes of supported lipid

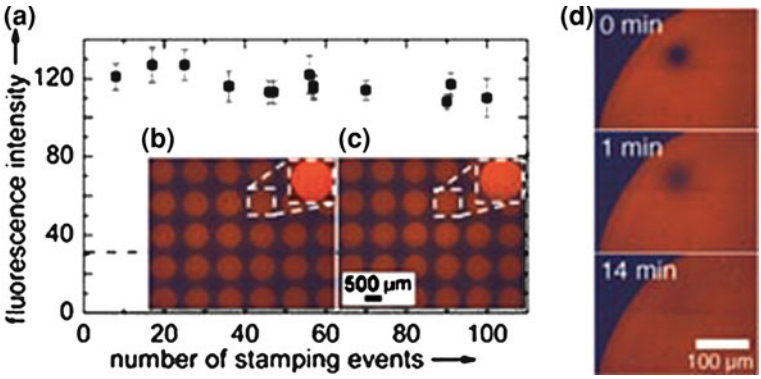

Fig. 10 Fluorescence intensity after stamping of 100 arrays of Rh-PE doped membranes by using a hydrogel stamp (without intermediate inking) and a test of bilayer fluidity. **a** Mean fluorescence intensity of supported bilayers as a function of the number of stamping events. **b** and **c** Micrograph of spots of supported bilayers after the 6th and 100th stamping events, respectively. **d** Fluorescence images from a FRAP experiment performed on the array from the last (100th) stamping event. Reproduced with permission from Ref. [52]. Copyright 2005 Wiley-VCH

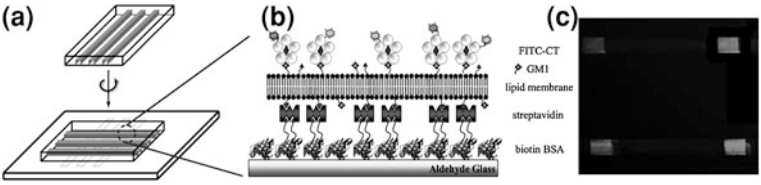

Fig. 11 Schematic of the general array configuration: **a** the orthogonal alignment of the PDMS chip for generation of the membrane squares; **b** structure of the membrane with based biointerface. **c** Fluorescence image of a lipid bilayer array [57]. Reproduced by permission of The Royal Society of Chemistry

bilayer membranes on a silica surface. One example is illustrated in Fig. 11a, b [57]. The square patterns of lipid bilayer membranes were constructed by a crosspatterned method: first, the biotinylated bovine serum albumin (biotin-BSA) (0.5 mg mL^{-1}) was injected through three channels (200 µm × 200 µm × 2 cm) and allowed to incubate for 30 min to form biotin-BSA lanes on an aldehyde modified glass slide; second, after rinsing, the PDMS chip was lifted off the slide, and another PDMS chip was then aligned perpendicularly across these biotin-BSA lanes; third, the surface aldehyde groups within the three channels were passivated with a 1 mg mL^{-1} solution of BSA for 1 h; fourth, streptavidin or avidin was co-injected with BSA at a concentration of 0.20 mg mL^{-1} and incubated for 1 h in order to allow sufficient binding to the small biotin-BSA zones; fifth, after rinsing with PBS, biotinylated vesicles were injected into the microchannels, incubated for 1 h, and subsequently rinsed. The fabricated lipid bilayer array is shown in Fig. 11c. This work demonstrated a lipid bilayer array that was fabricated using a

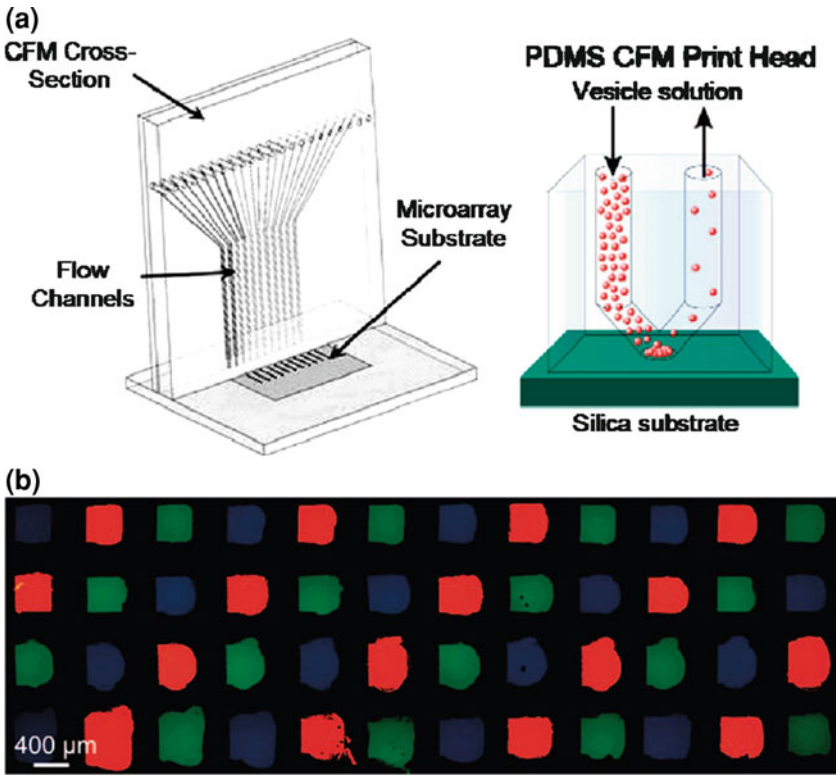

Fig. 12 **a** Schematic of the CFM apparatus and close-up of the CFM print head in contact with a silica substrate used for bilayer formation. The *arrows* represent the direction of fluid flow in the sealed channel created by contacting the PDMS print head with the silica substrate. **b** A 48-element lipid bilayer array of DOPC containing either 1.0 % Rh-PE (*red*), 1.0 % Oregon *Green*-DHPE (*green*), or 3.0 % Marina *Blue*-DHPE (*blue*). Reprinted with permission from Ref. [67]. Copyright 2008 American Chemical Society

2D microfluidics system. The next example will explore a 3D continuous flow microspotter (CFM) to form lipid bilayer arrays.

Conboy et al. [67, 68] used a 3D CFM system for the preparation of supported lipid bilayer arrays. This method can produce high density multicomponent lipid bilayer arrays. They fabricated the microspotter with PDMS material. The microspotter consists of a series of inlet and outlet wells connected by pairs of microfluidic channels embedded within PDMS. Once the PDMS print-head contacts the substrate, one continuous channel is formed between the inlet and outlet pairs (Fig. 12a). Each channel is individually addressable, allowing the production of multicomponent lipid bilayer arrays by injecting different vesicle solutions into each channel. Figure 12b confirmed the ability to create a multicomponent bilayer array containing three lipid compositions using this method. The diffusion coefficient of the resultant lipid bilayer was obtained to be $1.4 \pm 0.3\ \mu m^2\ s^{-1}$, which is within the same order of magnitude of the lipid bilayer on silica surface. This

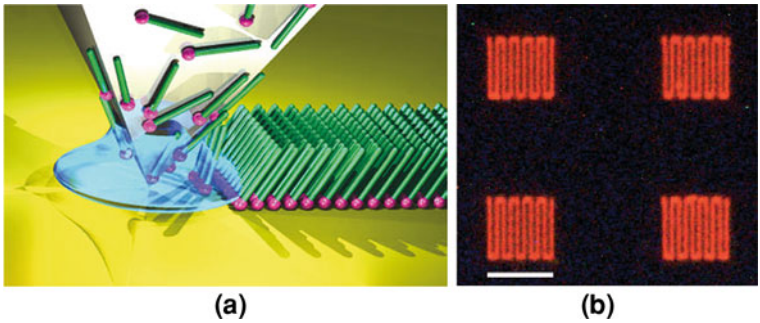

Fig. 13 **a** Schematic of DPN: an alkanethiol ink-coated AFM tip is brought into contact with a *gold* substrate. Molecules diffuse from the tip to the surface and assemble in the wake of the tip path to form a stable nanostructure. Reproduced with permission from Ref. [69]. Copyright 2007 Nature Publishing Group. **b** A contiguous 250-nm line features fluorophore-doped phospholipid patterns deposited onto a polystyrene petri dish. Reproduced with permission from Ref. [71]. Copyright 2007 Wiley-VCH

method does not require the use of a prepatterned substrate because lipid bilayers are effectively confined into discrete micrometer-sized domains by the residual PDMS deposited on the silica substrate when the PDMS microspotter is removed. The attractive features of this method include an easy washing process after vesicle fusion, the ability to address each element of the array individually if the print-head is maintained in contact with the substrate, and the capacity for high throughput multiply-analyte assay using multicomponent bilayer arrays after removing the print head from the surface.

Microfluidics offers a simple and low-cost alternative for creating multicomposition arrays and also could be used for membrane base-sensing applications in a lab-on-a-chip.

2.6 *Fabricating Lipid Membrane Arrays Using Dip Pen Nanolithography*

Dip Pen Nanolithography (DPN) is a novel scanning probe-based fabrication technique that uses an ink-coated AFM tip to pattern a surface [69]. The tip of AFM cantilever acts as a pen, which is coated with a chemical compound or mixture acting as an ink and put in contact with a substrate acting as the paper, as shown in Fig. 13a. The first demonstration of DPN was done with alkanethiol molecules [70]. Recently this technique was used to generate heterogeneous lipid membrane nanopatterns [71–73]. This method provides a lateral resolution down to 100 nm and an areal throughput of 5 cm^2 min^{-1} [71]. Lenhert et al. found that DOPC ($T_m = -16.5$ °C) is a suitable ink for DPN in higher humidities (>70 %). A fluorescence image of a serially patterned contiguous line array of DOPC doped with 1mol % of a rhodamine-labeled lipid is shown in Fig. 13b. Multicomponent

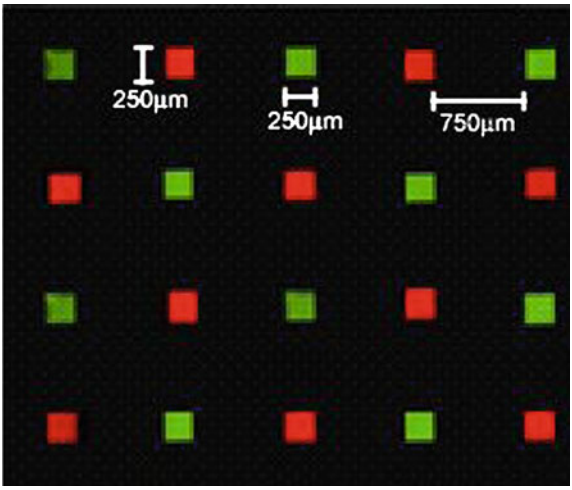

Fig. 14 Independently addressable lipid bilayer membrane arrays. A supported membrane array containing different molecules (1 mol % NBD-PG or 1 mol % TR-PE in Egg PC) in an alternating pattern was arrayed robotically. Reprinted with permission from Ref. [74]

patterns of lipid membranes can be easily fabricated with this state-of-the-art technology. However, it should be noted that the lipid membranes fabricated in this way are not single lipid bilayers, but multibilayers.

2.7 Forming Lipid Bilayer Arrays by a Robotic Spotter System

Ymazaki et al. [74] introduced a novel technology for generating lipid bilayer arrays using a commercially available microarrayer. The microarrayer (Cartesian technologies MycroSys^{TM} SQ series) was equipped with software (AxSys^{TM}) for programmable aspiration and dispensing of lipid solutions. The experiment was carried out in a humidified chamber ($\sim$98 % humidity) at room temperature to avoid evaporation because the drop size was very small (nanoliters). An automatic wash cycle was carried out before each sample aspiration to prevent contamination from carryover between different lipid solutions. After arraying, the arrayed elements were submerged in deionized water and washed three times with PBS. One example of a lipid bilayer array fabricated using this method is shown in Fig. 14. The bilayer membranes containing unique lipid compositions (*red* or *green*-fluorescent dopant lipids in this case) were arrayed at very high densities. This approach can be used to automatically generate addressable bilayer arrays.

2.8 Patterning Lipid Bilayers Using the Polymer Liftoff Technique

Craighead et al. [75–78] developed a method for creating lipid bilayer arrays down to 1 µm resolution using a photolithographically patterned polymer liftoff technique. The bilayer patterns are realized as the polymer is mechanically peeled

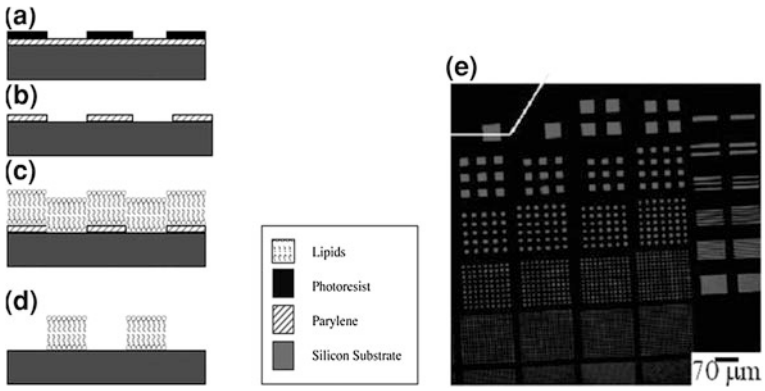

Fig. 15 Schematic of the fabrication steps of the polymer lift-off method: **a** photoresist patterning using optical lithography; **b** reactive ion etching of parylene and removal of the top photoresist layer; **c** POPC lipid immobilization; **d** peeling of parylene resulting in a patterned lipid bilayer. **e** Fluorescence image of lipid bilayer arrays created using this method. Reproduced with permission from Ref. [75]. Copyright 2003 the Biophysical Society

away from the substrate in one contiguous piece in solution. The fabrication process is illustrated in Fig. 15a–d. Di-*para*-xylylene (Parylene) is vapor deposited on a silicon substrate to produce a conformal polymer film that adheres weakly to the surface. After coating with a photoresist, the film is patterned using standard photolithography (Fig. 15a), and is then subjected to a controlled reactive ion etch (RIE) to remove exposed regions of Parylene from the silicon dioxide substrate (Fig. 15b). A more hydrophilic silicon dioxide surface is created by the RIE in the exposed regions compared to the nonexposed regions of the substrate. The resultant surface is immersed into lipid vesicle solution to form lipid bilayers, both on silicon dioxide regions and polymer regions (Fig. 15c). The lipid bilayer array was formed after removing Parylene (Fig. 15d). The fluorescent image of lipid bilayer arrays fabricated using this method is shown in Fig. 15e. The bright regions are lipid bilayers. Lipid bilayer arrays can be easily fabricated with sizes ranging from 1 to 76 μm in width.

2.9 Forming Lipid Bilayer Membranes on Nanopore Arrays

Solid supported lipid bilayers have limitations for reconstituted transmembrane proteins due to the thin water layer ($\sim$1 nm) adjacent to the solid surface. Free-standing lipid bilayers can overcome this problem because they are accessible from both sides of the lipid bilayer membrane. Attempts have been made in the past decade to develop free-standing bilayer lipid membranes over micrometer- or nanometer- sized pores [3, 6, 79–88]. Another advantage of this type of bilayer array is its long-term stability over conventional black lipid membranes.

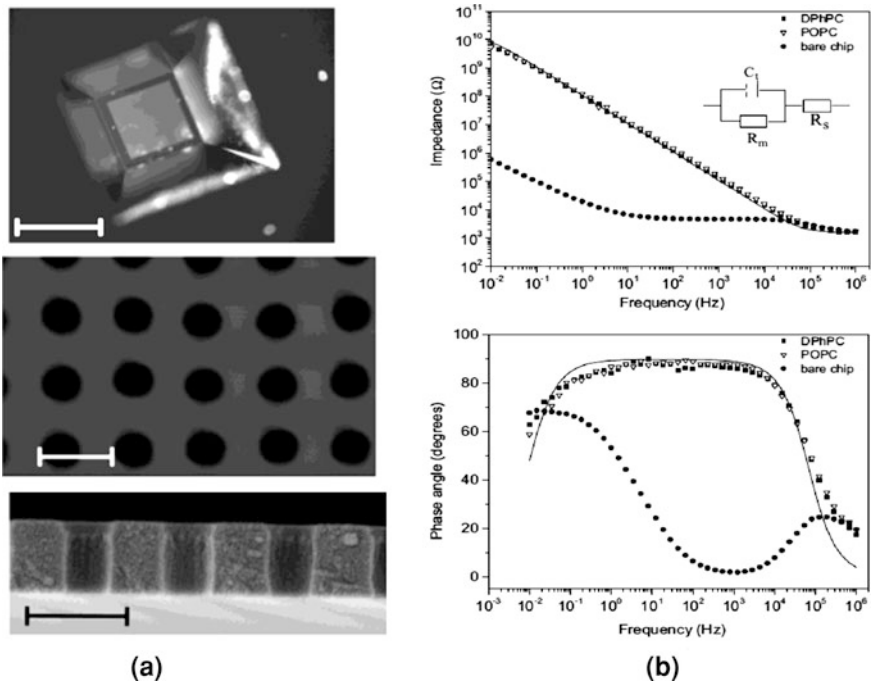

Fig. 16 **a** The bright field image of the chip (*top* graph) and SEM images of silicon nitride nanopore arrays (*top* view, *middle* graph; *side* view, *bottom* graph). Scale bars are 500 μm for the *top* graph and 400 nm for the *middle* and *bottom* images respectively, **b** Impedance spectra of silanized chip in 0.1 M KCl before (*Bullet*) and 1h after painting lipid solution of DPhPC (*Square*) and POPC (*Upside down triangle*) onto the chip. The *solid* lines represent the fitted data using the equivalent circuit shown. Reproduced with permission from Ref. [3]. Copyright 2007 Wiley-VCH

Han et al. [3] used nanopore array chips (as shown in Fig. 16a) to fabricate lipid bilayer arrays from naturally occurring lipids. All chips, fabricated using a method detailed elsewhere [89], had a small window (0.5 × 0.5 mm) of silicon nitride membrane (SNM) containing tens of thousands of nanopores. The chips were silanized with fluorosilane to render the surface hydrophobic. The method used to form lipid bilayer membranes on the nanopore arrays is the Mueller-Rudin technique [8], i.e. 'painting' of a lipid solution over the pores. The lipid solution undergoes a thinning process to single lipid bilayer thickness in the center of each pore. Formation of the lipid membrane is clearly recognized as a jump in the impedance value during lipid painting, because the impedance of bilayers at low frequencies is several orders of magnitude higher than the impedance of a bare chip (top graph in Fig. 16b). From fitting the impedance spectra, the resistance and the capacitance values were obtained to be 12.1 ± 2.4 GΩ and ∼1 μF cm^{-2} respectively. This type of lipid bilayer can survive from several days to a week. The chips used in this study have a very low aspect ratio (defined as the thickness of the silicon nitride membrane to the

diameter of a pore) of ~ 0.375, which makes this system suitable for studying mass transportation across the lipid bilayer membranes because the ions and molecules can easily access to both side of the bilayer.

3 Applications of Lipid Bilayer Arrays

3.1 Cell Adhesion and Activation Study Using Lipid Bilayer Arrays

It is well known that the chemical and physical characteristics of a surface can influence cellular behavior dramatically [90, 91]. For example, a surface containing poly (ethylene glycol) (PEG) moieties prevents cell adhesion by blocking the extracellular matrix (ECM). On the contrary, a hydrophobic surface tends to promote cell adhesion.

Solid supported lipid bilayers were originally developed for studies of cell–cell recognition in the immune system [92, 93] and have proven to be effective artificial cell surfaces for immunological studies involving interactions with living cells (T-lymphocytes [92, 94], neutrophils [95, 96]). Since the emergence of lipid bilayer arrays, they have been used to regulate cell behavior by adjusting the lipid composition [23] or reconstituting lipid modified receptors for cell adhesion and stimulation. These receptors include DNP-cap-DPPE [78], GPI modified E-cadherin proteins (hEFG) [64], and RGD peptide amphiphiles [24].

Groves et al. [23] demonstrated that lipid composition in lipid bilayer arrays can influence the adhesion and growth of cells on solid substrates. They found that the bilayer containing PS promotes cell adhesion and growth, as shown in Fig. 17. Figure 17a, b are the fluorescence and phase contrast images of the same lipid bilayer array, respectively; both were taken 24 h after inoculation with cells. The lipid bilayers in the upper two boxes contained 5 % PS/94 % PC/1 % TR-PE, while the bilayers in the lower two boxes contained 5 % PG/94 % PC/1 % NBD-PE. It is easily to see cells deposited in PS-containing bilayer regions, but not on PG-containing bilayer regions, although they have the same charge property. This result allowed us to direct cell adhesion to specified positions in a bilayer array.

T cells, B cells, and other specialized cells in the immune system are activated by clustering antigenic receptors on their plasma membrane surfaces. Thus, rather than simply adjusting the naturally occurring lipid composition in the bilayer, lipid modified receptors were included in the membrane. Orth et al. [78] fabricated bilayer arrays containing haptenated lipid to investigate signaling pathways of cellular response. In their experiments, DNP-cap-DPPE was used for the specific binding of anti-DNP IgE. The DNP-cap-DPPE containing lipid bilayer can facilitate the rat basophilic leukemia (RBL) mast cell adhesion because RBL expresses cell surface immunoglobulin E (IgE) receptors.

After incubating RBL cells at 37 °C with patterned lipid bilayers, cells settled onto the wafer and became adherent within 30 min, as shown in Fig. 18. In the

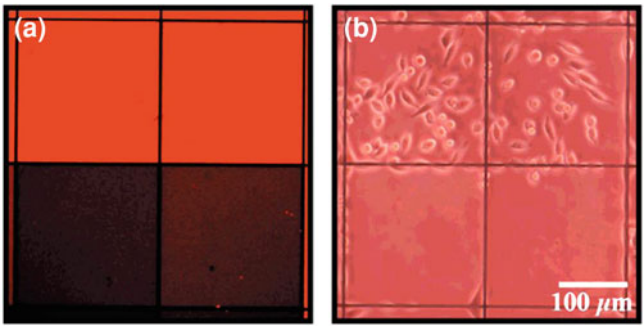

Fig. 17 Patterned cell growth on lipid bilayer arrays. **a** Fluorescence image of four membrane corrals in an array. **b** Phase contrast image of the same four corrals in (**a**) illustrating cell positioning. Reprinted with permission from Ref. [23]. Copyright 2001 American Chemical Society

regions with no DNP-cap-DPPE, the cells remain rounded and mostly detached from the patched features (Fig. 18a). In the patterned lipid bilayer containing DNP-cap-DPPE, the cells near or on lipid patches flatten and spread out. The labeled IgE receptors are distinctly polarized toward the edges of the lipid patches, if the periodic spacing is larger than 10 μm (Fig. 18b). Cells settle over several patches if the periodic spacing is smaller than 10 μm (Fig. 18c). Cells may settle between the patches or on top of one or more, and the IgE-receptors polarize toward the edge or cluster on top, respectively, if the periodic spacing is similar to 10 μm (Fig. 18d). Clustering IgE receptors on mast cells initiates signal transduction that leads to degranulation and release of chemical mediators. This process is accompanied by polymerization of cytoskeletal actins, leading to spread of the rounded cell. This clear morphological change allowed us to establish that receptors clustered by the haptenated lipid patches stimulate a cellular response.

Perez et al. [64] reported a patterned bilayer system for investigating how the lateral mobility of signaling protein influences cadherin-based cell signaling. The GPI modified E-cadherin proteins (hEFG) containing lipid bilayers were formed on the surface. In the bilayer, hEFG exhibits a diffusion coefficient of $0.6 \pm 0.3\ \mu m^2\ s^{-1}$ and mobile fraction of 30–60 %. The authors observed that MCF-7 cells recognized and clustered hEFG, but did not exhibit cell spreading. However, by micropatterning small anchors into the supported lipid bilayer, they achieved cell spreading across the bilayer surface.

Stroumpoulis et al. [24] created RGD peptide amphiphiles (a peptide-lipid conjugate molecule containing the RGD amino acid sequence, home synthesized) containing lipid bilayer patterns for controlling the ability of these surfaces to support cell adhesion and growth. They found mouse fibroblast cell adhesion was prevented on PC bilayers in the absence of RGD, but promoted in the presence of accessible RGD amphiphiles. The total area of adhered and spread cells increased with the peptide concentration but leveled off at high concentrations. Developing

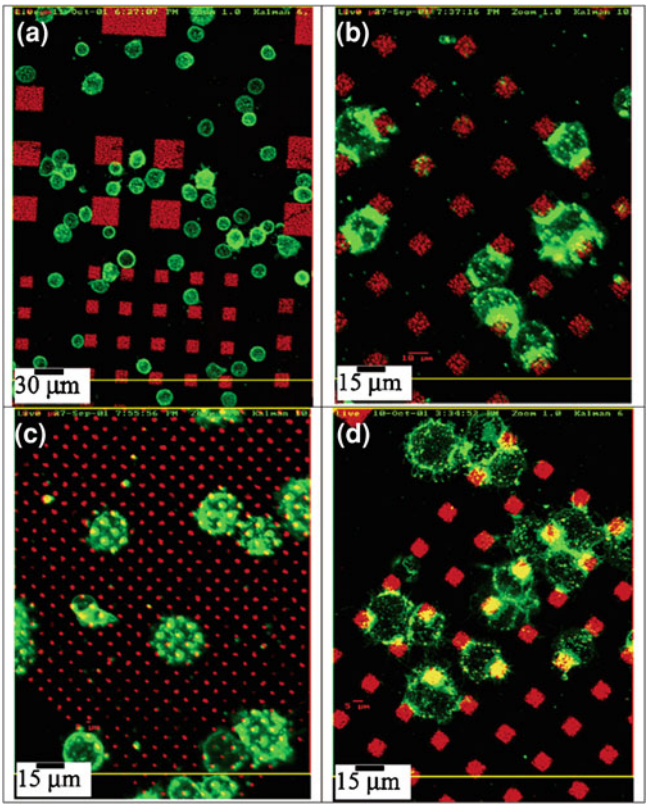

Fig. 18 Interaction between RBL cells and the patterned lipid bilayers. **a–d**, Confocal images of RBL cells sensitized with Alexa 488 anti-DNP IgE (*green*) on either **a** DPPC/DiI (*red*) with molar ratio 99.5:0.5 or **b–d** DPPC/DNP-cap-DPPC/DiI (*red*) with molar ratio 94.5:5:0.5. **a** 16 × objective; 5, 30, 60 μm pattern. **b** 40 × objective, 10 μm pattern, 20 μm period. **c** 40 × objective, 1.5 μm pattern, 5 μm period. **d** 40 × objective, 6 μm pattern, 16 μm period. Reprinted with permission from Ref. [78]. Copyright 2003 American Chemical Society

peptide composition gradients in a membrane environment has been demonstrated as an effective method to screen biological probes for cell adhesion and growth.

More recently, Oliver et al. [38] formed lipid bilayer arrays with bilayer patches surrounded by lipid monolayers using the deep UV patterned SAM method. They found that human retinal pigment epithelial (ARPE-19) cells adhered and grew in the lipid monolayer regions, not on bilayer regions, when the membrane contained POPC lipid only. The reason comes from the subtle variations in the physical properties (membrane tension and out-of-plane undulations) of the lipid mono- and bilayers, because essentially they have identical surface chemicals and structural character. After introducing PS into the patterned membrane surface, the cell-patterning capability disappeared.

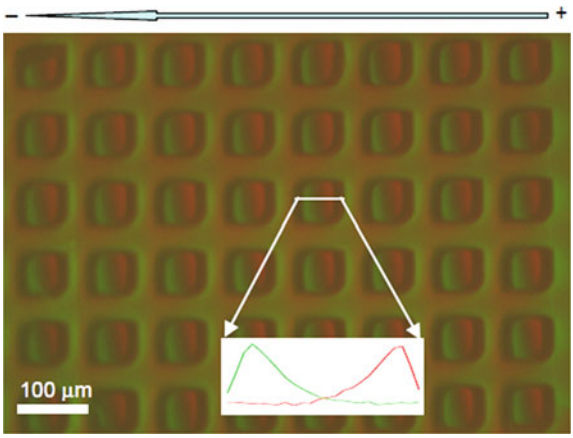

Fig. 19 Separation of charged lipids of TR-PE (q = −1e) and D 291 (q = +1e) under the application of a 50 V cm^{-1} field for 10 min. [33] – Reproduced by permission of The Royal Society of Chemistry

3.2 2D Membrane Electrophoresis in Patterned Lipid Bilayers

Membrane proteins are the main target of nearly 50 % of known drugs. In most cases, the membrane proteins lose their structure and functions when removed from their membranous environment. Thus there is significant interest in creating a platform to manipulate (separate, concentrate) membrane proteins in lipid bilayer environments. Because the proteins are chargeable by varying the solution pH, electric fields can be used to manipulate the charged species in the lipid bilayer. 2D electrophoresis in supported lipid bilayers has been demonstrated [18, 22, 33, 97], since Poo et al. [98] first reported in 1977 that electric fields could induce redistribution of charged membrane components (concanavalin A receptors).

Figure 19 demonstrates the separation of oppositely charged lipids in the membrane. TR-PE (q = −1e) (red color) and D 291 (q = +1e) (green color) lipids were separated upon application of a 50 Vcm^{-1} field for 10 min. The TR-PE moved to the positive electrode side, while D 291 moved to the negative electrode side. The separation was clearly shown by the fluorescent intensity line profile of these two dye labeled lipids (the inset of Fig. 19).

Lipids with the same charge polarity can also be separated. Figure 20 shows the separation of TR-PE (q = −1e) and NBD PS (q = −2e) under an electric field. Initially both TR-PE and NBD PS were driven to the left side of the square by applying a 30 Vcm^{-1} field (left to right direction) for 90 min (Fig. 20a). After changing the field direction, the field strength was increased to 75 V cm^{-1} to rapidly separate the two lipids. From the line profiles, a gradual peak separation can be seen (Fig. 20b–d). The red and the green curves correspond to TR-PE and NBD PS, respectively.

Apart from manipulating simple charged lipids in the bilayer using 2D electrophoresis, the more complicated systems of, membrane associated proteins were also studied [22, 33]. As mentioned above, the migration of charged lipids in an electric field is mainly controlled by electrophoresis, but this is not true of proteins bound to lipid membranes. Han et al. [33] took FITC-labeled streptavidin as a

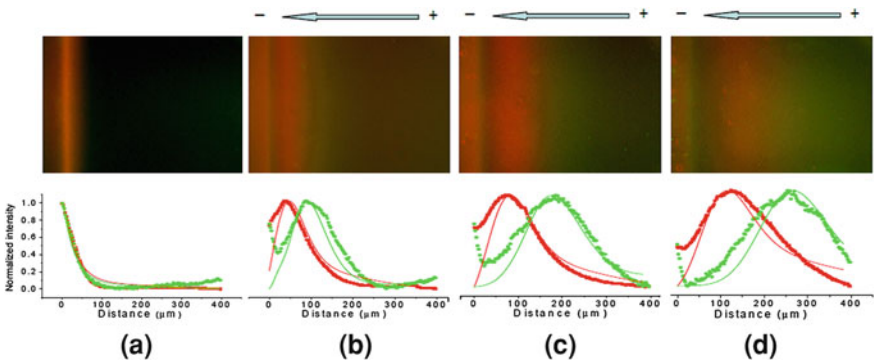

Fig. 20 Fluorescence images of a lipid bilayer containing 0.67 % TR-PE and 1.33 % NBD PS before **a** and after applying 75 Vcm^{-1} for 5 **b**, 10 **c**, and 15 min **d**. The *red* and *green* dotted curves under each image represent the average intensity profile of TR-PE and NBD PS, respectively. [33] – Reproduced by permission of The Royal Society of Chemistry

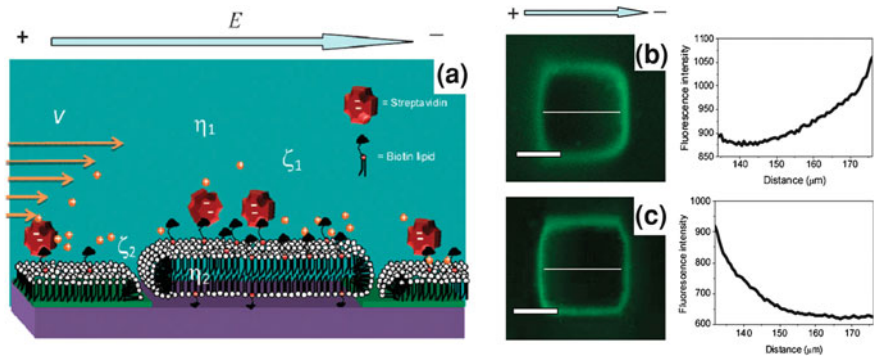

Fig. 21 **a** Schematic model of streptavidin attached to the biotinylated lipid 'doped' lipid membrane under an electric field. Fluorescence images of FITC-labeled streptavidin-bound lipid membrane **b** containing 0.5 % biotinylated lipid and c) 0.5 % biotinylated lipid + 0.5 % DOTAP, after applying an electric field of 5 Vcm^{-1} for 10 min. The curves are the intensity profiles in the bilayer regions for each image. The scale bar is 25 μm. [33] – Reproduced with permission from The Royal Society of Chemistry

model for a membrane-associated protein and investigated its migration behavior in the electric field. The schematic model of the system is illustrated in Fig. 21a. After applying an electric field, the negatively charged streptavidin (under their experimental conditions) moved towards the negative electrode (Fig. 21b), which suggested that electro osmosis flow caused by negatively charged biotinylated lipid in the bilayer is also important for the movement of membrane associated proteins. By adding enough positively charged lipids (DOTAP in this case) into the bilayer, the streptavidin can be tuned to move towards the positive electrode (Fig. 21c).

Similarly, electric fields were used to manipulate and concentrate GPI-tethered proteins in planar supported bilayers [22]. Naturally GPI-linked CD48, along with engineered forms of l-Ek and B7-2 in which the transmembrane domains were genetically replaced with the GPI linkage, were studied under an electrical field. All three protein complexes are mobile and migrate toward the cathode, but the B7-2 and CD48, each tethered to the membrane by a single GPI linker, moved significantly faster than the l-Ek, which has two GPI linkers. Close-packed densities were also achieved while preserving the fluidity and structure of the supported membrane in the fields. These results demonstrated that the patterned lipid bilayer provides a suitable environment for the electrical manipulation of GPI-tethered proteins.

Yoshina-Ishii et al. [44] reported a dynamic response of individual DNA-tethered vesicles in lipid bilayer membrane arrays in an electric field applied in parallel to the substrate. Vesicles respond to the field by moving in the direction of electro-osmotic flow, and this can be used to reversibly concentrate tethered vesicles against a barrier. The mobility of tethered vesicles can be increased by adding negatively charged PS to the lipid bilayer to enhance electro-osmosis, while their speed can be slowed by increasing the amount of negative charge on the tethered vesicle. The response of vesicles to an electric field can be finely tuned because the composition of the lipid bilayer in the arrays can be independently addressed. This expands the versatility of DNA-tethered vesicles for studying membrane–membrane interactions.

3.3 High-throughput Binding Assays Using Lipid Bilayer Arrays

Supported lipid bilayer membranes have long been known to be inherently biocompatible substrates for performing biological assays. Bilayer surfaces containing phosphocholine headgroups have been shown to be highly resistant to nonspecific protein adsorption due in part to their charge neutrality and hydration of the headgroups. Once a lipid bilayer contains protein receptors, it can be used to study binding events with corresponding proteins. It results in an important application of lipid bilayer arrays, i.e. detecting proteins that attach to or interact with lipid-soluble receptors and elucidating their binding characteristics [99]. So far, many binding pairs including biotin/avidin [25, 59, 66, 67], gangliosides GM1/cholera toxin(CT) [57, 67, 68, 74, 76], ganglioside GT1b/tetanus toxin fragment C (TTC) [76], and antidinitrophenyl (DNP)/DNP-antibody [67], have been used for binding assays using lipid bilayer arrays. In this section, several examples will be presented.

Cremer et al. demonstrated the selective binding of streptavidin to a biotin functionalized patterned lipid bilayer [25]. They created four 50 μm × 50 μm boxes by standard lithography. Box 1, 2 and 4 were formed with a lipid bilayer containing 3 % NBD-PE and 2, 0, and 1 % biotinylated lipid, respectively, as shown in Fig. 22a. Box three was left empty. After exposure of the substrate to a 10 μM Texas red-labeled streptavidin solution, the streptavidin was selectively and quantitatively absorbed onto the bilayer patches. There was no streptavidin

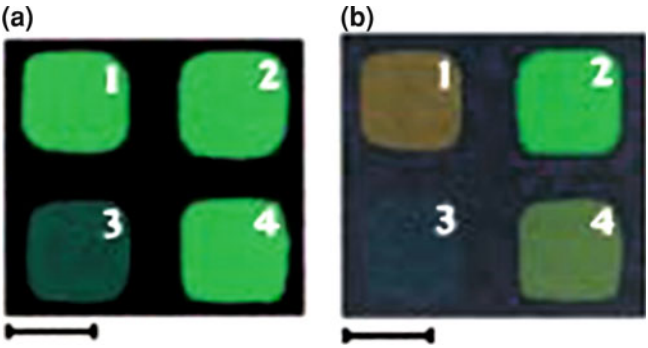

Fig. 22 An epifluorescence image of membranes containing various concentrations of biotinylated lipids **a** before and **b** after exposure to streptavidin. The scale bar is 500 μm. Reprinted with permission from Ref. [25]. Copyright 1999 American Chemical Society

adsorption on box two due to the lack of biotinylated lipid. As expected, box one adsorbed more streptavidin than box four because it contained double the concentration of biotinylated lipid (Fig. 22b).

Gangliosides, a family of negatively charged ceramide-based glycolipids with one or more *sialic acid* residues, are membrane-imbedded receptors that several bacterial toxins recognize and bind to in order to infect the host cell. Cholera toxin is an oligomeric protein produced by *Vibrio cholera*. Its B subunit (CTB) is a 12-kDa domain of cholera toxin that binds in pentamers to the intestinal cell surface via five identical gangliosides GM1 [100]. Similarly, tetanus neurotoxin released by the bacteria *Clostridium tetanii* binds to gangliosides presented on the surface of neural cells [101]. Tetanus toxin binds with higher affinity to ganglioside GT1b [102]. The carboxyl terminus of (TTC) (57 kDa) is responsible for binding to ganglioside GT1b. To explore these binding activities, Moran-Mirabal et al. [76] used micron-sized lipid bilayer arrays containing gangliosides GT1b or GM1 to assay the binding of bacterial toxins. They studied the binding of cholera toxin B subunit or TTC to GM1 or GT1b using this platform. The apparent dissociation constants of 370 nM and 1.1 μM have been calculated for CTB and TTC, respectively. They also fabricated patterned lipid bilayer arrays in microfluidic channels for segregating toxins from a binary mixture and detecting them independently.

Taylor et al. [57] demonstrated the addressable GM1-containing lipid bilayer arrays can be used to biosense cholera toxin (CT). The authors fabricated lipid bilayer arrays containing 5 % GM1 receptor in the microfluidic channels. Three concentrations of FITC-CT were delivered to the bilayers through three channels. The fluorescence intensity increased with the concentration of CT from top to bottom as shown in Fig. 23. The brighter squares indicate more CT binding on the bilayer. The lowest concentration is 0.833 nM, demonstrating a relatively high sensitivity for the approach.

Smith et al. [67] demonstrated a more complicated lipid bilayer array system for binding assays. They selectively incorporated biotin-cap DOPE, DNP(antidinitrophenyl)-cap-DOPE, and GM1 into the same bilayer array for binding avidin,

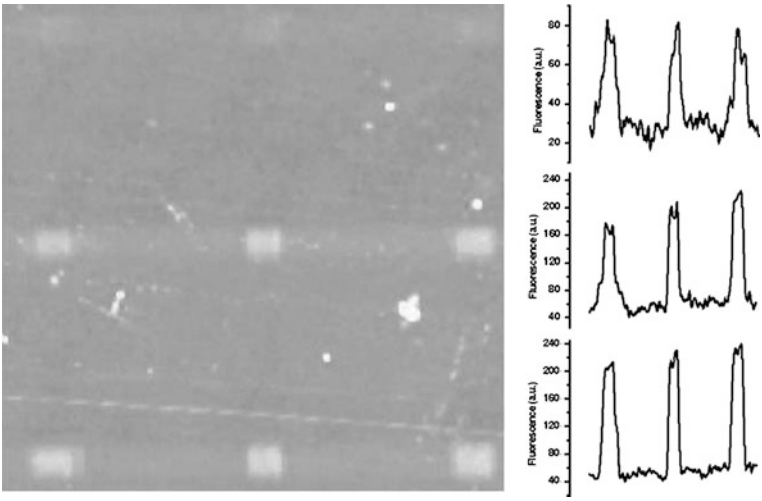

Fig. 23 Fluorescent characterization of FITC-CT binding on the GM1-functionalized lipid bilayer arrays. Profiles for each channel are displayed to on the right. Solution concentrations of CT from *top* channel to *bottom* channel are 1×10^{-5}, 4×10^{-5}, and 7×10^{-5} mg mL^{-1} respectively. The square size is 200 × 200 μm [57]. – Reproduced by permission of The Royal Society of Chemistry

anti-DNP antibody, and CTB, respectively. In Fig. 24, rows one, two, three contained different concentrations of GM1, DNP-cap-DOPE, and biotin-cap DOPE, respectively. After incubating the substrate into a solution containing CTB (200 nM), NeutrAvidin (500 nM), and anti-DNP (500 nM), fluorescence images with three different filter sets—one for each of the fluorescently labeled proteins, CTB in the red (Fig. 24a), anti-DNP in the green (Fig. 24b), and neutrAvidin in the blue channel (Fig. 24c)—were taken to quantify binding events. Each row has two series of increasing concentrations of ligand (two adjacent sets) from left to right. As expected, each analyte was selectively and quantitatively bound to the right ligand. The plotted data represent the average of the two reproduced bilayer spots of identical lipid composition, which shows the intensity of corresponding fluorescence increased with ligand concentration in the bilayers. This work demonstrated the usefulness of the lipid bilayer array for high-throughput binding assays.

The lipid bilayer arrays were also used for controlled chemical release [79] and measuring ion channel activities [9, 82].

4 Outlook

This review provided an overview of the fabricating methods and applications of for lipid bilayer arrays. While in the past the focus has been on the assembly of lipid bilayers in an array format, the core area of the field has already started to implement functionality into the bilayer arrays. One way to functionalize bilayer

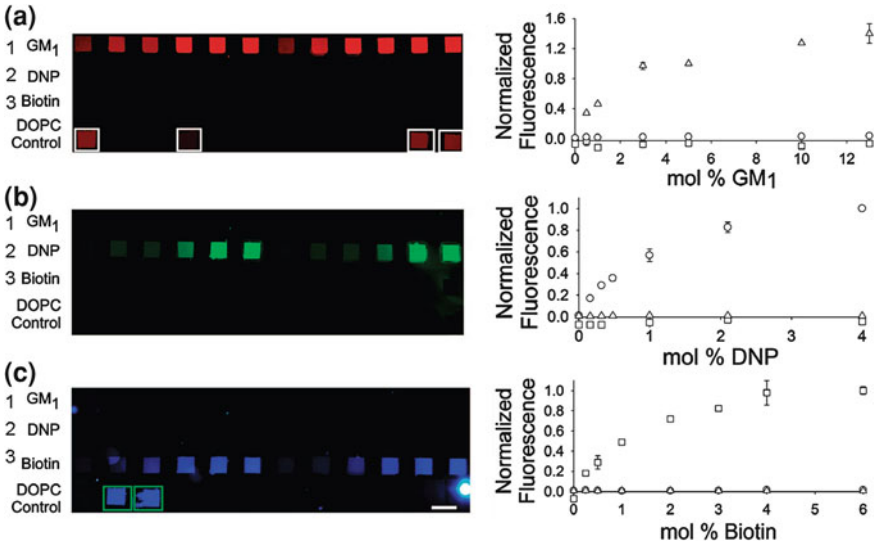

Fig. 24 Multiligand lipid bilayer arrays containing the following: (row 1) GM1 at 0.5, 1.0, 3.0, 5.0, 10.0, and 13.0 mol % in DOPC; (row 2) DNP-cap-PE at 0.2, 0.3, 0.5, 1.0, 2.1, and 4.0 mol % in DOPC; and (row 3) biotin-cap-DOPE at 0.25, 0.5, 1.0, 2.0, 3.0, and 4.0 mol % in DOPC. Each ligand concentration is present in two sequential sets going from the left to right in each row. The array was imaged under the red (**a**), green (**b**), and blue (**c**) filter sets to obtain the images. The representative binding curves to the right of the images represent the average fluorescence intensity of the duplicate bilayers from rows one, two, and three obtained under the red (open triangles), green (open circles), and blue (open squares) filter sets. The scale bar represents 600 μm. Reprinted with permission from Ref. [67]. Copyright 2008 American Chemical Society

arrays is to reconstitute multiple lipid-based receptors in heterogeneous bilayer arrays; the other way is to reconstitute membrane proteins in the bilayer to form membrane protein arrays. In the lipid bilayer environment, the membrane proteins keep their native functions. In the future, the functionalized bilayer arrays will play an important role in following areas. First, they are useful tools on screening surface properties for cell adhesion, growth, or migration. Second, the bilayer arrays containing integral membrane proteins (such as ion channels or transporters) will be highly useful for high-throughput drug screening or drug discovery since approximately half of the known drugs target membrane-associated proteins [103]. Third, by combining microfluidic platforms, the functionalized bilayer arrays are excellent high-throughput analysis systems, which could be optimized to make a biochip that is applicable in clinical diagnostics, such as, detecting low abundant predefined proteins in blood or urine for early diagnosis.

Acknowledgments This work was supported by the National Natural Science Foundation of China (Grant No. 21003032) and the program for New Century Excellent Talents in University (Grant No. NCET-09-0054).

References

1. Singer SJ, Nicolson GL (1972) Fluid mosaic model of structure of cell-membranes. Science 175:720–731
2. Danelon C, Perez JB, Santschi C, Brugger J, Vogel H (2006) Cell membranes suspended across nanoaperture arrays. Langmuir 22:22–25
3. Han XJ, Studer A, Sehr H, Geissbuhler I, Di Berardino M, Winkler FK, Tiefenauer LX (2007) Nanopore arrays for stable and functional free-standing lipid bilayers. Adv Mater 19:4466–4470
4. Hirano-Iwata A, Aoto K, Oshima A, Taira T, Yamaguchi RT, Kimura Y, Niwano M (2010) Free-standing lipid bilayers in silicon chips-membrane stabilization based on microfabricated apertures with a nanometer-scale smoothness. Langmuir 26:1949–1952
5. Romer W, Steinem C (2004) Impedance analysis and single-channel recordings on nano-black lipid membranes based on porous alumina. Biophys J 86:955–965
6. Im H, Wittenberg NJ, Lesuffleur A, Lindquist N, COh SH, (2010) Membrane protein biosensing with plasmonic nanopore arrays and pore-spanning lipid membranes. Chem Sci 1:688–696
7. Mueller P, Rudin DO, Tien HT, Wescott WC (1962) Reconstitution of cell membrane structure in vitro and its transformation into an excitable system. Nature 194:979–980
8. Mueller P, Rudin DO (1968) Action potentials induced in biomolecular lipid membranes. Nature 217:713–719
9. Studer A, Han XJ, Winkler FK, Tiefenauer LX (2009) Formation of individual protein channels in lipid bilayers suspended in nanopores. Colloid Surface B 73:325–331
10. Han XJ, Pradeep SND, Critchley K, Sheikh K, Bushby RJ, Evans SD (2007) Supported bilayer lipid membrane arrays on photopatterned self-assembled monolavers. Chem Eur J 13:7957–7964
11. Tanaka M, Sackmann E (2005) Polymer-supported membranes as models of the cell surface. Nature 437:656–663
12. Cremer PS, Boxer SG (1999) Formation and spreading of lipid bilayers on planar glass supports. J Phys Chem B 103:2554–2559
13. Kam L, Boxer SG (2001) Cell adhesion to protein-micropatterned-supported lipid bilayer membranes. J Biomed Mater Res 55:487–495
14. Sackmann E, Tanaka M (2000) Supported membranes on soft polymer cushions: fabrication, characterization and applications. Trends Biotechnol 18:58–64
15. Sackmann E (1996) Supported membranes: scientific and practical applications. Science 271:43–48
16. Groves JT, Ulman N, Boxer SG (1997) Micropatterning fluid lipid bilayers on solid supports. Science 275:651–653
17. van Oudenaarden A, Boxer SG (1999) Brownian ratchets: molecular separations in lipid bilayers supported on patterned arrays. Science 285:1046–1048
18. Groves JT, Boxer SG (1995) Electric field-induced concentration gradients in planar supported bilayers. Biophys J 69:1972–1975
19. Bayerl TM, Bloom M (1990) Physical-properties of single phospholipid-bilayers adsorbed to micro glass-beads—A new vesicular model system studied by H-2-nuclear magnetic-resonance. Biophys J 58:357–362
20. Cremer PS, Groves JT, Kung LA, Boxer SG (1999) Writing and erasing barriers to lateral mobility into fluid phospholipid bilayers. Langmuir 15:3893–3896
21. Groves JT, Boxer SG, McConnell HM (2000) Electric field effects in multicomponent fluid lipid membranes. J Phys Chem B 104:119–124
22. Groves JT, Wulfing C, Boxer SG (1996) Electrical manipulation of glycan phosphatidyl inositol tethered proteins in planar supported bilayers. Biophys J 71:2716–2723
23. Groves JT, Mahal LK, Bertozzi CR (2001) Control of cell adhesion and growth with micropatterned supported lipid membranes. Langmuir 17:5129–5133

24. Stroumpoulis D, Zhang HN, Rubalcava L, Gliem J, Tirrell M (2007) Cell adhesion and growth to peptide-patterned supported lipid membranes. Langmuir 23:3849–3856
25. Cremer PS, Yang TL (1999) Creating spatially addressed arrays of planar supported fluid phospholipid membranes. J Am Chem Soc 121:8130–8131
26. Kumar A, Whitesides GM (1993) Features of gold having micrometer to centimeter dimensions can be formed through a combination of stamping with an elastomeric stamp and an alkanethiol ink followed by chemical etching. Appl Phys Lett 63:2002–2004
27. Kumar A, Whitesides GM (1994) Patterned condensation figures as optical diffraction gratings. Science 263:60–62
28. Wilbur JL, Kumar A, Kim E, Whitesides GM (1994) Microfabrication by microcontact printing of self-assembled monolayers. Adv Mater 6:600–604
29. Jenkins ATA, Boden N, Bushby RJ, Evans SD, Knowles PF, Miles RE, Ogier SD, Schonherr H, Vancso GJ (1999) Microcontact printing of lipophilic self-assembled monolayers for the attachment of biomimetic lipid bilayers to surfaces. J Am Chem Soc 121:5274–5280
30. Mrksich M, Whitesides GM (1995) Patterning self-assembled monolayers using microcontact printing–a new technology for biosensors. Trends Biotechnol 13:228–235
31. Han XJ, Critchley K, Zhang LX, Pradeep SND, Bushby RJ, Evans SD (2007) A novel method to fabricate patterned bilayer lipid membranes. Langmuir 23:1354–1358
32. Han XJ, Achalkumar AS, Bushby RJ, Evans SD (2009) A cholesterol-based tether for creating photopatterned lipid membrane arrays on both a silica and gold surface. Chem Eur J 15:6363–6370
33. Han XJ, Cheetham MR, Sheikh K, Olmsted PD, Bushby RJ, Evans SD (2009) Manipulation and charge determination of proteins in photopatterned solid supported bilayers. Integr Biol 1:205–211
34. Howland MC, Sapuri-Butti AR, Dixit SS, Dattelbaum AM, Shreve AP, Parikh AN (2005) Phospholipid morphologies on photochemically patterned silane monolayers. J Am Chem Soc 127:6752–6765
35. Howland MC, Szmodis AW, Sanii B, Parikh AN (2007) Characterization of physical properties of supported phospholipid membranes using imaging ellipsometry at optical wavelengths. Biophys J 92:1306–1317
36. Sanii B, Parikh AN (2007) Surface-energy dependent spreading of lipid monolayers and bilayers. Soft Matter 3:974–977
37. Shreve AP, Howland MC, Sapuri-Butti AR, Allen TW, Parikh AN (2008) Evidence for leaflet-dependent redistribution of charged molecules in fluid supported phospholipid bilayers. Langmuir 24:13250–13253
38. Oliver AE, Ngassam V, Dang P, Sanii B, Wu HW, Yee CK, Yeh Y, Parikh AN (2009) Cell attachment behavior on solid and fluid substrates exhibiting spatial patterns of physical properties. Langmuir 25:6992–6996
39. Okazaki T, Tatsu Y, Morigaki K (2010) Phase separation of lipid microdomains controlled by polymerized lipid bilayer matrices. Langmuir 26:4126–4129
40. Morigaki K, Baumgart T, Jonas U, Offenhausser AM, Knoll W (2002) Photopolymerization of diacetylene lipid bilayers and its application to the construction of micropatterned biomimetic membranes. Langmuir 18:4082–4089
41. Morigaki K, Baumgart T, Offenhausser Am, Knoll W (2001) Patterning solid-supported lipid bilayer membranes by lithographic polymerization of a diacetylene lipid. Angew Chem Int Edit 40:172–174
42. Shi JJ, Chen JX, Cremer PS (2008) Sub-100 nm Patterning of supported bilayers by nanoshaving lithography. J Am Chem Soc 130:2718–2719
43. Kung LA, Kam L, Hovis JS, Boxer SG (2000) Patterning hybrid surfaces of proteins and supported lipid bilayers. Langmuir 16:6773–6776
44. Yoshina-Ishii C, Boxer SG (2006) Controlling two-dimensional tethered vesicle motion using an electric field: interplay of electrophoresis and electro-osmosis. Langmuir 22: 2384–2391

45. Yoshina-Ishii C, Miller GP, Kraft ML, Kool ET, Boxer SG (2005) General method for modification of liposomes for encoded assembly on supported bilayers. J Am Chem Soc 127:1356–1357
46. Yoshina-Ishii C, Boxer SG (2003) Arrays of mobile tethered vesicles on supported lipid bilayers. J Am Chem Soc 125:3696–3697
47. Yee CK, Amweg ML, Parikh AN (2004) Direct photochemical patterning and refunctionalization of supported phospholipid bilayers. J Am Chem Soc 126:13962–13972
48. Yee CK, Amweg ML, Parikh AN (2004) Membrane photolithography: direct micropatterning and manipulation of fluid phospholipid membranes in the aqueous phase using deep-UV light. Adv Mater 16:1184–1189
49. Yu CH, Parikh AN, Groves JT (2005) Direct patterning of membrane-derivatized colloids using in situ UV-ozone photolithography. Adv Mater 17:1477–1480
50. Hovis JS, Boxer SG (2000) Patterning barriers to lateral diffusion in supported lipid bilayer membranes by blotting and stamping. Langmuir 16:894–897
51. Hovis JS, Boxer SG (2001) Patterning and composition arrays of supported lipid bilayers by microcontact printing. Langmuir 17:3400–3405
52. Majd S, Mayer M (2005) Hydrogel stamping of arrays of supported lipid bilayers with various lipid compositions for the screening of drug-membrane and protein-membrane interactions. Angew Chem Int Edit 44:6697–6700
53. Martin BD, Gaber BP, Patterson CH, Turner DC (1998) Direct protein microarray fabrication using a hydrogel "stamper". Langmuir 14:3971–3975
54. Mayer M, Yang J, Gitlin I, Gracias DH, Whitesides GM (2004) Micropatterned agarose gels for stamping arrays of proteins and gradients of proteins. Proteomics 4:2366–2376
55. Weibel DB, Lee A, Mayer M, Brady SF, Bruzewicz D, Yang J, DiLuzio WR, Clardy J, Whitesides GM (2005) Bacterial printing press that regenerates its ink: contact-printing bacteria using hydrogel stamps. Langmuir 21:6436–6442
56. Stevens MM, Mayer M, Anderson DG, Weibel DB, Whitesides GM, Langer R (2005) Direct patterning of mammalian cells onto porous tissue engineering substrates using agarose stamps. Biomaterials 26:7636–7641
57. Taylor JD, Phillips KS, Cheng Q (2007) Microfluidic fabrication of addressable tethered lipid bilayer arrays and optimization using SPR with silane-derivatized nanoglassy substrates. Lab Chip 7:927–930
58. Shi JJ, Yang TL, Kataoka S, Zhang YJ, Diaz AJ, Cremer PS (2007) GM(1) clustering inhibits cholera toxin binding in supported phospholipid membranes. J Am Chem Soc 129:5954–5961
59. Burridge KA, Figa MA, Wong JY (2004) Patterning adjacent supported lipid bilayers of desired composition to investigate receptor-ligand binding under shear flow. Langmuir 20:10252–10259
60. Phillips KS, Dong Y, Carter D, Cheng Q (2005) Stable and fluid ethylphosphocholine membranes in a poly(dimethylsiloxane) microsensor for toxin detection in flooded waters. Anal Chem 77:2960–2965
61. Phillips KS, Cheng Q (2005) Microfluidic immunoassay for bacterial toxins with supported phospholipid bilayer membranes on poly(dimethylsiloxane). Anal Chem 77:327–334
62. Kam L, Boxer SG (2000) Formation of supported lipid bilayer composition arrays by controlled mixing and surface capture. J Am Chem Soc 122:12901–12902
63. Kam L, Boxer SG (2003) Spatially selective manipulation of supported lipid bilayers by laminar flow: steps toward biomembrane microfluidics. Langmuir 19:1624–1631
64. Perez TD, Nelson WJ, Boxer SG, Kam L (2005) E-cadherin tethered to micropatterned supported lipid bilayers as a model for cell adhesion. Langmuir 21:11963–11968
65. Dutta D, Pulsipher A, Yousaf MN (2010) Selective tethering of ligands and proteins to a microfluidically patterned electroactive fluid lipid bilayer array. Langmuir 26:9835–9841
66. Albertorio F, Diaz AJ, Yang TL, Chapa VA, Kataoka S, Castellana ET, Cremer PS (2005) Fluid and air-stable lipopolymer membranes for biosensor applications. Langmuir 21: 7476–7482

67. Smith KA, Gale BK, Conboy JC (2008) Micropatterned fluid lipid bilayer arrays created using a continuous flow microspotter. Anal Chem 80:7980–7987
68. Joubert JR, Smith KA, Johnson E, Keogh JP, Wysocki VH, Gale BK, Conboy JC, Saavedra SS (2009) Stable, ligand-doped, poly(bis-SorbPC) lipid bilayer arrays for protein binding and detection. Acs Appl Mater Inter 1:1310–1315
69. Salaita K, Wang YH, Mirkin CA (2007) Applications of dip-pen nanolithography. Nat Nano technol 2:145–155
70. Piner RD, Zhu J, Xu F, Hong SH, Mirkin CA (1999) "Dip-pen" nanolithography. Science 283:661–663
71. Lenhert S, Sun P, Wang YH, Fuchs H, Mirkin CA (2007) Massively parallel dip-pen nanolithography of heterogeneous supported phospholipid multilayer patterns. Small 3:71–75
72. Lenhert S, Mirkin CA, Fuchs H (2010) In situ lipid dip-pen nanolithography under water. Scanning 32:15–23
73. Lenhert S, Brinkmann F, Laue T, Walheim S, Vannahme C, Klinkhammer S, Xu M, Sekula S, Mappes T, Schimmel T, Fuchs H (2010) Lipid multilayer gratings. Nat Nanotechnol 5:275–279
74. Yamazaki V, Sirenko O, Schafer RJ, Nguyen L, Gutsmann T, Brade L, Groves JT (2005) Cell membrane array fabrication and assay technology. BMC Biotechnol. doi: 10.1186/1472-6750-5-18
75. Orth RN, Kameoka J, Zipfel WR, Ilic B, Webb WW, Clark TG, Craighead HG (2003) Creating biological membranes on the micron scale: forming patterned lipid bilayers using a polymer lift-off technique. Biophys J 85:3066–3073
76. Moran-Mirabal JM, Edel JB, Meyer GD, Throckmorton D, Singh AK, Craighead HG (2005) Micrometer-sized supported lipid bilayer arrays for bacterial toxin binding studies through total internal reflection fluorescence microscopy. Biophys J 89:296–305
77. Wu M, Holowka D, Craighead HG, Baird B (2004) Visualization of plasma membrane compartmentalization with patterned lipid bilayers. P Natl Acad Sci USA 101:13798–13803
78. Orth RN, Wu M, Holowka DA, Craighead HG, Baird BA (2003) Mast cell activation on patterned lipid bilayers of subcellular dimensions. Langmuir 19:1599–1605
79. Mager MD, Melosh NA (2008) Nanopore-spanning lipid bilayers for controlled chemical release. Adv Mater 20:4423–4427
80. Kresak S, Hianik T, Naumann RLC (2009) Giga-seal solvent-free bilayer lipid membranes: from single nanopores to nanopore arrays. Soft Matter 5:4021–4032
81. Tiefenauer LX, Studer A (2008) Nano for bio: Nanopore arrays for stable and functional lipid bilayer membranes (Mini Review). Biointerphases 3: FA74-FA79
82. Schmitt EK, Vrouenraets M, Steinem C (2006) Channel activity of OmpF monitored in nano-BLMs. Biophys J 91:2163–2171
83. Romer W, Lam YH, Fischer D, Watts A, Fischer WB, Goring P, Wehrspohn RB, Gosele U, Steinem C (2004) Channel activity of a viral transmembrane peptide in micro-BLMs: vpu(1–32) from HIV-1. J Am Chem Soc 126:16267–16274
84. Mayer M, Kriebel JK, Tosteson MT, Whitesides GM (2003) Microfabricated teflon membranes for low-noise recordings of ion channels in planar lipid bilayers. Biophys J 85:2684–2695
85. Hansen JS, Perry M, Vogel J, Groth JS, Vissing T, Larsen MS, Geschke O, Emneus J, Bohr H, Nielsen CH (2009) Large scale biomimetic membrane arrays. Anal Bioanal Chem 395:719–727
86. Hansen JS, Perry M, Vogel J, Vissing T, Hansen CR, Geschke O, Emneus J, Nielsen CH (2009) Development of an automation technique for the establishment of functional lipid bilayer arrays. J Micromech Microeng. doi:10.1088/0960-1317/19/2/025014
87. Vogel J, Perry M, Hansen JS, Bolinger PY, Nielsen CH, Geschke O (2009) A support structure for biomimetic applications. J Micromech Microeng. doi:10.1088/0960-1317/19/2/025026
88. Koynov S, Brandt MS, Stutzmann M (2009) Ordered Si nanoaperture arrays for the measurement of ion currents across lipid membranes. Appl Phys Lett doi:10.1063/1.3171931

89. Heyderman LJ, Ketterer B, Bachle D, Glaus F, Haas B, Schift H, Vogelsang K, Gobrecht J, Tiefenauer L, Dubochet O, Surbled P, Hessler T (2003) High volume fabrication of customised nanopore membrane chips. Microelectron Eng 67–68:208–213
90. Chen CS, Mrksich M, Huang S, Whitesides GM, Ingber DE (1997) Geometric control of cell life and death. Science 276:1425–1428
91. Singhvi R, Kumar A, Lopez GP, Stephanopoulos GN, Wang DIC, Whitesides GM, Ingber DE (1994) Engineering cell-shape and function. Science 264:696–698
92. Mcconnell HM, Watts TH, Weis RM, Brian AA (1986) Supported planar membranes in studies of cell–cell recognition in the immune-system. Biochim Biophys Acta 864:95–106
93. Watts TH, Mcconnell HM (1987) Biophysical aspects of antigen recognition by t-cells. Annu Rev Immunol 5:461–475
94. Grakoui A, Bromley SK, Sumen C, Davis MM, Shaw AS, Allen PM, Dustin ML (1999) The immunological synapse: a molecular machine controlling T cell activation. Science 285:221–227
95. Lawrence MB, Springer TA (1991) Leukocytes roll on a selectin at physiological flow-rates—distinction from and prerequisite for adhesion through integrins. Cell 65:859–873
96. Alon R, Hammer DA, Springer TA (1995) Lifetime of the *p*-selectin-carbohydrate bond and its response to tensile force in hydrodynamic flow. Nature 374:539–542
97. Stelzle M, Miehlich R, Sackmann E (1992) 2-Dimensional microelectrophoresis in supported lipid bilayers. Biophys J 63:1346–1354
98. Poo MM, Robinson KR (1977) Electrophoresis of concanavalin-A receptors along embryonic muscle-cell membrane. Nature 265:602–605
99. Lieto AM, Cush RC, Thompson NL (2003) Ligand-receptor kinetics measured by total internal reflection with fluorescence correlation spectroscopy. Biophys J 85:3294–3302
100. Merritt EA, Sarfaty S, Vandenakker F, Lhoir C, Martial JA, Hol WGJ (1994) Crystal-structure of cholera-toxin b-pentamer bound to receptor G(M1) pentasaccharide. Protein Sci 3:166–175
101. Herreros J, Schiavo G (2002) Lipid microdomains are involved in neurospecific binding and internalisation of clostridial neurotoxins. Inter J Med Microbiol 291:447–453
102. Angstrom J, Teneberg S, Karlsson KA (1994) Delineation and comparison of ganglioside-binding epitopes for the toxins of *Vibrio-cholerae*, *Escherichia-coli*, and *Clostridium-tetani*–evidence for overlapping epitopes. P Natl Acad Sci U S A 91:11859–11863
103. Drews J (2000) Drug discovery: a historical perspective. Science 257:1960–1964

Adv Biochem Eng Biotechnol (2013) 131: 153–169
DOI: 10.1007/10_2012_136

Published Online: 11 April 2012

RNA Aptamers: A Review of Recent Trends and Applications

Kyung-Nam Kang and Yoon-Sik Lee

Abstract RNA aptamers, small oligonucleotides derived by an in-vitro selection process called SELEX (Systematic Evolution of Ligands by EXperimental enrichment), are important candidates for therapeutic and diagnostic applications. RNA aptamers have high affinity and specificity for their target molecules. In this review, we describe methods for generating RNA aptamers (the SELEX technique and modified SELEX processes) and therapeutic applications for diseases such as neovascular age-related macular degeneration (AMD), inflammatory diseases, and obesity. We also analyze the social networks among researchers and organizations (universities, research institutes, firms, etc.) that are active in the pursuit of aptamer-based therapeutic approaches. This study provides relevant information on recent research trends in RNA aptamers.

Keywords RNA aptamer · Therapeutic application · Social networks

Abbreviations

CAD	Coronary artery disease
CNV	Choroidal neovascularization
MCP-1	Monocyte chemoattractant Protein 1
NIH	National Institutes of Health
OECD	Organization for Economic Cooperation and Development
PCI	Percutaneous coronary intervention
PEG	Polyethylene glycol
RADAR	A Randomized, partially-blinded, multi-center, active-controlled, dose-ranging study assessing the safety, efficacy, and pharmacodynamics

K.-N. Kang
Korea Institute of Intellectual Property, KIPS Center, 9th FL. 647-9,
Yeoksam-dong, Gangnam-gu, Seoul 135-980, Korea
e-mail: knkang75@snu.ac.kr

Y.-S. Lee (✉)
School of Chemical and Biological Engineering, Seoul National University,
Seoul 151-747, Korea
e-mail: yslee@snu.ac.kr

	of the REG1 anticoagulation system compared to unfractionated heparin or low molecular heparin in subjects with acute coronary syndromes
SDF-1	Stromal cell-derived factor-1
SELEX	Systematic evolution of ligands by exponential enrichment
SMEs	Small- and medium-sized enterprises
VEGF	Vascular endothelial growth factor

Contents

1 Introduction

In 1990, an in-vitro selection procedure for generating novel RNA molecules that bind target molecules was introduced. The isolated RNA molecules were called “RNA aptamers” (from the Latin word *aptus*, which means “fitting”) [1]. During the past decade, much progress has been made in the use of RNA aptamers for therapeutic or diagnostic applications. In particular, selection strategies have been improved and post-modification methods for enhancing the biostability of RNA aptamers have been developed. Many researchers have developed RNA aptamers for therapeutic and diagnostic purposes. Here, we describe methods for generating RNA aptamers and their therapeutic and diagnostic applications. We also analyze collaborative activities among researchers and organizations (firms, universities, hospitals, etc.) that are active in pursuing therapeutic approaches, and outline future prospects for the application of these RNA aptamers.

2 Methods for Generating RNA Aptamers

2.1 The SELEX Method

In 1990, three research teams independently developed methods for generating catalytic or ligand-binding RNA molecules from RNA libraries [2–5]. The process, which was termed SELEX (Systematic Evolution of Ligands by EXponential enrichment) by Tuerk and Gold [4], is a powerful tool for the in-vitro selection of nucleic acids with a desired property, such as catalytic activity or target affinity, from libraries of synthetic DNA or RNA with diversities of up to 10^{15} different molecules and possible secondary and tertiary structures [6].

For SELEX, an oligonucleotide is chemically synthesized to contain a central randomized region, commonly consisting of 15–75 random positions, flanked by conserved regions that are designed as primer-binding sites for reverse transcription and PCR amplification [6]. Usually, a T7 promoter site is used as a conserved region and the original RNA pool is produced by in-vitro transcription with T7-RNA polymerase on the double-stranded DNA templates, creating a library containing at least 10^{12} different sequences and possible 3-dimensional structures [6]. RNA molecules in the initial pool are purified and folded. The RNA pool is then mixed with its target molecules, and RNAs that bind with high affinity are eluted from the target molecules by phenol/chloroform denaturation of the target proteins. These selected RNA molecules are amplified by RT-PCR to produce the next-generation DNA pool. In-vitro transcription of the new DNA pool provides the RNA pool for the next selection cycle. The affinity of the RNA population for the target molecules is usually maximized after 6–20 rounds of selection and amplification and does not increase further with additional rounds. The RNA molecules in the final pool are then purified, reverse-transcribed to DNA, and cloned. Isolated clones are identified by DNA sequencing [6].

The major drawback of aptamers is their instability in biological fluids. Several different approaches to producing nuclease-resistant RNA molecules have been described. For the most part, modifications of the nucleotide sugar residues, phosphates, or bases have been employed for this purpose [7]. Post-SELEX modification methods, including the addition of 3′-3′-linked dinucleotide caps (usually conjugated deoxythymidine caps) and attachment of macromolecules such as polyethylene glycol (PEG) chains or cholesterol, have been developed to improve aptamer stability and reduce clearance from the bloodstream [7] (see Fig. 1a for a depiction of the SELEX process and Table 1for details of the modification methods described).

2.2 Modified SELEX

Various modifications that greatly improve the stability, affinity, and/or specificity of the original SELEX process have been developed since 1990. These improved

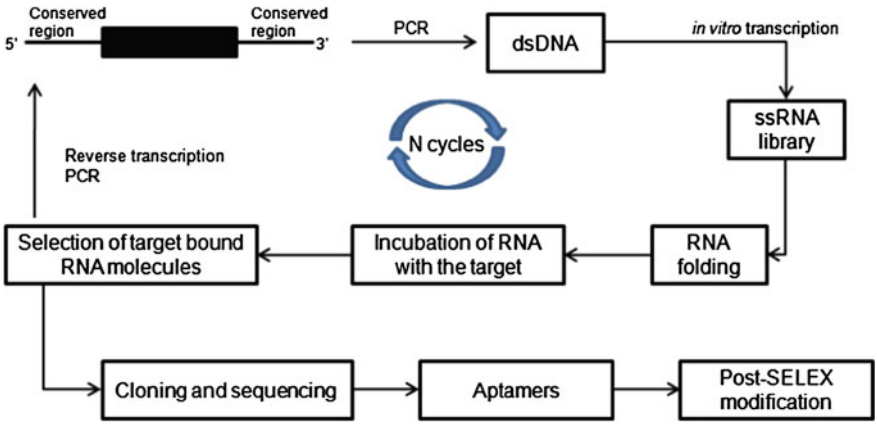

Fig. 1a A depiction of SELEX process

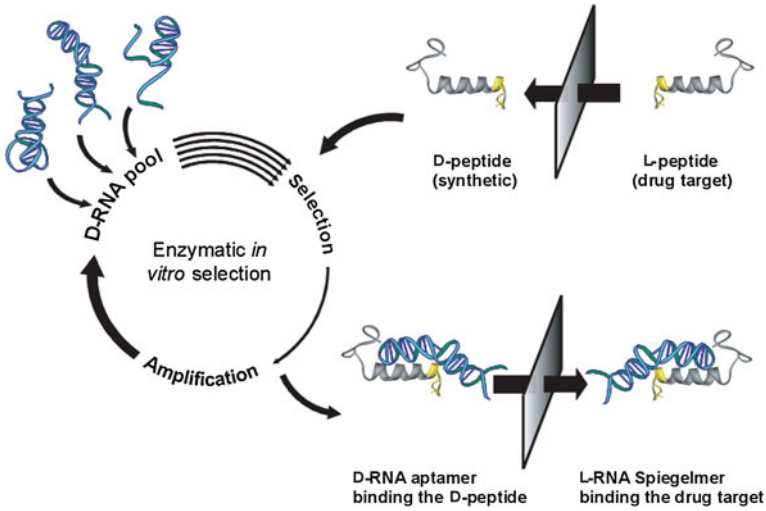

Fig. 1b The process of mirror-image in-vitro selection. Adapted from [5, 10]

processes include automated SELEX, toggle-SELEX, photoSELEX, mirror-image SELEX, and intramers. In automated systems, multiple targets can be handled with parallel processes and selection cycles can be conducted without any direct intervention with an automated aptamer selection procedure coupled to an in-vitro translation system for the target protein [8, 9]. Toggle-SELEX assays have been developed to facilitate the generation of aptamers that are cross-reactive between species [9, 10]. The photoSELEX method increases binding affinity via UV-induced cross-linking between aptamers and their target molecules [9]. Intramers, which use retroviral vectors to encode aptamers, have been developed to solve the delivery

Table 1 Modifications to RNA aptamers

Position of modification	Details of modification
Sugar residues	2′-fluoro
	2′-NH_2
	2′-*O*-methyl
	2′-*O*-methoxyethyl
	2′-*O*-dimethylallyl
Phosphate	phosphorothioate
	methylphosphonate
Nucleotide base	propenyl
	5-(*N*′-aminoalkyl) carbamoyluracil
	methyl
	trifluoromethyl
	phenyl
	2-thiopyrimidine
5′- or 3′-terminus	3′-3′-linked dinucleotide caps
	polyethylene glycol (PEG) chains
	cholesterol group

problem, which is particularly serious when the target is located inside the cell [1, 9]. Yang et al. [9] reviewed all of these methods except for mirror-image SELEX. In this paper, we introduce the mirror-image SELEX method in detail.

For therapeutic or diagnostic purposes, the major weakness of aptamers is their insufficient stability in vivo. Mirror-image (chiral) nucleotides have been used to solve this stability problem. Stereochemistry and chirality have become invaluable tools for targeted inhibition of intermolecular interactions [5]. Mirror-image in-vitro selection yields nuclease-resistant mirror-image L-oligonucleotides that bind biological target molecules. Furste et al. [12] invented this method, which relies on the synthesis of the selection target in its non-biological enantiomeric form (e.g., a peptide target synthesized from D-amino acids) [5]. As with traditional SELEX, repeated selection and amplification cycles are performed, and the target-binding nucleic acid species are identified through cloning and sequencing. The best candidates may then be chemically synthesized from mirror-image nucleotides. These L-oligonucleotides consequently bind to the natural target of interest [5]. As they are exact mirror images of their parent aptamers, the L-oligonucleotides were termed "spiegelmers" (from the German word *Spiegel*, which means mirror).

3 Applications of RNA Aptamers

3.1 Therapeutic Approaches

Aptamers show high affinity and specificity for their targets, with dissociation constants in the picomolar to nanomolar range [13, 14] and better specificity than control antibodies [14, 15]. Aptamers showed potential for superior target binding

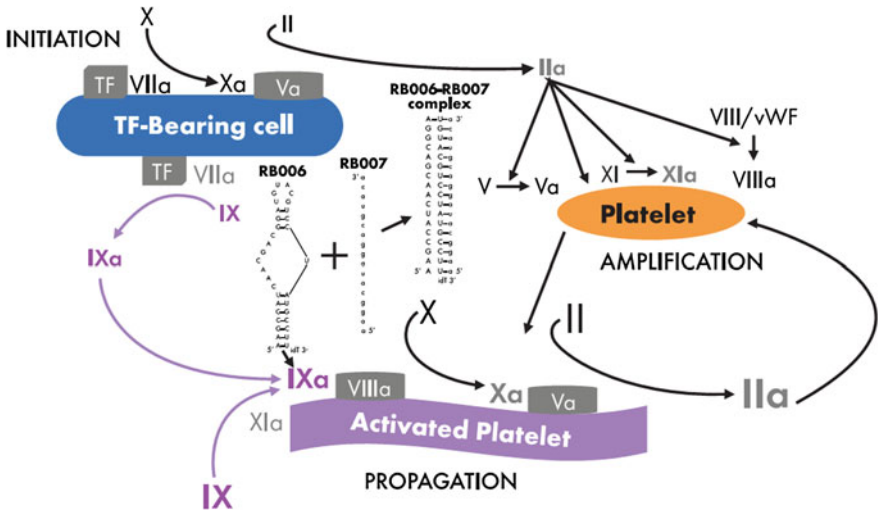

Fig. 2 Factor IXa and RB006-RB007 interactions. vWF indicates von Willebrand factor. Adapted from [28, 27]

compared with naturally occurring RNA or DNA molecules [13]. Furthermore, aptamers allow for adaptive recognition such as conformational alteration of either the protein or the aptamer, which further increases binding affinity [13]. During the past decade, much progress has been made in the therapeutic use of aptamers. In this study, we describe RNA aptamers in clinical development, including pegaptanib, REG1, NOX-E36, NOX-A12, and ARC1905. The targets, compositions, and clinical statuses of therapeutic RNA aptamers are summarized in Table 2.

3.1.1 Pegaptanib

Pegaptanib is an RNA aptamer with a 3-dimensional structure that facilitates binding to vascular endothelial growth factor (VEGF) [16]. The target (VEGF) has been linked to angiogenesis in age-related macular degeneration (AMD), and $VEGF_{165}$ is the predominant isoform [7]. AMD is the leading cause of severe, irreversible vision loss [17], and angiogenesis is an important factor in AMD and other pathophysiological conditions [18].

Using the SELEX process, Ruckman et al. [19] isolated RNA aptamers to human $VEGF_{165}$ and identified three families of aptamers with affinities in the low picomolar range [7]. A representative aptamer selected from each family was chemically modified after SELEX (with 2′-fluorine-modified pyrimidines and 2′-*O*-methyl instead of 2′-hydroxyl at all but 2 purine positions). The 5′ terminus of each aptamer was also conjugated to a 40-kDa polyethylene glycol (PEG) chain and a deoxythymidine linked to the 3′ terminus via a 3′-3′ linkage [19, 20]. The

Table 2 List of RNA aptamers in clinical development

Aptamer (Company)	Composition	Target	Condition	Status
Pegaptanib sodium (Eyetech/ Pfizer)	2′-O-methylpurine/ 2′-fluoropyrimidine with two 2′-ribopurines conjugated to 40 kDa PEG, 3′ inverted dT	Vascular endothelial growth factor (VEGF-165)	Age-related macular degeneration (AMD)	Approved in the US and EU
REG1 (RB006-RB007) (Regado Biosciences)	2′-fluoropyrimidines/ 2′-O-methypurines/ 2′-O-methylpyrimidines/ with a single 2′-OH residue conjugated to 40 kDa PEG (5′end), 3′-3′ dT cap (3′ end) (RB006), 2′-O-methyl antidote	Coagulation factor IXa	Percutaneous coronary intervention	Phase II
NOX-E36 (NOXXON pharma)	L-RNA conjugated to 40 kDa PEG	MCP-1 (CCL2) (monocyte chemoattractant protein 1)	Complications of Type II diabetes incl. nephropathy and lupus nephritis	Phase I
NOX-A12 (NOXXON Pharma)	L-RNA conjugated to 40 kDa PEG	SDF-1 (CXCL12) (stromal cell-derived factor-1)	Hematopoietic stem cell mobilization, hematological and solid tumors	Phase I
ARC1905 (Archemix/ Ophthotech)	2′-ribopurine/ 2′-fluoropyrimidine conjugated to 40 kDa PEG, 3′ inverted dT	Complement component 5	Age-related macular degeneration	Phase I

aptamer that showed the highest affinity for $VEGF_{165}$, NX1838 (dissociation constant $\sim$50 pM), was finally translated to pegaptanib [7, 16].

In-vitro studies using human umbilical vein endothelial cells found that pegaptanib inhibited VEGF binding as well as signal transduction, calcium mobilization, and cell proliferation mediated by $VEGF_{165}$ [16, adapted from 21]. The pharmacokinetic parameters of pegaptanib were evaluated in plasma and vitreous humor of rhesus monkeys, and intravitreal pharmacokinetics were studied in 18 New Zealand white rabbits [16]. The effects of pegaptanib were also studied in animal models of vascular leakage and ocular neovascularization such as the Miles assay, the rat corneal angiogenesis model, and the mouse retinopathy of prematurity (ROP) model [22]. A phase 1a single ascending dose study using intravitreal

injections of the drug was then performed in 15 patients with subfoveal choroidal neovascularization (CNV) secondary to exudative AMD, which revealed a good safety profile [22, 23]. The Eyetech Study Group next conducted a phase 2 multiple-injection study with and without photodynamic therapy for patients with subfoveal CNV secondary to AMD, which revealed that multiple intravitreal injections of pegaptanib were also well tolerated [23]. Gragoudas et al. [17] conducted two concurrent, prospective, randomized, double-blind, multicenter, dose-ranging, controlled clinical trials to test the safety and effectiveness of pegaptanib in patients and reported that pegaptanib showed treatment benefit in a broad spectrum of patients with neovascular AMD, regardless of the size or angiographic subtype of the lesion or the baseline visual acuity [17]. A series of clinical trials led to FDA approval for the commercialization of pegaptanib for the treatment of all types of neovascular AMD in December 2004, and pegaptanib became the first aptamer-based therapeutic agent [7, 13].

3.1.2 REG1

Anticoagulant therapeutic agents are widely administered due to the high prevalence of cardiovascular, cerebrovascular, and peripheral vascular diseases [24]. However, there are significant risks, such as bleeding, that increase patient morbidity and mortality [25]. In 2002, Rusconi et al. [25] devised a unique approach to the effective regulation of aptamer function by adding an antidote [7]. Their strategy was to develop drug–antidote pairs in which the aptamer can be controlled by an antidote with a complementary sequence.

Using the SELEX process, Rusconi et al. [25] isolated an aptamer specific for coagulation factor IXa, which plays critical roles in both the initial and propagation phases of coagulation [24]. The aptamer was then modified with 2′-fluoropyrimidines, 2′-O-methylpurines and 2′-O-methylpyrimidines with a single 2′-OH residue, and conjugated to a 40-kDa PEG and a 3′-3′ inverted deoxythymidine cap in order to enhance its bioavailability; the modified aptamer is referred to as RB006. Then, in order to rapidly and effectively inactivate the aptamer, Rusconi et al. designed a series of antidote oligonucleotides complementary to different portions of RB006. In preclinical trials, RB006 systematically induced anticoagulation in pigs and inhibited thrombosis in mice [24]. The antidote (referred to as RB007) inactivated RB006-mediated anticoagulation in surgically challenged animals [24].

The phase 1a study on dose, initial safety, and duration of effect in 85 healthy volunteers was successfully completed in 2005 [7, 26]. Chan et al. performed a randomized repeat-dose study of REG1 (a name for the combination of RB006 and RB007) and demonstrated its graded active reversibility [27]. In the phase 1b study, the safety, tolerability, and pharmacodynamic profile of REG1 were evaluated in patients with stable coronary artery disease (CAD) on maintenance single or dual antiplatelet therapy [28]. Povsic et al. performed detailed modeling to translate these phase 1 results into an appropriate phase 2 dose selection [29].

In a phase 2a clinical trial completed in September 2009, the feasibility and safety for percutaneous coronary intervention (PCI) of the REG1 anti-coagulation system were compared with those of heparin [30]. In addition, a phase 2b pharmacokinetic and pharmacodynamic substudy was completed and supported the weight-adjusted dose of 1 mg/kg of RB006 (pegnivacogin) selected for the RADAR study [31].

3.1.3 Spiegelmers (NOX-E36 and NOX-A12)

Several spiegelmers (aptamers based on L-ribose) are in clinical development, and the most advanced is the spiegelmer raised against monocyte chemoattractant protein-1 (MCP-1/CCL2). MCP-1, which is also known as CCL2, is a key chemokine in the regulation of the migration and infiltration of monocytes/macrophages. Both MCP-1 and its receptor CCR2 have been demonstrated to be upregulated and involved in a variety of inflammatory diseases, including nephritis, and are also associated with type 2 diabetes.

Aptamers that showed high affinity to D-mCCL2 were identified after 11 rounds of in-vitro selection [32]. The final candidate, mNOX-E36, was linked to 40-kDa PEG and referred to as NOX-E36 [32]. An in-vivo study in diabetic mice demonstrated that NOX-E36 delayed decline in kidney function and disease progression [33]. A first-in-human clinical trial was completed in late 2009 and showed a dose-dependent effect on blood monocytes, consistent with the proposed mode of action of NOX-E36 [7]. A double-blinded, placebo-controlled phase I study to evaluate the safety, tolerability, pharmacokinetics, and pharmacodynamics of NOX-E36 in healthy volunteers and non-insulin-dependent diabetic patients was initiated in mid-2010 [7, 34].

NOX-A12, an L-ribose-based aptamer raised against stromal cell-derived factor-1 (SDF-1) has also been developed. SDF-1 has been shown to bind to several chemokine receptors and play important roles in vasculogenesis, tumor growth, and metastasis. Therefore, inhibition of SDF-1 would be an effective method for the treatment of many types of cancer. NOXXON has announced the successful completion of the first-in-human phase I clinical trial [7, 34].

3.1.4 Arc1905

ARC1905, which is an aptamer against complement component 5 (C5), interrupts the complement cascade by inhibiting factor C5. This inhibition of C5-mediated inflammation makes ARC1905 a promising potential therapeutic agent for both dry and wet AMD. An open-label multicenter phase 1 clinical study of ARC1905 in combination with an anti-VEGF agent (ranibizumab) in patients with wet AMD is ongoing. In addition, a phase 1 clinical study in patients with dry AMD was initiated in 2009 [35].

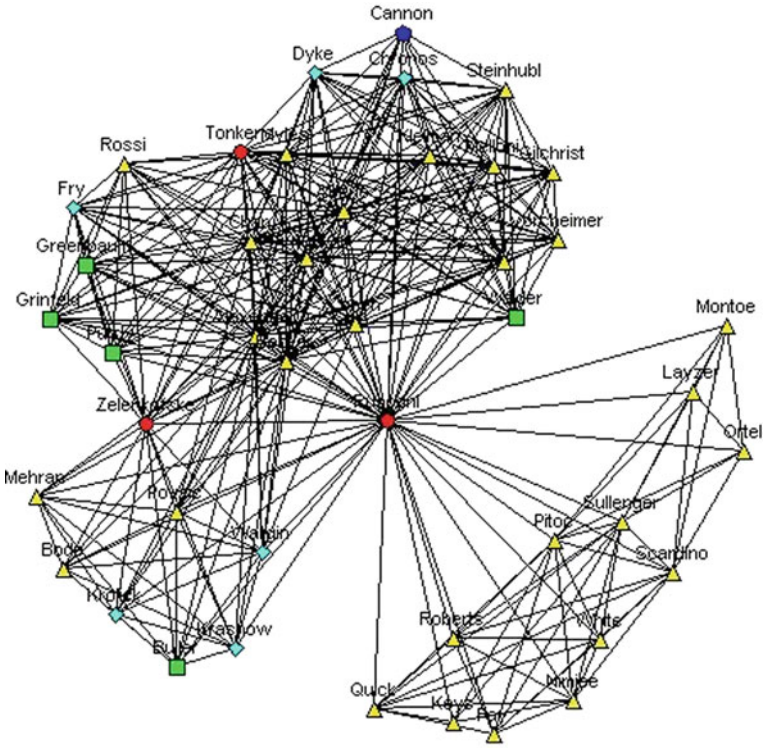

Fig. 3a Social networks among researchers who conducted studies related to the discovery and development of REG1. *Red circle*: Regado (Biotech SME), *yellow triangle*: university, *green square*: hospital, *light blue diamond*: private research institute, *dark blue pentagon*: national institute

3.2 Diagnostic Approaches

As previously described, aptamers show high affinity and specificity for their targets, making them potentially useful as diagnostic reagents. For diagnostic applications of aptamers, post-SELEX modifications such as fluorescence labeling and quantum dot coupling are employed [6].

RNA aptamers can be used in place of antibodies because they bind their targets with equal or better specificity [14, 15]. Therefore, aptamers conjugated to signaling molecules can substitute for antibodies in enzyme-linked immunosorbent assays (ELISAs), Western blot assays, and chip-based technologies [6, 36–38]. For example, Davis et al. [39] developed fluorophore-tagged RNA aptamers for flow cytometry. Bagalkot et al. [40] reported a novel quantum dot–aptamer–doxorubicin conjugate as a targeted combined cancer imaging, therapy, and sensing system. Quantum dots are novel fluorophores, each having a distinct sharp

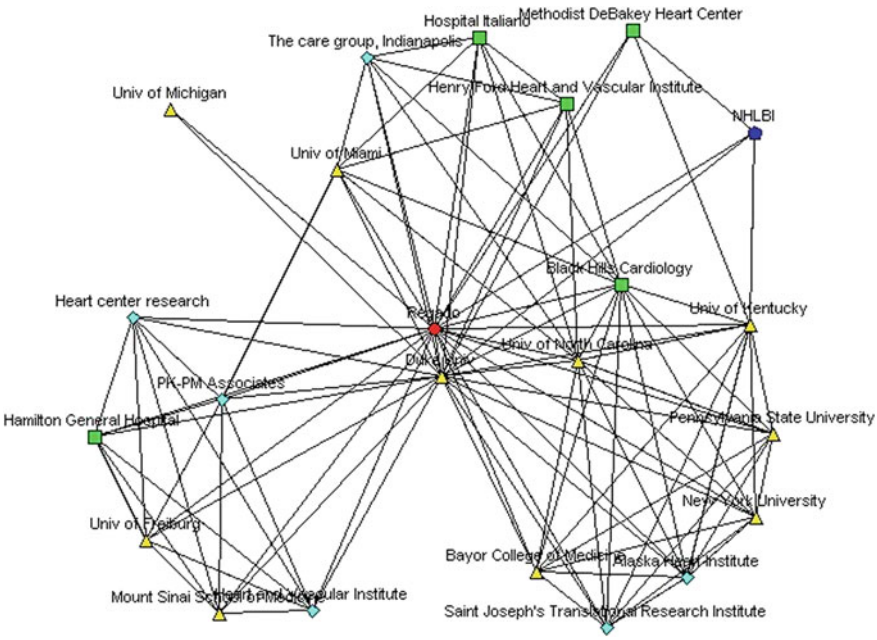

Fig. 3b Social networks among organizations involved in the discovery and development of REG1. NHLBI indicates National Heart, Lung, and Blood Institute. *Red circle*: Regado (Biotech SME), *yellow triangle*: university, *green square*: hospital, *light blue diamond*: private research institute, *dark blue pentagon*: national institute

emission profile [1]. Ulich argued that coupling aptamers to quantum dots may greatly facilitate high-throughput chip-based screening systems because quantum dots allow the simultaneous use of many intensity levels and colors [6]. Recently, Gold et al. created a new class of aptamer, the Slow Off-rate Modified Aptamer (SOMAmer). These aptamers contain chemically modified nucleotides and kinetic manipulations that support the construction of diagnostic tools [41]. Multiplex SOMAmer affinity assays allow large-scale comparison of proteome profiles among discrete populations [41].

4 Social Networks in Therapeutic Applications of RNA Aptamers

In this section, we introduce brief histories related to the development of pegaptanib and REG1. We also describe the social networks among researchers involved in REG1, which is in clinical development, by analyzing published research papers. For social network analysis, we used NetMiner II ver. 2.6 (Cyram Co., Ltd)

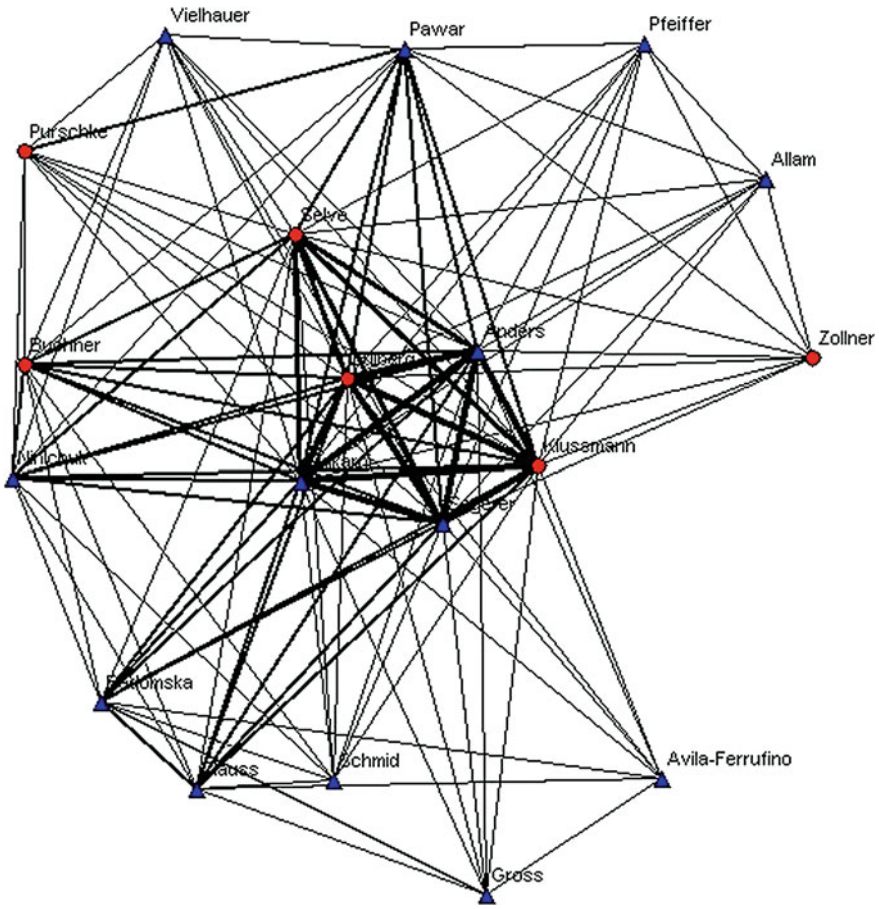

Fig. 3c Social networks among researchers who conducted studies related to the discovery and development of NOX-E36. The line width is proportional to the number of co-authorships. *Red circle*: NOXXON (Biotech SME), *blue triangle*: university

and employed spring-embedding algorithms, especially Spring-KK (Kamada–Kawai), to visualize the results.

4.1 Discovery and Development of Pegaptanib

The discovery of and preclinical development work on pegaptanib were conducted by NeXstar and began in 1994 [13]. NeXstar may be advanced in the field because they owned the patent related to the SELEX process, which is essential for studying aptamers. When NeXstar was acquired by Gilead Sciences, Gilead and Eyetech entered into an exclusive license agreement in which Eyetech received the

rights to use pegaptanib for therapeutic applications [21]. Eyetech then tested pegaptanib in humans in a phase 1 clinical trial. Since December 2002, Eyetech has collaborated with Pfizer to jointly develop and commercialize pegaptanib [21]. The history of the development of pegaptanib shows the importance of patents in research tools. The NIH (National Institutes of Health) defines research tools as "embracing the full range of tools that scientists use in the laboratory" [42]. According to the OECD (Organization for Economic Cooperation and Development), "research tools may be considered as compositions or methods used in conducting experiments. This term could embrace a broad range of resources that scientists use in the laboratory including, but not limited to, cell lines, monoclonal antibodies, reagents, animal models, growth factors, combinational chemistry, genomic and proteomic libraries, drug and drug targets, clones and cloning tools, methods, laboratory equipment and machines, databases and software" [43]. In the field of biotechnology, research tool patents have enormous power because the patented inventions are of crucial importance to researchers [44]. Under these circumstances, the owner of a research tool has priority for its use and thereby influences subsequent studies.

4.2 Discovery and Development of REG1

Rusconi et al. designed the aptamer against coagulation factor IXa and its antidote in 2002 [24]. Rusconi then founded a biopharmaceutical firm named Regado-Bioscience (Regado). Regado continuously collaborated with researchers at Duke University to develop REG1. For clinical development, Regado still collaborates with Duke University as well as other organizations including several universities, hospitals, and public and private research institutes.

We used co-authorships of published research papers to analyze the social networks among researchers who conducted studies on REG1 [24–31, 45]. We also analyzed the social networks among the organizations where the researchers were employed.

As depicted in Figs. 3a and b, Regado has collaborated with various organizations. Many previous studies have revealed that interaction with other actors is a positive influence on the research performance of biotech small- and medium-sized enterprises (SMEs) [48–53]. These interactions help biotech SMEs to overcome deficiencies in their scientific knowledge, human and financial resources, and complementary competencies [51, 54, 55].

Deep collaboration between a biotech SME and universities was also observed in the development of NOX-E36 [32, 33, 46, 47]. As depicted in Fig. 3c, NOXXON has collaborated with universities to form "dense" networks. A major benefit of networking with universities is that these interactions increase a firm's stock of knowledge. The results of several empirical studies show that companies which collaborated with a university had higher levels of innovative output [49].

5 Future Prospects

Considerable effort is being directed towards improving the affinity, specificity, and biostability of RNA aptamers. Therapeutic applications of RNA aptamers have been broadened in a number of fields. Some RNA aptamers have been used in clinical trials, as described in this study, and in-vitro studies are being conducted for the development of RNA aptamers against targets such as human immunodeficiency virus (HIV), hepatitis C virus (HCV), and angiopoietin 2. According to BCC Research, the global market for aptamers was valued at $10 million in 2009 and is expected to be valued at nearly $1.8 billion by 2014, with a compound annual growth rate of 67.5% [60]. With this extension of the market, it is expected that research into the therapeutic and diagnostic applications yof RNA aptamers will increase. It seems likely that firms that are currently using RNA aptamers will maintain their collaborative activities in order to continue their prior occupation of the market.

References

1. Bunka DHJ, Stockley PG (2006) Aptamers come of age—at last. Nat Rev Microbiol 4:588–596
2. Ellington AD, Szostak JW (1990) In vitro selection of RNA molecules that bind specific ligands. Nature 346:818–822
3. Robertson DL, Joyce GF (1990) Selection in vitro of an RNA enzyme that specifically cleaves single-stranded DNA. Nature 344:467–468
4. Tuerk C, Gold L (1990) Systematic evolution of ligands by exponential enrichment: RNA ligands to bacteriophage T4 DNA-polymerase. Science 249:505–510
5. Vater A, Klussman S (2003) Toward third-generation aptamers: Spiegelmers and their therapeutic prospects. Curr Opin Drug Discov Devel 6:253–261
6. Ulrich H (2006) RNA aptamers: from basic science towards therapy. Handb Exp Pharmacol 173:305–326
7. Bunka DHJ, Platonova O, Stockley PG (2010) Development of aptamer therapeutics. Curr Opin Pharmacol 10:557–562
8. Cox JC, Hayhurst A, Hesselberth J et al (2002) Automated selection of aptamers against protein targets translated in vitro: from gene to aptamer. Nucleic Acids Res 30:e108
9. Yang Y, Yang D, Schluesener HJ et al (2007) Advances in SELEX and application of aptamers in the central nervous system. Biomol Eng 24(6):583–592
10. White R, Rusconi C, Scardino E et al (2001) Generation of species cross-reactive aptamers using "Toggle" SELEX. Mol Ther 4:567–573
11. Vater A, Jarosch F, Buchner K et al (2003) Short bioactive Spiegelmers to migraine-associated calcitonin gene-related peptide rapidly identified by a novel approach: tailored-SELEX. Nucleic Acids Res 31:e130
12. Fruste JP, Bald R, Erdmann VA (2002) Mirror-symmetrical selection and evolution of nucleic acids. EP-00934331
13. Ng EWM, Shima DT, Calias P et al (2006) Pegaptanib, a targeted anti-VEGF aptamer for ocular vascular disease. Nat Rev Drug Discov 5(2):123–132
14. Lee JF, Stovall GM, Ellington AD (2006) Aptamer therapeutics advance. Curr Opin Chem Biol 10(3):282–289

15. Bless NM, Smith D, Charlton J et al (1997) Protective effects of an aptamer inhibitor of neutrophil elastase in lung inflammatory injury. Curr Biol 7:877–880
16. Kourlas H, Schiller DS (2006) Pegaptanib sodium for the treatment of neovascular age-related macular degeneration: a review. Clin Ther 28(1):36–44
17. Gragoudas ES, Adamis AP, Cunningham ET Jr et al (2004) Pegaptanib for neovascular age-related macular degeneration. N Engl J Med 351:2805–2816
18. Tucker CE, Chen L-S, Judkins MB et al (1999) Detection and plasma pharmacokinetics of an anti-vascular endothelial growth factor oligonucleotide-aptamer (NX1838) in rhesus monkeys. J Chromatogr B Biomed Sci Appl 732:203–212
19. Ruckman J, Green LS, Beeson J et al (1998) 2′-Fluoropyrimidine RNA-based aptamers to the 165-amino acid form of vascular endothelial growth factor (VEGF165). Inhibition of receptor binding and VEGF-induced vascular permeability through interactions requiring the exon 7-encoded domain. J Biol Chem 273(32):20556–20567
20. Drolet DW, Nelson J, Tucker CE et al (2000) Pharmacokinetics and safety of an anti-vascular endothelial growth factor aptamer (NX1838) following injection into the vitreous humor of rhesus monkeys. Pharm Res 17(12):1503–1510
21. Vinores SA (2003) Technology evaluation: pegaptanib Eyetech/Pfizer. Curr Opin Mol Ther 5(6):673–679
22. Eyetech Study Group (2002) Preclinical and phase 1A clinical evaluation of an anti-VEGF pegylated aptamer (EYE001) for the treatment of exudative age-related macular degeneration. Retina 22:143–152
23. Eyetech Study Group (2003) Anti-vascular endothelial growth factor therapy for subfoveal choroidal neovascularization secondary to age-related macular degeneration: phase II study results. Ophthalmology 110:979–986
24. Rusconi CP, Roberts JD, Pitoc GA et al (2004) Antidote-mediated control of an anticoagulant aptamer in vivo. Nat Biotechnol 22:1423–1428
25. Rusconi CP, Scardino E, Layzer J et al (2002) RNA aptamers as reversible antagonists of coagulation factor IXa. Nature 419:90–94
26. Dyke CK, Steinhubl SR, Kleiman NS et al (2006) First-in-human experience of an antidote-controlled anticoagulant using RNA aptamer technology: a phase 1a pharmacodynamic evaluation of a drug-antidote pair for the controlled regulation of factor IXa activity. Circulation 114(23):2490–2497
27. Chan MY, Rusconi CP, Alexander JH et al (2008) A randomized, repeat-dose, pharmacodynamic and safety study of an antidote-controlled factor IXa inhibitor. J Thromb Haemost 6:789–796
28. Chan MY, Cohen MG, Dyke CK et al (2008) Phase 1b randomized study of antidote-controlled modulation of factor IXa activity in patients with stable coronary artery disease. Circulation 117(22):2865–2874
29. Povsic TJ, Cohen MG, Chan MY et al (2011) Dose selection for a direct and selective factor IXa inhibitor and its complementary reversal agent: translating pharmacokinetic and pharmacodynamic properties of the REG1system to clinical trial design. J Thromb Thrombolysis 32:21–31
30. Cohen MG, Purdy DA, Rossi JS et al (2010) First clinical application of an actively reversible direct factor IXa inhibitor as an anticoagulation strategy in patients undergoing percutaneous coronary intervention. Circulation 122(6):614–622
31. Povsic TJ, Wargin WA, Alexander JH et al (2011) Pegnivacogin results in near complete FIX inhibition in acute coronary syndrome patients: RADAR pharmacokinetic and pharmacodynamic substudy. Eur Heart J 32(19):2412–2419
32. Kulkarni O, Pawar RD, Purschke W et al (2007) Spiegelmer inhibition of CCL2/MCP-1 ameliorates lupus nephritis in MRL-(Fas)lpr mice. J Am Soc Nephrol 18:2350–2358
33. Ninichuk V, Clauss S, Kulkarni O et al (2008) Late onset of Ccl2 blockade with the spiegelmer mNOX-E36–3′PEG prevents glomerulosclerosis and improves glomerular filtration rate in db/db mice. Am J Pathol 172(3):628–637
34. NOXXON homepage http://145.253.103.53/noxxon16/downloads/FactSheet.pdf

35. Ophthotech homepage http://www.ophthotech.com/products/arc1905/
36. Drolet DW, Moon-McDermott L, Romig TS (1996) An enzyme-linked oligonucleotide assay. Nat Biotechnol 14:1021–1025
37. McCauley TG, Hamaguchi N, Stanton M (2003) Aptamer-based biosensor arrays for detection and quantification of biological macromolecules. Anal Biochem 319:244–250
38. Ulrich H, Martins AH, Pesquero JB (2004) RNA and DNA aptamers in cytomics analysis. Cytometry A 59:220–231
39. Davis KA, Lin Y, Abrams B et al (1998) Staining of cell surface human CD4 with 2′-F-pyrimidine-containing RNA aptamers for flow cytometry. Nucleic Acids Res 26(17): 3915–3924
40. Bagalkot V, Zhang L, Levy-Nissenbaum E et al (2007) Quantum dot-aptamer conjugates for synchronous cancer imaging, therapy, and sensing of drug delivery based on bi-fluorescence resonance energy transfer. Nano Lett 7(10):3065–3070
41. Gold L, Ayers D, Bertino J et al (2010) Aptamer-based multiplexed proteomic technology for biomarker discovery. PLoS ONE 5(12):e15004. doi:10.1371/journal.pone.0015004
42. NIH homepage www.nih.gov/news/researchtools/
43. OECD homepage www.oecd.org/dataoecd/39/38/36198812.pdf
44. Kang KN, Ryu TK, Lee YS (2009) Effects of research tool patents on biotechnology innovation in a developing country: a case study of South Korea. BMC Biotechnol 9:25
45. Nimjee SM, Keys JR, Pitoc GA et al (2006) A novel antidote-controlled anticoagulant reduces thrombin generation and inflammation and improves cardiac function in cardiopulmonary bypass surgery. Mol Ther 14(3):408–415
46. Kulkarni O, Eulberg D, Selve N et al (2009) Anti-Ccl2 Spiegelmer permits 75% dose reduction of cyclophosphamide to control diffuse proliferative lupus nephritis and pneumonitis in MRL-Fas(lpr) mice. J Pharmacol Exp Ther 28(2):371–377
47. Clauss S, Gross O, Kulkarni O et al (2009) Ccl2/Mcp-1 blockade reduces glomerular and interstitial macrophages but does not ameliorate renal pathology in collagen4A3-deficient mice with autosomal recessive Alport nephropathy. J Pathol 218(1):40–47
48. Baum JAC, Calabrese T, Silverman BS (2000) Don't go it alone: alliance network composition and startup's performance in Canadian biotechnology. Strateg Manag J 21:267–294
49. George G, Zahra SA, Wood DR (2002) The effects of business–university alliances on innovative output and financial performance: a study of publicly traded biotechnology companies. J Bus Ventur 17:577–609
50. Hagedoorn J (1993) Understanding the rationale of strategic technology partnering: interorganizational modes of cooperation and sectoral differences. Strateg Manag J 14:371–385
51. Romijn H, Albaladejo M (2002) Determinants of innovation capability in small electronics and software firms in Southeast England. Res Policy 31:1053–1067
52. Rothaermel FT, Deeds DL (2006) Alliance type, alliance experience and alliance management capability in high-technology ventures. J Bus Ventur 21:429–460
53. Shan W, Walker G, Kogut B (1994) Interfirm cooperation and startup innovation in the biotechnology industry. Strateg Manag J 15:387–394
54. Becheikh N, Landry R, Amara N (2006) Lessons from innovation empirical studies in the manufacturing sector: a systematic review of the literature from 1993–2003. Technovation 26:644–664
55. Kang KN, Lee YS (2008) What affects the innovation performance of small and medium-sized enterprises (SMEs) in the biotechnology industry? An empirical study on Korean biotech SMEs. Biotechnol Lett 30:1699–1704
56. Azoulay P, Ding W, Stuart T (2007) The determinants of faculty patenting behavior: demographics or opportunities? J Econ Behav Organ 63:599–623
57. Zucker LG, Darby MR (2001) Capturing technological opportunity via Japan's star scientists: evidence from Japanese firms' biotech patents and products. J Technol Transf 26(1–2):37–58

58. Zucker LG, Darby MR, Brewer MB (1998) Intellectual human capital and the birth of U.S. biotechnology enterprises. Am Econ Rev 88(1):290–306
59. Zucker LG, Darby MR, Armstrong JS (2002) Commercializing knowledge: university science, knowledge capture, and firm performance in biotechnology. Manag Sci 48(1):138–153
60. BCC Research (2010) Nucleic acid aptamers for diagnostics and therapeutics: global markets. (Report BIO071A)

Adv Biochem Eng Biotechnol (2013) 131: 171–172
DOI: 10.1007/978-3-642-36508-9

Index